

WESTERN SYDNEY UNIVERSITY



Analysis of AR/AR-V7 Signalling Pathways in Circulating Tumour Cells of Prostate Cancer Patients

Tanzila Khan

Supervisors:

Prof Paul de Souza

A/Prof Therese Becker

A/Prof Kieran Scott

Dr. John Lock

This thesis is submitted as fulfilment of the requirements for the degree:

Doctor of Philosophy

School of Medicine, Western Sydney University

Campbelltown, NSW, Australia

July, 2022

Acknowledgements

First of all, I would like to say thanks to Allah for completing this journey and making things easy. Then, I would like to acknowledge the immense contribution of my supervisors, A/Prof Therese Becker, A/Prof Kieran Scott, Prof Paul de Souza and Dr John Lock. I am very lucky to have you people during this journey. Thank you for arranging the scholarship for me and for teaching me everything. I am really thankful to you all. It was a totally different environment, but you made it easy for me. Kieran, thank you for your mentoring also.

I would like to acknowledge Yafeng Ma-You also worked like a mini-supervisor. Thank you for a lot of help in systematic review and also laboratory training.

I would like to acknowledge A/Prof Kevin Spring for all the help during this journey.

I would like to acknowledge A/Prof David Harman and team for their help in mass spectroscopy. I would like to acknowledge HDR director A/Prof Tara Robert.

I would like to acknowledge Dusica Maric for all the support during my studies.

I would like to acknowledge Nicole Caixeiro who helped me a lot. You are really a great person. I would like to acknowledge Joseph Po for all his help. I would like to acknowledge David Lynch. I always remember you for your nice attitude. I would like to acknowledge Alex James (you were like a problem solver for my experiments mainly westerns). I would like to acknowledge Branka, Sarah, Anshuli, Shadma, Mila, Tess, Tim and Heena. You all are great people. I am thankful for everything you did for me. I would like to acknowledge Noor for all the support during my studies.

I would like to acknowledge Alison and Natalie for laboratory support.

I would like to acknowledge Paul de Souza, Wei Chua and Bavanthi Balakrishnar for their help in providing access to patient samples. I would like to acknowledge WSU and Ingham Institute.

I would like to acknowledge patients for their agreement to provide samples in this study. I

would like to acknowledge my family-my mother, my sisters and my brothers. Thank you for supporting me during this journey.

Statement of Authentication

The work presented in this thesis is, to the best of my knowledge and belief, original except as acknowledged in the text. I hereby declare that I have not submitted this material, either in full or in part, for a degree at this or any other institution.

(Signed) _____  _____

Declarations/Co-authorship

The work presented in this thesis is, to the best of my knowledge and belief, original except as acknowledged in the text. I hereby declare that I have not submitted this material, either in full or in part, for a degree at this or any other institution.

Tanzila Khan

June 2022

COVID-19 Impact Statement

The project as planned originally was severely impacted by the COVID lockdowns in 2020 and 2021.

These impacted patient recruitment for the study, availability of supplies and laboratory access, in particular access to laboratories of our UNSW collaborator Dr John Lock with essential facilities for multiplex single cell staining.

As a result, the overall project was changed:

1. Chapter 3, an extensive systematic review of the clinical utility of liquid biopsy-based AR-V7 testing, not originally planned for this PhD project, was conducted and published.
2. In Chapter 5, some additional work in collaboration with A/Prof David Harman, WSU, was included. This comprised *in silico* analysis of potential cross-reactivities of the tested AR-V7 antibodies (protein blast) and analysis of putative cross-reactivity bands of interest detected by mass spectroscopy, followed by further *in silico* analysis of detected peptides.
3. Chapter 5, while initially planned to be more complex with multiplex immunostaining analysis of single cells (cultured cells and CTC), was reduced to the parts I was able to do in the Ingham Institute laboratories. It is essentially now a method development chapter with a view of future single cell multiplex analysis beyond this PhD project.

Publications

Journal Articles

- **Khan T**, Lock J, Ma Y, Harman D, Souza PD, Chua W, Balakrishnar B, Scott KF, Becker TM. *Choice of antibody is critical for specific and sensitive detection of androgen receptor splice variant-7 in circulating tumour cells*. Scientific Reports, 2022 (under revision).
- **Khan T**, Becker TM, Po J, Chua W, Ma Y, *Single Circulating Tumour Cell Whole Genome Amplification to Unravel Cancer Heterogeneity and Actionable Biomarkers* International Journal of Molecular Sciences, (submitted).
- **Khan T**, Becker TM, Scott KF, Descallar J, Souza PD, Chua W, Ma Y. *Prognostic and Predictive Value of Liquid Biopsy-Derived Androgen Receptor Variant 7 (AR-V7) in Prostate Cancer: A Systematic Review and Meta-Analysis*. Frontiers in Oncology, **2022**:12. doi.org/10.3389/fonc.2022.868031.
- **Khan T**, Scott KF, Becker TM, Lock J, Nimir, M, Ma Y and Souza PD. *Prospect of Identifying Resistance Mechanisms for Castrate Resistant Prostate Cancer using Circulating Tumour Cells: is Epithelial to Mesenchymal Transition a Key Player?* Prostate Cancer, **2020**:7938280, doi.org/10.1155/2020/7938280.
- Nimir, N., Ma, Y., Jeffreys, S.A., Opperman, T., Young, F., Ding, P., **Khan, T.**, Chua, W., Balakrishna, B., Cooper, A., de Souza, P., Becker, T.M. *Detection of AR-V7 in liquid biopsies of castrate resistant prostate cancer patients: a comparison of AR-V7 analysis in circulating tumour cells, circulating tumour RNA and exosomal RNA*. Cells, **2019**: 8(7). doi: [10.3390/cells8070688](https://doi.org/10.3390/cells8070688)

Conference Presentations

Khan, T., Scott, K., De Souza, P., Ma, Y., Lock, J., Becker, T. Towards Multiple Protein Biomarker Detection in Advanced Prostate Cancer Circulating Tumour Cells. 8th Thomas Ashworth CTC & Liquid Biopsy Symposium, Oct 2021 Sydney (*poster with virtual oral presentation*)

Khan, T., Better Diagnosis to Improve Survival In Prostate Cancer. WSU School of Medicine Three Minute Thesis Competition, WSU Campbelltown Campus, 2021 Sydney (*oral presentation*)

Khan, T., Scott, K., De Souza, P., Ma, Y., Lock, J., Becker, T. Towards Multiple Protein Biomarker Detection in Advanced Prostate Cancer Circulating Tumour Cells. 29th ASMR NSW Annual Scientific Meeting, 2021 Sydney (*poster*)

Khan, T., Scott, K., De Souza, P., Ma, Y., Lock, J., Becker, T. Towards Multiple Protein Biomarker Detection in Advanced Prostate Cancer Circulating Tumour Cells. CONCERT Virtual Showcase Dec 2020 Sydney (*selected for short oral presentation*)

Khan, T., Scott, K., De Souza, P., Ma, Y., Lock, J., Becker, T. Towards Multiple Protein Biomarker Detection in Advanced Prostate Cancer Circulating Tumour Cells. 7th Thomas Ashworth CTC & Liquid Biopsy Symposium, Oct 2020 Sydney (*poster*)

Khan, T., Towards Multiple Protein Biomarker Detection in Advanced Prostate Cancer Circulating Tumour Cells. 2nd annual CONCERT All Members Day, 2019 (Oral presentation)

Becker, T.M., Ma, Y., Nimir M., Chua, W., Balakrishnar, B., Cooper, A., **Khan, T.**, Young, F., Luk A.W.L., Opperman T., de Souza P. *Circulating tumour cell analysis for prostate cancer biomarkers*. 6th Thomas Ashworth CTC and Liquid Biopsy Symposium, Oct 2019, Sydney (*abstract invited oral presentation by T. Becker*)

Khan, T., Scott, K., Lock, J., Ma, Y., de Souza, P., Becker, T.M. *Towards Multiple Protein Biomarker Detection in Advanced Prostate Cancer Circulating Tumour Cells*. 6th Thomas Ashworth CTC and Liquid Biopsy Symposium, Oct 2019, Sydney (*poster abstract*)

Nimir, M., Ma, Y., Jeffreys, S., Opperman, T., Young, F., **Khan, T.**, Ding, P., Chua, W., Balakrishnar, B., Cooper, A., De Souza, P., Becker, T.M. *Detection of AR-V7 in liquid biopsies of castrate resistant prostate cancer patients: a comparison of AR-V7 analysis in circulating tumour cells, circulating tumour RNA and exosomes*. 6th Thomas Ashworth CTC and Liquid Biopsy Symposium, Oct 2019, Sydney (*abstract selected for oral presentation by M Nimir, won best presentation award*)

Khan, T., Better Diagnosis to Improve Survival In Prostate Cancer. WSU School of Medicine Three Minute Thesis Competition, WSU Campbelltown Campus, 2019 Sydney (*oral presentation*)

*Opperman T., Ma Y; Ding P; Cooper A; Chua W; **Khan T**; de Souza P; Becker T., *Predictive Biomarkers for Advanced Prostate Cancer in Circulating Tumour Cells: AR we ready to Akt?* Translational Cancer Research Workshop, Oct 2018, Wollongong (*poster abstract*)

*Opperman T., Ma Y; Ding P; Cooper A; Chua W; **Khan T**; de Souza P; Becker T. *Dissecting the PTEN/Akt and AR pathways in Circulating Tumour Cells: Towards a Biomarker Assay for Castrate Resistant Prostate Cancer*, Thomas Ashworth CTC and Liquid Biopsy Symposium, Sydney 2018- (*poster abstract, best poster prize*)

Table of Contents

Acknowledgements.....	II
Statement of Authentication	IV
Declarations/Co-authorship	V
COVID-19 Impact Statement	VI
Publications.....	VII
Journal Articles	VII
Conference Presentations	VIII
Table of Contents.....	X
List of Figures	XV
List of Tables	XVII
Abstract	XIX
Abbreviation	XXII
Chapter 1: Introduction and Literature Review	1
1.1 Introduction.....	1
1.2 Circulating Tumour Cells and EMT in Metastasis.....	6
1.3 Clinical Relevance of EMT Markers in PCa.....	16
1.4 AR, ADT, EMT and Drug Resistance.....	19
1.5 AKT Pathway in mCRPC	20
1.6 Hippo Signalling Pathway and Its Role in CRPC and EMT.....	22
1.7 YAP Cross Talk with AR and AKT Pathways	27

1.8 Analysis of PCa CTCs to Explore the AR-AKT-YAP Connection and EMT.....	29
1.9 CTC Enrichment and Analysis Strategies.....	32
1.10 Hypothesis.....	34
1.11 Aims	34
Chapter 2: Material and Methods	35
2.1 Chemicals and Research Consumables.....	35
2.2 Equipment	37
2.3 General Methods	38
2.3.1 Patient Recruitment	38
2.3.2 Tissue Culture.....	38
2.3.3 Western Blotting.....	39
2.3.4 Immunocytostaining and Fluorescence Microscopy	40
2.3.5 CTC isolation from Patient Blood.....	40
2.3.6 RNA Isolation.....	41
2.3.7 Droplet Digital PCR (ddPCR).....	41
2.3.8 Primers and probes	42
Chapter 3: Prognostic and Predictive Value of Liquid-Biopsy-Derived Androgen Receptor Variant 7 (AR-V7) in Prostate Cancer: A Systematic Review and Meta-Analysis.....	43
3.1 Introductory Background	43
3.1.1 Published Manuscript	44
3.2 Abstract	45
3.3 Introduction	46

3.4 Methods.....	47
3.4.1 Study Design and Literature Searches.....	47
3.4.2 Selection Criteria.....	47
3.4.3 Data Extraction and Quality Assessment.....	48
3.4.4 Statistical Analysis.....	49
3.5 Results.....	49
3.5.1 Search Results, Study and Patient Characteristics.....	49
3.5.2 Predictive Value of AR-V7 for ARSi-Treatment.....	58
3.5.3 Chemotherapy-Treated Patients and Outcome Association with AR-V7.....	62
3.5.4 AR-V7 Effect on Non-Defined (Miscellaneous) Treatments.....	62
3.5.5 ARSi vs. Chemotherapy in AR-V7 Positive or Negative Patients.....	62
3.5.6 Quality Assessment, Publication Bias and Sensitivity Analysis.....	64
3.6 Discussion.....	64
3.7 Supplementary Material.....	68
3.8 Conclusion.....	87
Chapter 4: Establishing Reliable Immunocytostaining for AR-V7.....	88
4.1 Introduction.....	88
4.1.1 Published Manuscript.....	89
4.2 Abbreviation.....	90
4.3 Abstract.....	91
4.4 Introduction.....	92

4.5 Methods.....	93
4.5.1 Cell Lines.....	93
4.5.2 Antibodies.....	94
4.5.3 Droplet Digital PCR (ddPCR).....	95
4.5.4 Western Blotting.....	95
4.5.5 Immunocytostaining of Cell Lines	96
4.5.6 CTC Enrichment and Immunocytostaining.....	96
4.5.7 Image Analysis and Statistics.....	97
4.6 Results	97
4.7 Discussion	110
4.8 Supplementary Material	112
4.9 Conclusion.....	113
Chapter 5: Method Development for Single Cell Multiplex Proteomic Microscopy with a View to Study Relationships Among the AR, AKT and Hippo Signalling Pathways in Prostate Cancer	114
5.1 Introduction.....	114
5.2 CTC Enrichment	120
5.2.1 Foundations for CTC Enrichment Experiments	120
5.2.2 Comparison of CTC Enrichment Using RosetteSep CD36-kit vs. CD45-kit.....	124
5.2.3 CD36-kit CTC Isolation vs. OncoQuick CTC Enrichment Isolation.....	129
5.2.4 CD36-kit vs. AutoMacs CTC Enrichment Comparison.....	136
5.2.5 Preliminary Discussion of CTC Enrichment Method Comparison.....	144

5.2.6 Additional CD36-kit Considerations and Tests.....	147
5.3 CTC Immobilisation.....	152
5.3.1 Results and Discussion of CTC Adhesion Optimisation.....	153
5.4 Antigen and Antibody Selection and Optimisation.....	157
5.4.1 Results	167
5.5 Mass spectrometry.....	171
5.6 Discussion	180
5.7 Limitations	182
5.8 Future directions.....	183
Chapter 6: General Discussion.....	184
6.1 Implications and Considerations for Clinical Translation.....	186
6.2 Limitations of This Project.....	189
6.2 Future Directions.....	192
6.3 Conclusion.....	193
Chapter 7: References	195
7.1 References	195
Appendices.....	211

List of Figures

Figure 1. 1 AR and AR-V7 gene and protein	4
Figure 1. 2 EMT in Cancer Metastasis	9
Figure 1. 3 Hippo signalling pathway	23
Figure 1. 4 AR AKT and YAP interaction	28
Figure 3. 1 Flow chart of literature search and study selection.....	50
Figure 3. 2 Forest plot of hazard ratios (HRs) for association of liquid biopsy AR-V7 status with overall survival (OS) in all included studies	59
Figure 3. 3 Forest plot of hazard ratios (HRs) for association of liquid biopsy AR-V7 status with PFS in all studies.....	60
Figure 3. 4 Forest plot of hazard ratios (HRs) for association of liquid biopsy AR-V7 status with PSA-PFS in all studies.....	61
Figure 3. 5 Forest plots for association of liquid biopsy AR-V7 status with OS in (A) AR-V7 positive (ARSi vs. Chemotherapy) and (B) AR-V7 negative patients (ARSi. vs. Chemotherapy).....	63
Supplemental Figure 3. 1 Inverted funnel plot to evaluate potential publication bias in OS (A) and PFS (B) of ARSi treated patients.....	83
Supplemental Figure 3. 2 Forest plot of hazard ratios (HRs) for association of liquid biopsy AR-V7 status with OS (A), PFS (B), PSA-PFS (C) in all studies.....	86
Figure 4. 1 AR-V7 specific peptide and antigens for antibody generation.....	99

Figure 4. 2 AR-V7 staining with different antibodies in AR-V7 positive and negative cells	104
.....	
Figure 4. 3 AR-V7 staining nuclear intensity	106
Figure 4. 4 AR-V7 CTC detection	109
Figure 5. 1 Multiplex CTC analysis methods development	117
Figure 5. 2 The comparison of CD36-kit vs. CD45 kit for the isolation of CTCs	128
Figure 5. 3 The comparison of CD36-kit vs. OncoQuick CTC enrichment	133
Figure 5. 4 The OncoQuick CTC enrichment (left) and CD36 kit (right)	135
Figure 5. 5 CD36-kit vs. AutoMacs CTC enrichment	140
Figure 5. 6 CTC enrichment method comparison	143
Figure 5. 7 Comparison of four CTC enrichment methods	146
Figure 5. 8 Anucleated cells vs. nucleated cells	150
Figure 5. 9 Cell immobilisation by using Cell-Tak	156
Figure 5. 10 Steps in multiplex proteomics	158
Figure 5. 11 AR-FL antibody staining	170
Figure 5. 12 Isolation of cross-reacting bands identified on SDS PAGE gel electrophoresis and western blot with antibody EPR15656	172

List of Tables

Table 1. 1 Signalling Pathways implicated in EMT and relevance to PCa	12
Table 1. 2 EMT markers detected in PCa tissue.....	18
Table 3. 1 The basic characteristics of eligible studies	52
Supplemental Table 3. 1 Definitions of OS, PFS, PSA-PFS and tumour stages in each included study.....	68
Supplemental Table 3. 2 Quality assessment of included studies based on adapted NOS scales.....	77
Supplemental Table 3. 3 Sensitivity analysis of subgroups with more than 6 studies.....	78
Table 4. 1 AR-V7 staining CTC detection by antibody.....	108
Supplemental Table 4. 1 Anti-AR-V7 antibodies and working dilutions	112
Table 5. 1 Example of calculated cell counts vs. input control cell counts	123
Table 5. 2 Proportion of recovered with CD36-kit vs. CD45-kit.....	126
Table 5. 3 Proportion of recovered CTCs with CD36-kit vs. OncoQuick CTC enrichment	131
Table 5. 4 Proportion of recovered CTCs with CD36-kit vs. AutoMacs CTC enrichment	138
Table 5. 5 Number of CTCs after immunostaining	151
Table 5. 6 List of shortlisted antigens for the AR/AR-V7–AKT–Hippo pathway study including cell line status for antibody optimisation	160

Table 5. 7 List of antibodies with company details, species and results	164
Table 5. 8 22RV1 Band 1 (1)	176
Table 5. 9 22RV1 Band 1 (duplicate)	176
Table 5. 10 22RV1 Band 2 (1)	176
Table 5. 11 22RV1 Band 2 (duplicate)	177
Table 5. 12 22RV1 Band 3 (1)	177
Table 5. 13 22RV1 Band 3 (duplicate)	177
Table 5. 14 PC3 Band 4 (1).....	178
Table 5. 15 PC3 Band 4 (duplicate).....	178
Table 5. 16 PC3 Band 5 (1).....	178
Table 5. 17 PC3 Band 5 (duplicate).....	179

Abstract

Biomarkers detected in liquid biopsy (such as circulating tumour cells, CTCs) demonstrate high concordance with biomarkers detected in conventional tissue biopsy. Prostate cancer, when metastatic, is treated with androgen deprivation therapy (ADT). However, resistance to ADT evolves into a clinical state referred to as castrate resistant prostate cancer (CRPC), in which increased, abnormal, androgen receptor (AR) signalling through changed AR structures (amplification, point mutations or variant expression) occurs. Although CRPC also facilitates development of other, complex signalling pathways that promote cell survival, our hypothesis is that the abnormal AR signalling is tightly linked to PTEN/AKT and Hippo/YAP pathways that contribute to the oncogenic driver role that confers ADT resistance.

This PhD project aims to evaluate the role of AR, PTEN, and Hippo driver pathways in CRPC through analysis of CTCs, which have become important biological correlates and sources to study tumour biology in prostate cancer. The main focus was on the AR splice variant 7 (AR-V7), a promising predictive and prognostic CRPC biomarker.

Outcomes:

- Initially a comprehensive literature review indicated a likely triangular relationship between AR/AR-V7, the PTEN/AKT signalling pathway and the Hippo/YAP pathway in CRPC. This is summarized in the Introduction chapter (and is in parts published ([1], attachment 1). Thus, demonstrating the linkage of these pathways through multiplex staining of CTCs for markers of these pathways became a goal of this project.
- This was followed by systematic review to evaluate whether there was sufficient evidence in the current literature to support the concept of ARV7 within liquid biopsies as an important clinical (prognostic and predictive) biomarker of CRPC. An extensive

meta-analysis (Chapter 3, published in *Frontiers in Oncology* [2], attachment 2) confirmed that liquid biopsy-based detectable AR-V7 significantly associates with worse overall survival (OS), progression free survival (PFS), PSA-PFS in general and in the context of specific therapy. Thus, we can conclude that AR-V7 is an important biomarker that is useful in guiding therapy and to potentially stratify patients for clinical trials.

- Our team had previously developed the most sensitive method in the world to detect AR-V7 transcript in CTCs. Here we aimed to add analysis of AR-V7 protein in CTCs. While there are 7 commercial antibodies in theory capable of selective AR-V7 detection, our initial observation of antibody binding to AR-V7 negative cells suggested that a thorough comparison of all available anti-AR-V7 antibodies was needed. The work in Chapter 4 (corresponding manuscript under revision with the journal *Scientific Reports* (attachment 3)) is based on identifying the best anti-AR-V7 antibody [clone E308L] to detect AR-V7 by immunocytostaining; we found that the number of CRPC CTCs detected varies considerably, depending on the antibody used in the methodology.
- Chapter 5 summarises integral steps of method development, such as CTC enrichment, CTC immobilization to optical surfaces (slides, glass bottom plates) for extensive multiplex immunocytostaining analysis (“proteomic microscopy”), and optimisation of a range of antibodies to detect relevant biomarkers in cultured cells (and ultimately CTCs).

The overall outcomes of this PhD project were to (i) investigate the role of AR, PTEN, and Hippo pathways implicated in CRPC, (ii) validate liquid-biopsy-detected AR-V7 as a CRPC biomarker, (iii) define the best antibody to detect AR-V7 CTCs in CRPC patient blood, and

(iv) optimise methods that enable multiplex immunocytostaining of prostate cancer cells, including CTCs with a view to conduct ‘proteomic microscopy’ in the future.

This work in this PhD puts in place basic procedures and methods that will enable CTC multiplex “proteomic microscopy” a method that could change the current paradigm of CTC analysis by allowing analysis of these rare cells for multiple markers targeting multiple biological pathways at the same time.

Abbreviation

CE3 Cryptic Exon 3

ADT Androgen Deprivation Therapy

AKT-mTOR Phosphoinositide 3 Kinase (PI3K)/AKT-Mammalian Target of Rapamycin

AR Androgen Receptor

ARE Androgen Response Elements

CRPC Castration Resistant Prostate Cancer

CSPC Castration Sensitive Prostate Cancer Cells

CTCs Circulating Tumour Cells

CtDNA Circulating Tumour DNA

DBD DNA-Binding Domain

DHT Dihydrotestosterone

EMT Epithelial to Mesenchymal Transition

EMT-TFs EMT-Causing Transcription Factors

HIF Hypoxia-Inducible Factor

HSP90 Heat-Shock Protein 90

LATS ½ Large Tumour Suppressor ½ Kinases

LBD Ligand-Binding Domain

mCRPC metastatic Castration Resistant Prostate Cancer

MET Mesenchymal to Epithelial Transition

miRNA MicroRNA

MST ½ Mammalian Sterile 20- Like 1 And 2 Kinases

NTD Amino-Terminal Domain

PCa Prostate Cancer

PSA Prostate-Specific Antigen

PTEN Phosphatase and Tensin Homologue

TEAD Transcriptional Enhanced Associate Domain

YAP Yes Associated Protein

Chapter 1: Introduction and Literature Review

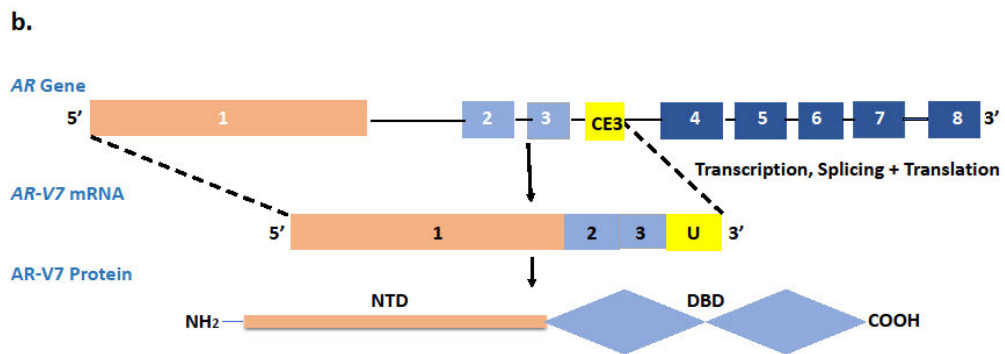
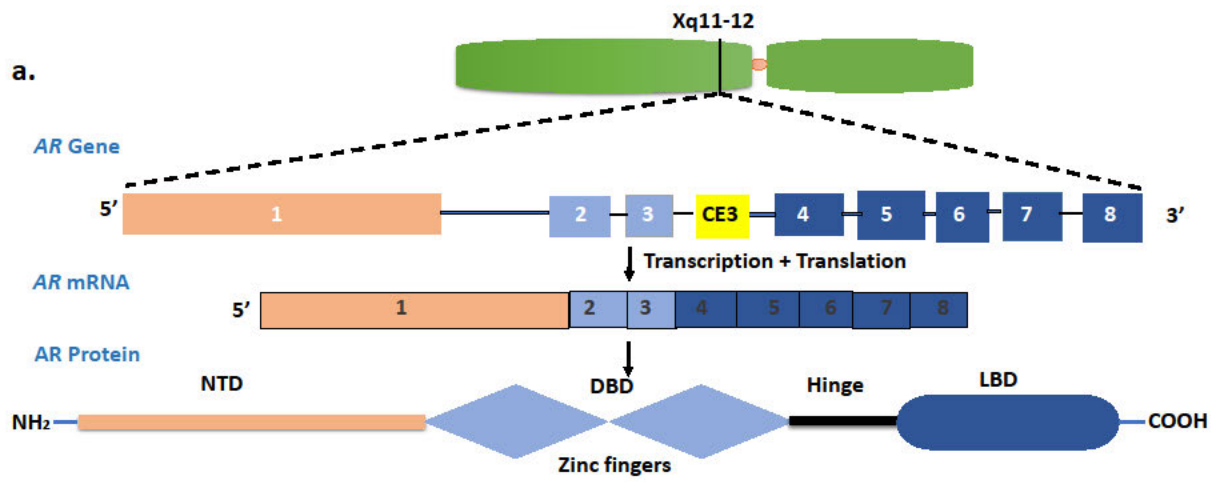
Note, extensive parts of this chapter have been published as a review manuscript [1]: *Prospect of Identifying Resistance Mechanisms for Castrate Resistant Prostate Cancer using Circulating Tumour Cells: is Epithelial to Mesenchymal Transition a Key Player?* Prostate Cancer, **2020** :7938280, doi.org/10.1155/2020/7938280 (Attachment 1 is the published pdf document).

1.1 Introduction

Prostate cancer (PCa) is highly prevalent in the Western world; it ranks sixth among cancers in regards to mortality among men [3]. In 2021 there were 18,110 new cases of PCa diagnosed in Australia and 3,323 PCa deaths [4]. Despite dramatic improvements in five-year survival, mortality from PCa is poised to remain a major health problem due to increasing longevity, particularly in western countries. The most significant factors associated with morbidity and mortality are the development of metastatic spread to other organs, particularly bone, and emerging resistance to therapy.

In the 1940s Charles Huggins found that androgen deprivation reduced PCa growth [5]. This was followed in the 1960s by discovering the role of androgen receptor (AR) signalling in the progression of PCa [6-8]. The AR, located on the X chromosome (Figure 1.1a), is a hormone dependent transcription factor [9]. In the unstimulated state, the receptor is cytoplasmic and bound by heat-shock proteins [10]. When its ligand, dihydrotestosterone (DHT) or testosterone, binds *via* the AR ligand binding domain (LBD) (Figure 1.1a), a structural change results in the detachment of AR from the heat-shock protein 90 (HSP90) complex, homo-dimerization of the receptor, and nuclear translocation.

In the nucleus, AR acts as a transcription factor by binding to androgen-response elements (AREs) in the promoter region of androgen-regulated genes [11, 12]. AR transactivates genes which are responsible for cell growth, differentiation and cell survival [13]. Consequently, increased AR signalling can potentially transform normal prostate cells into malignant PCa cells. Moreover, it has been shown that androgen deprivation therapy (ADT) can select for cancer cells with further increased AR activity, for example due to *AR* gene amplification [14].



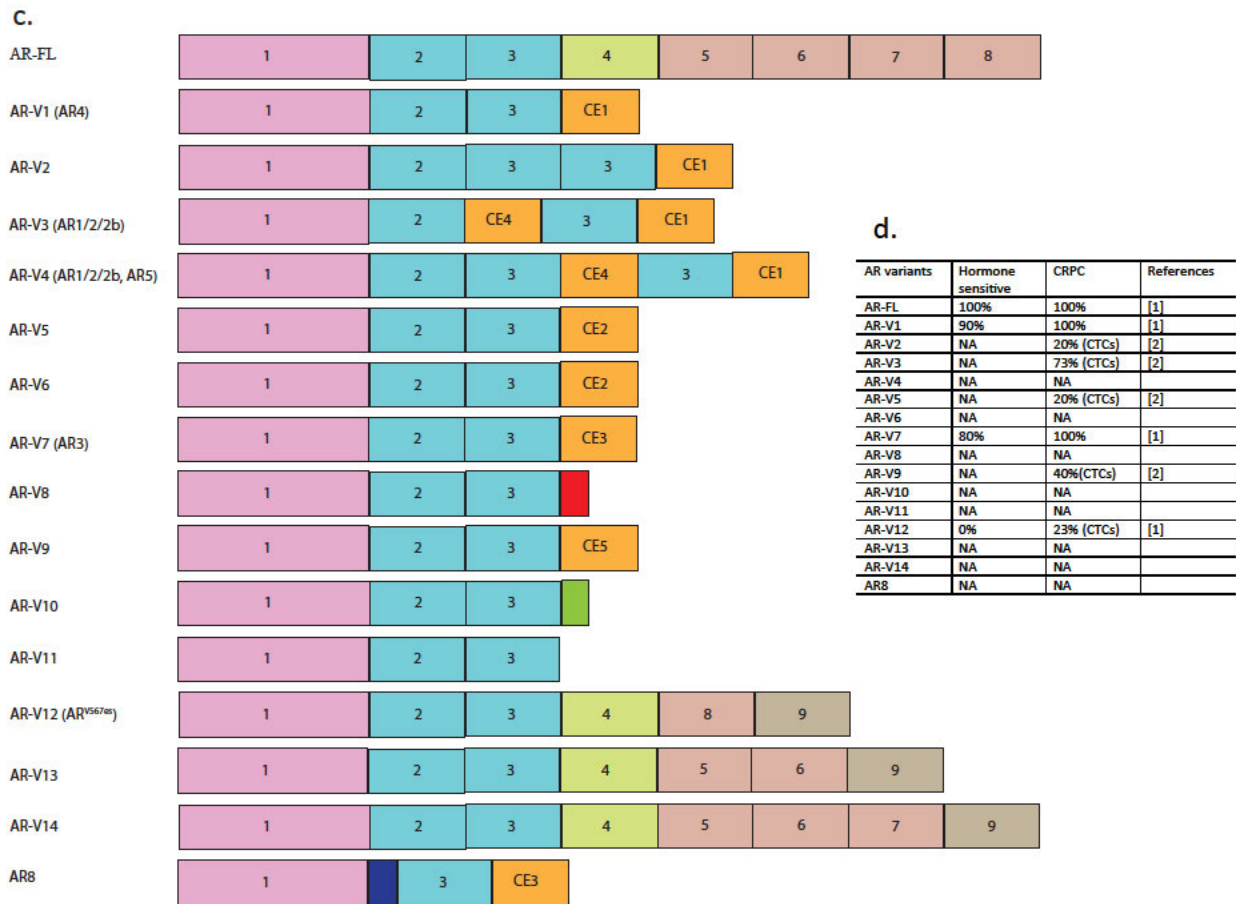


Figure 1. 1 AR and AR-V7 gene and protein

The schematic indicates (a) the structural organisation of the *AR* gene and protein (NTD: amino terminal domain, DBD: DNA binding domain, LBD: ligand binding domain) (b) shows the transcription and translation of the splice variant AR-V7 protein, including the exon/intron composition of the *AR*, highlighting the CE3 (middle) and indicates domains of the AR retained in the AR-V7 protein (bottom) (c) *AR* splice variants structures (d) *AR* splice variants frequency in hormone sensitive and CRPC.

The expression of alternative *AR* splice variants (shown in Figure 1c and 1d) has been proposed as a mechanism underlying resistance to ADT [15, 16]. Most splice variants result in the translation of a truncated AR protein lacking a functional C-terminal LBD but containing a functional transactivating N-terminal domain. Without being capable of binding ligand, the

resulting proteins are constitutively active as transcription factors and able to promote expression of certain target genes [13, 17]. At least 20 splice variants of *AR* have been identified in human prostate tissue and have been implicated in the development of mCRPC [17-20]. Amongst *AR* variants, *AR-V7* is highly expressed in mCRPC and is the most frequently disease associated variant identified in the clinic [21, 22]. The *AR-V7* transcript results from alternative splicing of the *AR* gene such that the transcript contains exon 1, 2 and 3 together with a cryptic exon 3 (CE3) resulting in a truncated transcript (U), resulting in premature transcriptional termination (Figure 1.1b). *AR-V7* is constitutively active irrespective of androgen binding, which is a proposed mechanism of escape from ADT [23, 24].

Many alternative signalling pathways are involved in the development of CRPC [25]. In 40% CRPC, *AR* independent signalling results in ADT resistance [26, 27]. On the molecular level, PCa is almost always initially driven by excessive signalling through the *AR* pathway (reviewed in [28]). Consequently, men with metastatic PCa will be offered ADT as the primary treatment. After a median of around 18-24 months, the disease tends to become resistant to hormonal manipulation and progresses towards so called metastatic castration-resistant prostate cancer (mCRPC). In mCRPC, the concentration of the current blood-based clinical PCa biomarker, prostate-specific antigen (PSA), continues to increase over time. As PSA is regulated *via* *AR* signalling this suggests in general, the common ongoing involvement of *AR* signalling in disease progression to mCRPC [29-32]. Abiraterone [33, 34] and enzalutamide [35, 36] have been developed to be used for mCRPC, as ‘second generation’ ADT treatments, and responses are generally good, but a median progression – free survival of 5.6 months [33] suggests resistance to treatment once again supervenes. Indeed, despite the difference in mechanisms of action, cross-resistance between enzalutamide and abiraterone is very common [33, 37-39], suggesting the development of true hormone resistance following second line ADT therapy, as opposed to castrate-resistance. Thus, androgen signalling through *AR* within the

context of the oncogenic effect of other signalling pathways, remains an important area of research. There are, as yet no effective treatments or markers for true hormone resistance. This study explores the involvement of two critical signalling pathways, the phosphatidylinositol-3-kinase/AKT (PI3K/AKT) and Hippo/YAP pathway, which interact with the AR pathway in mCRPC and which have links to epithelial to mesenchymal transition (EMT). EMT is thought to play an important role in the development of both metastasis and therapy resistance [40, 41]. A special focus of this project is the AR variant 7 (AR-V7), a transcriptional variant that has been associated with and may be a cause of mCRPC [21, 22]. Indeed, the presence of AR-V7 may differently affect the interplay of the PI3K/AKT and the Hippo/YAP pathway and EMT regulation in PCa. The data generated in this project initiate a path to analyse AR, AR-V7 and the PI3K/AKT and the Hippo/YAP pathway in circulating tumour cells (CTCs) derived from PCa patient liquid biopsies.

CTCs are cells that dislodge from tumour tissue and enter the blood stream. In blood, CTC number is small relative to number of blood cells. CTCs express tumour markers that allow the differentiation of different stages of cancer. In addition, CTCs are identifiable by their physical properties such as their size is generally larger than blood cells. CTC isolation and characterization may help in better treatment selection because AR-V7 expression in CTCs might be associated with resistance to second generation anti-androgens in mCRPC [42-44]. Antonarakis *et al.* found a correlation between the expression of AR-V7 in CTCs, decreased PSA response rates, shorter progression free survival and overall survival in mCRPC patients treated with enzalutamide or abiraterone [45].

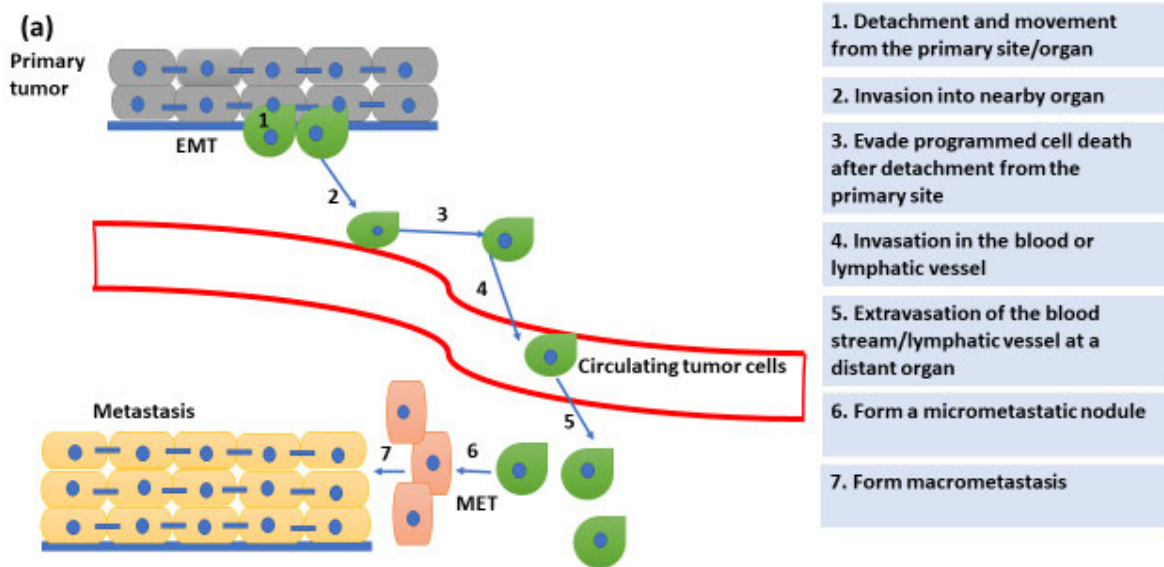
1.2 Circulating Tumour Cells and EMT in Metastasis

In solid tumours including PCa, tissue biopsy, while used for diagnosis and staging, is rarely available for ongoing analysis of the disease. The challenges in the management of PCa

includes but is not limited to, heterogenous signalling mechanisms, limitation of tissue biopsies and limited biomarkers to guide treatment of PCa. In the case of the latter, CTCs are used as tumour biopsy surrogates, through liquid biopsy [46-48]. While CTCs are generally rare in early disease, recent technologies allow us to enrich CTCs from the billions of other cells in a blood sample [49, 50], which allows detailed analysis for genetic and proteomic characteristics that can be used as biomarkers to monitor disease and importantly guide best treatment options. CTCs from various solid cancers have been successfully analysed for cancer associated mutations, gene expression, amplifications, protein expression and phenotype [51-53]. Moreover, CTCs are thought to “get a ride” to distant organs *via* the circulation, enabling distant cancer metastases to be established [54]. Several methods have been used for the detection and isolation of CTCs [55].

At the cellular level, metastasis involves a sequence of steps, and current evidence suggests that EMT as well as the reverse process mesenchymal to epithelial transition (MET) (reviewed by [56]) are important mechanisms by which tumour cells migrate and re-establish themselves at distant sites. Cancer cells are believed to lose their tight adhesion to neighbouring cells and become more mobile when undergoing EMT, which in turn, favours their ability to shed from the tumour mass, intravasate into the blood stream and thus become CTCs. MET on the other hand is thought to aid CTCs after leaving the vascular system to be able to settle in other tissue and form new tumours [54, 57] (Figure 1.2). Thus, CTC counts in the bloodstream have been recognized as a marker of metastatic disease, and importantly, EMT markers have been found in patient CTCs including those with PCa. For instance, of 54 patients, 53% of whom had advanced metastatic disease, intermittent epithelial to mesenchymal phenotype of CTCs correlated with metastasis in these patients, while another study found that the mesenchymal CTC phenotype correlated with increased rates of progression to CRPC in a cohort of 108 PCa

patients recruited with high volume metastatic disease whilst hormone sensitive, and longitudinally followed during the study [58-60].



(b)

Environmental factors	Signaling molecules	Signaling cascades	Transcription regulators/co-activators
Hypoxia Radiation	EGF, Hedgehog, Wnt, FGF, Notch, TGF- β , HGF, FGF,	Notch, NF-KB, Hippo , MAPK, AKT , Wnt/ β - catenin, AR	ZEB1, TCF4, YAP1 , Snail 1, Twist, FOXC2 and Snail 2

(c)

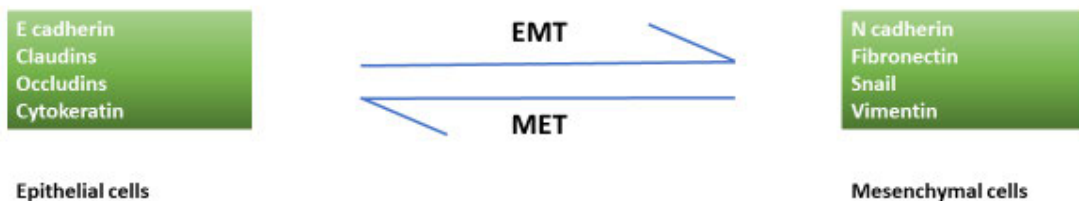


Figure 1. 2 EMT in Cancer Metastasis

(a) Schematic representation of the role of EMT in cancer metastasis, (b) A cascade of transcriptional regulation underlies the transition from an epithelial to mesenchymal phenotype, (c) During EMT, epithelial markers are downregulated while mesenchymal markers are upregulated.

Metastatic spread of cancer is thought to involve different stages (Figure 1.2a) in which cancer cells (i) lose cell-cell tight junctions and detach from the primary site/organ, (ii) penetrate the basal lamina and enter nearby tissue, (iii) evade programmed cell death normally induced by loss of substrate adhesion (anoikis), (iv) breach blood or lymphatic vessels and migrate to other sites *via* blood/lymphatic circulation, (v) leave the blood stream or lymphatic vessels at distant organs (vi) form a micro-metastatic core and finally (vii) adjust and reprogram the surrounding stroma to form detectable macro-metastases [61]. At a molecular level, EMT has been studied in various cancers, including PCa. In the development of mCRPC, it has been proposed that activation of transcription factors (TFs) results in the loss of epithelial properties and acquisition of mesenchymal characteristics as well as the change of cell shape-change, leading to enhanced invasion and increased mortality [62, 63].

EMT is inducible by environmental factors such as radiation or hypoxia (Figure 1.2b) and there is accumulating evidence that radiation or chemotherapy, used to treat earlier stage PCa, may induce EMT changes [64, 65]. Hypoxia induces the production of hypoxia-inducible factor (HIF), and HIF-1 α stimulates transcription factors (TF's), such as Snail and Twist, to trigger EMT [66, 67]. EMT then results from activation of a mesenchymal transcriptional program induced by specific transcription factors (EMT-TF's) [64]. Mechanistically, central EMT- TF's ZEB1, Snail, Slug, Twist, along with other TFs such as TCF4 and FOXC2 suppress the expression of key epithelial markers such as cytokeratin, E-cadherin, occludin and claudin while causing upregulation of mesenchymal markers such as N-cadherin, fibronectin, and vimentin, which enable cancer cells to be more motile and consequently more aggressive (Figure 1.2c).

Regulation by signalling cascades and signalling molecules including EGF, Hedgehog, Wnt, FGF, Notch, TGF- β and HGF in turn, induce signalling *via* NF- κ B, MAPK, PI3K/AKT, or Wnt/ β -catenin pathways to regulate EMT-TFs and ultimately induce EMT phenotypic changes.

More recently the Hippo-pathway has been implicated in regulating EMT *via* its down-stream transcriptional modulator Yes associated protein (YAP) and the transcriptional coactivator TAZ [66, 68-76]. Importantly, there is evidence in the literature that these pathways can be successfully analysed in CTCs even though in some cases these analyses may not have yet been reported for PCa CTCs. Table 1.1 summarises key evidence implicating signalling pathways in PCa EMT as well as the analysis of these pathways, available mainly from other cancers, in CTCs. Nevertheless, this analysis indicates pathways where examination in PCa CTCs may be warranted.

Table 1. 1 Signalling Pathways implicated in EMT and relevance to PCa

Pathway	Implication in cancer-related EMT	Roles in PCa	CTC analysis
AR	Opposing data: Elevation of AR expression and AR signalling in prostate tumours promotes PCa metastasis by induction of EMT [77], other data suggest AR reverses EMT and ADT can induce EMT [78, 79]	Cell proliferation and tumour progression [80, 81]	Different AR expression patterns, amplification, mutation and variant expression in PCa CTC [51, 82-84]
AKT	PI3K-AKT directly or in crosstalk with other signalling pathways can induce EMT [85, 86]. Drugs inhibiting EMT <i>via</i> the AKT/GSK-3 β /Snail pathway, decrease the invasiveness of PCa cells [87]	Implicated in PCa cell proliferation and resistance to apoptosis [88, 89]	Phosphorylated EGFR and PI3K/AKT signalling kinases detected in breast cancer patient CTCs [90], pERK/AKT pathway in CTCs in hepatocellular carcinoma patients [91], PTEN loss in circulating tumour cells in CRPC patients [92]. No report in PCa CTCs.

Hippo	Deregulation of the Hippo pathway contributes to EMT in colorectal cancer [93], FZD2 could promote clinically relevant EMT in hepatocellular carcinoma involving Hippo pathway [94]	Emerging roles in PCa development, progression, EMT and mCRPC [95, 96]	TAZ expression detected in NSCLC CTCs [97], YAP association with metastasis in human gastric cancer [98]. No report in PCa CTCs.
MAPK	MAPK mediates epithelial to mesenchymal transition in cooperation with TGF- β / Smad2 signalling and increased Snail, Twist expression [99, 100] [101]	Linked to proliferation, early relapse and development of mCRPC [102, 103]	MAPK gene expression signature shown in pancreatic CTCs [104], detection of mutant RAS and RAF in CRC and in melanoma CTCs [105, 106]. No report in PCa CTCs.
NF-κB	Hypoxia or overexpression of HIF-1 α induces the EMT <i>via</i> NF- κ B in pancreatic cancer cells [107] and inhibition of NF- κ B deregulates EMT [108]	Promotes PCa cell survival, tumour invasion, metastasis and chemoresistance [109, 110]	NSCLC- CTC gene expression profile was associated with cellular movement, cell adhesion and differentiation, and cell-to-cell signalling

			linked to PI3K/AKT, ERK1/2 and NF- κ B pathways [111]. No report in PCa CTCs.
JAK / STAT	IFN γ can induce epithelial to mesenchymal transition (EMT) in PCa cells <i>via</i> the JAK–STAT signalling pathway [112], STAT3 may directly mediate EMT progression and regulate ZEB1 expression in CRC [113]	PCa progression, cell proliferation and inhibition of apoptosis [88, 89]	No direct analysis of these pathways in CTCs.
Wnt/β-Catenin	Dysregulation of Wnt/ β -catenin signalling have been implicated in the development of cancer in different tissues like lung, skin, liver and prostate [89], <i>via</i> regulating Zeb1 in CRC [114]	Wnt/ β -catenin pathway promotes the metastatic spread of PCa cells by inducing EMT [115]	Epithelial type CTCs and activation of Wnt/ β -catenin signalling in lung cancer cells [116]. No report in PCa CTCs.
Notch	Crosstalk between the Jagged1/Notch and	Notch signalling results in prostate	Increased production of ROS results in the

JAK/STAT3 signalling pathways by promoting EMT through Jagged-1 in ovarian cancer [117]	tumour recurrence <i>via</i> EMT [118]	upregulation of Notch1 in CTCs in metastatic breast and melanoma cancer [119]. No report in PCa CTCs.
---	--	--

1.3 Clinical Relevance of EMT Markers in PCa

Several studies have assessed EMT markers for their clinical importance at various stages of human PCa. Table 1.2 shows typical EMT markers detected in PCa tissue. A possible clinical utility of these EMT markers at different phases of the disease is suggested by their prognostic correlation with both recurrence-free and overall survival. For example, the presence of EMT markers Twist and vimentin as measured by immunohistochemistry in radical prostatectomy samples - are independent markers for biochemical recurrence as defined by a resurgence in serum prostate-specific antigen (PSA) levels post-surgery [120, 121]. A recent study found that Cathepsin L (Cat L), which is an EMT-associated target of the EMT-TF Snail may be a biomarker of PCa progression [122]. In addition, loss of membrane-bound E-cadherin staining appears to be linked with higher Gleason score, advanced clinical stage, and poor prognosis in PCa [123]. EMT markers like Zeb1, E-cadherin and vimentin play important roles at different stages of disease progression from primary tumour stage 2 to CRPC. In CRPC, increased expression of Zeb1 correlated with decreased survival [120]. Further, in a study of 108 patients with newly diagnosed castrate sensitive PCa, expression of mesenchymal markers in CTCs at baseline was found to be an independent prognostic factor that was predictive of time to progression to CRPC following standard ADT. Patients who had mesenchymal CTCs at baseline showed a significantly shorter time to progression to CRPC than patients without CTCs or patients whose CTCs were negative for mesenchymal markers [59]. Several studies show that E-cadherin suppresses invasion and metastasis *in vitro* and consistent with these findings, E-cadherin staining in tumour tissue correlates with longer overall survival [120]. However, the relationship of E-cadherin to metastasis is not clear in all cases since, in a recent study, it has been shown that loss of E-cadherin reduced metastatic potential in invasive ductal carcinomas [124], suggesting that E-cadherin plays opposing roles in tumour progression by suppressing cancer cell invasion while promoting metastasis. Nonetheless, on balance, the data

suggest that EMT markers may have predictive value with respect to recurrence and overall survival both in tissues and in CTCs [120]. Different studies show that E-cadherin suppresses invasion and metastasis. However, in a recent study it has been shown that loss of E-cadherin reduced metastatic potential in invasive ductal carcinomas [124].

Table 1. 2 EMT markers detected in PCa tissue

Epithelial markers	Mesenchymal markers
	Snail, Cat L [122]
E-cadherin [120]	Vimentin, N-cadherin [120]
Cytokeratin[125]	Vimentin [125]
	Twist [126, 127]
E-cadherin[128]	N-cadherin [128]
E-cadherin, Cytokeratin [129]	

1.4 AR, ADT, EMT and Drug Resistance

There is no clear consensus with respect to the role of androgen signalling in the regulation of EMT. An early study using cell lines showed that androgen stimulation promoted EMT in both LNCaP and PC-3 cells but that there was an inverse relationship between AR receptor levels and androgen-mediated EMT marker expression and EMT-associated cytoskeletal changes. The use of shRNA to reduce AR levels, promoted PCa cell metastatic ability by inducing EMT while high AR levels did not [130]. In contrast, a recent study has shown that AR mRNA and protein expression is higher in metastatic tumour tissues than in primary tumours and increases with tumour stage and Gleason score. Patients with higher AR expression showed shorter recurrence-free survival, indicating a positive association between AR expression and tumour progression. Further, knockdown of AR using siRNA in C4-2B cells, suppressed functional markers of EMT, *viz* cell migration and invasion and mesenchymal marker proteins associated with EMT, while increasing the epithelial marker E-cadherin. These effects were recapitulated by treatment with the antiandrogen bicalutamide [77]. Thus, it appears that AR stimulation induces or suppresses EMT in cell culture in a cell-type dependent fashion. More work is needed to clarify how AR affects EMT in such a context-specific manner.

Studies with both normal mouse prostate and human prostate tumour models in mice have shown that androgen deprivation through surgical castration, while suppressing tumour growth, induces EMT mesenchymal markers and markers of a stem cell phenotype, while suppressing epithelial markers. These changes were also seen in tissues of patients treated with ADT [131], supporting the view that AR signalling suppresses EMT, while ADT promotes it.

In further support of this view, ADT with enzalutamide in C4-2 cells (a clonal cell line derived from parental LNCaP cells), but not in PC-3 cells, induced EMT markers in a Snail-dependent fashion. Induction of EMT required both suppression of AR signalling and activation of Snail.

Interestingly, Snail was downregulated by androgen in AR-expressing C4-2 and VCaP cells but again, not in PC-3 cells. Importantly the inverse correlation between AR signalling and Snail expression observed in C4-2 xenografts, castration-resistant patient-derived metastases in mice and in clinical samples supports the view that the induction of EMT is an adaptive response to ADT with enzalutamide [78]. ADT may favour acquisition of stem cell and EMT characteristics, expression of oncogenes or suppression of tumour suppressor genes in AR-positive PCa cells, implying that mCRPC at least in part is achieved through EMT [79, 131-135].

Other data suggests that AR splice variants are involved in the development of drug resistance in PCa [21, 136-138]. One corollary of this hypothesis is that inhibition of the AR variants or their specific function might lead to reversal of EMT phenotype and that might in turn inhibit tumour spread [79, 139]. Overall, however, this area remains understudied, and more data are needed to fully understand how the AR pathway and its manipulation during therapy may regulate EMT and potentially, as a result, regulate metastasis. Since mCRPC is ultimately the principal cause of death in many patients, the fundamental biological processes for the development and establishment of mCRPC need to be understood [140]. It is noteworthy that there is now mounting evidence in CTCs that the expression of EMT markers is associated with mCRPC [141, 142], highlighting the potential benefit in the analysis of CTCs to address the role of AR in metastasis and drug resistance.

1.5 AKT Pathway in mCRPC

As indicated above, due to the hormone-independent nature of mCRPC, it is unresponsive to all current forms of ADT. At this stage AR expression may even be completely lost [143-145], raising the question as to how survival and proliferation of PCa cells occurs. The main oncogenic signalling pathway implicated at this juncture, is the PI3K/AKT-pathway,

predominantly activated through frequent functional loss of the inhibitory tumour suppressor phosphatase and tensin homolog (PTEN), which is less common in localised PCa (20-30%) but becomes more dominant and is found in up to 50-60% of mCRPCs. The result is uncontrolled, oncogenic AKT signalling (reviewed by [146, 147]). The PI3K/AKT and AR pathways are highly networked with both positive and negative feedback loops [146] and in mCRPC, current literature indicates that negative feedback dominates. That is, inhibition of one pathway leads to reciprocal activation of the other [148-151]. Carver and colleagues have elucidated part of this interaction, demonstrating that the AR reduces AKT activation through the intermediary PHLPP, while AKT can transcriptionally down-regulate AR output *via* HER kinase activity [148]. The exact role of PTEN in mediating this interaction is controversial. On one hand PTEN deletion has been associated with AKT activation and reduced AR levels [149, 152], on the other hand it may independently increase AR gene expression by removing transcriptional repression [151, 153-155]. Given the interconnected signalling network, outcomes of AR and AKT signalling, or silencing may affect overall outcomes in a context-specific fashion, which is likely dependent on the presence and activity of other proteins that can affect the balance of feedback loops. For example, it has been shown that AR can transcriptionally repress PTEN expression in PCa cells while it increases PTEN expression in breast cancer cells and the report suggested this may be due to tissue dependent availability of transcriptional co-factors [156]. Moreover, ADT may also affect the balance in these interconnected signalling pathways. Importantly, loss of *PTEN* has been associated with EMT driven through the AKT pathway or in cooperation with RAS signalling, thereby lack of PTEN function could promote metastasis [157, 158].

1.6 Hippo Signalling Pathway and Its Role in CRPC and EMT

As indicated above, several signalling pathways may contribute to the induction of EMT and ultimately metastasis, with the AKT pathway of importance in the context of PCa. More recently the YAP1 transcriptional co-activator regulated by the Hippo-pathway has emerged as an important player in this scenario and in regulating PCa cell motility [159]. In the context of gastric cancer PTEN inactivation has been proposed to link the Hippo and PI3K/AKT pathways to promote cancer development and tumorigenesis [160]. In normal tissue, the Hippo signalling pathway appears central to cell growth control and limits organ size by coordinating cell proliferation, growth and death [161]. Different signals like cell polarity, cell-cell contact, extracellular matrix characteristics and stress can result in the activation of the Hippo pathway (reviewed in [162]). Hippo signalling through a kinase-cascade results in phosphorylation of oncogenic co-transcription factors known as YAP and TAZ, promoting their cytoplasmic retention and proteasomal degradation [163-165] (Figure 1.3).

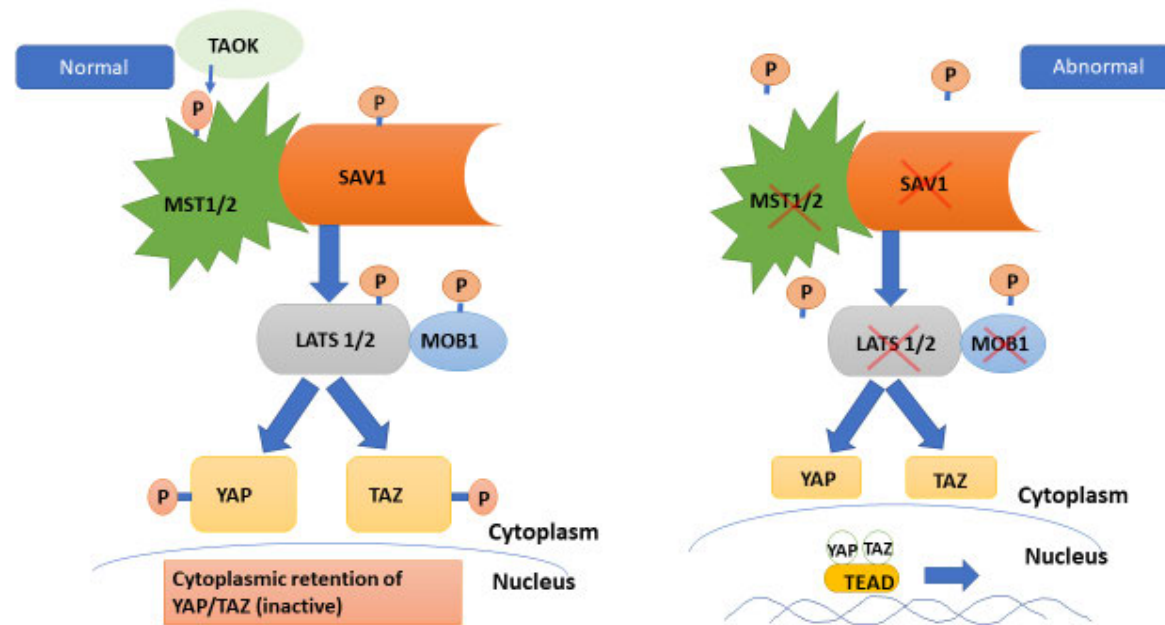


Figure 1. 3 Hippo signalling pathway

Active Hippo signalling represses YAP and TAZ *via* phosphorylation (left), while inactive Hippo leads to dephosphorylation, nuclear translocation and thus activation of TFs (right).

Inactivation of the Hippo pathway allows for YAP and TAZ activation *via* dephosphorylation, which is required for translocation into the nucleus. Although TAZ and YAP lack intrinsic DNA-binding domains, they are recruited by and enhance the activity of other TFs at their target promoters [166, 167]. Nuclear YAP results in castration resistance and metastasis [168].

Hippo signalling can act as a tumour suppressor. Functional impairment of Hippo signalling is often due to the loss of MST1/2 or LATS1/2 function or due to *YAP1* gene amplification. YAP1 is the most studied YAP isoform and aberrant YAP1 activation is associated with the etiology of various malignancies including stomach [169] thyroid [170], lung [171], colon [172], head and neck [173] ovarian [174], liver [175] and PCa [176].

Most interestingly, YAP1 and AR directly interact in PCa cells. One study demonstrates that unlike in hormone sensitive PCa cells, YAP1-AR interactions are androgen insensitive and may cause resistance to enzalutamide in mCRPC cells. The WW/SH3 domain of YAP1 most likely facilitates the interaction with the AR amino terminal domain (NTD) [177].

One study proposes that increased nuclear YAP1, possibly due to the loss of Hippo signalling, may lead to increased complex formation between AR and YAP1 leading to androgen-independent binding of the complex to AREs located in AR-driven promoters resulting in aberrant AR target gene expression possibly promoting mCRPC [95].

Importantly, YAP has been shown to promote metastasis through several mechanisms including EMT, and there is some evidence that the PTEN - AKT axis is involved in YAP1 induced EMT [166, 178, 179]. The underlying mechanisms of EMT regulation by YAP are still emerging but given the role of YAP as a transcriptional co-regulator it is not surprising that the pathways centrally involve EMT-TFs. Critically, YAP1 has been shown to network with the main EMT-TFs. For instance, high glucose-induced polyubiquitination of PTEN results in alteration of its phosphatase targets, including an increased focus on

dephosphorylation and activation of EMT regulators like Twist, Snail and YAP1 [180]. YAP1 was also reported to drive EMT and likely NSCLC metastasis by TEAD dependent transcriptional induction of *SLUG* [181]. Focusing on YAP's role in osteoblast differentiation one study identified two links between YAP and Snail/Slug. In Snail/Slug-null skeletal stem/stromal cells the levels of both YAP and TAZ were reduced *via* protein degradation due to activation of the Hippo pathway, while direct interaction of YAP with Snail and with Slug was shown to alter YAP/TEAD transcriptional activity [182]. Another study found that Twist-induced EMT in breast cancer cells is dependent on TAZ activity. The mechanism involved increased expression of the Hippo pathway inhibitors PAR-1 and PAR-3, which drive TAZ nuclear localisation. One would expect that YAP nuclear localisation may also be induced *via* PAR-1/-3 in this context, although this was not examined [183]. Another study revealed that increased extracellular matrix stiffness can induce EMT in breast cancer cells and that blocking β 1-integrin-mediated matrix stiffness prevented both Twist and YAP nuclear translocation albeit, interestingly, by different mechanisms [184].

In epithelial cells, cells are connected to each other by membrane structures called tight junctions, adherens junctions and desmosomes. Any dysregulation in these junctions is implicated in metastasis and EMT [185, 186]. Zona occludens-1 (ZO-1) is a tight junction protein that is present in normal epithelial cells. Though not yet studied in PCa, in melanoma, lung cancer cells and breast cancer, ZO-1 expression correlates with the invasive properties of cancer cells [187-189]. One study found that YAP overexpression resulted in downregulation of ZO-1 and induced metastasis through EMT in NSCLC [181].

YAP (but not TAZ) has been shown to interact directly with ZEB1 and remarkably, this interaction turns this transcriptional repressor into an activator. This is highlighted by the fact that ZEB1-mediated *CDHI* (E-cadherin) repression is independent of YAP binding. Critically, gene upregulation by the ZEB1-YAP complex correlated with gene expression signatures of

claudin-low breast cancer, a breast cancer subtype overall exhibiting an EMT phenotype. More importantly ZEB1-YAP complex-mediated gene expression was related to poor patient survival in hormone-independent breast cancers and linked to drug resistance and metastasis [190]. ZEB1 is known to repress several EMT-related miRNAs including miR375, which is associated with an epithelial phenotype. Nevertheless, miR375, a known YAP target, is commonly over expressed in PCa and in fact has been indicated as a plasma marker of PCa. The suggested mechanism by which miR375 supports an epithelial phenotype is *via* feedback regulation, such that it targets and suppresses YAP transcript and thus YAP protein levels and thereby reversing EMT in PCa cells. Surprisingly however, high plasma miR375 level were associated with CTC positivity [191], suggesting that further investigations are needed to understand the complex network between YAP, ZEB1, miR375, EMT and CTC formation. Additionally, hypoxia may, at least in part, induce EMT by stabilizing YAP and its nuclear translocation in PCa cell lines [192].

Not surprisingly, another study showed that inhibiting a key characteristic of epithelial tissue, namely E-cadherin-mediated cell-cell interaction, resulted in EMT and increased dissemination of Madin-Darby canine kidney cells. Interestingly, dissemination could be partially prevented by YAP knock-down. The same study found that not only is YAP required to allow nuclear entry of the MET initiating Wilms Tumour protein 1 (WT1), but both WT1 and YAP form a complex at the *CDHI* (E-cadherin) promoter and repress its transcription. These data, together with confirmation that E-cadherin inhibition upregulates YAP levels, indicates double-negative feedback where E-cadherin and YAP mutually inhibit each other. This may be part of a switch between EMT and MET, thus potentially explaining the plasticity of the EMT process [193].

1.7 YAP Cross Talk with AR and AKT Pathways

One possible mechanism for PTEN loss of function is mediated by YAP. The pathway involves nuclear YAP-mediated activation of the TEAD family of transcription factors, leading to synthesis of the PTEN transcriptional repressor miRNA29c. Conversely, when YAP is inactivated *via* phosphorylation PTEN levels are restored and the oncogenic function of YAP is inhibited [194]. Moreover, as mentioned above, PTEN ubiquitination can dephosphorylate and thus activate YAP causing its nuclear accumulation indicating a possible positive feedback regulation [180].

On the other hand, PTEN was identified as a negative regulator of AR activity such that the AR/PTEN interaction may mediate a tumour suppressor role for PTEN *via* suppression of AR and apoptosis induction in PCa cells [195]. However, as outlined above, the PTEN and AR network is still poorly understood, and data are conflicting. This is exemplified by another study with opposing findings, wherein PTEN deletion reduces both AR expression and AR transcriptional activity in PCa [152].

Taken together, emerging evidence indicates that YAP is part of the complex functional network that connects the AR and AKT pathways and thereby modulates PCa and mCRPC - at least in part - *via* EMT (Figure 1.4). However, more work is needed to better understand this interplay and its implications for the development of strategies to treat advanced PCa.

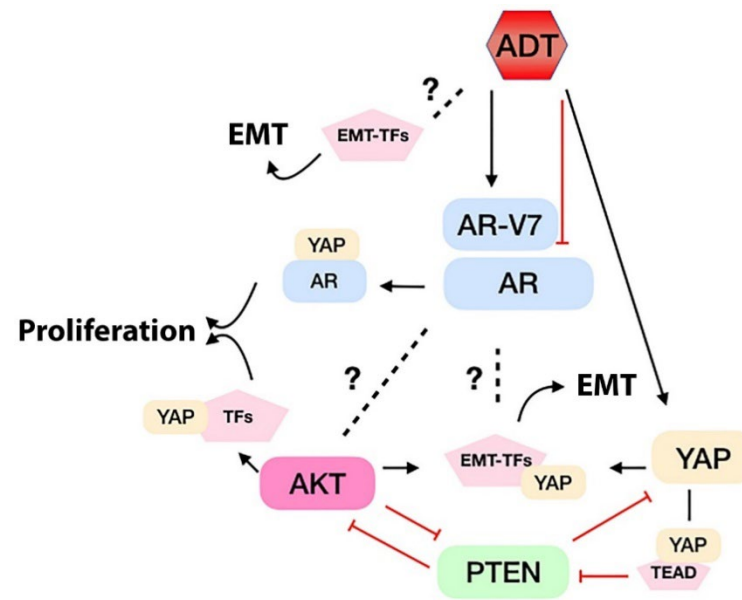


Figure 1. 4 AR AKT and YAP interaction

Schematic presentation of reported and likely (dotted lines) network connections between ADT, AR, AKT and YAP.

1.8 Analysis of PCa CTCs to Explore the AR-AKT-YAP Connection and EMT

The evaluation of molecular pathways underlying mCRPC is challenging because tissue biopsies are generally not available from late disease stages and animal models; further, although examination of tissue can provide some signalling pathway information, this mode of studying PCa has limitations. Liquid biopsies, and analysis of mCRPC CTCs, may be an alternative. While diagnostic CTC analysis in PCa is still in its infancy, there is ample evidence of its utility in this disease. Certainly, CTCs have been investigated by imaging and molecular technologies for expression of proteins, gene amplifications, mutations and transcript expression on both targeted and comprehensive levels [196]. For PCa, increased CTC counts are associated with earlier disease progression and shorter OS, with enumeration of PCa CTCs using the CellSearch CTC platform gaining FDA approval as a prognostic indicator [197]. While common CTC isolation and analysis techniques favour epithelial CTCs, there have been numerous advances in improving capture, detection and analysis of EMT-CTCs by screening for epithelial and mesenchymal marker expression [198-203]. Equally, as Table 1.1 shows, several major signalling pathways implicated in EMT have, to some extent, been analysed in CTC samples. This project focusses on the AR, AKT and Hippo pathways as being central to mCRPC, at least in part *via* EMT regulation. It is important to consider how these pathways have been explored in CTCs, in order to gauge the potential for CTC analysis to advance our understanding of these pathways in mCRPC. Accordingly, we note that DNA-, RNA- and protein-centric analyses for AR and AR-V7 levels in isolated CTCs has become a busy field of PCa research. In the US, epic sciences is a commercially available test for identification of AR-V7 in CTCs and its localisation in single CTCs [42]. Moreover, efforts are being made to translate CTC-based AR and AR-V7 detection into clinical settings aimed initially at stratifying

patients to define either eligibility criteria or outcome markers for clinical trials (<https://clinicaltrials.gov>) [204].

mCRPC associated AR amplification and mutation analysis has been performed in CTCs using hybridisation techniques such as fluorescent *in-situ* hybridization (FISH) and other molecular approaches. In general, these studies were able to validate association of CTC-based AR amplification or mutation with mCRPC, while the relevance of AR cellular localisation in CTCs was shown in mCRPC and in response to taxanes [52, 83, 84, 205-208]. The presence of full-length AR and AR-V7 in CTCs has been studied extensively at the RNA level and CTC-based AR-V7 in particular was found to correlate with mCRPC and primary resistance to abiraterone and enzalutamide [45, 51, 204, 206, 209]. There have also been efforts at detecting both AR and AR-V7 as biomarkers in other liquid biopsy entities, including plasma-derived circulating tumour RNA (ctRNA), exosomes or even in urine. We recently compared some of these strategies and found both AR full length and V7 RNA detection is more sensitive and specific if performed on CTC samples, as compared to ctRNA or exosomes [210]. Our lab also demonstrated that AR-V7 is detectable from CTC-RNA up to 48 hrs post blood draw into common EDTA vacutubes [211]. With improved AR-V7-specific antibody availability, CTC immunocytostaining more recently provided evidence that specific detection of AR-V7 in CTC nuclei may be an even better predictor of overall survival (OS) and progression free survival (PFS) in CRPC patients [42, 43]. Different studies were conducted to study the prognostic and predictive value of AR-V7 in PCa patients. AR-V7 in CTCs was associated with worse OS and PFS [45]. Wang *et al.* showed that AR-V7 positive patients do not respond well to ARS compared to AR-V7 negative patients. Taxane treatment is a better option for AR-V7 positive patients [212]. Thus, the detection of AR-V7 before treatment may assist the selection of the best treatment option.

In general, it appears nuclear AR-V7 is found in most CTCs positive for AR-V7 RNA, reflecting the predominant tendency for AR-V7 to be nuclear localised in mCRPC tissue [209, 213]. In CRPC patients, AR-V7 positive CTCs have been shown to correlate with enzalutamide and abiraterone resistance [45]. In any case, when investigating the interplay of AR/AR-V7 with other pathways, especially transcriptional co-activators, immunocyto-detection in CTCs appears to be the most logical strategy. In particular, high resolution immunodetection of AR-V7 in CTCs may also open opportunities to investigate colocalisation with other proteins or cellular structures and this capability may help refine the utility of AR-V7 as an important CRPC biomarker.

Several studies have also analysed PTEN loss in CTCs, which as outlined above, may allow oncogenic activation of the AKT pathway and is an important PCa biomarker. Loss of *PTEN* and gain of *AR* copy numbers was reported in PCa CTCs [214-216], while testing for activation of the AKT pathway has been performed for example by phospho-AKT or phospho-S6 kinase immunostaining in breast cancer CTCs [217].

Reports on hippo signalling and YAP1 analysis in CTCs, by contrast, are still scarce. One study assessed expression of TAZ using RNA in situ hybridization (RNAish) probing of NSCLC CTCs. TAZ expression was detected more frequently in EGFR wild type cancers while its expression in CTCs was associated with lymph node status of the disease [97]. It is likely that YAP1 could be analysed in a similar fashion in CTCs or preferentially using immunocytostaining, as the latter would also reveal cellular localisation and thus activity as well as co-localisation with other proteins. However, to our knowledge direct detection of YAP1 in CTCs has not yet been reported, although the relationship of YAP1 to EMT suggests that activated YAP1 should correlate with increased formation of CTCs. Some indirect evidence lends further strength to this idea, as a recent report showed that the Rho GTPase activating protein 29 (ARHGAP29) is a transcriptional target of YAP1 in gastric cancer. High

ARHGAP29 levels were shown to regulate cytoskeletal actin and cell migration. Importantly, the authors also demonstrated using a mouse model that CTCs exhibited increased ARHGAP29 RNA levels compared with primary tumour site cells [98, 218]. Final proof of a YAP1-ARHGAP29 connection in CTCs remains pending, however. Another transcriptional target of YAP is miR375 which was associated with CTC positivity, yet a direct connection could not be shown in CTCs [191].

Taken together, the reviewed data suggest that AR-AKT-YAP1 network can be analysed in CTCs. Since tumour tissue is rarely available in the mCRPC setting, whereas blood samples can be easily taken, future endeavours in CTC analysis could open the way to better understand ADT resistance and thereby inform the development of improved diagnostic, prognostic and therapeutic capabilities.

1.9 CTC Enrichment and Analysis Strategies

Analysis of CTCs has provided a foundation for liquid biopsy, especially in the absence of biopsy tissue. However, there are serious challenges with CTC isolation, detection and downstream analysis. One is that CTC numbers are relatively small within large populations of blood cells and the volume of blood that can be taken depends on the patient's general condition. CTCs are quite heterogenous in terms of physical properties (size, elasticity, surface charge), biological characteristics and expression of different tumour markers making enrichment or isolation of all CTCs difficult (reviewed by [219]). Various methods to enrich, detect and analyse CTCs have been developed. In general CTCs are isolated according to their physical properties such as larger size than most blood cells and differences in plasticity or more commonly CTC cell surface markers are immuno-targeted by magnetic beads or other techniques. CTC enrichment methods might include density dependent isolation, size-based isolation and positive selection or blood cell depletion using immunomagnetic beads. Most

commonly the cell surface marker EpCAM is targeted to capture CTCs. Apart from single cell picking or compartmentalisation most methods will lead to an CTC enriched sample containing CTCs and hundreds to thousands of residual blood cells and additional analysis helps to distinguish CTCs. Immunostaining to exclude cells expressing the CD45 lymphocyte marker and positive detection of CTCs using for example cytokeratin staining is common. Specific cancer markers can also be stained for such as AR or prostate specific membrane antigen (PSMA) as a marker for PCa CTC detection (reviewed by [220]).

In general, the low CTC counts make down-stream analysis of CTCs another challenge and the main method of CTC isolation is positive selection of cells that express the cell surface marker and epithelial protein EpCAM [55]. Given CTC heterogeneity and the downregulation of EpCAM during EMT, which in turn is implicated in CTC formation as outlined above, unbiased CTC enrichment using depletion of lymphocytes [221] may result in a more complete representation of heterogeneity in CTC enriched samples. Moreover, protein detection in CTCs is usually based on immunocytostaining which relies on antibody-based detection limited to the number of microscope channels available with 3 usually dedicated to detection of a CTC marker (often cytokeratin), a nuclear marker such as DAPI or Hoechst and exclusion of a blood cell marker usually CD45. Nevertheless, some studies have detected additional proteins such as EMT markers [59, 60, 198] or post translational modifications such as phosphorylation of pFAK, pPI3K, pSRC, pEGFR and pAKT [90, 222-225].

This project planned to generate the foundations for a new technology of extensive multiplex immunostaining of CTCs to overcome the technical limitation of detecting insufficient markers using immunocytostaining by traditional methods. In brief, this method relies on a semi-automated workflow that allows for cells to be stained for various markers using immunofluorescence and then imaged, followed by elution of the first staining cycle antibodies and re-staining and re-imaging of the same cells for a suite of new antigens in cycle 2 and

subsequent staining cycles. A sophisticated artificial intelligence-based machine learning analysis pipeline can then be used to correlate high resolution cellular and subcellular staining with patient data. Adaptation of this single cell analysis method to CTCs is part of this project.

1.10 Hypothesis

The overarching hypothesis of this PhD project is that PCa patient CTCs can be analysed using a multiplex staining approach for single cells.

1.11 Aims

Embedded in this overall hypothesis and in order to lay important foundations to enable testing it in future, this PhD project addressed the following aims:

Aim 1: To systematically review and perform meta-analysis on the clinical relevance of liquid biopsy detection of the known CRPC biomarker AR-V7.

Aim 2: To determine the best anti-AR-V7 antibody to reliably detect AR-V7 in CTCs.

Aim 3: To optimise a range of methods as a prerequisite and preparation for the use of multiplex immunofluorescence to analyse AR, AR-V7, AKT and Hippo pathway components, as well as markers for EMT using both cultured cells and CTCs.

Chapter 2: Material and Methods

2.1 Chemicals and Research Consumables

All chemicals used in this study were analytical grade. Chemicals and consumables used, together with suppliers are listed below:

96-well plate (Greiner-Bio-One, Frickenhausen, Germany)

BioRad DC protein quantification kit (Bio-Rad Laboratories, Hercules, CA)

Bovine Serum Albumin (BSA) (Sigma-Aldrich, Castle Hill, Australia)

Cell scraper (Sigma-Aldrich)

Cell tracker (Invitrogen, Life Technologies)

Coverslips 13 mm (Menzel-Glaser, Braunschweig, Germany)

Cryovials (Interpath, Melbourne, Australia)

Dimethyl sulfoxide (DMSO; Sigma-Aldrich)

Dulbecco's modified eagle medium (DMEM; Lonza, Basel, Switzerland)

EDTA vacutubes (Greiner-Bio-One)

Ethanol 100% (Sigma-Aldrich)

Ethylenediaminetetraacetic acid (EDTA; Sigma-Aldrich)

Falcon tubes (50 mL, 15 mL; ThermoFisher, Scoresby, Australia)

Foetal bovine serum (FBS; Interpath, Melbourne, Australia)

Formaldehyde (VMR International, Tingalpa, Australia)

Goat serum (Sigma-Aldrich)

HCl (Sigma-Aldrich)

HEPES (Lonza)

Heraeus Pico 21 Microcentrifuge (ThermoFisher)

Hoechst (ThermoFisher)

L-glutamine (Sigma-Aldrich)

Lymphoprep (Stemcell Technologies, Vancouver, Canada)

Minimum Essential Medium (MEM; Gibco, ThermoFisher)

Methanol (Univar, Downers Grove, IL)

NaCl (Rowe Scientific, Sydney, Australia)

Paraformaldehyde (Sigma-Aldrich)

Phosphate buffered saline (PBS, Life Technologies, Mulgrave, Australia)

Polyvinyl difluoride (PVDF) membrane (Amersham, GE Healthcare, Buckinghamshire, UK)

Precast 4-12% polyacrylamide gels (Invitrogen)

ProLong Gold Antifade reagent (ThermoFisher)

RosetteSepTM CTC enrichment cocktail Containing Anti-CD36 (Stemcell Technologies, Victoria, Australia) (Catalogue number 15167)

RosetteSepTM Human CD45 depletion cocktail (Stemcell Technologies) (Catalogue number 15162)

Roswell Park Memorial Institute 1640 medium (RPMI; Lonza)

SepMate tubes (Stemcell Technologies)

Skim milk powder (Woolworths, Sydney, Australia)

Superfrost glass slides (Menzel-Glaser)

T25 cm² and T75 cm² tissue culture flasks (Corning, MA, US)

Tris base (Sigma-Aldrich)

Triton X-100 (Sigma-Aldrich)

Tween-20 (Sigma-Aldrich)

2.2 Equipment

BX53 microscope (Olympus, Notting Hill, Australia)

Haemocytometer (Sigma, Castle Hill, Australia)

IX71 microscope (Olympus, Notting Hill, Australia)

Milli-Q water (Merck, Bayswater, Australia)

Mr. Frosty freezing container (ThermoFisher)

NanoDropTM2000 spectrophotometer (ThermoFisher)

Odyssey Gel documentation system (LI-Cor Biosciences, Lincoln, NE)

Zeiss LSM 800 confocal microscope (Zeiss, Oberkochen, Germany)

2.3 General Methods

The methods below are commonly used throughout Chapters 4 and 5 and are described here in detail, and briefly described in Chapters 4 and 5, with any minor changes/deviations noted.

2.3.1 Patient Recruitment

Patients were recruited from Liverpool Cancer Therapy Centre and St George Private Hospital. Clinical information was sourced from patient medical records. Clinical information at time of blood sampling was collected including age, sex, primary cancer site and stage. Treatment information was collected including chemotherapy regimen, previous lines of therapy prior to circulating tumour cell (CTC) isolation, serum biomarker levels and radiological assessments. Blood samples from healthy individuals were collected as controls for initial optimisation studies. All studies were undertaken with approval from the South Western Sydney Local Health District (SWSLHD) human ethics committee (HREC/13/LPOOL/158), and patients gave written consent to participate.

2.3.2 Tissue Culture

PCa cell lines 22RV1, LNCaP, VCaP and PC3 were maintained in DMEM medium supplemented with 10% Foetal bovine serum (FBS), 2 mM L-glutamine and HEPES in a humidified atmosphere with 5% CO² at 37°C. DU145 cell line was maintained in MEM medium, supplemented as above, in a humidified atmosphere with 5% CO² at 37°C. All cell lines were grown from frozen stocks that were STR authenticated and confirmed to be free of mycoplasma at time of freezing (Australian Genome Research Facility Ltd, Melbourne, Australia) and maintained for no more than 35 passages. Cells were seeded at 15-20% confluency and cultured for three to four days before passaging. When growing cell lines, media was changed twice a week. When cells reached 80-90% confluency, cell were split as follows. Cells were washed with PBS, 2 mM trypsin-EDTA (2 mM) was added to detach the

cells and the flask was kept at 37°C 5% CO₂ for 3-5 minutes. Trypsin-EDTA was then neutralized in the required medium (containing 10% FBS) at 1:5 or 1:10 dilution depending on types of cells, transferred to a new flask, and kept at 37°C.

2.3.3 Western Blotting

Cells were lysed in 50 mM Tris-HCl pH 7.5, 150 mM NaCl, 0.5% Triton X-100, 2 mM EDTA, 2 mM EGTA 25 mM NaF, 25 mM β -glycerophosphate, 10% glycerol, phosphatase inhibitor and 1x protease inhibitors (Roche) for 30 minutes on ice followed by clearing at 4000 g at 4°C. Protein concentrations were measured with SPECTRAMAX M2^e Plate reader (Molecular Devices, USA). 30 μ g of total protein per sample was SDS PAGE separated on 4-12% Bis-Tris gels and transferred to PVDF membranes. The primary antibodies were prepared in 1x Tris buffered saline containing 0.05% Tween-20 (TBS-T) containing 5% skim milk powder and incubated with membranes overnight under gentle agitation at 4°C. After washing the membrane in TBS-T (3 times), membranes were incubated with ECLTM Anti-Rabbit IgG, Horseradish Peroxidase linked whole antibody (from donkey) (Lot 9526417) and ECLTM Anti-mouse IgG, Horseradish Peroxidase linked F(ab')₂ fragment (from sheep) (Lot 312511) (Life technologies, Eugene, OR, USA) for 1 hour at room temperature, washed 3 times in TBS-T and images were developed by using Western LightningTM Plus-ECL Enhanced Luminol Reagent Plus (LOT 275-13481) and Western LightningTM Plus-ECL Oxidizing Reagent Plus (LOT 265-13481) (PerkinElmer, Waltham, MA). Membranes were washed in TBS-T after taking images by using an Odyssey imager and reprobod for GAPDH primary antibody overnight. After washing 3 times in TBS-T, membranes were incubated with ECLTM Anti-Rabbit IgG, Horseradish Peroxidase linked whole antibody (from donkey) (Lot 9526417). The images were taken by using an Odyssey imager (Li-Cor Biosciences, Lincoln, NE).

2.3.4 Immunocytostaining and Fluorescence Microscopy

Cells were seeded at $\sim 2 \times 10^4$ cells onto sterile coverslips in 6-well plates. After approx. three days, cells were fixed by using 3.7% paraformaldehyde (PFA) for 10 minutes. Cells were washed with PBS (2x) and kept in PBS until staining was done. Fixed cells were permeabilized by using 0.2% Triton X-100 for 10 minutes followed by washing with PBS. Permeabilized cells were blocked with 10% goat serum in PBS for 30 minutes and washed with PBS. Cells were stained with specific antibody in 0.5% goat serum and incubated for an hour. Coverslips were washed three times with PBS containing 0.5% Tween-20 (PBST), followed by PBS (1x). The cells were stained with Hoechst in PBS for 10 minutes, followed by washes with PBST (3x), PBS (1x) and a Milli-Q water rinse. The coverslips were mounted onto glass slides with ProLong Gold Antifade reagent. Cells were visualised with a BX53 or IX71 fluorescence microscope (Olympus). Images were captured with the 20X objective with Cell Sens Dimension imaging software (1.18, Build 16686).

2.3.5 CTC isolation from Patient Blood

Patient blood was drawn into 9 mL EDTA vacutubes (Greiner Bio-One) and processed within 24 hours. RosetteSep CD36 enrichment kits were used to isolate CTCs. The blood was incubated with antibody cocktail (50 μ L/mL of blood sample) for 10 minutes and diluted with recommended medium (2% FBS in PBS). Then diluted blood sample was transferred to a Sepmate tube containing 15 mL density-gradient medium and centrifuged at 1200 x g for 10 minutes with brakes on. After centrifugation, supernatant was transferred to a 50 mL falcon tube and topped up with recommended media. The tube was centrifuged again at 300 x g for 10 minutes with low brake. The supernatant was discarded, and the tube was resuspended by tapping manually in residual supernatant. The tube was refilled with recommended media and once again centrifuged at 300 x g for 10 minutes with low brakes. After discarding the

supernatant, the pellet was resuspended in 2 mL recommended media and split into 3 different wells of 24-well glass bottom plate. The plate was centrifuged at 200 x g for 10 minutes and the cells were fixed with 3.7% formaldehyde in PBS for 10 minutes followed by washing with 1 x PBS (2 times). There was 500 μ L PBS in the wells and CTCs were stored for up to 1-2 days at 4°C before doing staining.

2.3.6 RNA Isolation

Total RNA from cell lines was extracted with the ISOLATE II RNA Micro Kit (Bioline, Sydney, Australia) and any residual genomic DNA contamination was removed by on-column DNase I treatment for 15 minutes. RNA was eluted in 50 μ L RNase-free H₂O. RNA quality and quantity were measured using the NanoDrop 2000 (Thermo Scientific, Waltham, MA). cDNA synthesis was performed from 1 μ g total RNA with the SensiFAST cDNA Synthesis kit (Bioline, Sydney, Australia). Total RNA from CTC samples or healthy control PBMCs was extracted with the RNA purification Mini kit (Norgen Biotek Corp., Thorold, Canada) and double-eluted in a total volume of 30 μ L RNase-free H₂O. 15 μ L of this RNA was converted into cDNA with the SensiFAST cDNA Synthesis kit (Bioline, Sydney, Australia).

2.3.7 Droplet Digital PCR (ddPCR)

Primers and TaqMan probes were designed by our team using NCI primer software <https://www.ncbi.nlm.nih.gov/tools/primer-blast/>. ddPCR samples for total AR and AR-V7 were set up with 20 μ L reaction mixture containing 10 μ L ddPCR Supermix for probes, no dUTP (Bio-Rad, Hercules, CA, USA), each forward primer (FP, 500 nM) and reverse primer (RP, 500 nM) and probes (FAM and HEX, each 250 nM). Droplets were generated with 70 μ L oil using a QX200 droplet generator (Bio-Rad). Amplification was performed at 95°C, 10 minutes; followed by 40 cycles of 94°C, 30 s and 55°C (or 60°C for actin) 1 minute using a

C1000 Touch thermocycler (Bio-Rad). After amplification, the droplets were read on a QX200 droplet reader (Bio-Rad) and analysed with QuantaSoft software V1.7.4 (Bio-Rad).

2.3.8 Primers and probes

AR-Species	Primers	Probes
Total AR	FP: 5'- GGAATTCCTGTGCATGAAAGC-3' RP: 5'- CGATCGAGTTCCTTGATGTAGTTC- 3'	5'-[HEX] CTCAGCATTATTCCAGTG[BHQ1] -3'
AR-V7	FP: 5'- CGGAAATGTTATGAAGCAGGGATG A-3' RP: 5'- CTGGTCATTTTGAGATGCTTGCAAT- 3'	5'-[6FAM] CGGAATTTTCTCCCAGA[BHQ1]- 3'
GAPDH	FP: 5'- CGGGAAGCTTGTCATCAATGG-3' RP: 5'- CTCCACGACGTA CT CAGCG-3'	5'- [FAM]TCTTCCAGGAGCGAGATCCC T-[BQ1]- 3'

Chapter 3: Prognostic and Predictive Value of Liquid-Biopsy-Derived Androgen Receptor Variant 7 (AR-V7) in Prostate Cancer: A Systematic Review and Meta-Analysis

3.1 Introductory Background

As detailed in Chapter 1, Section 1.8, Androgen receptor variant 7 (AR-V7) is an important biomarker in PCa, particularly when castrate resistant prostate cancer (CRPC) develops. Current therapies for CRPC include second-generation androgen axis inhibitors, such as abiraterone or enzalutamide, docetaxel, cabazitaxel, or other agents more generally available in the US, such as Radium 223, and sipueluecel T. Docetaxel chemotherapy is now aimed at AR-V7 positive CRPC patients, and eligibility for recruitment onto the current clinical trials includes expression of AR-V7 [204]. However, in advanced stage PCa, recent tissue biopsies are often unavailable and archival tissue may not reflect current AR-V7 status. This challenge has prompted exploratory studies to detect AR-V7 from other tissues, specifically easily accessible and repeatable liquid biopsies. Chapter 3 reviewed the evidence for and assessed the importance of AR-V7 in PCa patients as detected in liquid biopsy compartments, namely CTCs, ctDNA, exosomes and whole blood. For this purpose, a meta-analysis was performed according to systematic guidelines. Our meta-analysis showed significant association of liquid biopsy-based AR-V7 with overall survival and in context of specific therapies, as outlined here.

3.1.1 Published Manuscript

This study was published as a systematic review.

Front Oncol. 2022; 12: 868031. doi: 10.3389/fonc.2022.868031. Published online 2022 Mar 18. (Attachment 2).

Publication Details: Tanzila Khan, Therese M. Becker, Kieran F. Scott, Joseph Descallar, Paul de Souza, Wei Chua, Yafeng Ma.

Contribution of Authors:

Project development, methodology, data collection and analysis: TK and YM;
Conceptualization: YM and TK; Project development: TB, KS, PDS and WC; Statistics: JD, TK and YM; Manuscript writing, editing, and reviewing: all authors; All authors read and approved the final manuscript.

3.2 Abstract

In advanced PCa, access to recent diagnostic tissue samples is restricted, and this affects the analysis of the association of evolving biomarkers such as AR-V7 with metastatic castrate resistance. Liquid biopsies are emerging as alternative analytes to traditional tissue biopsies. To clarify the clinical value of AR-V7 detection from liquid biopsies, here we performed a meta-analysis on the prognostic and predictive value of androgen receptor variant 7 (AR-V7) detected from liquid biopsy for patients with prostate cancer (PCa). Three databases (Embase, Medline and Scopus) were searched up to September 2021. A total of 37 studies were included. The effects of liquid biopsy AR-V7 status on overall survival (OS), radiographic progression-free survival (PFS) and prostate-specific antigen (PSA)-PFS were calculated with RevMan 5.3 software. AR-V7 positivity detected in liquid biopsy significantly associates with worse OS, PFS and PSA-PFS ($P < 0.00001$). A subgroup analysis of patients treated with androgen receptor signalling inhibitors (ARSi such as abiraterone and enzalutamide) showed a significant association of AR-V7 positivity with poorer OS, PFS and PSA-PFS. A statistically significant association with OS was also found in taxane-treated patients ($P = 0.04$), but not for PFS ($P = 0.21$) or PSA-PFS ($P = 0.93$). For AR-V7 positive patients, taxane treatment has better OS outcomes than ARSi ($P = 0.01$). Study quality, publication bias and sensitivity analysis were integrated in the assessment. Our data suggest that liquid biopsy AR-V7 may be a clinically useful biomarker that is associated with poor outcomes of ARSi-treated castrate resistant PCa (CRPC) patients and thus has the potential to guide patient management as well as to stratify patients for clinical trials. More studies on chemotherapy treated ARV7+ patients are warranted.

3.3 Introduction

Prostate cancer (PCa) is one of the most common male cancers. The androgen receptor (AR) pathway is critical in maintaining normal prostate tissue homeostasis, cancer development and progression [226]. Therapies for PCa include surgery and radiation for localised or early-stage cancer, while for advanced or metastatic PCa, androgen deprivation therapy (ADT), with or without chemotherapy, is standard of care. However, patients eventually develop castration resistant PCa (CRPC). Recent incorporation of novel androgen receptor signalling inhibitors (ARSi, e.g., enzalutamide (Enz), abiraterone (Abi)) and taxane-based chemotherapy have improved outcomes of CRPC patients over the past two decades [227].

Biomarkers detected in liquid biopsy (such as circulating tumour cells and cell-free tumour DNA) demonstrate good concordance with biomarkers detected in conventional tissue biopsy, especially for metastatic CRPC [228]. Liquid biopsy is emerging as a reliable source of biological data for biomarker discovery, especially in advanced PCa, when tissue biopsy is often not obtainable or cannot be used longitudinally to monitor tumour evolution and changes in biomarker characteristics. In CRPC, one of the most promising prognostic markers is the constitutively active AR splice variant 7 (AR-V7). AR-V7 lacks the ligand binding domain and substitutes for functional AR even in absence of the ligand testosterone, and differentially regulates AR-dependent gene expression [229]. Thus far, the current literature suggests that expression or nuclear subcellular location of AR-V7 is associated with overall survival (OS) and progression free survival (PFS) when found in tissue biopsy [209] or liquid biopsy [whole blood [230, 231], circulating tumour cells [232], exosomes [233, 234]]. However, the statistical power of studies varies, depending on cohort sizes, clinical stages of patients under study, and also treatment options; the clinical relevance of AR-V7, especially liquid biopsy detectable AR-V7, is still not clear or widely accepted, and needs further investigation.

To clarify the clinical utility of AR-V7 detection from liquid biopsies, we undertook a comprehensive systematic review and meta-analysis to evaluate the available data from clinical studies published up to September 2021. Prognostic and predictive value of liquid biopsy derived AR-V7 data in PCa patients were evaluated from 37 studies that met inclusion criteria.

3.4 Methods

3.4.1 Study Design and Literature Searches

This study was conducted according to preferred reporting items for systematic reviews and meta-analysis (PRISMA) [235]. The protocol has been registered on PROSPERO (CRD42021239353). Detailed literature searches up to September 10, 2021, in the Embase, PubMed and Scopus databases were conducted thoroughly to check the prognostic role of AR-V7 in PCa. The used search terms were (~Androgen Receptor Variant 7) OR (~ARV7) OR (~AR3) AND (~"prostate cancer"). The searched study citations were imported to EndNote (version X9) for duplicate checking and title and/or abstract screening and then uploaded to online systematic review research tool Rayyan (<https://www.rayyan.ai/>) for independent systematic review according to selection criteria. Two independent, blinded observers (TK and YM) reviewed all candidate articles. Any discrepancies in the article selections were resolved by discussion.

3.4.2 Selection Criteria

Pre-set exclusion criteria of this study were: (1) publication type: review articles, letters, comments, questionnaires, conference papers, corrections, reply to editor, case reports, book chapters, abstracts only, research highlights, summaries; (2) non-human studies (animal or cell line study); (3) non-prostate cancer; (4) AR-V7 data are not derived from human; (5) survival data not related to AR-V7 or with insufficient data to calculate hazard ratios (HRs) and 95% confidence intervals (Cis), or insufficient data from the Kaplan-Meier (K-M) curves that

prevented calculation of HRs and 95% CI parameters. Finally, studies were only included when they met the following criteria: (1) AR-V7 assayed in liquid biopsies (whole blood, circulating tumour cells, PBMC, plasma, exosome); (2) A reported relationship between AR-V7 and prognostic/predictive indicators, including OS, PFS and PSA-PFS; (3) patient cohorts with n >25, and (4) English language only.

3.4.3 Data Extraction and Quality Assessment

This study focuses on the prognostic value of AR-V7 detected from liquid biopsy and its predictive value for ARSi and chemotherapy outcomes. According to a pre-designed table, items of data extraction included the last name of the first author, publication year, study country, number of patients included, age of patient, sample resource (processing method) and AR-V7 detection method, type of therapies, endpoints of oncological outcomes, HRs and 95% CIs (from univariate or multivariate Cox analysis), follow-up durations and definitions of OS, PFS and PSA-PFS (Supplemental Table 3.1). When HRs and 95% CIs were not presented in the study, an Engauge Digitizer (version 12.1) was used to digitalise the K-M survival curve to re-calculate HRs and 95% CI as described previously [236]. Data was extracted by two authors (TK and YM) independently and any inconsistencies were resolved by discussion. Notably, when several publications were retrieved that reported the same trial or patient cohort or were from same author(s), the study question and data from this publication were discussed by two authors (TK and YM) and uniqueness of the included data was ensured.

The adapted Newcastle-Ottawa Scale (NOS) scales for cohort study [237] were used to evaluate the quality of enrolled studies, which embraced three aspects, namely, patient selection, comparability, and assessment of outcome with a total score of 9. In addition, the quality of statistical evaluation was assessed to give a maximal score of 1 as described in

Supplemental Table 3.2; a score of 7 or more is considered as high-quality and a score of 6 or less is considered as low quality.

3.4.2 Statistical Analysis

Pooled HR and 95% CI were used to evaluate the prognostic and predictive value of AR-V7 presence or high expression (in some studies, authors set a threshold to discriminate high or low expression level) on the patient survival parameters (OS, PFS, PFA-PFS) in Review Manager 5.3 software (RevMan v.5.3, Denmark). The Cochran Q and I^2 statistical methods were applied to evaluate the heterogeneity among included studies and a random effects model was used for data consolidation. If the heterogeneity was very high, only a descriptive score was given. Further subgroup analysis based on patient treatment was also conducted. The inverted funnel plots with Egger's test were used to analyse potential publication bias with R software. A sensitivity analysis was carried out to assess the influence of each individual study on the pooled results by sequentially excluding each study. A two-tailed p-value <0.05 was regarded as statistically significant.

3.5 Results

3.5.1 Search Results, Study and Patient Characteristics

The flowchart outlining the results of the literature search and application of the strategic inclusion and exclusion criteria is presented in Figure 3.1.

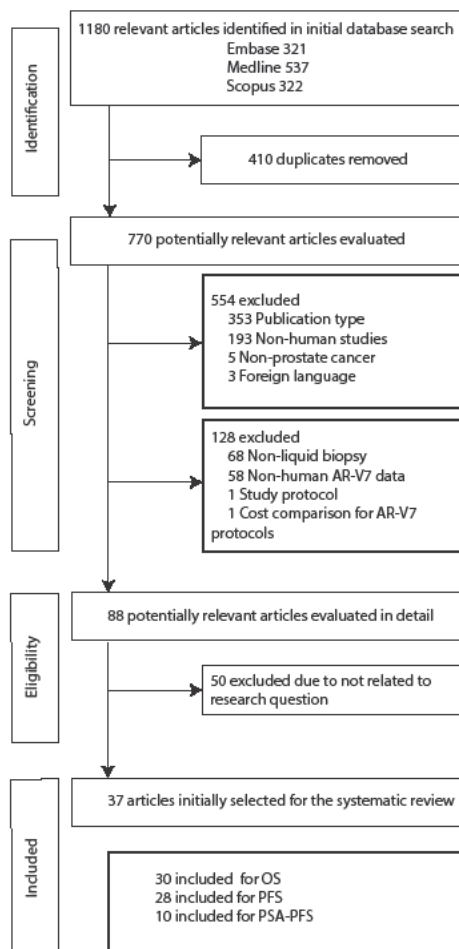


Figure 3. 1 Flow chart of literature search and study selection

A total of 1,180 relevant articles were identified in initial database searches (Embase: 321, Medline: 537, Scopus: 322). After screening research title and abstract to remove duplicates (n = 410) and excluding the non-relevant studies based on publication type (n = 353), non-human studies (n = 193), non-prostate cancer (n = 5) and foreign language (n = 3) followed by a review of full text for eligibility, 37 articles were identified based on inclusion criteria 'human data', 'AR-V7', 'liquid biopsy', and 'survival'. Although we initially only searched quite a broad terminology 'prostate cancer', all 37 studies investigated CRPC (n = 4) or metastatic CRPC (mCRPC) (n = 33) as defined in the reports (Supplemental Table 3.1). Baseline characteristics of all eligible articles are listed in Table 3.1. All articles were published from 2014 to 2021 and included studies from Europe (46%), America and Canada (46%) and Asia-Pacific (8%). Liquid biopsy AR-V7 was detected from CTC (n = 28), PBMC (n = 2), whole blood (n = 4) or exosomes (n = 3). The patient cohort size ranged from 26 to 202 and the median or mean patient age ranged from 56 to 78. CTC enrichment methods included (modified) AdnaTest® (Qiagen) (n = 13), OncoQuick® (Greiner Bio-One GmbH) (n = 1), red blood cell (RBC) lysis (n = 3), and immunomagnetic beads-based methods (such as CellSearch® or IsoFlux®, dynabeads) (n = 9). The method of AR-V7 detection was primarily by PCR (quantitative PCR and droplet digital PCR, 92%). Endpoint of patient outcomes include OS (n = 30), PFS (n = 28) and PSA-PFS (n = 10) (Table 3.1).

Table 3. 1 The basic characteristics of eligible studies

Study	Year, country	Study type	Patients	Age	Resource, method	Treatment	Endpoint outcome	Follow up(month)	NOS score
Antonarakis et al. [238]	2015 US	Pros	37 CTC+	67 (46-82) ^B	CTCs (mAdna), qRT-PCR	Taxane	OS, PFS, PSA-PFS	7.7 (0.7-19.0) ^B	10
Antonarakis et al. [239]	2017 US	Pros	53 CTC-, 113 CTC+ /AR-V7-, 36 CTC+ /AR-V7+	70 71 70 ^A	CTCs (mAdna), qRT-PCR	Abi/Enz	OS, PFS, PSA-PFS	CTC-:15.0 CTC+/ARV7-:21.7 CTC+/ARV7+:14.6 ^A	9
Antonarakis et al. [45]	2014 US	Pros	Enz:31, Abi: 31	Enz:70 (56-84), Abi:69 (48-79) ^B	CTCs (mAdna), qRT-PCR	Abi/Enz	OS, rPFS, PSA-PFS	Enz: 5.4 (1.4-9.9) Abi: 4.6 (0.9-8.2) ^B	9
Armstrong et al. [204]	2019 US	Pros, blinded, multi-center	118	73 (45-92) ^B	CTCs (Adna, CellSearch), qRT-PCR	Abi/Enz	OS, PFS	19.6 ^A	10
Armstrong et al. [240]	2020 US	Pros, blinded	ARSi:118 Taxane: 51	72(48-82) 72(45-87) ^B	CTCs (Adna, CellSearch), qRT-PCR	ARSi, Taxane	OS, PFS	ARSi:35 Tax:23 ^A	9
Belderbos et al. [241]	2019 Netherlands	Pros	94	69 (65-75) ^C	CTCs (CellSearch), qRT-PCR)	Cabazitaxel ARSi	OS	NA	9
Cattrini et al. [242]	2019 Italy	Pros	39	72 (56-84) ^B	CTCs (Adna), qRT-PCR	ARSi, Taxane	OS	NA	8
Chung et al. [243]	2019 US	Pros	37	72 (67-79) ^C	CTCs (Dynabeads), qRT-PCR	Abi/Enz	OS, rPFS, PSA-PFS	11.4 (4.7-21.3) ^C	7
De Laere et al. [244]	2019 Belgium	Pros	168	76 ± 7.7 ^E	CTCs (CellSearch),	Abi/Enz	OS, PFS	12.4 (7-17.3) ^C	10

		multi-center			RNA-seq				
Del Re et al. [245]	2017 Italy	Pros	36	66 (51-81) ^B	Plasma exosomes (exoRNeasy), ddPCR	ARSi	OS, PFS	9 (2.0-31.0) ^B	8
Del Re et al. [233]	2021 Italy	Retros	84	78 (47-91) ^B	Plasma exosomes (exoRNeasy), ddPCR	ARSi	OS, PFS	NA	9
Del Re et al. [234]	2019 Italy	Retros	73	NA	Plasma exosomes (exoRNeasy), ddPCR	Abi/Enz	OS, PFS	NA	7
Erb et al. [246]	2020 Germany	Pros	26	74.3 ± 9 ^A	CTCs (OncoQuick), IHC	ARSi, Taxane	PFS	NA	6
Graf et al. [247]	2020 US	Pros, cross-sectional	193	69 (62.5-75) ^C	CTCs (RBC lysis), IF	ARSi, Taxane	OS	28.4 (24.4 - 33.0) ^C	9
Gupta et al. [248]	2019 US	Pros	ARSi:120 Radium:20	ARSi:73 (45-92) Radium:72 (54-86) ^B	CTCs (Adna, CellSearch), qRT-PCR and Epic assay	Abi/Enz, Radium	PFS	NA	9
Joncas et al. [249]	2019 Canada	Pros	35	75 (67,79) ^C	EVs (UC, miRNeasy), ddPCR	ARSi, Taxane	OS, PFS	27 (16,33) ^C	8
Kwan et al. [250]	2019 Australia	Pros	115	72 (46-91) ^B	WB, qRT-PCR	ARSi, Taxane	OS	15.5 (1.4 -29) ^B	10
Lorenzo et al. [251]	2021 Italy	Pros, multi-center	53 (data only)	72.1 (54-86) ^B	CTCs, (Flow cytometry)	Enz	OS, rPFS	27 ^A	10
Maillet et al. [252]	2019 France	Pros	41	73 ^A	CTCs (AdnaTest),	ARSi	OS, rPFS,	31 ARSi treated patients: 10.5 ^A	8

					qRT-PCR		PSA-PFS		
Marín et al. [253]	2020 Spain	Pros	136	ARSi:70.2 (53.3-93.3) Tax: 62.8 (32.8-79.4) ^B	PBMC and CTCs (IsoFlux) qRT-PCR	Abi/Enz, Taxane	OS, rPFS, PSA-PFS	ARSi:14.9 (1.5-57.9) Tax:13.8 (1.37-82.27) ^A	10
Markowski et al. [254]	2021 US	Multicohort phase II	Post-Abi: 29, Post-Enz: 30	Post-Abi: 71(49-85) Post-Enz: 74(50-89) ^B	CTCs (Adna), qRT-PCR	BAT, ARSi	rPFS	NA	7
Miyamoto et al. [255]	2018 US	Pros	27	67 ^D	CTCs (CTC-iChip), ddPCR	Abi	OS, rPFS	13.0 ^A	8
Okegawa et al. [256]	2018 Japan	Retros	49 CTC -, 23 CTC +/AR-V7 -, 26 CTC +/AR-V7 +	69, 71, 72 ^D	CTCs (on-chip FC), PCR	Abi/Enz	OS, rPFS, PSA-PFS	20.7 (3.0-37.0) ^B	9
Onstenk et al. [257]	2015 Netherlands	Pros, multicenter, phase II	29	70 ± 7 ^E	CTCs (CellSearch), qRT-PCR	Cabazitaxel	OS, PFS	7 (2-27) ^B	7
Qu et al. [258]	2017 US	Retros	Abi: 81, Enz: 51	Abi: 68.3 (62-74) Enz:69.0 (63-74) ^C	PBMC(Ficol), ddPCR	Abi/Enz	OS, PFS (TTF)	29.7 (3.6- 47.5) 23.9 (0.9- 48.3) ^B	10
Scher et al. [259]	2018 US	Pros, cross-sectional	142	69.5 ± 9.6 ^E	CTCs (RBC lysis), IF	ARSi, Taxane	OS	4.3 years	8

Scher et al. [43]	2017 US	Pros, cross-sectional	161	68 (45-91) ^b	CTCs (RBC lysis), IF	ARSi, Taxane	OS	11 (1-30) ^A	9
Scher et al. [42]	2016 US	Pros, cross-sectional	161	68 (45-91) ^B	CTCs, IF	ARSi, Taxane	OS, PFS	36	10
Seitz et al. [260]	2017 Germany	Pros	85	71 (66-74) ^C	WB, ddPCR	Abi/Enz	OS, rPFS, PSA-PFS	7.6 (4.7-12.7) ^C	8
Sepe et al. [261]	2019 Italy	Pros	Abi:26, Enz: 11	75 (68-80) ^B	CTCs (Adna), qRT-PCR	Abi/Enz	OS, rPFS, PSA-PFS	25 ^A	9
Sharp et al. [232]	2019 UK	Pros	181	CTC -:71.0 (66.8-75.6), CTC +/AR-V7 - : 69.6 (64.9-72.3), CTC +/AR-V7 - : 70.4 (65.3-74.6) ^C	CTCs (Adna, CellSearch), qRT-PCR	ARSi, Taxane	OS	19 (11-31) ^C	10
Škereňová et al. [262]	2018 Czech Republic	Retros	41	71 (54-82) ^B	CTCs (Adna), qRT-PCR	Docetaxel	OS	23.5 ^A	7
Stuopelyte et al. [230]	2020 Lithuania	Pros	102	75.4 (11.4) ^C	WB, qRT-PCR	Abi	PFS, OS	30.5 ^A	9
Tagawa et al. [263]	2019 US	Pros	54	71 (53-84) ^B	CTCs, ddPCR	Taxane	PFS	NA	7
Todenhöfer et al. [231]	2016, Canada	Pros	37	70 (53-87) ^B	WB, qRT-PCR	Abi	OS, PSA-PFS	NA	8

Tommasi et al. [264]	2018 Italy	Pros	44	71.5 (55-87) ^B	CTCs (Adna), qRT-PCR	ARSi, Taxane	PFS	20.5 ^A	7
Wang et al. [265]	2018 China	Pros	36	56.2 ± 8.6 ^E	CTCs (immuno- beads), qRT-PCR	Abi/Enz	PFS	NA	6

Studies are labelled as last name of first author, et al. and presented in alphabetical order; Patient number and age are all patients included in study; Pros: prospective; Retros: retrospective; ^a: median, ^b: median (range), ^c: median IQR, ^d: mean, ^e: mean ± STD; WB: whole blood; CTC: circulating tumour cells; RBC: red blood cell lysis; PBMC: peripheral blood mononuclear cell; Ficoll: density gradient medium; Adna: AdnaTest ProstateCancerPanel AR-V7; mAdna: modified Adna; IF: immunofluorescent staining; qRT-PCR: quantitative real time-polymerase chain reaction; ddPCR: droplet digital PCR; UC: ultracentrifuge; FC: flow cytometry; ARSi: androgen receptor signalling inhibitor; Abi: abiraterone; Enz: Enzalutamide; BAT: bipolar androgen therapy; NA: not available; some studies include healthy control for threshold setting or discovery cohort (the data is insufficient and not included in table).

Thirty studies including 976 AR-V7 positive (or high level, as defined by authors) and 2,056 AR-V7 negative (or low level) patients were used for OS comparison, while 28 studies including 697 AR-V7 positive and 1,553 AR-V7 negative patients were used for PFS analysis and 10 studies including 216 AR-V7 positive and 425 AR-V7 negative patients for PSA-PFS analysis. Most patients in the cohort of studies were treated with ARSi (either enzalutamide, abiraterone, or not specified) or taxane-based chemotherapy. Some reports included miscellaneous treatments [such as Bipolar Androgen-based therapy [254]]. Overall AR-V7 positive patients had significantly worse OS (HR 3.36, 95% CI 2.56-4.41, $P < 0.00001$), PFS (HR 2.96, 95% CI 2.20-3.98, $P < 0.00001$) and PSA-PFS (HR 4.34, 95% CI 2.15-8.76, $P < 0.00001$) than AR-V7 negative patients. Due to significant study heterogeneity ($I^2 \geq 80\%$), random effects model was applied to calculate HR value and 95% CI for all survival parameters.

3.5.2 Predictive Value of AR-V7 for ARSi-Treatment

AR-V7 positive patients treated with ARSi (enzalutamide or abiraterone) had significant poorer OS (HR 4.34, 95% CI 3.00-6.28, $P < 0.00001$), PFS (HR 2.89, 95% CI 2.15-3.87, $P < 0.00001$) and PSA-PFS (HR 4.69, 95% CI 2.50-8.82, $P < 0.0001$) compared with AR-V7 negative patients (Figure 3.2-3.4). When analysed based on specific treatment, compared to negative patients, AR-V7 positive patients also had significant worse OS (Enz: HR 2.93, 95% CI 1.71-5.01, $P < 0.0001$; Abi: HR 6.59, 95% CI 2.18-19.94, $P = 0.0008$, respectively) (Figure 3.2), PFS (Enz: HR 4.38, 95% CI 2.44-7.84, $P < 0.0001$; Abi: HR 6.88, 95% CI 1.99-23.73, $P = 0.002$, respectively) (Figure 3.3) and PSA-PFS (Enz: HR 7.40, 95% CI 2.66-20.60, one study, $P = 0.0008$; Abi: HR 11.39, 95% CI 4.53-28.67, two studies, $P < 0.00001$, respectively) (Figure 3.4).

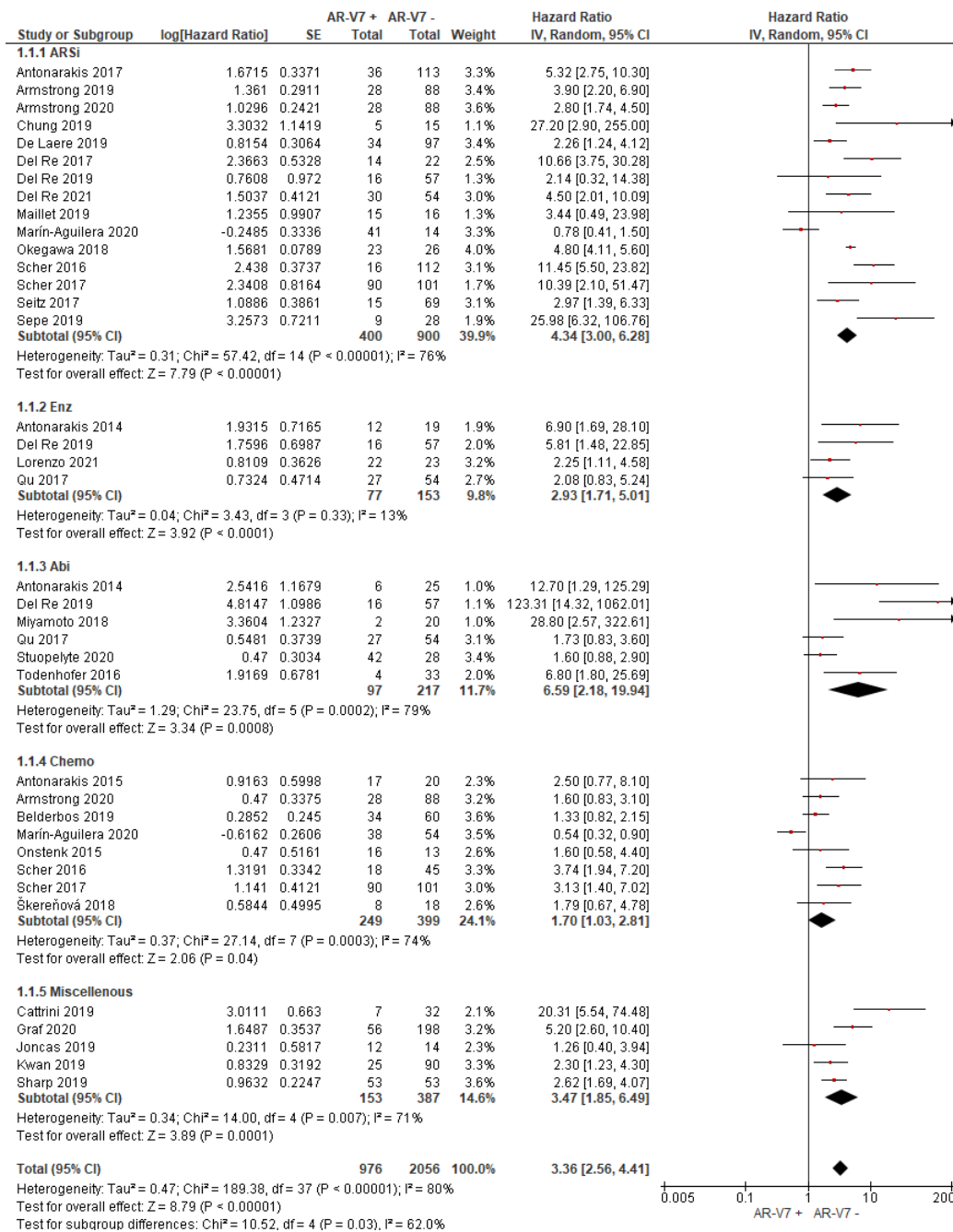


Figure 3. 2 Forest plot of hazard ratios (HRs) for association of liquid biopsy AR-V7 status with overall survival (OS) in all included studies

Pooled HRs were calculated using random effect model. AR-V7, androgen receptor splice variant 7; CI, confidence interval and bars indicate 95% CIs. Subgroup analysis (ARSi, enzalutamide or abiraterone; Enz, enzalutamide; Abi, abiraterone; Chemo, taxane based chemotherapy; Miscellaneous, treatments that do not belong to above treatments or not clearly defined) were assessed.

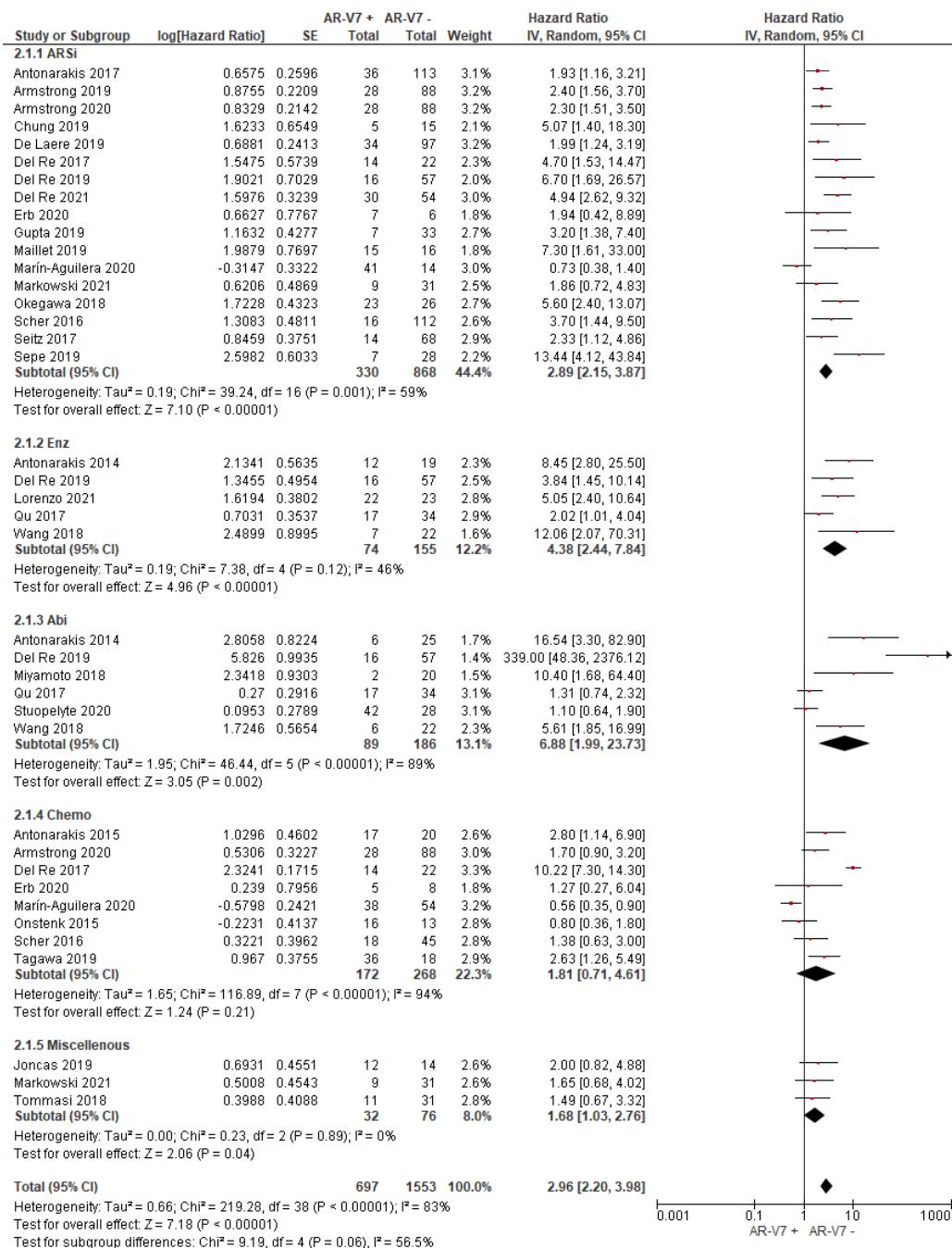


Figure 3. 3 Forest plot of hazard ratios (HRs) for association of liquid biopsy AR-V7 status with PFS in all studies

Pooled HRs were calculated using random effect model. AR-V7, androgen receptor splice variant 7. CI, confidence interval and bars indicate 95% CIs. Subgroup analysis (ARSi, enzalutamide or abiraterone; Enz, enzalutamide; Abi, abiraterone; Chemo, taxane based chemotherapy; Miscellaneous, treatments that do not belong to above treatments or not clearly defined) were assessed.

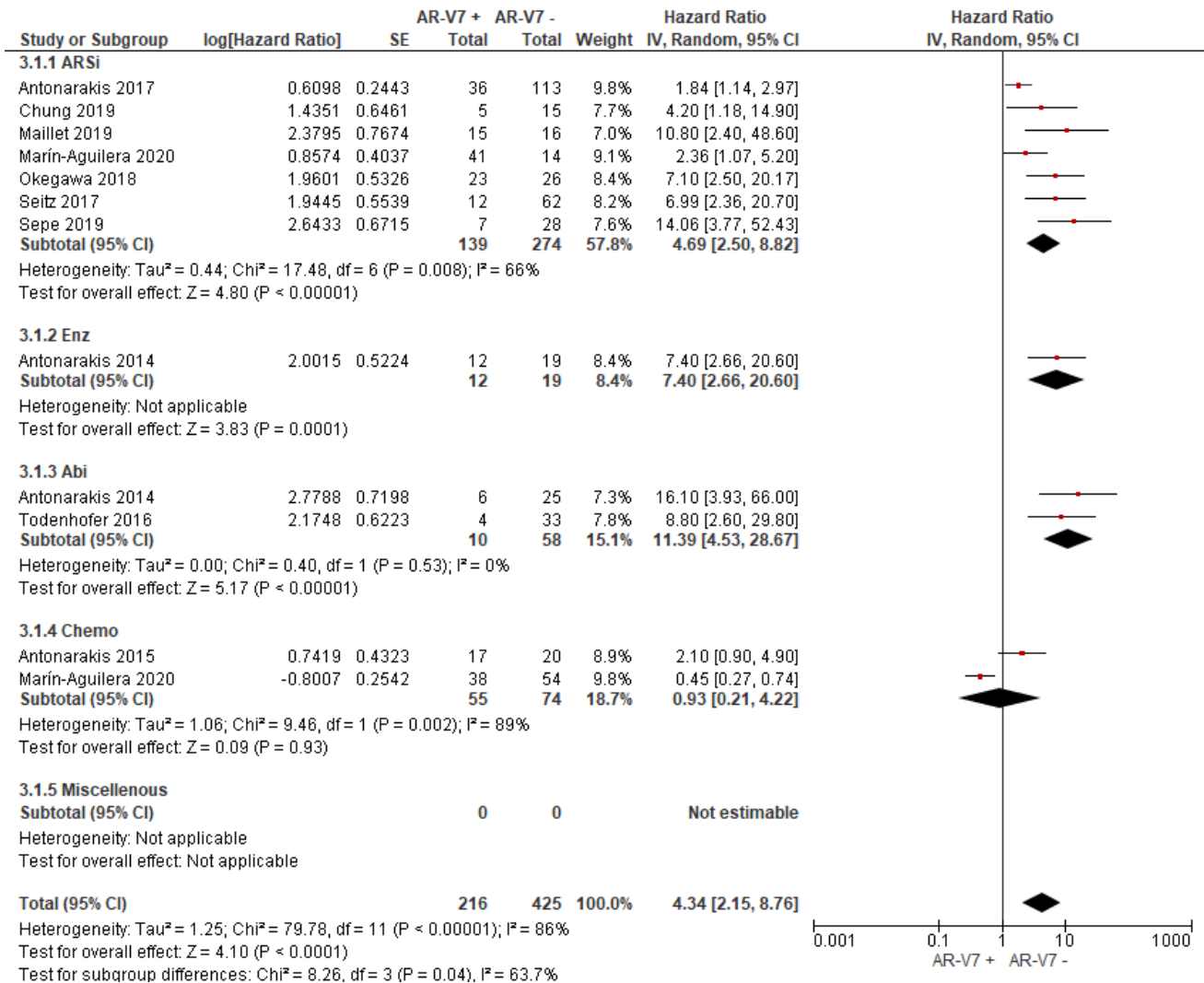


Figure 3. 4 Forest plot of hazard ratios (HRs) for association of liquid biopsy AR-V7 status with PSA-PFS in all studies

Pooled HRs were calculated using random effect model. AR-V7, androgen receptor splice variant 7. CI, confidence interval and bars indicate 95% CIs. Subgroup analysis (ARSi, enzalutamide or abiraterone; Enz, enzalutamide; Abi, abiraterone; Chemo, taxane based chemotherapy; Miscellaneous, treatments that do not belong to above treatments or not clearly defined) were assessed.

3.5.3 Chemotherapy-Treated Patients and Outcome Association with AR-V7

In the subgroup analysis of the patients treated with taxane-based chemotherapy, the association of AR-V7 positivity with worse OS was observed (HR 1.70, 95% CI 1.03-2.81, P = 0.04) (Figure 3.2), but no conclusive association between AR-V7 positive status and worse PFS and PSA-PFS were apparent, likely due to inadequate power (PFS: HR 1.81, 95% CI 0.71-4.61, P = 0.21, Figure 3.3; PSA-PFS: HR 0.93, 95% CI 0.21-4.22, P = 0.93, Figure 3.4). It is to be emphasised that data is only derived from two studies and a total of 129 patients (Figure 3.4).

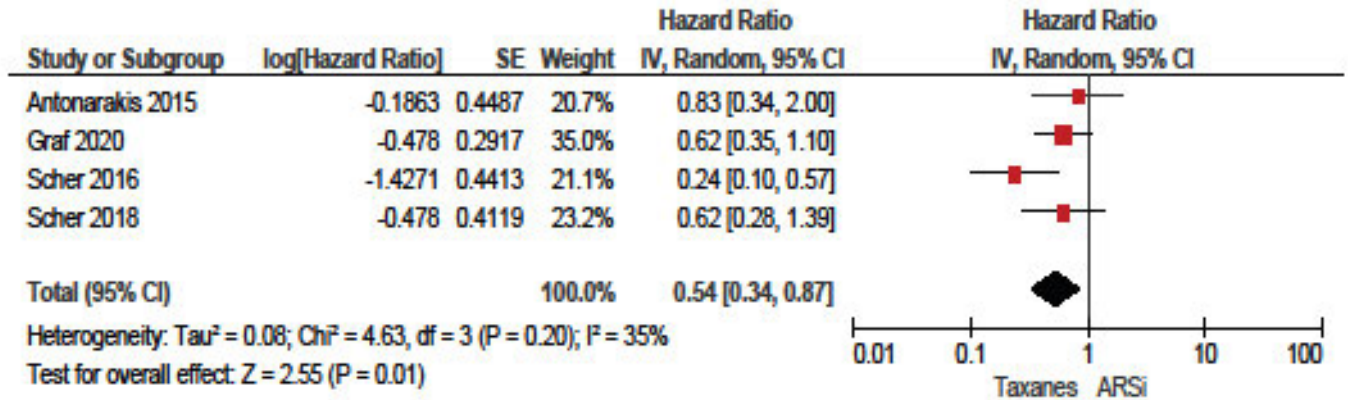
3.5.4 AR-V7 Effect on Non-Defined (Miscellaneous) Treatments

For the studies in which the authors did not clarify treatments and were unable to be classified as either ARSi or taxane chemotherapy, AR-V7 presence is associated with worse OS (HR 3.47, 95% CI 1.85-6.49, P = 0.0001, 5 studies) and PFS (3 studies, HR 1.68, 95% CI 1.03-2.76, P = 0.04) (Figure 3.2 and 3.3).

3.5.5 ARSi vs. Chemotherapy in AR-V7 Positive or Negative Patients

Four studies compared treatment response in AR-V7 positive or negative patients. Taxane treatment is linked to superior OS (HR 0.54, 95% CI 0.34-0.87, P = 0.01) in patients positive for AR-V7, compared to ARSi (Figure 3.5A). In contrast, for AR-V7 negative patients, OS in taxane or ARSi treated patients is not significantly different (HR 1.17, 95% CI 0.71-1.92, P = 0.54) (Figure 3.5B).

A



B

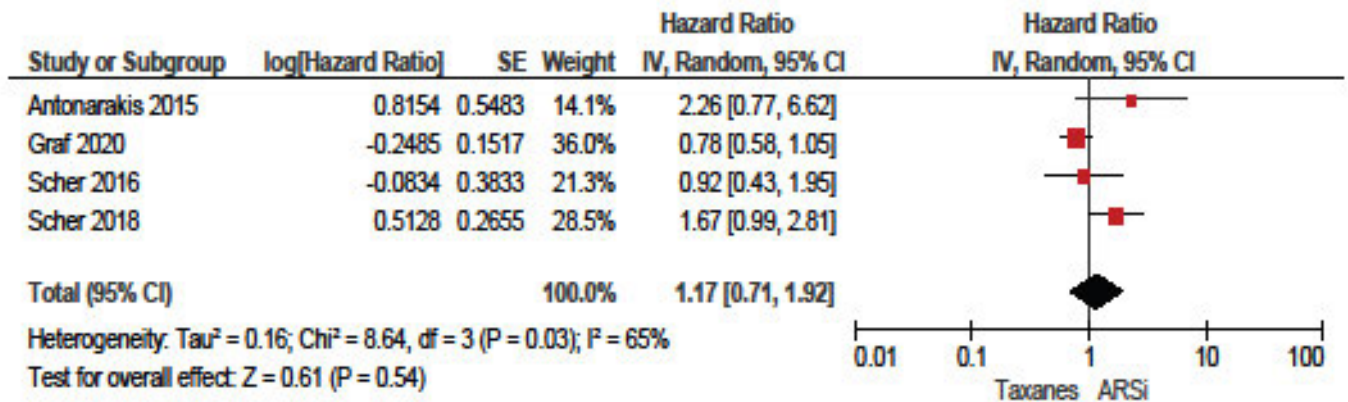


Figure 3. 5 Forest plots for association of liquid biopsy AR-V7 status with OS in (A) AR-V7

positive (ARSi vs. Chemotherapy) and (B) AR-V7 negative patients (ARSi. vs. Chemotherapy)

Pooled HRs were calculated using random effect model. AR-V7, androgen receptor splice variant 7;

CI, confidence interval and bars indicate 95% CIs.

3.5.6 Quality Assessment, Publication Bias and Sensitivity Analysis

Thirty-five articles were assessed as high-quality studies while 2 were deemed low quality studies (Table 3.1 and Supplemental Table 3.2). Overall, the average quality of studies is 8.5. Publication biases were evaluated for subgroups with more than 10 publications; no publication bias was observed for OS (Egger's test $P = 0.9925$, 15 publications, Supplemental Figure 3.1A) whereas publication bias was observed for PFS (Egger's test $P = 0.0411$, 17 publications, Supplemental Figure 3.1B) in ARSi-treated subgroups. Sensitivity analyses were performed on the subgroups of more than 6 studies and the results were relatively stable except for overall survival in chemotherapy-treated group, where missing data in one study [253] had a significant effect on data outcome (Supplemental Table 3.3).

3.6 Discussion

AR splice variants have been proposed as a cause of resistance to ARSi and taxane-based chemotherapy [266]. AR-V7, the most well-studied AR splice variant, is emerging as a clinically relevant biomarker in CRPC, with a detection incidence ranging between 20-60%, depending on biopsy source, detection methods and disease stage. Given that tumour tissue of advanced PCa is rarely available and archival tissue may not reflect the biology of the current tumour stage, liquid biopsies, mainly blood, are becoming attractive resources for AR-V7 and other biomarker evaluation. The majority of studies were conducted on CTC analysis (see table 3.1) and separate meta-analysis of the few studies conducted on other liquid biopsy forms was not statistically meaningful. Those studies did however generally have outcomes in line with the CTC based studies and were not excluded from overall analysis. Nevertheless, analysis of the data plus/minus these studies was performed to evaluate their impact on overall data. Technical advances, different detection methods for AR-V7 from liquid biopsies are now available, including modified AdnaTest Prostate Cancer, and droplet digital PCR of CTCs enriched by various platforms (see Table 3.1). We recently confirmed CTC-based AR-V7 testing is more reliable

than exosomal RNA and cell free tumour RNA in plasma [210]. Accumulating reports on the association of AR-V7 detectability in liquid biopsy with therapy response and patient survival have prompted us to perform this systematic review and meta-analysis on the prognostic and predictive utility of liquid biopsy-based AR-V7 identification. Our data show that liquid biopsy detectable AR-V7 significantly associates with poor outcomes to ARSi treatment as shown for OS, PFS, PSA-PFS ($P < 0.001$). This strongly supports the notion that AR-V7 detection from CRPC patient liquid biopsies has prognostic and predictive power. This observation is highly clinically relevant and could affect how clinicians make treatment decisions for patients with (metastatic) CRPC and when to transition patients to taxane-based chemotherapy.

While on taxane-based treatment, the association of AR-V7 presence with poorer outcome is still significant ($P = 0.04$) for OS data and lack adequate power for PFS ($P = 0.21$) or PSA-PFS ($P = 0.93$). However, there are relatively fewer publications in this subgroup, so these conclusions are based on weaker datasets compared to the ARSi treated subgroup; for instance, omitting one publication changes the P-value, and AR-V7 impact on OS would no longer be significant (Supplemental Table 3.3). Our data agree with a recent report that AR-V7 may contribute to taxane resistance by circumventing taxane-induced inhibitory effects both *in vitro* (cell lines) and *in vivo* (PCa tissue) [263, 267]. On the other hand, we cannot exclude the possibility that AR-V7 expression was induced in CRPC patients who had received ARSi prior to chemotherapy, and that its effect on OS has not been completely washed out by taxanes. We note that four studies suggest that chemotherapy would be a better option compared to ARSi (HR 0.54, $P = 0.01$) in AR-V7 positive CRPC, suggesting that AR-V7 determination is important in chemotherapy-treated patients. More studies in this subgroup are warranted.

Three other meta-analyses on AR-V7 prognostication [212, 237, 268] have been published recently, but given the common inaccessibility of current tissue biopsies, our meta-analysis exclusively focuses on liquid biopsies and includes the most up-to-date studies. Further, we not only include all studies

with author self-reported HR and 95% CI, but also calculate HR and 95% CI with established methods [236] for some papers with insufficient and incomplete statistical reporting. Nevertheless, our systematic review has limitations. We only examined OS, PFS and PSA-PFS, and did not assess other treatment outcomes such as PSA response. Discrepancies in the definition of PSA response (e.g., extent of PSA fall in a specific timeframe) exist across studies and given our selection criteria, papers were excluded if they only reported PSA response without survival data. Secondly, statistical power was limited by the numbers of studies available and small sample sizes in some of the subgroups analysed. Thirdly, included study designs differed greatly in biological material investigated (type of liquid biopsy and content such as CTCs or exosomes). For some studies, patients were enrolled from a single centre, potentially leading to publication bias and selection bias. Also, no randomized study has ever directly compared the predictive value of AR-V7 in patients treated with chemotherapy vs. ARSi. Therefore, the findings here are considered preliminary. Lastly, the variability of techniques used to determine AR-V7 positivity, namely, qRT-PCR and ddPCR of mRNA derived from CTC, whole blood, exosome, could result in differing conclusions. The cut-off value is essential in defining and interpretation of AR-V7 positivity, due to the continuous nature of this variable; more work is required to answer the question of whether the degree of AR-V7 presence is important. Last but not least, other CTC AR detection methods have been adopted such as RNA-seq and immunostaining. Despite the variety of methodologies, we found that liquid biopsy detectable AR-V7 correlates with disease outcomes (Supplemental Figure 3.2).

In conclusion, ARSi and taxane-based chemotherapy are approved treatment options for CPRC patients and are used globally. Use of emerging methodologies, such as liquid biopsy- determined AR-V7, to optimise utility of a known predictive biomarker could help to guide the optimal treatment sequencing pathway for each patient in a personalised manner and is therefore of clinical importance. Standardisation of liquid biopsy AR-V7 detection would underpin utility in clinical practice. Avoiding

ineffective therapies or early switching to more effective approaches should ensure better outcomes for patients. However, further studies on chemotherapy-treated patient cohort and direct comparison of chemotherapy vs. ARSi are warranted.

3.7 Supplementary Material

Supplemental Table 3. 1 Definitions of OS, PFS, PSA-PFS and tumour stages in each included study

Study	Outcome	Stage of disease	OS	PFS	PSA-PFS
Antonarakis et al 2015	OS, PFS, PSA-PFS	mCRPC	The time to death from any cause	Symptomatic progression and radiologic progression or death, whichever occurred first	NA
Antonarakis et al 2017	OS, PFS, PSA-PFS	CRPC	The interval from enrolment to death from any cause	Same as above	NA
Antonarakis et al 2014	OS, PFS, PSA-PFS	mCRPC	Same as above in 1	Same as above in 1	NA
Armstrong et al 2019	OS, PFS	mCRPC	NA	From date of registration to clinical/radiographic progression or death, whichever occurred first	
Armstrong et al 2020	OS, PFS	mCRPC	NA	Same as above in 4	
Belderbos et al 2019	OS	mCRPC	The date from enrolment to death from any cause		
Cattrin et al 2019	OS	mCRPC	The time elapsed from blood collection date and the date of death for any cause		

Chung et al 2019	OS, rPFS, PSA-PFS	mCRPC	NA	A $\geq 20\%$ increase in the sum of the soft tissue lesion diameters during computed tomography, $\gg 2$ new bone lesions on nuclear medicine bone scan, or symptomatic progression (pain aggravation or cancer-related complications)	PSA progression was defined using the Prostate Cancer Working Group 3 definition as a $\geq 25\%$ increase in PSA levels above the nadir (and by $\gg 2$ ng/ml), with confirmation ≥ 4 weeks later
De Laere et al 2019	OS, PFS	mCRPC	NA	According to Prostate Cancer Clinical Trials Working Group 3 criteria	
Del Re et al 2017	OS, PFS	CRPC		Patients must have had at least three increasing serum PSA values taken at least 2 wk before the last value of at least 2.0 ng/ml, consistent with the Prostate Cancer Working Group-2 guidelines	
Del Re et al 2021	OS, PFS	mCRPC		According to Prostate Cancer Clinical Trials Working Group 3 (PCWG3) guidelines	
Del Re et al 2019	OS, PFS	CRPC		The Prostate Cancer Working Group-2 guidelines	
Erb et al 2020	PFS	mCRPC			
Graf et al 2020	OS	mCRPC	From the time of treatment decision to death		

Gupta et al 2019	PFS	mCRPC		The date from registration to radiographic progression using PCWG2 criteria, clinical progression requiring a change in systemic therapy, or death, whichever came first	
Joncas et al 2019	OS, PFS	CRPC	NA	NA	
Kwan et al 2019	OS	mCRPC	Time from systemic treatment commencement to death from any cause		
Lorenzo et al 2021	OS, rPFS	mCRPC	The time from the date of the enrolment to the date of death due to any cause	The time from enrolment to radiographic progressive disease or death due to any cause	
Maillet et al 2019	OS, rPFS, PSA-PFS	mCRPC	NA	Radiological progression was defined using PCWG3 criteria	PSA progression was defined using PCWG3 criteria as a post-treatment PSA level increase of >25% above the nadir, which is confirmed by a second value 3 wk later and a PSA measurement of 2ng/ ml
Marín et al 2020	OS, r-PFS, PSA-PFS	mCRPC	Calculated from the date of treatment initiation to	Calculated from the date of treatment initiation to RX progression	Calculated from the date of treatment initiation to date of progression

			death or last follow-up visit		
Markowski et al 2021	rPFS	mCRPC		Clinical or radiographic progression was defined by RECIST 1.1 (soft tissue lesions) and PCWG2 (clinical and bone lesions)	
Miyamoto et al 2018	OS, rPFS	CRPC	The interval between the start of therapy and the date of death or censor	The interval between the start of therapy and the date of radiographic progression, death, or censor	
Okegawa et al 2018	OS, rPFS, PSA-PFS	CRPC	NA	Determined by independent blinded review of available radionuclide bone scans, CT, or MRI, using the PCWG2 criteria (rPFS was defined as ≥ 2 new lesions on an 8-week bone scan plus two additional lesions on a confirmatory scan, ≥ 2 new confirmed lesions on any scan ≥ 12 weeks after random assignment, progression in nodes or viscera on cross-sectional imaging, or death.)	PSA progression was determined by PSAWG2; a patient was considered as experiencing biochemical failure if their PSA post-treatment determination increased by 50% and PSA measurement was ≥ 2 ng/mL
Onstenk et al 2015	OS, PFS	mCRPC		Reported end points were based on the Prostate Cancer Working Group 2 guidelines	

Qu et al 2017	OS, PFS (TTF)	CRPC	Time from treatment initiation to death from any cause, censored at the date of last follow-up for patients who were still alive	Time from treatment initiation until the date of drug discontinuation for any reason, censored at the date of last follow-up for patients who were still on therapy
Scher et al 2018	OS	mCRPC	NA	
Scher et al 2017	OS	mCRPC	Calculated from initiation of therapy to death from any cause, with right censoring for patients alive at last follow-up	
Scher et al 2016	OS, PFS	mCRPC	Calculated from initiation of therapy to death from any cause. Patients still alive at time of last follow-up were right-censored	Radiographic progression was determined by independent blinded review of available radionuclide bone scans, CTs, or MRIs, using the PCWG2 criteria, ¹⁷ and calculated from therapy initiation until radiologically confirmed progression or death owing to any cause within 60 days of stopping treatment. Patients without evidence of radiologic progression at

				the time of last stable scan or end of therapy, whichever occurred later, were right censored	
Seitz et al 2017	OS, rPFS, PSA-PFS	mCRPC	NA	Clinical progression was defined as worsening of disease related symptoms or new cancer-related complications, radiographic progression according to Response Evaluation Criteria In Solid Tumours, two or more new bone lesions on bone scan, or death, whichever occurred first	PSA progression-free survival (PSA-PFS) according to PCWG2 criteria
Sepe et al 2019	OS, rPFS, PSA-PFS	mCRPC	The time from the date of the start of treatment to death from any cause	Defined as the time from the start of treatment to the first objective evidence of radiographic disease progression	Defined as freedom time from PSA progression
Sharp et al 2019	OS	mCRPC	Defined as time from PB draw to date of death or last follow up/contact		
Škereňová et al 2018	OS	CRPC	NA		
Stuopelyte et al 2020	PFS, OS	CRPC	The time from the initiation of the AA treatment until	The time from the initiation of the AA treatment until documented evidence of disease progression	

death from any cause				
Tagawa et al 2019	PFS	mCRPC		The time between randomization and the first documentation of radiographic tumour progression (using RECIST 1.1), clinical progression (including skeletal-related events, increasing pain requiring escalation of narcotic analgesics, urinary obstruction, etc.), PSA progression, or death from any cause. PFS was required to be confirmed at least 3 weeks after initial assessment
Todenhöfer et al 2016	OS PSA-PFS	mCRPC	NA	PSA progression according to Prostate Cancer Working Group 2 criteria
Tommasi et al 2018	PFS	CRPC		NA

**Wang
et al 2018**

PFS

CRPC

NA

Supplemental Table 3. 2 Quality assessment of included studies based on adapted NOS scales

It was hard to display this table in Excel format in Word document. Please follow the link to view this table.

https://www.ncbi.nlm.nih.gov/pmc/articles/PMC8971301/bin/Table_2.xlsx.

Supplemental Table 3. 3 Sensitivity analysis of subgroups with more than 6 studies

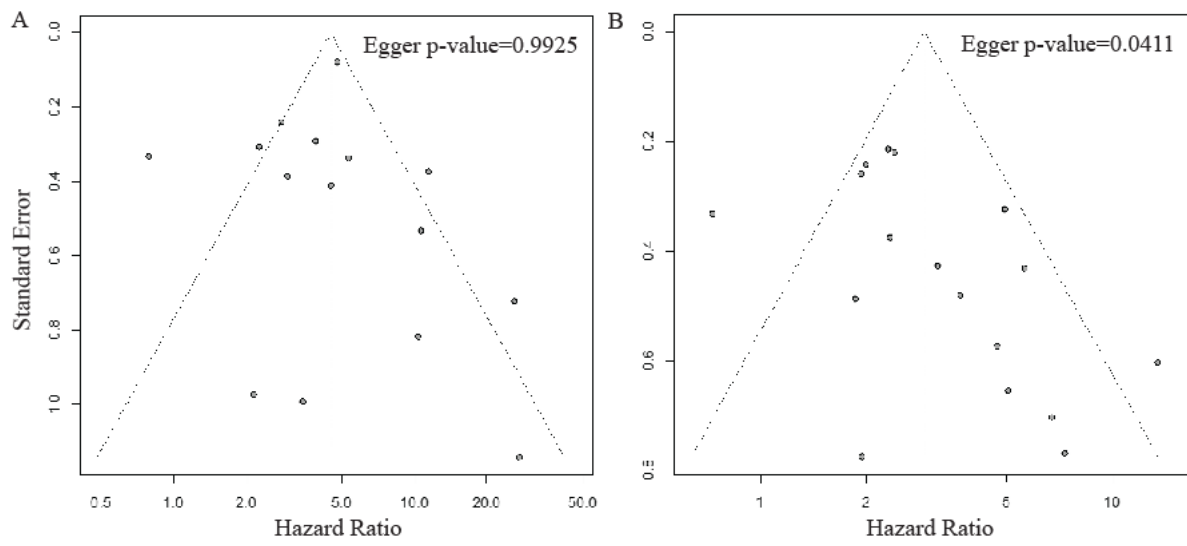
OS		
ARSi	HR (95% CI)	Test for overall effect: Z (p-value)
Antonarakis 2017	4.30 [2.88, 6.41]	7.14 (<0.00001)
Armstrong 2019	4.44 [2.95, 6.66]	7.18 (<0.00001)
Armstrong 2020	4.59 [3.06, 6.88]	7.37 (<0.00001)
Chung 2019	4.16 [2.88, 6.02]	7.56 (<0.00001)
De Laere 2019	4.63 [3.14, 6.84]	7.71 (<0.00001)
Del Re 2017	4.10 [2.80, 5.99]	7.28 (<0.00001)
Del Re 2019	4.44 [3.04, 6.48]	7.74 (<0.00001)
Del Re 2021	4.36 [2.93, 6.47]	7.30 (<0.00001)
Maillet 2019	4.38 [3.00, 6.40]	7.65 (<0.00001)
Marín-Aguilera 2020	4.83 [3.59, 6.49]	10.39 (<0.00001)
Okegawa 2018	4.46 [2.80, 7.11]	6.29 (<0.00001)
Scher 2016	3.98 [2.73, 5.79]	7.20 (<0.00001)
Scher 2017	4.20 [2.88, 6.13]	7.45 (<0.00001)
Seitz 2017	4.51 [3.04, 6.68]	7.49 (<0.00001)
Sepe 2019	3.99 [2.77, 5.74]	7.46 (<0.00001)
All included	4.34 [3.00, 6.28]	7.79 (<0.00001)
Abi		
Antonarakis 2014	6.06 [1.84, 19.89]	2.97 (0.003)
Del Re 2019	3.52 [1.50, 8.28]	2.88 (0.004)
Miyamoto 2018	5.31 [1.72, 16.42]	2.90 (0.004)
Qu 2017	11.20 [2.24, 56.03]	2.94 (0.003)

Stuopelyte 2020	11.31 [2.41, 53.11]	3.07 (0.002)
Todenhofer 2016	6.85 [1.88, 24.87]	2.92 (0.003)
All included	6.59 [2.18, 19.94]	3.34 (0.0008)
Chemo		
Antonarakis 2015	1.64 [0.95, 2.81]	1.78 (0.07)
Armstrong 2020	1.73 [0.96, 3.11]	1.82 (0.07)
Belderbos 2019	1.79 [0.96, 3.34]	1.84 (0.07)
Marín-Aguilera 2020	2.02 [1.44, 2.83]	4.10 (< 0.0001)
Onstenk 2015	1.72 [0.98, 3.00]	1.90 (0.06)
Scher 2016	1.47 [0.91, 2.39]	1.57 (0.12)
Scher 2017	1.56 [0.91, 2.65]	1.63 (0.10)
Škereňová 2018	1.69 [0.97, 2.96]	1.85 (0.06)
All included	1.70 [1.03, 2.81]	2.06 (0.04)

PFS		
ARSi	HR (95% CI)	Test for overall effect: Z (p-value)
Antonarakis 2017	3.02 [2.20, 4.14]	6.84 (< 0.00001)
Armstrong 2019	2.98 [2.15, 4.13]	6.56 (< 0.00001)
Armstrong 2020	2.99 [2.16, 4.15]	6.57 (< 0.00001)
Chung 2019	2.83 [2.10, 3.82]	6.81 (< 0.00001)
De Laere 2019	3.02 [2.19, 4.15]	6.78 (< 0.00001)
Del Re 2017	2.83 [2.09, 3.82]	6.77 (< 0.00001)
Del Re 2019	2.80 [2.09, 3.77]	6.84 (< 0.00001)
Del Re 2021	2.75 [2.04, 3.70]	6.67 (< 0.00001)
Erb 2020	2.93 [2.17, 3.96]	6.99 (< 0.00001)
Gupta 2019	2.88 [2.12, 3.93]	6.72 (< 0.00001)
Maillet 2019	2.81 [2.09, 3.77]	6.86 (< 0.00001)
Marín-Aguilera 2020	3.06 [2.39, 3.90]	8.94 (< 0.00001)
Markowski 2021	2.97 [2.19, 4.03]	6.97 (< 0.00001)
Okegawa 2018	2.76 [2.05, 3.71]	6.72 (< 0.00001)
Scher 2016	2.86 [2.11, 3.88]	6.74 (< 0.00001)
Seitz 2017	2.95 [2.16, 4.03]	6.79 (< 0.00001)
Sepe 2019	2.67 [2.03, 3.50]	7.05 (< 0.00001)
All included	2.89 [2.15, 3.87]	7.10 (< 0.00001)
Abi		
Antonarakis 2014	5.80 [1.56, 21.59]	2.62 (0.009)
Del Re 2019	3.24 [1.30, 8.06]	2.53 (0.01)

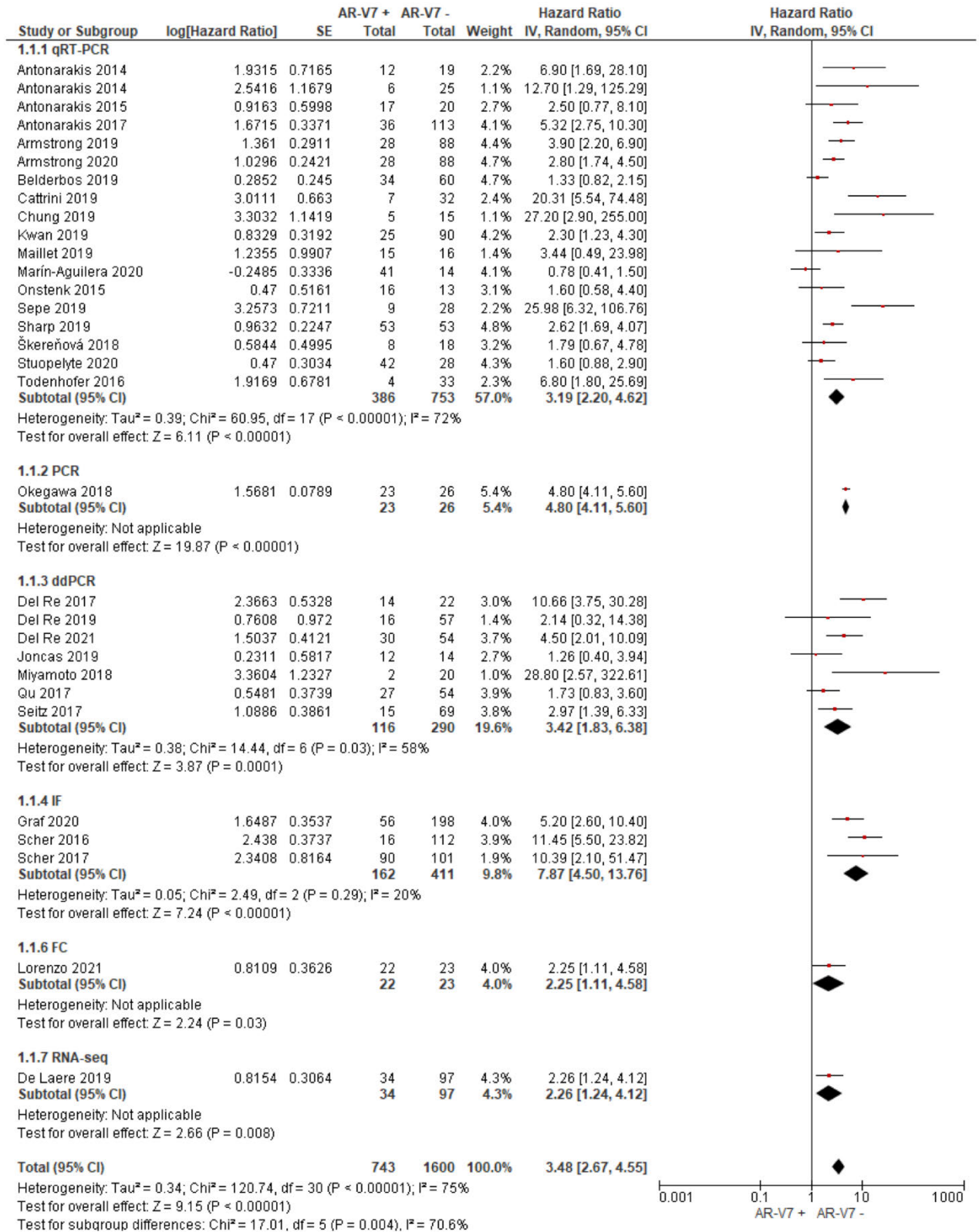
Miyamoto 2018	6.45 [1.67, 24.84]	2.71 (0.007)
Qu 2017	11.33 [1.86, 68.97]	2.63 (0.008)
Stuopelyte 2020	11.65 [2.08, 65.12]	2.80 (0.005)
Wang 2018	7.42 [1.74, 31.51]	2.71 (P0.007)
All included	6.88 [1.99, 23.73]	3.05 (0.002)
Chemo		
Antonarakis 2015	1.70 [0.60, 4.82]	1.00 (0.32)
Armstrong 2020	1.82 [0.62, 5.37]	1.09 (0.28)
Del Re 2017	1.35 [0.80, 2.28]	1.11 (0.27)
Erb 2020	1.88 [0.69, 5.11]	1.24 (0.22)
Marín-Aguilera 2020	2.19 [0.93, 5.19]	1.78 (0.07)
Onstenk 2015	2.03 [0.74, 5.59]	1.37 (0.17)
Scher 2016	1.88 [0.66, 5.35]	1.18 (0.24)
Tagawa 2019	1.71 [0.59, 4.97]	0.98 (0.32)
All included	1.81 [0.71, 4.61]	1.24 (0.21)

PSA-PFS		
ARSi	HR (95% CI)	Test for overall effect: Z (p-value)
Antonarakis 2017	5.72 [3.24, 10.12]	6.00 (< 0.00001)
Chung 2019	4.86 [2.37, 9.96]	4.32 (< 0.0001)
Maillet 2019	4.25 [2.22, 8.15]	4.36 (< 0.0001)
Marín-Aguilera 2020	5.59 [2.58, 12.09]	4.36 (< 0.0001)
Okegawa 2018	4.40 [2.20, 8.78]	4.20 (< 0.0001)
Seitz 2017	4.43 [2.22, 8.85]	4.21 (< 0.0001)
Sepe 2019	3.94 [2.15, 7.20]	4.45 (< 0.00001)
All included	4.69 [2.50, 8.82]	4.80 (< 0.00001)

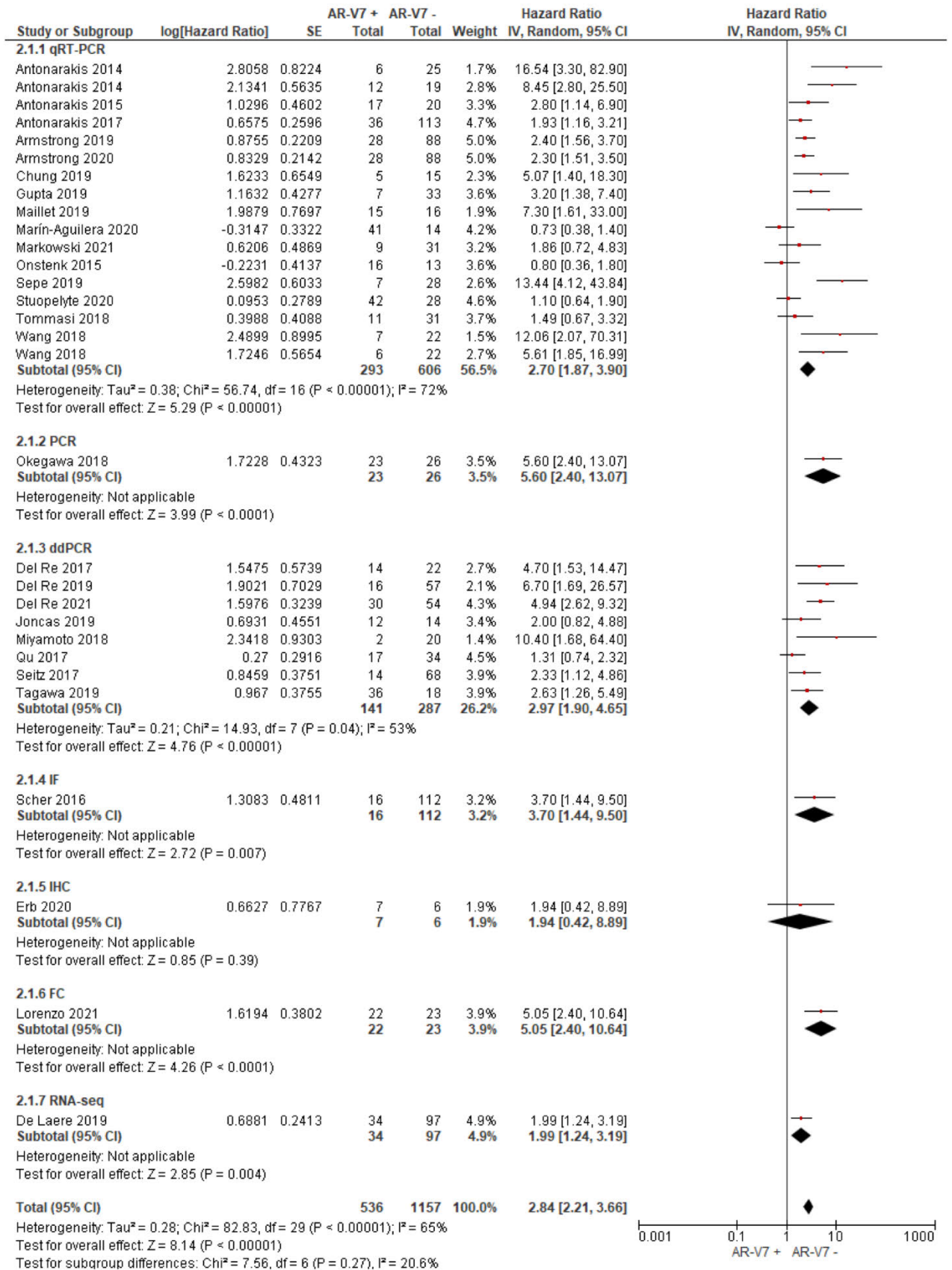


Supplemental Figure 3. 1 Inverted funnel plot to evaluate potential publication bias in OS (A) and PFS (B) of ARSi treated patients

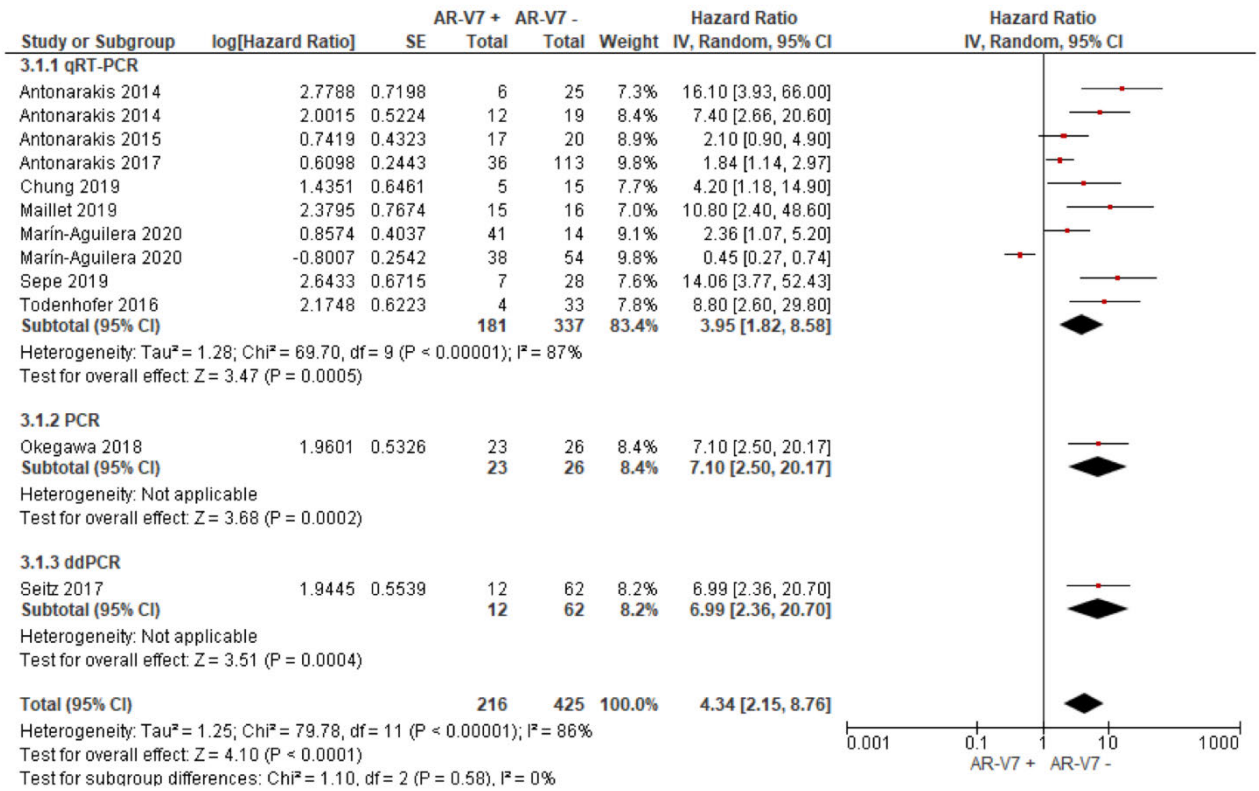
A



B



C



Supplemental Figure 3. 2 Forest plot of hazard ratios (HRs) for association of liquid biopsy AR-V7 status with OS (A), PFS (B), PSA-PFS (C) in all studies

Subgroup analyses were performed based on AR-V7 detection technique type. Pooled HRs were calculated using random effect model. AR-V7: androgen receptor splice variant 7. CI: confidence interval and bars indicate 95% CIs. PCR: polymerase chain reaction; qRT-PCR: quantitative real time PCR; ddPCR: droplet digital PCR; IF: immunofluorescence; IHC: marker immunohistochemistry; FC: flow cytometry; RNA-seq: RNA-sequencing.

3.8 Conclusion

This study establishes, using a systematic metanalysis of current literature, that use of new methodologies like liquid biopsies based ARV7 detection can help in the selection of individual best treatment option, and ultimately would be expected to improve treatment outcomes. These findings provide strong evidence that further exploration of AR-V7 as a predictive marker for CRPC, both alone and in combination with other potential biomarkers is warranted. In this study, we found that by selecting a specific therapeutic option, AR-V7 shows strong association with worse OS, PFS and PSA-PFS and thus might be useful to guide the therapy and to stratify patients for clinical trials as some trials have been done (<https://beta.clinicaltrials.gov/>). AR-V7 presence might indicate poor response to current treatment options and help decision to consider clinical trials options for the patient.

Chapter 4: Establishing Reliable Immunocytostaining for AR-V7

4.1 Introduction

From the systematic analysis of the literature presented in Chapter 3, Section 3.5, we can see that AR-V7 is linked with CRPC progression and significantly associated with worse OS, PFS and PSA-PFS. These data emphasized AR-V7 as a potential biomarker in CTCs. To date, AR-V7 immunocytostaining in CTCs as reported in the literature has relied on the anti-AR-V7 antibody clone EPR15656 [259]. Our early studies, however, showed that EPR15656 was non-specific for AR-V7 in its staining pattern, as it stained known AR-V7-negative cell lines. Given the focus of this project was on AR-V7 immunocytostaining of CTCs, it became clear that the first task was to find a suitably specific antibody for AR-V7 detection. This chapter outlines a comparison of all commercially available anti-AR-V7 antibodies. As a critical resource, our lab has well - characterised PCa cell lines with known AR-V7 status [51]. Antibodies were ranked for their staining intensity and specificity in these cell lines and PCa patient CTCs.

4.1.1 Published Manuscript

The findings from this study have been published as a preprint (DOI: <https://doi.org/10.21203/rs.3.rs-1602818/v1>) and is currently in revision for publication in the journal Scientific Reports. The manuscript text is presented below.

Publication Details: Tanzila Khan, John Lock, Yafeng Ma, David Harman, Paul de Souza, Wei Chua, Bavanthi Balakrishnar, Kieran F. Scott, Therese M. Becker.

Authors' Contributions:

Conceptualisation: TK, JL, KS, TB; Experimental/Analysis: TK, JL, YM, DH, KS, TB; Patient recruitment: PdS, WC, BB; Manuscript drafting: TK, KS, TB; Manuscript finalisation: all authors.

4.2 Abbreviation

aa Amino Acid

ADT Androgen Deprivation Therapy

AR Androgen Receptor

AR-V7 Androgen Receptor Variant 7

CRPC Castration-Resistant Prostate Cancer

CTCs Circulating Tumour Cells

CE3 Cryptic Exon 3

DBD DNA Binding Domain

ddPCR Droplet Digital PCR

FBS Foetal Bovine Serum

AR-FL Full Length AR

Knime Konstanz Information Miner

LBD Ligand Binding Domain

NTD N-Terminal Domain

PVDF Polyvinyl Difluoride

PCa Prostate Cancer

TBS-T Tris-Buffered Saline with 0.1% Tween-20 Detergent

4.3 Abstract

Background: Androgen receptor variant 7 (AR-V7) is an important biomarker to guide treatment options for castration-resistant prostate cancer (CRPC) patients. Its detectability in circulating tumour cells (CTCs) opens non-invasive diagnostic avenues. While detectable at the transcript level, AR-V7 protein detection in CTCs may add additional information.

Aims: The aim of this study was to compare commercially available anti-AR-V7 antibodies and establish reliable AR-V7 immunocytochemistry applicable to CTCs from prostate cancer (PCa) patients.

Methods: We compared seven AR-V7 antibodies by western blotting and immunocytochemistry, using a set of PCa cell lines with known AR/AR-V7 status. The best antibody was then validated for detection of AR-V7 in CTCs from CRPC patients, enriched by negative depletion of leucocytes.

Results: The anti-AR-V7 antibody, clone E308L emerged as the best antibody in regard to signal to noise ratio with a specific nuclear signal. Moreover, this antibody detects CRPC CTCs more efficiently compared to an antibody previously shown to detect AR-V7 CTCs.

Conclusion: We have determined the best antibody for AR-V7 detection in CTCs, which will enable future studies to correlate AR-V7 subcellular localisation and potential co-localisation with other proteins and cellular structures to patient outcomes.

4.4 Introduction

First line therapy for patients with metastatic PCa is androgen deprivation therapy (ADT), which targets androgen receptor (AR) signalling [2, 226]. However, ADT resistance inevitably occurs with time, and the disease is then referred to as castrate resistant prostate cancer (CRPC).

The expression of altered AR proteins translated from alternative *AR* splice variants has been proposed as a mechanism of ADT resistance [15, 16]. Expression of the AR splice variant 7 (AR-V7), is correlated with the establishment of CRPC, and is the most frequently identified disease associated variant. AR-V7 is proposed to be ligand independent and constitutively active as a nuclear transcription factor [21, 22].

Splicing of the *AR* gene including exon 1, 2 and 3 together with a cryptic exon 3 (CE3) results in the *AR-V7* transcript (Figure 4.1A). The unique cryptic exon has allowed the generation of highly sensitive and specific assays to detect AR-V7 at the mRNA level [45, 239, 257, 258]. Importantly, given the general lack of matching tumour tissue for biomarker analysis at the CRPC stage, these methods have been used to successfully detect AR-V7 transcripts from liquid biopsies, such as urine, plasma, exosomes and circulating tumour cells (CTCs), with the most reliable data originating from AR-V7 analysis in CTCs [210]. Our recent metanalysis emphasises the potential of AR-V7 detection in liquid biopsies as clinical biomarker, as it demonstrates significant correlation with patient survival overall and in context of specific treatment [2]. The presence of full-length *AR* (AR-FL) and *AR-V7* in CTCs has been investigated at the RNA level in a number of studies and CTC-based *AR-V7* was found to correlate with metastatic CRPC and primary resistance to abiraterone and enzalutamide [45, 109, 204, 206, 209].

The AR-V7 protein has 16 distinctive C-terminal amino acids, encoded by an alternate cryptic exon 3 producing a unique AR- V7 C-terminal protein domain, allowing for generation of

specific antibodies to this part of the protein. To our knowledge, seven antibodies are now commercially available designated to specifically detect the AR-V7 protein and have been raised to C-terminal peptides (Figure 4.1A). AR-V7 protein detection opens opportunities for immunobiological analysis, however, as outlined above, tissue is rarely available for advanced PCa analysis. Liquid biopsy derived CTCs lend themselves for immunocytostaining of AR-V7 in addition to mRNA information that is readily obtained from these samples. Indeed, Scher et al. reported that information regarding AR-V7 subcellular localisation within CTCs may add important information correlating to disease progression and therapy response [204, 240, 259]. This is an important finding, as it potentially increases the value of AR-V7 screening as a biomarker in PCa. Additionally, cellular AR-V7 protein analysis may enable future detailed investigations into interactions of AR-V7 with other proteins and nucleic acids to help understanding its CRPC - related functions.

Here, using a cohort of well characterised PCa cell lines with known and experimentally validated AR-V7 expression, we tested the seven commercially available AR-V7 antibodies for their ability to truly detect AR-V7 by immunoblotting and immunocytostaining. Our findings highlight the sensitivity, specificity and cross reactivities of antibodies and point towards an antibody of choice for AR-V7 immunocytostaining of CTCs. The antibody prioritised in this study performed well when employed for detection of CTCs from CRPC patients by immunocytostaining. Our finding is highly relevant for AR-V7 screening in patients to guide therapy decisions, or to stratify patients for relevant clinical trials.

4.5 Methods

4.5.1 Cell Lines

22RV1, LNCaP, VCaP, PC3 and DU145 PCa cell lines are here referred to as 22RV1^{AR+/AR-V7+++}, LNCaP^{AR+/AR-V7-}, VCaP^{AR+++/AR-V7+}, PC3^{AR(+)/AR-V7-}, DU145^{AR-/AR-V7-} according to their

published and in this study validated AR-FL and AR-V7 expression [17, 42, 269]. Cells were grown in DMEM supplemented with 10% Foetal Bovine Serum (FBS), 2 mM L-Glutamine, 4 nM HEPES or MEM supplemented with 10% FBS, 2 mM L-Glutamine, 4 nM HEPES at 37°C in 5% CO₂. Cell lines were tested to be mycoplasma free (MycoAlert Mycoplasma Detection Kit, Lonza, Rockland, USA) and STR authenticated (AGRF, Melbourne, Australia). Cells were seeded at approximately 30-40% confluency and harvested after 72 hours culture for immunoblotting and gene expression analysis.

4.5.2 Antibodies

Six rabbit anti-human-AR-V7 antibodies were compared in this study: clone EPR15656 (Abcam, VIC, Australia), clone E308L and polyclonal antibody (Cell Signaling, Danvers, MA, USA), clone SN8 (Creative Diagnostic, Shirley, NY, USA), clone DHH-1 (RQ4683, Assay Matrix, VIC, Australia), and clone RM7 (RevMab Biosciences, San Francisco, CA, USA), as well as the mouse anti-human-AR-V7 clone AG10008 (Precision Antibody, Columbia, MD, USA). The available information of antigens used for the anti-AR-V7 antibody generation is shown in Figure 4.1A. Additional antibodies used in this study are: mouse anti-human AR-FL, clone ER179 (Abcam, NSW, Australia), rabbit anti-GAPDH clone 14C10 (Cell Signaling, VIC, Australia), Alexa fluor 488 goat anti-rabbit IgG (H+L) (LOT 1423009) or Alexa fluor 488 goat anti-Mouse (H+L) (LOT 1252783) (Life technologies, Eugene, OR, USA), horseradish peroxidase-labelled donkey anti-Rabbit IgG (1:1000 dilution) (Lot 9526417, GE Healthcare, Buckinghamshire, UK) or sheep anti-mouse IgG, Horseradish Peroxidase linked F(ab')₂ fragment (1:1000 dilution) (Lot 312511, Amersham, GE Healthcare, Buckinghamshire, UK) and Alexa fluor 555 Phalloidin (Abcam, NSW, Australia).

4.5.3 Droplet Digital PCR (ddPCR)

In brief, total RNA was extracted with ISOLATE II RNA Mini Kit (Bioline, London, UK) from approximately 5×10^6 cells. The quality and quantity of RNA was tested using a fragment analyser (5200 Fragment Analyzer System, CA, USA). cDNA was synthesised from 1 μ g of total RNA per cell line using the SensiFAST cDNA Synthesis Kit (Bioline, London, UK). ddPCR to detect AR-V7 and full-length AR (AR-FL) was performed as described previously [109]. The quality of RNA was confirmed by conducting GAPDH ddPCR as described previously [210] (data not shown).

4.5.4 Western Blotting

Approximately 1×10^6 cultured cells were harvested and lysed in RIPA lysis buffer (50 mM Tris-Cl pH7.5, 150 mM NaCl, 0.5% Triton X-100, 2 mM EDTA, 2 mM EGTA 25 mM NaF, 10% glycerol) containing 1x protease inhibitors (Roche, Basel, Switzerland) for 30 minutes placed on ice, followed by maximum microfuge centrifugation speed (11,700g, 4°C, 20 minutes) and recovery of supernatant. Protein concentrations were determined using the DC protein assay kit (Bio-Rad Laboratories, Hercules, CA). 30 μ g total protein per sample was separated on 4-12% Bis-Tris gels (Invitrogen, Life Technologies) and transferred to Polyvinyl difluoride (PVDF) membrane (Amersham, GE Healthcare, Buckinghamshire, UK). Membranes were incubated with primary antibodies (dilutions see Supplemental Table 4.1) overnight under gentle agitation at 4°C. After three Tris-buffered saline with 0.1% Tween-20 detergent (TBS-T) washes, membranes were incubated with horseradish peroxidase-conjugated donkey anti-rabbit IgG (1:1000 dilution) or sheep anti-mouse IgG, horseradish peroxidase linked F(ab')₂ fragment (1:1000 dilution) for 1 hour at room temperature and again washed three times in TBS-T. Membranes were developed using Western Lightning™ Plus-ECL Enhanced Luminol Reagent Plus (LOT 275-13481) and Western Lightning™ Plus-ECL

Oxidizing Reagent Plus (LOT 265-13481) (PerkinElmer, Waltham, MA, USA) and imaging was performed with an Odyssey imager (LI-Cor Biosciences, Lincoln, NE).

4.5.5 Immunocytostaining of Cell Lines

For each cell line approximately 20,000 cells were seeded on sterile, round coverslips in 12-well plates and cultured for 72 hours followed by fixation with 3.7% paraformaldehyde for 10 minutes. Cells were permeabilized with 0.2% Triton X-100 for 10 minutes and blocked using 10% goat serum in PBS for 30 minutes. Primary antibodies were diluted in 0.5% FBS in PBS (Supplemental Table 4.1) and incubated for 1 hour. Secondary antibodies conjugated with Alexa fluor 488 goat anti-rabbit IgG (H+L) (1:5000) or Alexa fluor 488 goat anti-mouse (H+L) (1:5000) were diluted in PBS with 0.5% goat serum and incubated 30 minutes. Cells were stained with Alexa fluor 555 phalloidin for 30 minutes followed by nuclear staining by using 1x Hoechst (Fluorion, San Francisco, CA, USA) in PBS for 10 minutes. Coverslips were mounted with Pro LongTM Glass Antifade Mountant (Eugene, OR, USA). Images were taken with Olympus IX71 microscope (Olympus, Tokyo, Japan) at 20X magnification with consistent exposure times.

4.5.6 CTC Enrichment and Immunocytostaining

For each patient, 2 x 9 mL peripheral blood was collected into 2 EDTA vacutubes (Greiner Bio-One) and processed within 24 hours. Eighteen mL blood was used to isolate CTCs using RosetteSepTM CTC enrichment cocktail containing anti-CD36 (Stemcell Technologies, Victoria, Australia) according to the supplier's instructions. In brief, blood was incubated with antibody cocktail for 10 minutes and then diluted with 2% FBS in PBS as recommended by the manufacturer, transferred to a Sepmate tube containing lymphoprep density gradient medium (Stemcell technologies, VIC, Australia) and centrifuged at 1200 x g for 10 minutes. The supernatant with cellular layer was recovered and topped up to 50 mL with 2% FBS in PBS

and gently mixed. After a 10 minutes 300 x g spin, the supernatant was discarded, and cells were suspended in residual fluid by gentle tapping. Cells were washed once with PBS and spun again (300 x g, 10 minutes), resuspended in 1.5 mL PBS and transferred to a well of a 24-well glass bottom plate (Greiner Bio-One GmbH, Frickenhausen, Germany) coated with 3.5 µg of CellTak (FAL354240, InVitro technologies, VIC, Australia) per cm². After spinning the cells onto the glass (200 x g, 10 minutes) immunocytostaining was essentially performed as above including probing for CD45 to exclude lymphocytes and Hoechst to secure nucleated cellular identity.

4.5.7 Image Analysis and Statistics

Image J (1.53c, National Institute of Health, USA) was used for RGB stacking and merging of images before doing quantitative image analysis using CellProfiler (Broad Institute, MIT, Massachusetts, USA) an automated image analysis software to measure biological phenotypes in images [270]. CellProfiler segmented cell data for at least 150 cells per sample (nucleus and cytoplasm) based on staining and extracted data on nucleus, cell body and cytoplasm and AR-V7 intensity were saved in excel to transfer to Konstanz Information Miner (Knime) [271]. The quantitative data from CellProfiler was used in Knime to compare the intensity of AR-V7 detected by different antibodies as well as cellular localisation of AR-V7.

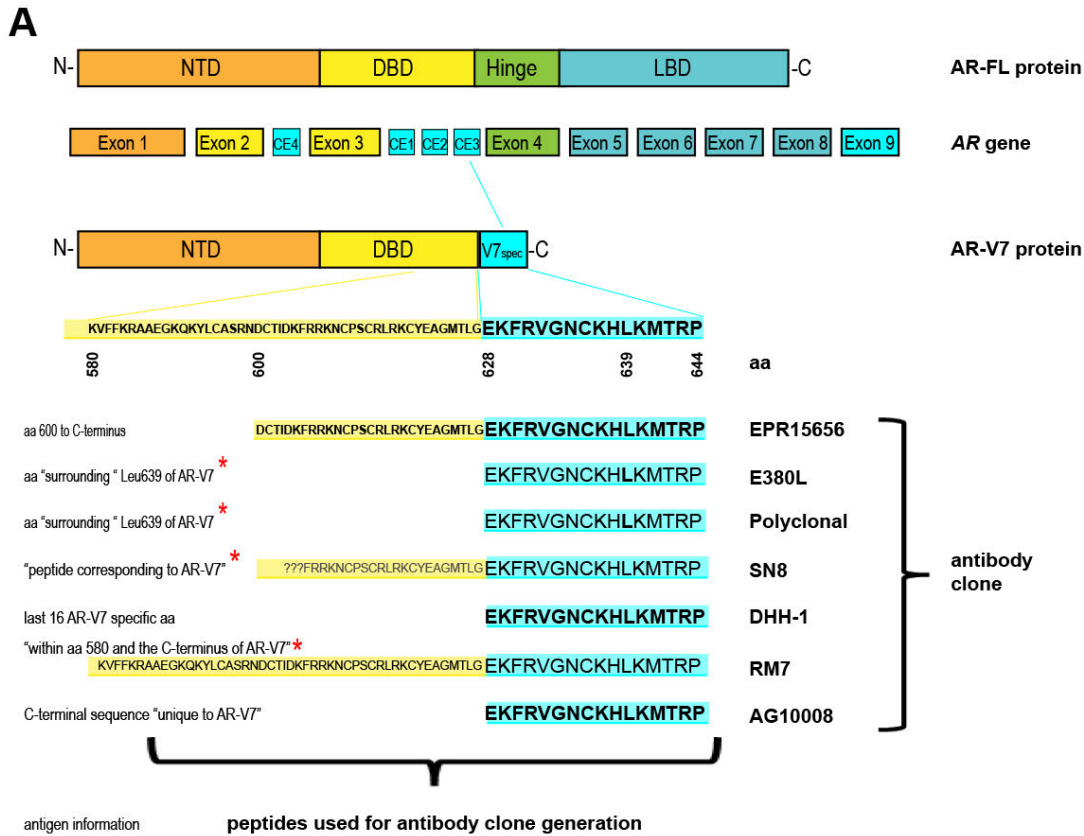
4.6 Results

For any antibody to be selective for AR-V7, it must recognise a C-terminal peptide epitope corresponding to the 16 amino acid peptide sequence (EKFRVGNCKHLKMRP) unique to AR-V7, encoded by the cryptic exon 3. Supplier information regarding the exact antigens used for antibody generation is considered imprecise for five of the seven antibodies tested here. Nevertheless, one can deduce that the entire 16 amino acids, or most, are part of any antigenic peptide used for antibody generation. Three of the antibodies are known or implied to have

antigen peptides containing parts of at least the DNA binding domain (DBD) shared by AR-V7 and AR-FL (Figure 4.1A) [51].

To be able to compare these antibodies, the AR-V7 status of several PCa cell lines was validated. ddPCR confirmed high and detectable AR-V7 in 22RV1^{AR+/AR-V7+++} and lower but readily detectable transcript AR-V7 expression in VCaP^{AR+++/AR-V7+}, while AR-V7 is negative for LNCaP^{AR+/AR-V7-}, PC3^{AR(+)/AR-V7-}, DU145^{AR-/ARV7-}, ddPCR also confirmed known AR-FL status for all lines (Figure 4.1B).

To test whether all of the anti-AR-V7 antibodies interact with a protein of the expected AR-V7 size of ~80 kDa in our AR-V7 expressing cell lines, or whether the antibodies may cross react with other proteins, we first tested the antibodies by immunoblotting of full protein lysates from all cell lines (Figure 4.1C). We also included an anti-AR-FL antibody to clarify whether the AR-V7 antibodies identified protein bands of AR-FL size. None of the specific anti-AR-V7 antibodies produced a band considered AR-FL. Interestingly, only the anti-AR-V7 antibody clones E308L, SN8, RM7 and AG1008 produced a distinct band appearing around the expected AR-V7 size for AR-V7 positive 22RV1^{AR+/AR-V7+++} and VCaP^{AR+++/AR-V7+} cells, while not detecting anything above background in AR-V7 negative cell lines in that protein size range. However, there was clearly some cross-reactivity detected for proteins of smaller size. We considered E308L was the “cleanest” antibody with negligible cross-reactivity detected for AR-V7 negative cell lines. SN8, RM7 and especially AG1008 produced strong reaction to proteins of other size than 80 kDa in all, including AR-V7 negative cell lines with one band appearing relatively dominant just below the 28 kDa range.



B

	22RV1 ^{AR+/AR-V7+++}	LNCaP ^{AR+/AR-V7-}	VCaP ^{AR+++/AR-V7+}	PC3 ^{AR(+)/AR-V7-}	DU145 ^{AR-/AR-V7-}
AR-FL	+	+	+++	(+/-)	-
AR-V7	+++	-	+	-	-

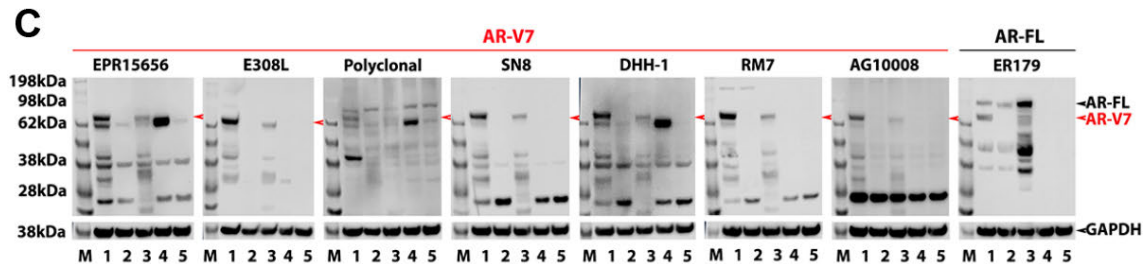


Figure 4. 1 AR-V7 specific peptide and antigens for antibody generation

(A) Schematic presentation of the *AR*-gene encoding full length androgen receptor (AR-FL) and androgen receptor variant 7 (AR-V7) proteins. Amino acid (aa) sequences of cryptic exon (CE) 3 encoded AR-V7 specific domain (V7_{spec}) and a section of DNA binding domain (DBD) shared with AR-FL are displayed and aa sequences representing antigens for antibody is indicated for the clones. Antigen information: as published by supplier or provided on request

(*: information is considered ambivalent for four peptides, consequently shown aa sequences may not reflect exact antigen peptides, but are based on “informed assumption” that the V7spec unique 16 aa are part of all peptides and uncertain proportions of the DBD shared with AR-FL as indicated); ???: DBD aa sequences uncertain; the epitope for AR-FL antibody ER179 is not publicly available. NTD: N-terminal domain; LBD: ligand binding domain; N-: N-terminal; -C: C-terminal. **(B)** Validation of AR-FL and AR-V7 mRNA expression in the indicated cell lines by ddPCR. -: no detection; + detection; +++ high levels of AR-V7 or AR-FL copies. The classification of cell lines in different groups was done according to the number of copies per 20 μ L. For AR-FL, if the number of copies was above 1000 copies per 20 μ L, the cell line was represented as +++ and if less than 1000, the cell line was classified as +. For AR-V7, if the number of copies was above 50 copies per 20 μ L, the cell line was represented as +++ and if less than 1000, the cell line was classified as +. If there is no expression of AR-FL or AR-V7, the cell line was classified as -. **(C)** Immunoblotting of total protein lysates from the indicated cell lines for AR-V7 (left panel), or AR-FL (right) using the indicated antibodies in reference to GAPDH. M: size marker, 1: 22RV1^{AR+/AR-V7+++}, 2: LNCaP^{AR+/AR-V7-}, 3: VCaP^{AR+++/AR-V7+}, 4: PC3^{AR(+)/AR-V7-}, 5: DU145^{AR-/AR-V7-}.

Two anti-AR-V7 antibodies (EPR15656 and DHH-1), while detecting protein bands corresponding to AR-V7 size in 22RV1^{AR+/AR-V7+++} and VCaP^{AR+++/AR-V7+} cells, also detected a very strong band in AR-V7 negative PC3^{AR(+)/AR-V7-} cells, while additional bands across cell lines suggested further cross-reactivity for these antibodies. The prominent PC3^{AR(+)/AR-V7-} protein band was just below the expected AR-V7 size. AR-V7 detection with the polyclonal antibody proved to be nonspecific. (Figure 4.1C).

Although there was a low likelihood that PC3^{AR(+)/AR-V7-} with undetectable AR-V7 transcript expressed a slightly truncated form of AR-V7, we wished to rule out the AR-V7 identity of this band detected close to 80 kDa. Firstly, we conducted protein Blast searches (blast.ncbi.nlm.nih.gov/Blast.cgi?PAGE=Proteins) of the full AR-V7 specific 16 amino acid sequence as well as the sequence from amino acid 580 and 600 (see Figure 4.1A) to the C-terminus of AR-V7 against the human protein database (<https://www.uniprot.org>), which identified only the AR-V7 splice variant and for the 580/600 to C-terminus peptide additionally to AR-V7 the partially homologue AR variant 5 (see ref [272] for review of AR variants). We were also able to elute the PC3^{AR-/AR-V7-} band of interest from a gel to perform mass spectroscopy, and the retrieved data confirmed our Blast data, with no proteins detected that share homology to AR-V7 or AR-FL in the excised protein band of interest from PC3^{AR-/AR-V7-} cells (data not shown).

With Western analysis already pointing towards clear specificity differences between the antibodies tested, we excluded two antibodies from further analysis - the polyclonal due to lack of specificity for AR-V7 detection sensitivity and specificity by Western analysis, and the mouse monoclonal AG10008. The latter was excluded due to very strong cross-reactivity in all cell lines with a protein band at ~28 kDa compared to specific AR-V7 band intensity. In our established CTC workflow, antibodies of rabbit origin are more easily integrated for technical reasons. Initial immunocytostaining analysis of the five remaining antibodies was performed,

focusing on the AR-V7-positive cell line, 22RV1^{AR+/AR-V7+++} and the AR-V7-negative cell line LNCaP^{AR+/AR-V7-}.

Representative immunocytostaining images of all remaining antibodies in the two cell lines used for monochromatic analysis of staining intensity and subcellular localisation are shown in Figure 4.2.

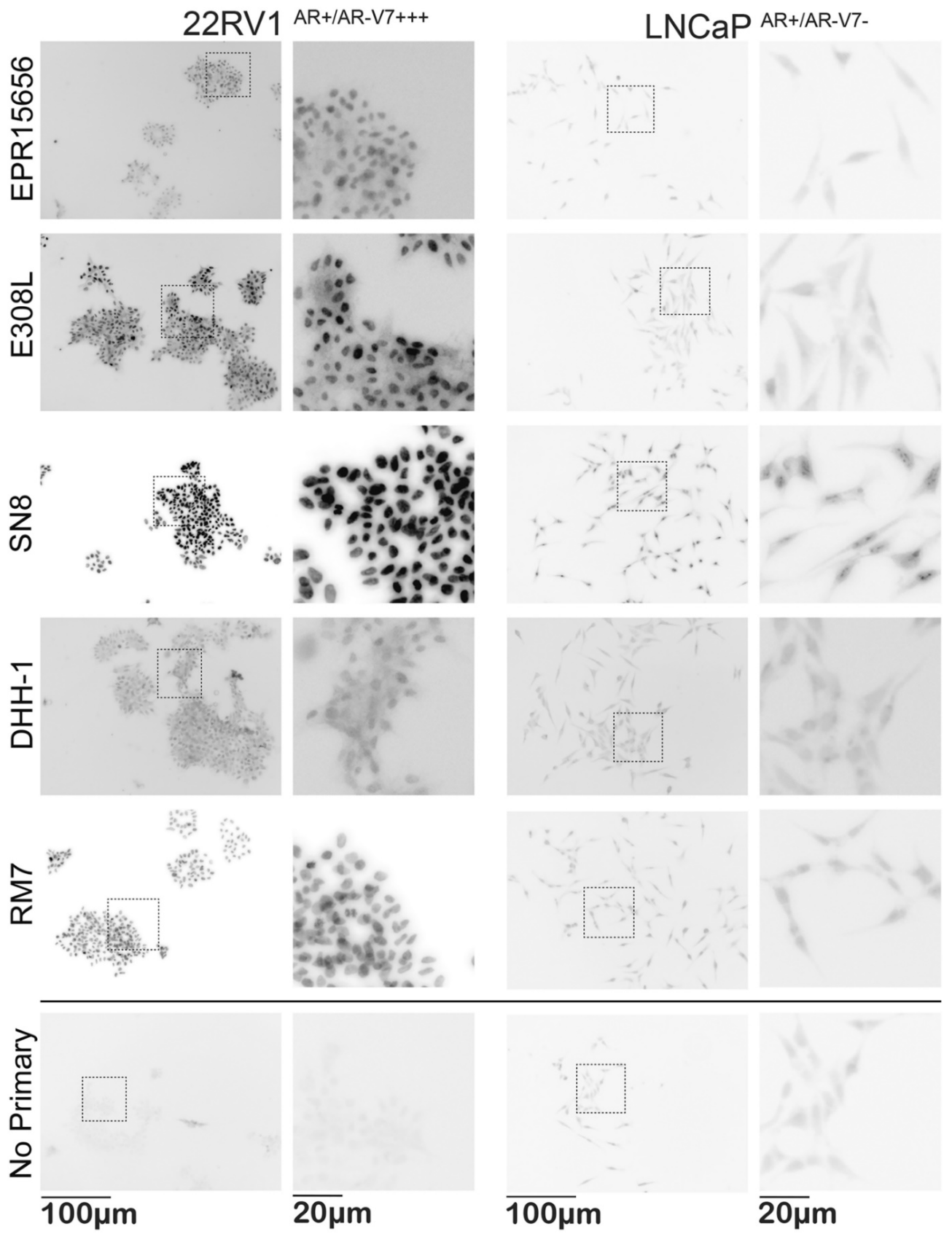


Figure 4. 2 AR-V7 staining with different antibodies in AR-V7 positive and negative cells

AR-V7 staining with different antibodies in AR-V7 positive and negative cells. Immunocytostaining was performed with the indicated antibodies on 22RV1^{AR+/AR-V7+++} and LNCaP^{AR+/AR-V7-} cells in comparison to no-primary antibody controls. Images were acquired with identical acquisition settings, with no pixel intensity saturation in the brightest cell labelling conditions. This enables quantitative comparison of intensity values across all antibodies and cell lines. Here, monochrome images are presented inverted, allowing easier visual detection of low intensity labelling patterns. Overview visual fields of stained cells are shown to the left with higher magnification images for representative regions (dotted boxes) to the right.

In comparison to “no primary” control staining, we analysed intensity of staining, and subcellular localisation of staining, as specific AR-V7 staining is expected to be predominantly nuclear [43]. Initial subjective visual analysis clearly favoured the E308L and SN8 antibodies that show distinct nuclear AR-V7 staining in 22RV1^{AR+/AR-V7+++}, however, SN8 produces what appears to be cross-reactivity with nucleolar structures in the negative control LNCaP^{AR+/AR-V7-} cells. EPR15656, DHH-1 and RM7 appear to produce less distinct staining in 22RV1^{AR+/AR-V7+++} vs. LNCaP^{AR+/AR-V7-} cells. Analysing images using unbiased digital image analysis essentially confirmed these observations, presented in Figure 4.3 for nuclear intensity.

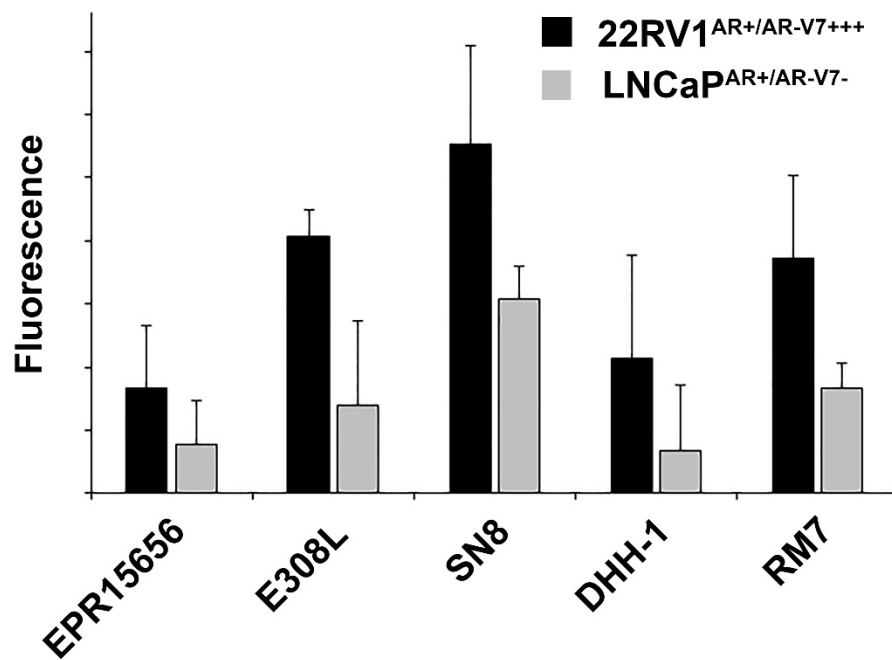


Figure 4. 3 AR-V7 staining nuclear intensity

AR-V7 staining nuclear intensity. Cells (imaged as presented in Fig. 4.2) were segmented using CellProfiler based on identification of Hoechst as a nuclear marker and Alexa fluor 555 phalloidin as a cell body marker. This permitted selective measurement of AR-V7 labelling intensities in individual whole cells, as well as in nuclear and cytoplasmic compartments, per cell. Here, nuclear AR-V7 labelling intensity (average and standard deviation of at least 150 cells per condition) is depicted after normalisation to control values (no primary antibody labelling), allowing comparison of antibody signals in 22RV1^{AR+/AR-V7+++} and LNCaP^{AR+/AR-V7-} cells. Fluorescence (Y-axis): in arbitrary units. The antibodies comparison between positive and negative cell lines P values are: EPR15656:0.77, E308L: 0.029, SN8: 0.059, NSJ: 0.258, RM7: 0.058 list all antibodies (Statistical test: student unpaired t test using prism).

E308L produced the second highest nuclear staining intensity after SN8 in 22RV1^{AR+/AR-V7+++} cells, and that corresponded to the second lowest nuclear staining intensity in AR-V7 negative LNCaP^{AR+/AR-V7-}. Since the staining in LNCaP^{AR+/AR-V7-} can be attributed to non-specific antibody binding, we concluded that E308L is the antibody with the best signal detection to noise ratio for AR-V7 immunocytostaining.

The goal of this study was to find the best suited anti-AR-V7 antibody to probe and analyse AR-V7 in CTCs. While EPR15656 has been solely used in the literature for AR-V7 immunocytostaining in CTCs [42, 43], our data suggested that E308L was better. A final comparison of both antibodies, E308L and EPR15656, was made by their ability to detect CTCs isolated from a small number of CRPC patients. Our data show that E308L detected PCa patient CTC counts in consistently higher numbers, indicating higher sensitivity. In addition, the heterogeneity of AR-V7 expression becomes more apparent since detection efficiencies are between 7-308% higher using E308L (Table 4.1). Representative CTC detection with both antibodies is shown in Figure 4.4.

Table 4. 1 AR-V7 staining CTC detection by antibody

Patient	CTC counts	
	E308L	EPR15656
1	38	23
2	29	20
3	69	64
4	45	5
5	173	95
6	184	45

P value = 0.03 (Wilcoxon matched pairs signed rank test was performed using using prism)

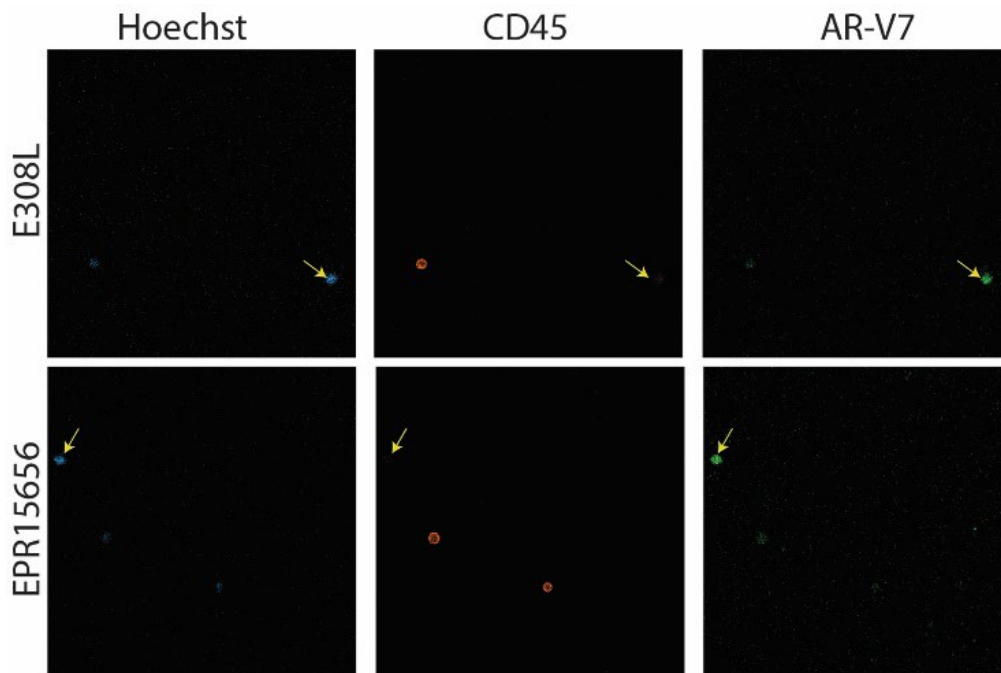


Figure 4. 4 AR-V7 CTC detection

Nucleated (blue, Hoechst) events were included in CTC counts if negative for CD45 (orange) and positive for AR-V7 (green).

4.7 Discussion

Here, we compared various antibodies in detection of AR-V7 by immunocytostaining with the ultimate focus of detecting AR-V7 positive CTCs from PCa patient blood samples. Initially PCa cell lines with known and confirmed status of AR-V7 expression (Figure 4.1B), provided the tools to test cross-reactivity of antibodies in AR-V7 negative cells while specific staining and its subcellular localisation could be determined in AR-V7 expressing cells. Western analysis helped to determine sensitivity and specificity of antibodies first, since higher cross-reactivity for immunocytostaining is suggested by the appearance of cross-reactive bands in AR-V7 negative cells, and for molecular weights other than the ~80 kDa of AR-V7 in positive cells. Indeed the “more specific” antibody by Western analysis, E308L, also emerged as our favoured antibody for immunocytostaining as well. The other antibody that performed well for immunocytostaining in AR-V7 positive 22RV1^{AR+/AR-V7+++} cells, clone SN8, caused clearly noticeable nuclear staining in AR-V7 negative LNCaP^{AR+/AR-V7-} cells, interestingly of nucleolar appearance. Therefore, the use of this antibody for CTC detection could cause false positive AR-V7 detection in the cellular compartment that has been linked to AR-V7 activity [43], confounding the potential for “true” biomarker detection.

AR-V7 detection in CTCs by immunocytostaining has been reported previously using the ERP15656 antibody [42, 43]. This prompted us to do a direct comparison of CTC detection in parallel patient blood samples with our favoured E308L as well as the ERP15656 antibody. The E308L did not only consistently detect more CTCs in liquid biopsies from a small cohort of 6 patients (Table 4.1), but did so to different extents, possibly reflecting heterogeneous AR-V7 protein levels in patient CTCs. Non-specific bands seen with Western would indicate that the relevant antibody would possibly also detect more cells with immunostaining, although likely due, in part, to non-specific binding. This is not what we saw. The more specific antibody E308L showed better sensitivity than EPR15656 and increased the number of CTCs stained.

However, we need to consider that detection by western is different from detection by immunocytochemistry as western uses SDS-page separation after complete denaturing of proteins while immunocytochemistry uses only fixing. Thus, western may well detect more unspecific proteins.

More work is needed to verify the extent and heterogeneity of AR-V7 levels in CTCs. So far EPR15656 staining has shown correlation of AR-V7 CTC staining with patient outcome [43]. Nevertheless, evaluation in larger patient cohorts is needed to clarify if AR-V7 detection in CTCs by immunocytochemistry is better suited to predict patient outcome than detection by mRNA, or if indeed a combination of both methods may have benefit. A clear benefit of detecting the AR-V7 protein rather than only mRNA in CTCs is that it opens opportunities to evaluate cell by cell heterogeneity and how AR-V7 expression and sub-cellular localisation is related to that of other proteins, which may not only add to our understanding of AR-V7 function but reveal ways of therapeutically targeting it in the future.

Here we evaluated the commercially available antibodies against AR-V7 for utility in immunocytochemistry of cell lines with known AR-V7 status and for CRPC patient CTCs. The clone E308L emerged as the favoured antibody, considering sensitivity and specificity, as shown by immunoblotting and signal to noise ratio in immunocytochemistry. With the growing appeal of liquid biopsies in diagnostic settings, identification of the best antibody to detect AR-V7 in CTCs should help to develop a standardised approach for AR-V7 screening in patient CTCs.

4.8 Supplementary Material

Supplemental Table 4. 1 Anti-AR-V7 antibodies and working dilutions

Host [Clone]	Western blot	Immuno- Cytostaining
R [EPR15656]	1:1000	1:100
R [E308L]	1:500	1:100
R [polyclonal]	1:1000	1:100
R [SN8]	1:2000	1:100
R [DHH-1]	1:500	1:50
R [RM7]	1:1000	1:100
M [AG10008]	1:250	1:100

R: rabbit; M: mouse;

4.9 Conclusion

This study not only enabled the identification of the best anti-AR-V7 antibody for immunocytostaining (i.e., E308L), the data clarify that AR-V7 CTC detection is more sensitive using E308L compared to detection with an anti-AR-V7 antibody previously reported for CTC probing. Furthermore, the data while preliminary and only relying on a small patient cohort (see COVID Impact Statement), suggest a degree of heterogeneity of AR-V7 levels in different CTCs, which needs further validation. Importantly for this project, given the higher specificity of E308L compared to other anti-AR-V7 antibodies, we predict it to perform more reliable in multiplex immunocytostaining of cells, including CTCs. Multiplex staining will allow for study of AR-V7 in different contexts including interaction with important signalling pathways in PCa in liquid biopsies (CTCs).

Chapter 5: Method Development for Single Cell Multiplex Proteomic Microscopy with a View to Study Relationships Among the AR, AKT and Hippo Signalling Pathways in Prostate Cancer

5.1 Introduction

As detailed in Chapter 1, Section 1.8, liquid biopsies are an alternative biomarker information source to tumour biopsies and are being utilised at least in research settings, in many cancers including prostate cancer. Liquid biopsies have the advantage, over tissue biopsy, of being minimally invasive and therefore may be repeated several times during a patient's cancer progression, thus providing an up-to-date analysis of the cancer both at therapy commencement and during treatment. CTCs are rare cells shed by the tumour into the bloodstream. These cells can be isolated and enriched from blood and subjected to detailed analysis for clinically relevant biomarkers [50]. The ultimate goal of this PhD project is to develop methodologies that will allow *future* detailed proteomic analysis of CTCs using multiplex immunocytostaining ("proteomic microscopy") and *future* evaluation of CTC multiplex staining for its potential to screen for clinically relevant biomarkers. These approaches will enable the study of relative expression and cellular localisation, at the single-cell level, of protein components of complex signalling networks [273] that are relevant in the progression of ADT-sensitive PCa to CRPC. In turn, this information may be useful in the stratification of PCa patients for clinical trials and in monitoring changes in the multiplex CTC profile in response to therapy. Ultimately, multiplex CTC analysis may guide treatment decisions.

The unique "proteomic microscopy" method of single cell analysis optimised by co-supervisor Dr John Lock [273], which we plan to transfer to CTC analysis, relies on a semi-automated workflow that allows for cells to be stained for various markers using immunofluorescence and

then imaged, followed by elution of the first staining cycle antibodies and re-staining and re-imaging of the same cells for a suite of new antigens in staining-imaging cycle 2 and further staining-imaging cycles. A sophisticated machine learning analysis pipeline can then be used to correlate high resolution cellular and subcellular staining with patient data [273].

To allow transfer of this method to multiplex immunocytostaining of CTCs, we have to consider a number of issues and develop approaches suitable for proteomic microscopy of CTCs (Figure 5.1).

a. CTC Enrichment: Since CTCs are very rare events with numbers of cells in a 10 mL blood sample often only in the single digits, we need to establish the best way of isolating or enriching these cells that is efficient to minimise cell loss, reliable and gentle to not alter cellular protein patterns. Ideally an unbiased method (not selecting for expression of certain proteins) would be used for the enrichment process.

b. CTC Immobilisation: To enable repeated cycles of staining, imaging, antibody elution and restaining it is an absolute prerequisite that the cells of interest, here CTCs, are reliably immobilised on glass slides or glass-bottom-plate wells, so they can be repeatedly located, phenotypically unchanged, for a series of imaging cycles. This allows for images from various cycles to be overlaid and merged to visualise expression and subcellular location and co-localisation of the various antigens of interest in individual cells.

c. Antibody Optimisation: All the antibodies used for this study need to be selected considering potential for parallel and sequential staining and need careful optimisation to achieve reliable staining.

The development of methods addressing these issues forms this chapter, which also contains some additional experimental work associated with Chapter 4, not mentioned in detail in that chapter.

Methods development

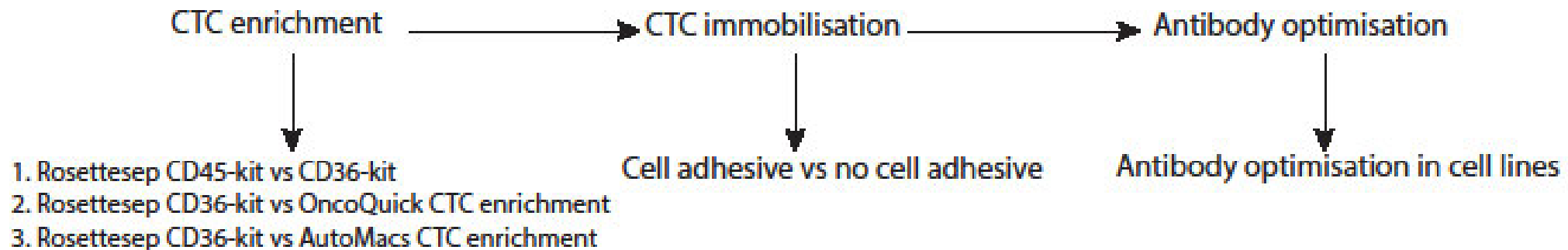


Figure 5. 1 Multiplex CTC analysis methods development

CTC enrichment by removing unwanted cells by immunodepletion followed by density centrifugation, immobilisation to attach CTC to the optical surface and antibody optimisation was initially established by mimicking CTCs by spiking defined numbers of cultured PCa cells into healthy donor blood.

As reviewed in Chapter 1, Section 1.9, traditionally, CTC enrichment protocols rely most commonly on immuno-targeted CTC capture by enriching cells that express tumour-specific cell surface proteins that are generally absent from normal blood cells. As indicated, this approach may miss certain CTCs not expressing these proteins. Specifically, the most common methods for targeted CTC isolation capture only CTCs that express the epithelial cell adhesion molecule (EpCAM) which may not be present on CTCs that have undergone EMT, or only at reduced levels [274-276]. EMT may be an important feature of cancer cells that have acquired resistance to therapy and thus this study aims to evaluate EMT phenotypes in CTCs, as well as the activity of signalling pathways. While there are targeted enrichment methods that can account for EMT CTCs [198], our team has previously successfully used an unbiased method of CTC isolation for culture of CTCs [277]. The method relies on the removal of blood cells rather than capture of CTCs using the RosetteSepTM CTC enrichment cocktail (Stemcell Technologies, Victoria, Australia) kit with anti-CD36, and is thus not biased towards specific protein presence. The advantage of the RosetteSep methods is that they are relatively gentle on the cells, evidenced by CTCs remaining viable as they can be grown in culture [277]. We considered that RosetteSep CTC enrichment should have minimal effects on the proteomic landscape of even rapidly changing proteins (such as phosphorylated proteins, relevant in signalling). There are two main candidate RosetteSep kits available here referred to as “CD36-kit” and “CD45-kit” (Stemcell technologies, Melbourne, VIC, Australia). The principal of the CD36-kit is based on enrichment of CTCs from fresh whole blood by negative depletion of blood cells. CD36-kit removes the unwanted cells by crosslinking lymphocytes through targeting a number of lymphocyte specific cell surface markers including CD2, CD16, CD19, CD36, CD38, CD45, CD66b with glycophorin A expressed on the surface of red blood cells (RBCs). Significant numbers of lymphocytes/undesired cells are then pelleted and removed together with RBCs using density centrifugation. Any enriched tumour cells will locate

together with the residual lymphocytes in the interface between plasma and density gradient medium. The CD45-kit crosslinks all nucleated blood cells to RBCs which are pelleted with density centrifugation. The tumour cells are present in the interface between density gradient medium and plasma together with residual lymphocytes. This chapter describes the comparison of these RosetteSep kits to define the best CTC recovery and lymphocyte removal (i.e., fewer residual lymphocytes in the final CTC sample). Additionally, our team also uses traditional CTC enrichment methods based on EpCAM-targeted CTC isolation with either the IsoFlux or the the AutoMacs cell isolation platforms [51, 210, 211, 278]. For PCa CTCs, our lab predominately uses AutoMacs CTC enrichment [211]. Thus, I designed experimental workflows to compare RosetteSep CTC enrichment kits with AutoMacs EpCAM-based CTC enrichment in several experiments. Finally, a new unbiased method of CTC enrichment, OncoQuick CTC enrichment, allegedly better than Ficoll-based density gradient centrifugation [279] has recently been released and despite some supply problems (see COVID impact statement) I was able to obtain this kit for testing.

It is important to emphasize that there are general considerations for CTC enrichment method comparisons: to make direct comparison of multiple methods would require the enrichment of CTCs from parallel drawn patient blood samples, and this is generally not feasible. For each method tested, 5-10 mL of patient blood is needed. Our ethics approval would not allow us to take 40- or 50-mL blood from a cancer patient to compare four or five methods. Generally, initial comparisons of CTC enrichments may be performed using healthy donor blood which is spiked with a defined number of cultured cells. However, the issue remains, and although we would be able to draw larger volumes of blood such as 50 mL from healthy donors, in reality recruitment of donors is quite difficult for more than 20-30 mL blood draws. Additionally, an ultimate test using patient samples is still desirable, as cultured cells usually represent a relatively homogeneous population of cells selected for by tissue culture conditions,

while CTCs are known to be relatively heterogeneous even if analysed from one patient, let alone different patients [280]. Our solution was that comparisons of methods were done sequentially. This strategy was also more practical as processing in some cases relies on quite different experimental manipulations which are difficult to perform in parallel by one operator.

5.2 CTC Enrichment

The first comparison for CTC enrichment to be conducted was the CD45-kit versus CD36-kit based RosetteSep enrichment, followed by the resulting better method being tested against either AutoMacs CTC enrichment or OncoQuick CTC enrichment-based CTC isolation protocols.

5.2.1 Foundations for CTC Enrichment Experiments

To test unbiased and targeted CTC enrichment methods, initially cultured PC3 cells (see Chapter 2, Section 2.3.2 for culture conditions) were used to model CTCs.

For all spiking experiments, in order to protect cell surface proteins, which may be degraded by trypsin digest, PC3 (or 22RV1) cells were detached by using 0.2 mM EDTA in PBS and cells spiked into 9 mL blood drawn from healthy donors into EDTA tubes (the same donor for each experimental comparison).

Enrichment experiments relied on either of two possible strategies of CTC detection for enumeration, labelling cultured cells prior to spiking with “Cell Tracker”, thereby allowing direct fluorescent microscopy CTC detection to distinguish PC3 CTCs from residual lymphocytes or immunocytostaining of non-labelled cells.

Cell Tracker: To allow easy detection of enriched modelled CTCs, cell tracker (AF555) (Invitrogen) was added to PC3 cells at 1:1000 dilution and cancer cells for intended spiking experiments preincubated for 20 minutes.

Immunocytostaining: Cells were not pre-labelled, and CTCs identified using immune detection of cytokeratin in nucleated (Hoechst positive) events and exclusion of CD45 staining.

Set up of cell spiking: Spiking of an exact relatively small cell number is not a trivial exercise. Haemocytometer counts have a user to user, but even a count to count, variation by the same operator. Generally, a count within $\pm 10\%$ is considered acceptable if the aim is to seed relatively high numbers of cells for culture. However, in using haemocytometer cell counts to determine dilution to produce accurate small numbers of cells, even a 10% variation is not preferred, since dilution steps will increase inaccuracies further by the likely introduction of an additional error of at least 10% variation (estimated by our laboratory). This issue has been reviewed for spiking cultured cells into blood to mimic CTCs [281, 282]. Essentially to improve accuracy, recounts of diluted cell suspensions are required. These recounts can be done in the diluted cell suspension before spiking, but that means delay of the spiking, which may affect the biology of mimicked CTCs, but also can further affect spiking accuracy as cancer cells are heavy enough to slowly precipitate, and suspensions need to be constantly agitated to increase the chance of maintaining a uniform cell density in suspension. The other way to proceed experimentally, is to accept the inaccuracy of haemocytometer counting and dilution to define a certain cell number in the spiked cell suspension volume (for example a diluted cell dilution is calculated to have 500 cells in 70 μL); this strategy relies on production of input controls. Example: 70 μL of cell suspension with the calculated cell number of 500 is pipetted onto a glass slide, then 70 μL of the same cell suspension each is spiked into 9 mL blood samples needed for CTC isolation comparisons, and then 70 μL is again pipetted onto a glass slide. This produces two input control slides (a pre- and a post spiking input) which will be airdried and from which, more accurate cell numbers will be enumerated. Quality experiments should ideally have less than 10% deviation between cell numbers of both input controls, and these will be averaged to more accurately determine the “real” spiked cell

number, which is the base of defining efficiencies of “CTC” capture. The second strategy is the method that was used in this project; see Table 5.1 for a typical example of calculated cell numbers compared to experimental input controls used in this project.

Table 5. 1 Example of calculated cell counts vs. input control cell counts

		Actual cell counts		
	Calculated cell count	Pre-input cell count	Post-input cell count	Average
CD36 CD45- 1	500	514	440	477
CD36 CD45- 2	500	491	449	470

The input controls are equivalent to the number of PCa cells spiked into 9 mL blood to mimic CTCs for different CTC isolation method comparisons. The average number is likely to be a better representation of the actual cell number and is used to calculate CTC isolation efficiencies.

For the CTC enrichment comparisons, PC3 cells were enumerated using haemocytometer counts, and diluted so a volume of 70 μL would contain calculated 500 PCa cells. 70 μL was spiked into each of two comparison 9 mL blood samples from the same blood draw of a healthy donor, in EDTA vacutubes. Two 70 μL input controls were pipetted on glass slides, one before and one after the spiking of the same volume into blood samples. The input controls were counted after airdrying using fluorescent microscopy for cell tracker (AF555) labelled cells or cytokeratin labelled cells.

5.2.2 Comparison of CTC Enrichment Using RosetteSep CD36-kit vs. CD45-kit

The method used for RosetteSep CD36/CD45-kits was followed according to the manufacturer's instructions. In brief, 50 $\mu\text{L}/\text{mL}$ RosetteSep cocktail CD36 or CD45 was added to each blood sample and incubated for 10 minutes at room temperature. Then the sample was diluted 1:1 with 2% FBS in PBS and mixed gently. The diluted sample was transferred to the top compartment of a Sepmate tube preloaded with 15 mL of lymphoprep density gradient medium in the bottom compartment and centrifuged at 1200 x g for 10 minutes with full brake. This process segregates the blood constituents into layers based on density, sequestering nucleated cells including PBMCs (peripheral blood mononuclear cells) and CTCs in a layer referred to as the buffy coat that is cushioned on the lymphoprep. The supernatant, together with this interphase, was transferred by a quick pouring step (quick to avoid contamination with the lymphoprep separated by the Sepmate compartment) to a 50 mL tube and topped up with 2% FBS in PBS to wash the cells, followed by centrifugation at 300 x g for 10 minutes with low brake. The supernatant was discarded, and the pellet was resuspended in PBS. The tube was again filled with further PBS to wash the cells and centrifuged as in the previous step. The supernatant was discarded, and the pellet was resuspended in 1.5 mL PBS. To account for the approximate number of residual lymphocytes retained in the sample, a 10 μL aliquot was taken at this point and diluted with 90 μL PBS to count lymphocytes by using a hemocytometer.

The remaining 1490 μ L PBS containing the enriched CTCs was equally distributed into 3 different wells of a 24-well glass bottom plate. The enriched cell tracker labelled PC3 cells “CTCs” were enumerated by fluorescence microscopy. The experiment was repeated four times.

The recovery rate was $55.3\% \pm 4.9\%$ for the CD36-kit compared to $43\% \pm 8.8\%$ for the CD45-kit (Table 5.2 and Figure 5.2). Residual lymphocyte numbers were 24765 vs. 41051 on average for the CD36-kit and the CD4-kit respectively (Table 5.2 and Figure 5.2). Despite some variation between the four experiments conducted, we conclude that the CD36-kit performs better than the CD45-kit for isolation of PCa CTCs.

Table 5. 2 Proportion of recovered with CD36-kit vs. CD45-kit

Experiment	CTCs [%]		Residual lymphocytes [n]	
	CD36-kit	CD45-kit	CD36-kit	CD45-kit
Experiment 1	54.92	40.88	18198	51176
Experiment 2	59.11	55.55	13482	62834
Experiment 3	48.51	37.23	27846	24393
Experiment 4	58.51	36.80	39536	25802
Average	55.3 ± 4.9	43 ± 8.8	24765 ± 11520	41051 ± 19035

500 PC3 cells were spiked into 9 mL healthy donor blood (same donor per experiment) and recovered using the indicated CTC isolation kit. Proportion [%] of recovered mimicked CTCs (PC3 cells) as calculated relative to the average input control in four independent experiments are presented together with the number of residual lymphocytes per experiment. P value for % CTC isolation comparison was 0.007 and for residual lymphocytes was 0.20 (Unpaired t-test with Welch's correction was performed using prism).

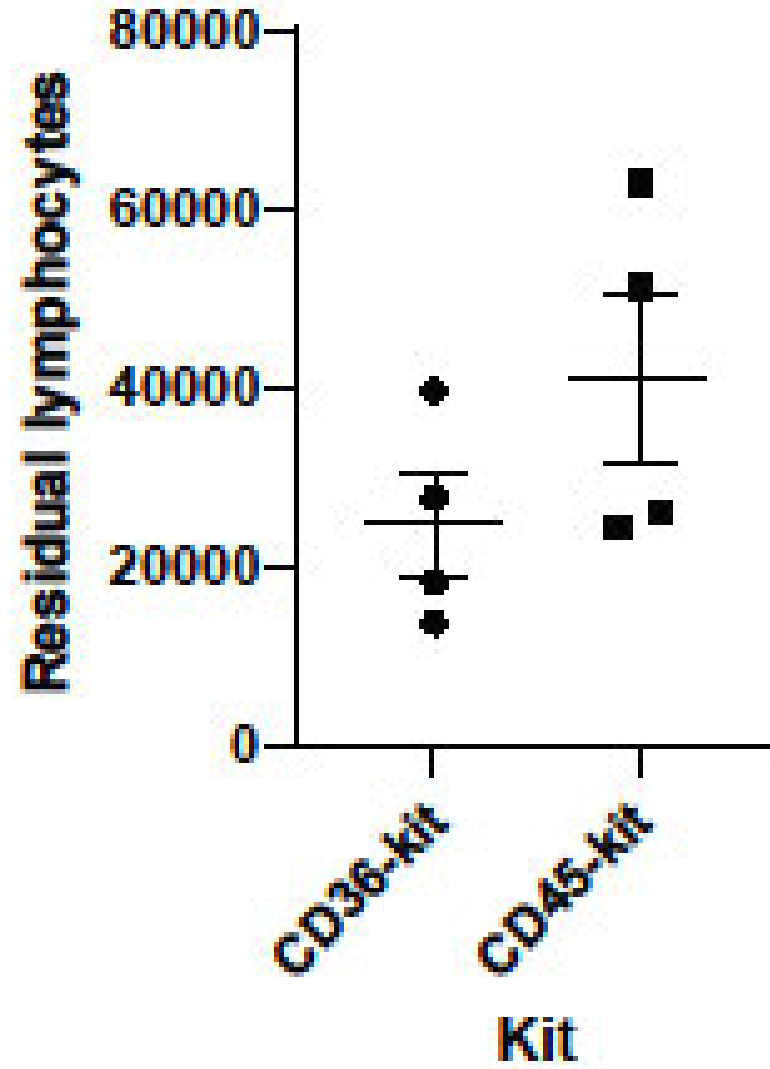
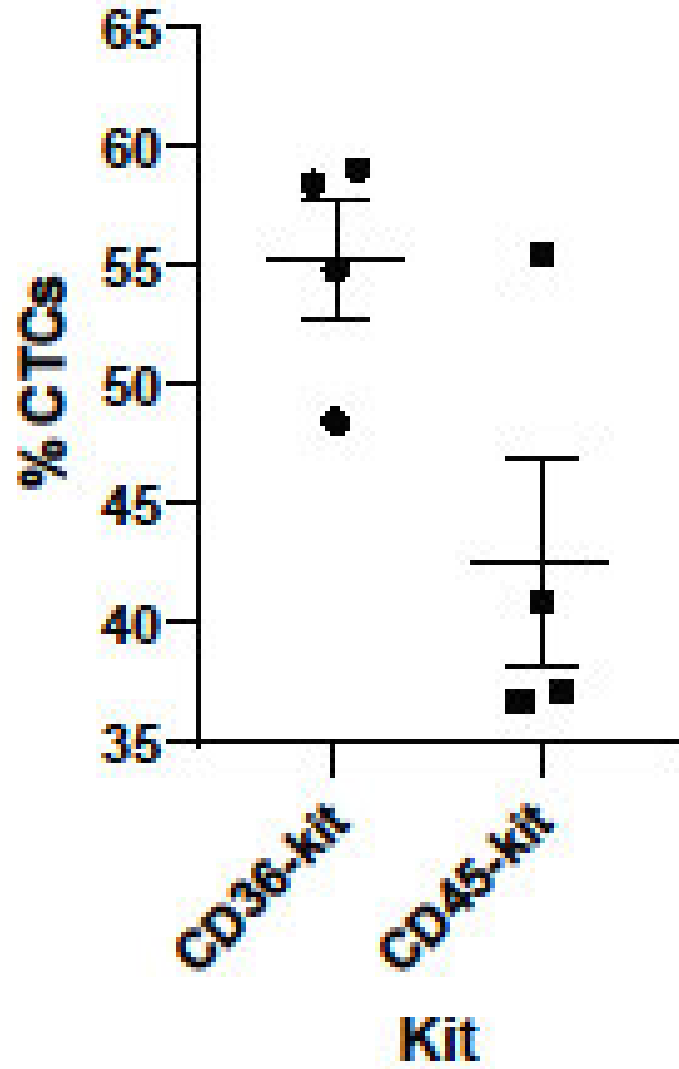


Figure 5. 2 The comparison of CD36-kit vs. CD45 kit for the isolation of CTCs

500 PC3 cells were spiked into 9 mL healthy donor blood and recovered using the indicated CTC isolation kit. Proportion [%] of recovered model CTCs (PC3 cells), as calculated relative to the average input control, in four independent experiments are presented together with the number of residual lymphocytes per experiment. (A) Proportion [%] of recovery of PC3 cells labelled with cell tracker using CD36-kit vs. CD45-kit, (B) the total number of residual lymphocytes for the same experiments.

5.2.3 CD36-kit CTC Isolation vs. OncoQuick CTC Enrichment Isolation

An additional kit for unbiased CTCs enrichment, OncoQuick, has recently been brought onto the market and the supplier (Greiner Bio-One) provided information suggesting CTC enrichment efficiencies of 87% [282]. Given that figure is significantly higher than a lot of published CTC isolation efficiencies, such as Ficoll (equivalent to lymphoprep) based density gradient medium centrifugation [279], including the one tested above, the CD36-kit (Section 5.2.2) was compared to the OncoQuick CTC isolation method.

Again, PC3 cells pre-labelled with cell tracker, as above, were used for this comparison.

5.2.3.1 OncoQuick CTC Enrichment

For this method both the OncoQuick tube, which includes a preloaded separation medium underneath a porous barrier, and the EDTA tube with the spiked blood specimen, were placed on ice for 10-15 minutes. Then the cooled whole blood (15-30 mL) was gently transferred into the upper compartment of the OncoQuick tube without disturbing the separation medium underneath the porous barrier and then centrifuged at 1600 x g at 4°C for 20 minutes with low acceleration and brake off. The supernatant containing the CTCs with the residual lymphocytes was transferred into a fresh centrifugation tube. The OncoQuick tube was washed with 5mL washing buffer (0.5% BSA in PBS) which was then transferred to the tube already containing the transferred liquid volume and the volume brought to a total of 50 mL with additional washing buffer. After mixing the suspension by gently inverting the tube 5 times, it was centrifuged at 200 x g for 10 minutes. 45 mL of supernatant was removed without disturbing the cell pellet which was left in the remaining 5 mL of washing buffer. The tube was tapped to loosen the pellet and to wash the cells, washing buffer was added to make up the volume up to 50 mL. The cells were mixed by gently inverting tube five times and centrifuged at 200 x g for

10 minutes. The supernatant was removed, and pellet was resuspended in 1.5 mL PBS and distributed in three wells of 24-well glass bottom plate.

To compare spiked “CTC” recovery by the CD36-kit vs. the OncoQuick tube, 500 PC3 cells were spiked into healthy human blood as outlined above. The tumour cell enrichment was done by a density gradient centrifugation as outlined for both the OncoQuick (Greiner BioOne, Frickenhausen, Germany) system and RosetteSep CD36 enrichment cocktail. The recovery rate was $51\% \pm 6\%$ for CD36 enrichment cocktail and $17\% \pm 8.6\%$ for the OncoQuick method (Table 5.3, Figure 5.3). While the capture performance of the OncoQuick method was below expectations, and below the CD36-kit, there was an additional drawback for this method. It produced a large amount of background (large aggregates of undefined origin or composition but interfering with cell visibility) when inspected by brightfield microscopy (Figure 5.4). Not only did this make it hard to count the cells, but we would expect interference of this background with future multiplex immunocytostaining as well.

Table 5. 3 Proportion of recovered CTCs with CD36-kit vs. OncoQuick CTC enrichment

Experiment	CTCs [%]		Residual lymphocytes [n]	
	CD36-kit	OncoQuick CTC enrichment	CD36-kit	OncoQuick CTC enrichment
Experiment 1	51.68	7.04	55355	78679
Experiment 2	55.85	23.37	45442	8137
Experiment 3	43.97	19.85	3220	56101
Average	51 ± 6	17 ± 8.6	34672 ± 27686	47639 ± 36024

500 PC3 cells were spiked into 9 mL healthy donor blood, each, and recovered using the indicated CTC isolation kit. Proportion [%] of recovered mimicked CTCs (PC3 cells), as calculated relative to the average input control, in three independent experiments are presented together with the total number of residual lymphocytes per experiment. P value for % CTC was 0.007 and for residual lymphocytes was 0.64 (Unpaired t-test with Welch’s correction was performed using prism).

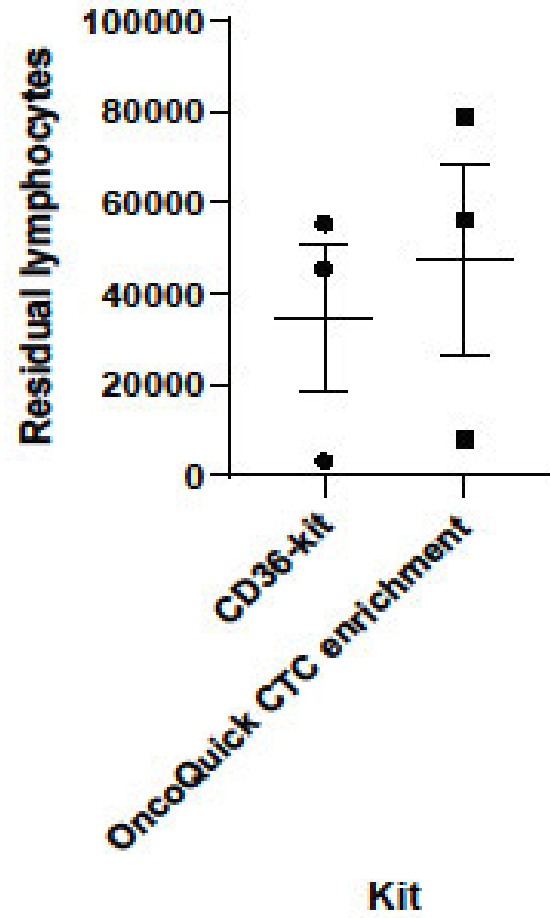
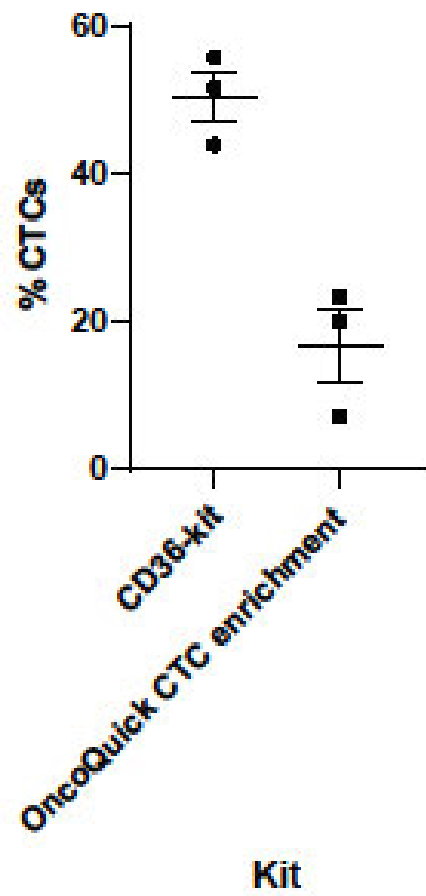
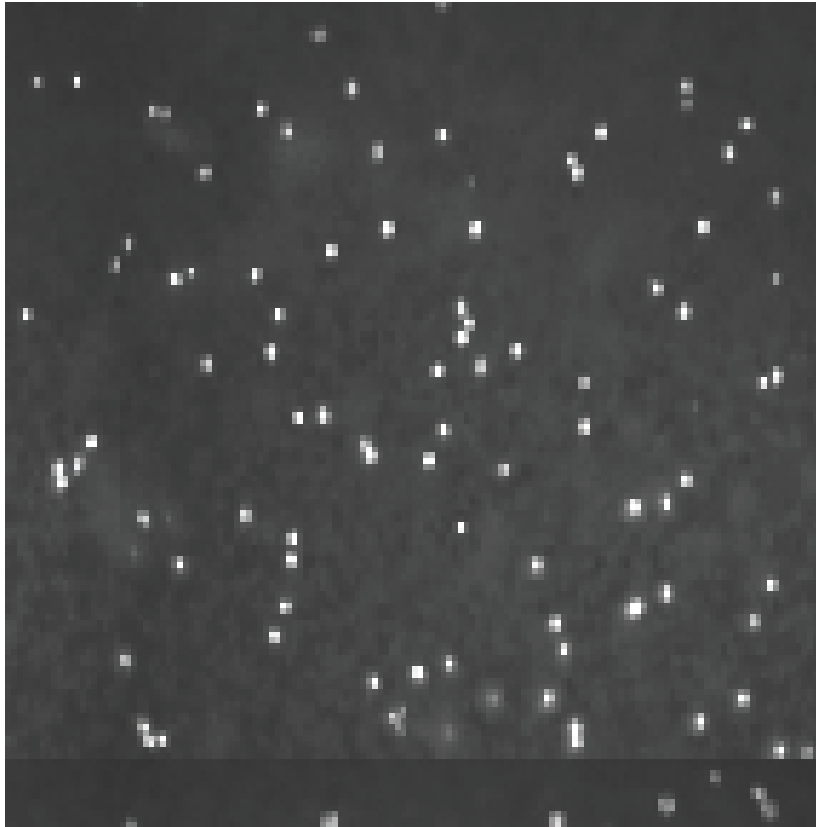


Figure 5. 3 The comparison of CD36-kit vs. OncoQuick CTC enrichment

500 PC3 cells were spiked into 9 mL healthy donor blood and recovered using the indicated CTC isolation kit. Proportion [%] of recovered mimicked CTCs (PC3 cells), as calculated relative to the average input control, in three independent experiments are presented together with the total number of residual lymphocytes per experiment. (A) Recovery of PC3 cells labelled with cell tracker using CD36-kit and using OncoQuick CTC enrichment, (B) the number of residual lymphocytes for the same experiment. CD36-kit performance was higher (51%) than OncoQuick CTC enrichment (17%).

CD36-kit



OncoQuick CTC enrichment

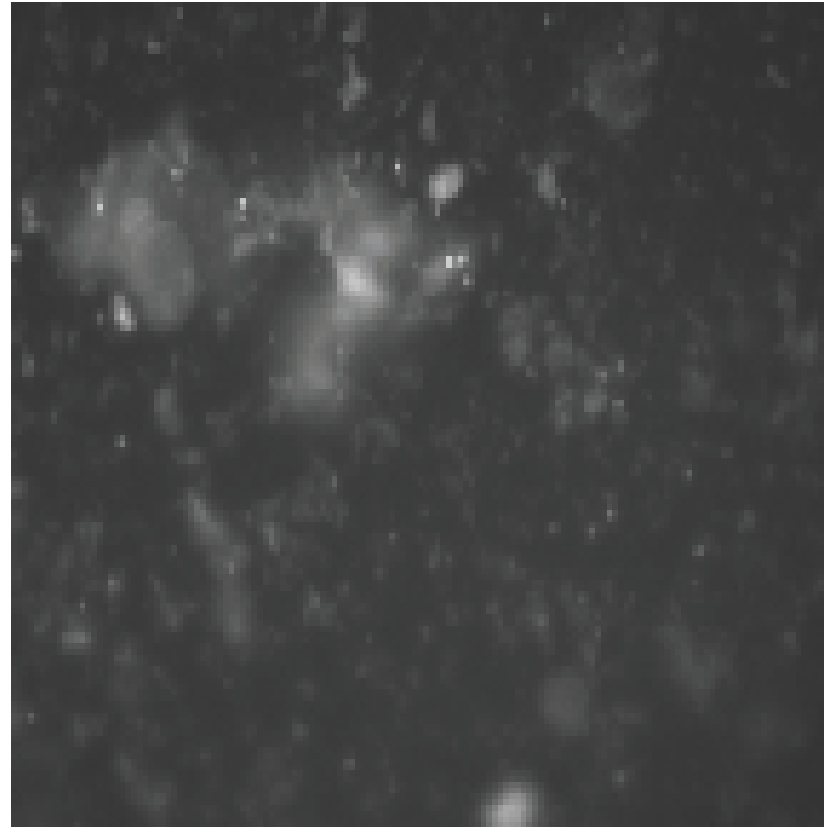


Figure 5. 4 The OncoQuick CTC enrichment (left) and CD36 kit (right)

500 PC3 cells labelled with cell tracker were spiked into 9 mL healthy donor blood and recovered using the indicated CTC isolation kit (CD36-kit vs. OncoQuick CTC enrichment). Recovery of PC3 cells labelled with cell tracker using CD36-kit and using OncoQuick CTC enrichment was done. The image on the right demonstrated large aggregates typically seen with OncoQuick CTC enrichment in comparison to easy visibility of cells enriched by the CD36-kit (left).

Due to a low recovery rate and interfering aggregate residues, the OncoQuick CTC enrichment was ruled out for CTC enrichment.

5.2.4 CD36-kit vs. AutoMacs CTC Enrichment Comparison

Comparison of the CD36-kit with traditional CTC capture by EpCAM targeted AutoMacs CTC enrichment was also performed. However, this comparison was done using the 22RV1 cell line as this was growing in culture at the time, and with lab access varying (see COVID impact statement), DU145 cells were not used for this comparison.

5.2.4.1 AutoMacs CTC Enrichment

22RV1 (500) cells each were spiked into two 9 mL blood draws from healthy donors. Blood from each EDTA tube was layered over 15 mL lymphoprep in a 50 mL Sepmate tube. To remove any cells left behind the EDTA tube was washed with 9 mL PBS, which was added to the aqueous layer of the Sepmate tube, and the sample was spun at 1200 x g for 10 minutes with no brakes. The buffy coat and plasma layers were decanted into a sterile 50 mL tube and the top compartment of the Sepmate tube was washed with 7 mL of PBS. The wash was combined with the buffy coat in the 50 mL tube, and the cells were centrifuged for 10 minutes at 200 x g at room temperature. After centrifugation, the supernatant was removed, and the cells were resuspended in 5 mL of separation buffer (PBS with 0.5% FBS and 2 mM EDTA) and transferred to a 15 mL tube. The 50 mL tube was washed with 5 mL of separation buffer which was also transferred to the 15 mL tube. The sample was then centrifuged for a further 10 minutes at 280 x g at room temperature. The supernatant was removed and leaving the pellet in approximately 200 μ L supernatant. The pellet was loosened by tapping the tube on the palm of the hand, followed by adding 25 μ L FcR blocking reagent and 25 μ L EpCAM (CD326) microbeads (human, Miltenyi Biotech). The pellet was resuspended and incubated for 30 minutes at 4°C. 10 mL separation buffer was added to the tube and centrifuged for 10 minutes

at 300 x g at room temperature, and the supernatant removed leaving 2 mL of supernatant in the tube. The pellet was then resuspended, and the sample loaded into the AutoMacs Pro Separator for isolation of EpCAM-positive cells using the inbuilt Posseld2 program. The eluted cells were then spun at 300 x g for 10 minutes at room temperature, resuspended in 2 mL separation buffer and transferred to a well of a 24-well glass bottom plate and the plate centrifuged at 200 x g for 10 minutes. After centrifugation, cells were fixed by using 4% PFA for 10 minutes followed by washing.

The CD36-kit cell isolation was essentially performed as described above with 22RV1 cells instead of PC3 cells spiked into the matched healthy donor bloods. After enrichment, these “CTCs” were placed into 3 wells of the 24-well glass bottom plate.

Cells were permeabilized with 0.2% Triton X-100 in PBS 10 minutes followed by blocking with 10% goat serum for 30 minutes. The cells were incubated with anti-CD45-PE and anti-Cytokeratin-647 in 0.5% goat serum for 30 minutes, followed by 1x Hoechst in PBS for nuclear staining. Olympus microscope was used for imaging.

The recovery rate for the CD36-kit in this study in the initial comparison experiments was 51-55% (Table 5.2 and 5.3). To check whether we could get better cell recovery, the CD36-kit was compared with another commercially available method known as AutoMacs CTC enrichment. In AutoMacs CTC enrichment, the isolation is based on epithelial markers. 22RV1 cells were spiked into healthy human blood and both methods were used to do the comparison by counting cytokeratin positive cells. The recovery rate was higher using the CD36-kit (55%) compared to AutoMacs (40%).

Table 5. 4 Proportion of recovered CTCs with CD36-kit vs. AutoMacs CTC enrichment

Experiment	CTCs [%]		Residual lymphocytes [n]	
	CD36-kit	AutoMacs CTC enrichment	CD36-kit	AutoMacs CTC enrichment
Experiment	55	40	115921	9075

500 22RV1 cells were spiked into 9 mL healthy donor blood, each, and recovered using the indicated CTC isolation kit. Proportion [%] of recovered mimicked CTCs (22RV1 cells), as calculated relative to the average input control, in three independent experiments are presented together with the total number of residual lymphocytes per experiment. This experiment could only be performed once (due to COVID impact). No statistical test was performed as there was only one experiment done.

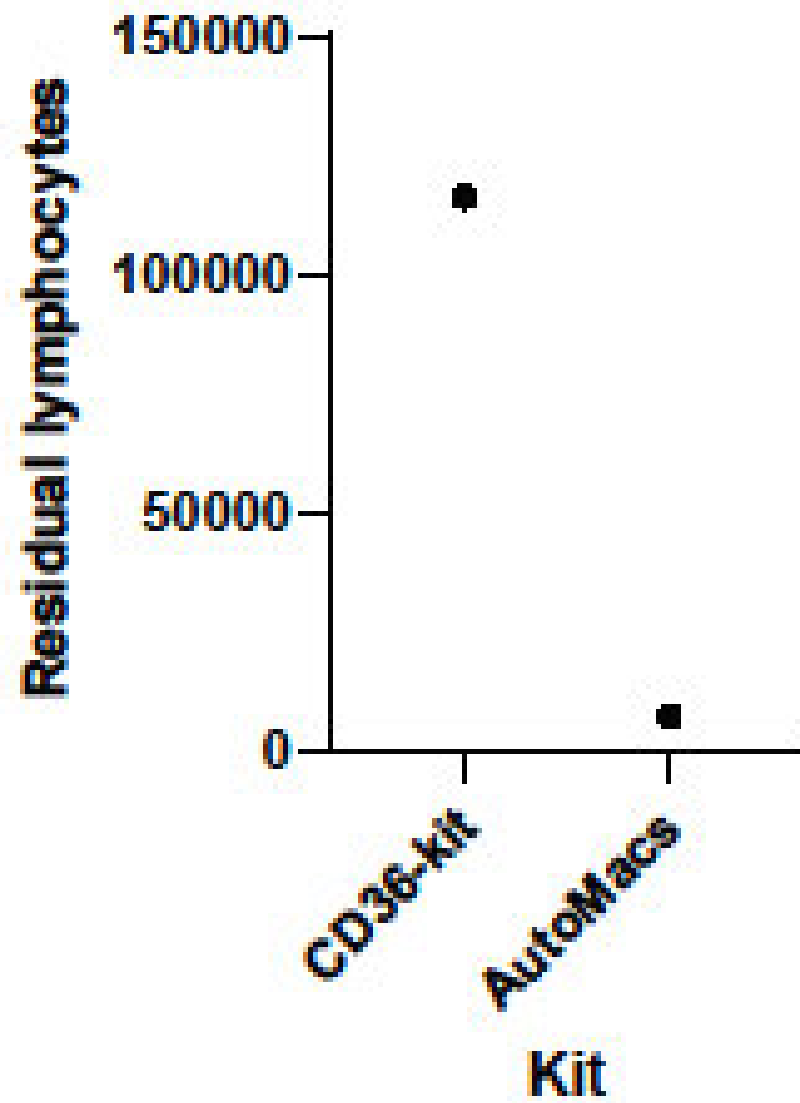
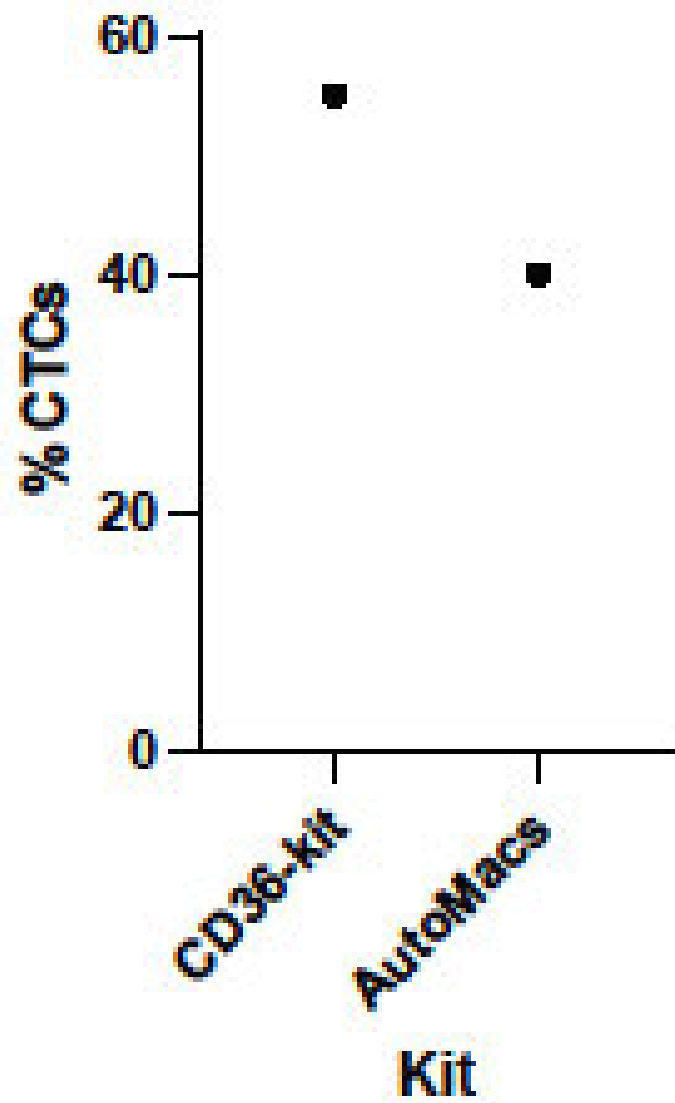


Figure 5. 5 CD36-kit vs. AutoMacs CTC enrichment

500 22RV1 cells were spiked into 9 mL healthy donor blood and recovered using the indicated CTC isolation kit. Proportion [%] of recovered mimicked CTCs (22RV1 cells), as calculated relative to the average input control, are presented together with the total number of residual lymphocytes per experiment. (A) Recovery of 22RV1 cells labelled with cell tracker using CD36-kit and by AutoMacs CTC enrichment, (B) the number of residual lymphocytes for the same experiment. CD36-kit performance was higher (55%) than AutoMacs CTC enrichment (40%)

In summary, the experiments that were done to design and validate the CTC isolation method, together with the conclusions from those experiments are shown in Figure 5.6. The first comparison for CTC enrichment to be conducted was the CD36-kit versus CD45-kit based RosetteSep enrichment, followed by the leading method (CD36-kit) being tested against AutoMacs CTC enrichment and OncoQuick CTC enrichment-based CTC isolation protocols.

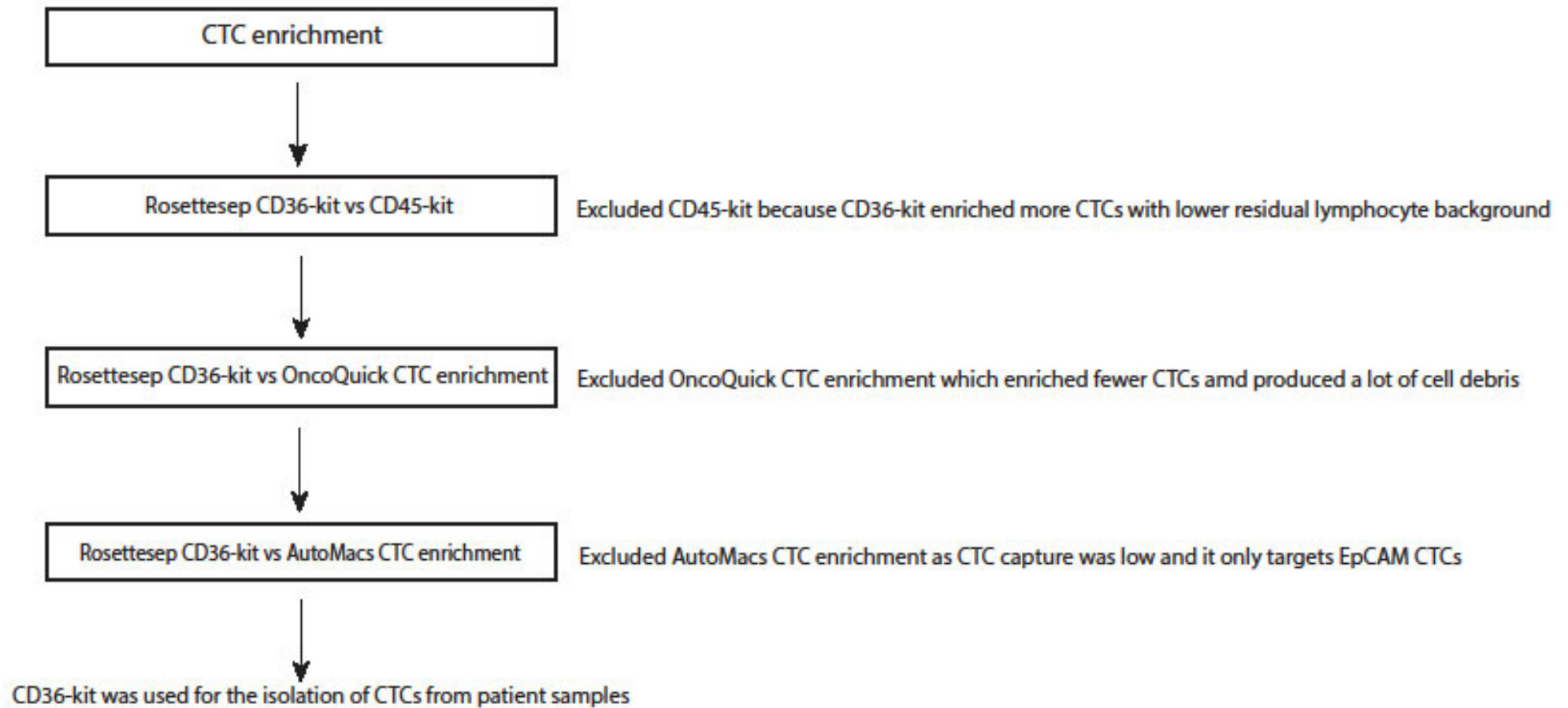


Figure 5. 6 CTC enrichment method comparison

Four different methods of CTC isolation were compared. These methods included CD36-kit, CD45-kit, OncoQuick CTC enrichment and AutoMacs CTC enrichment. The first two methods deplete blood cells expressing markers including CD2, CD16, CD19, CD36, CD45 while the OncoQuick includes “elimination of lymphocytes and mononuclear cells to a wide extent” by a not manufacturer specified mode of action. AutoMacs as used here is an EpCAM-based CTC enrichment method. Two kits were compared in each test and the best one chosen for comparison with another kit/method

5.2.5 Preliminary Discussion of CTC Enrichment Method Comparison

Comparing different methods for the isolation of CTCs showed that the CD36-kit was the leader, producing the highest CTC recovery rate. It is also the preferred method for CTC isolation as it results in lower residual lymphocytes compared to OncoQuick CTC enrichment. AutoMacs has lower residual lymphocyte contamination in comparison to CD36-kit (Table 5.4), but this procedure only isolates epithelial CTCs which results in biased isolation, and lower CTC yields ultimately (Figure 5.3, 5.4, 5.6, 5.7).

Overall, these experiments suggest CD36-kit is the best choice for CTC enrichment for future multiplex staining of CTCs. Although we still have high number of residual lymphocytes with this method, the advantage of our multiplex staining method is that we can clearly distinguish between CTCs and lymphocytes with many markers and the method can cope with even large number of residual lymphocytes. As long as individual CTCs are visible, we do not require further enrichment.

Conclusion for CTC enrichment method:

We conclude that CD36-kit is the best method of CTC isolation.

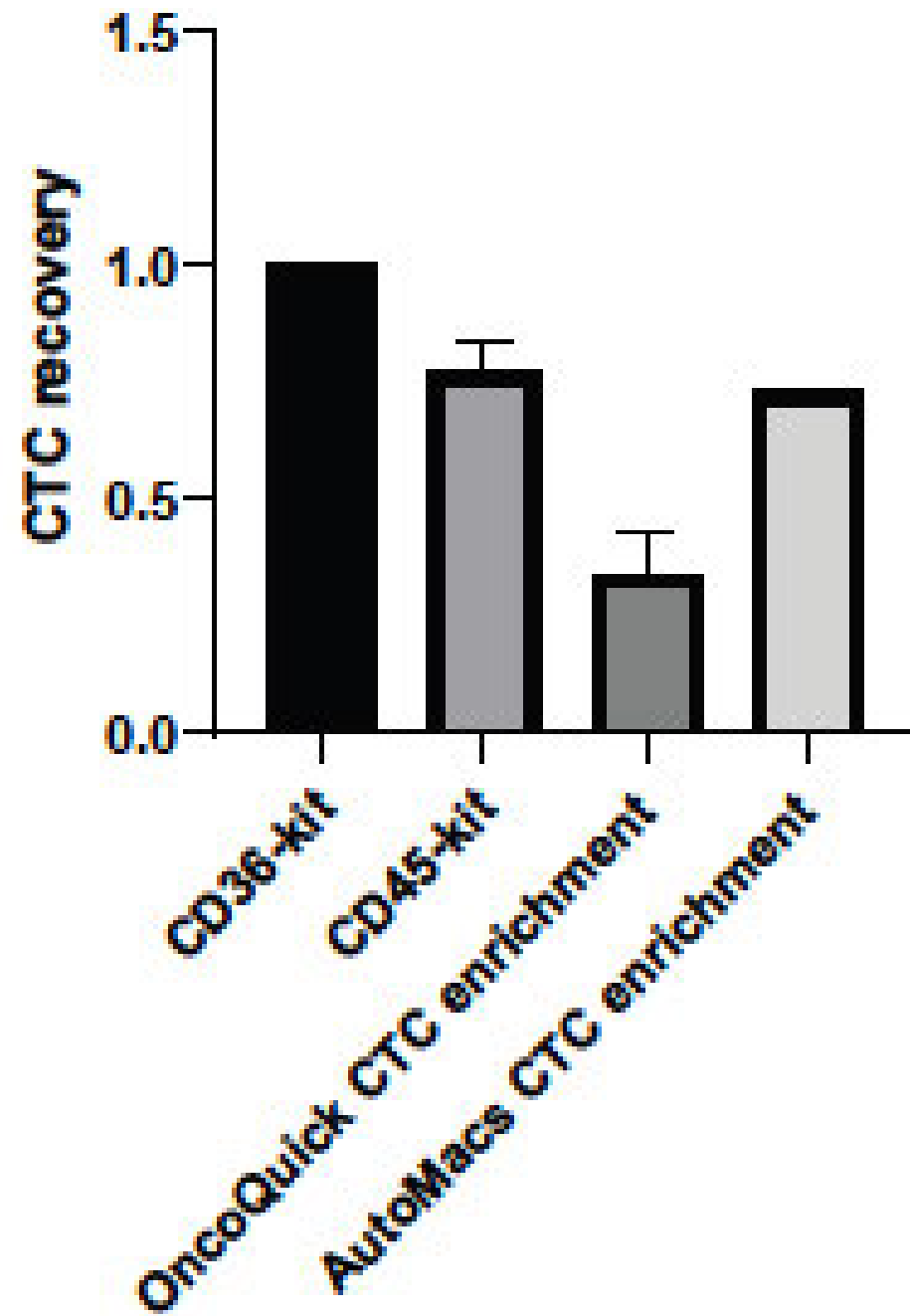


Figure 5. 7 Comparison of four CTC enrichment methods

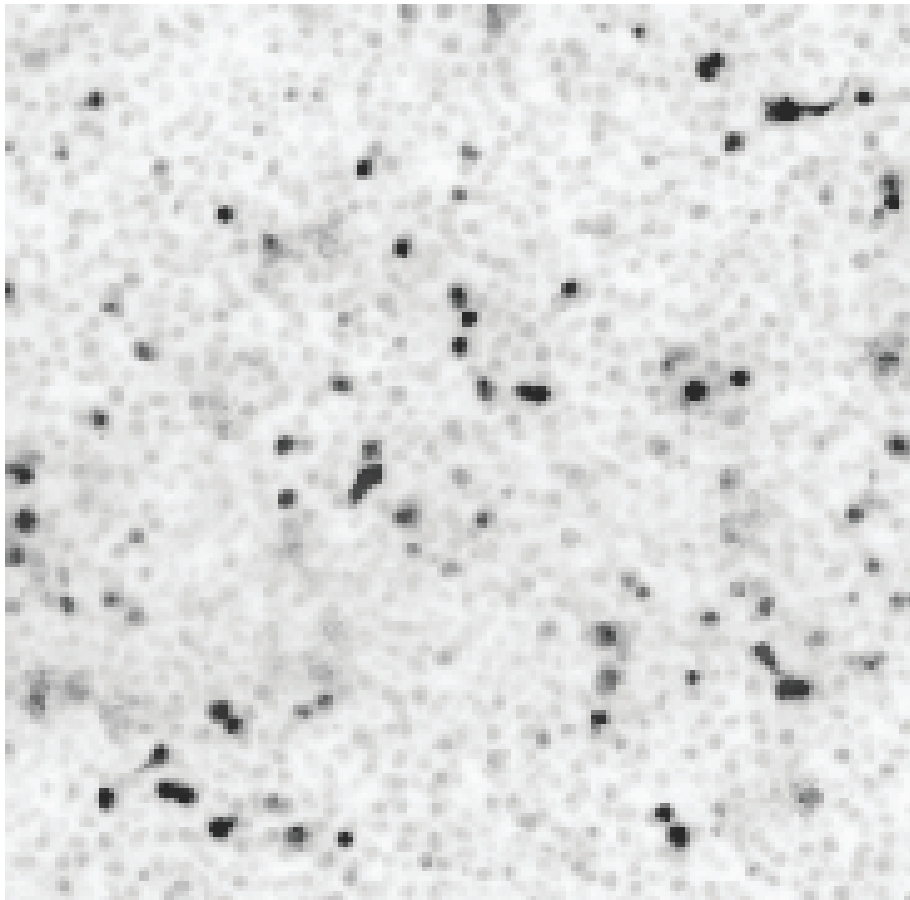
To compare the results of CTC isolation efficiencies from the different experiments, the efficiency with the CD36-kit (used in every experiment) was set as 1 and the other data normalised to that for each comparison to generate this graph. CD36-kit performs the best and other kits (CD45-kit, OncoQuick CTC enrichment and AutoMacs CTC enrichment) of CTC isolation were normalised against CD36-kit.

5.2.6 Additional CD36-kit Considerations and Tests

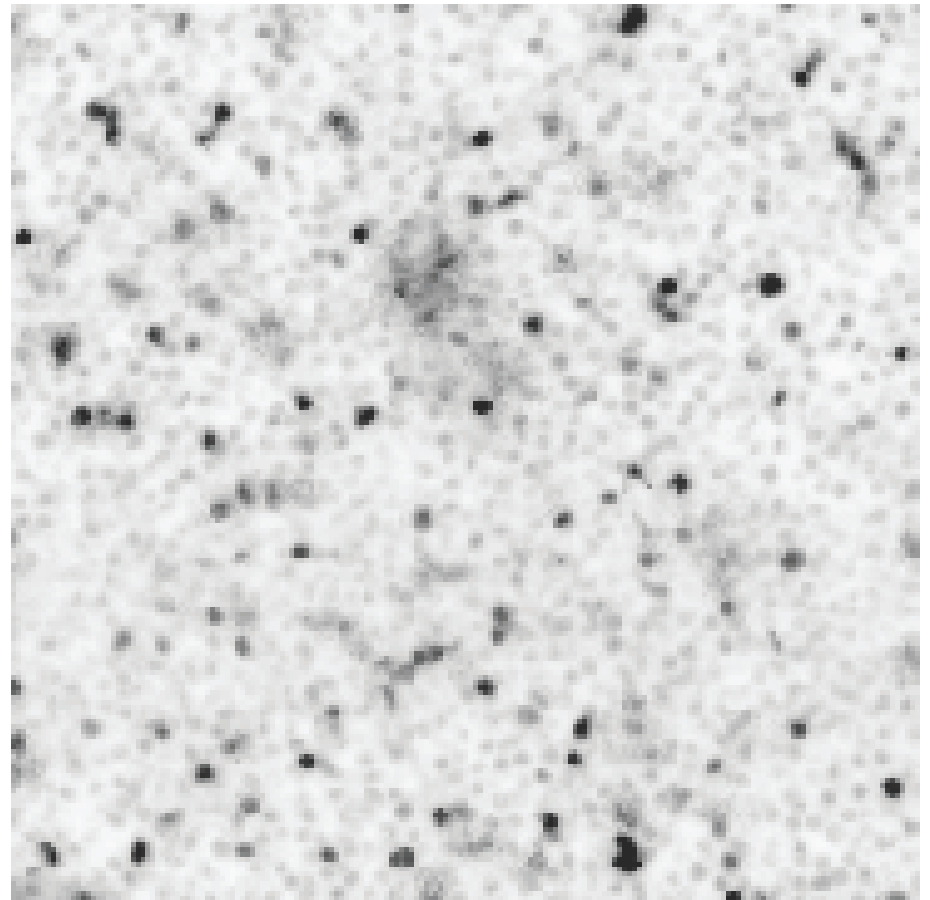
The use of the CD-36 kit identified one issue of concern. The CD36-kit produced events that, by brightfield microscopy, appeared to result in anucleated, small cells (Figure 5.8). Given these observations, we assumed it would be better to separate the sample over several (3) wells in a 24-well glass bottom plate so cancer cells would not need to compete for attachment surface. However, with a view towards multiplex immunocytostaining, this solution would mean an excessive need for antibodies to stain a 9 mL blood-derived patient CTC sample in 3 separate wells. In fact, this would make CTC multiplex staining an endeavour too expensive to be affordable in our team's research budget. Thus, we decided to do some troubleshooting: From the size of these cells, we speculated they may be platelets or less likely RBCs due to lack of haemoglobin. Referring to the Stemcell (CD36-kit manufacturer) website it appears that not removing platelets may explain our observations. Simply pouring the supernatant together with the PBMC/CTC layer into the new tube to recover cells after the gradient centrifugation step may contribute to the potential platelet contamination. The reasoning was that platelets are light (small size, lack of nuclei) and many are likely to have remained in the supernatant. To test this idea using the CD36-kit, we compared our easy pouring method with carefully pipetting off most of the top plasma layer before recovery of the cell layer after gradient centrifugation. The rest of the procedure was the same. However, no obvious difference in the "anucleated" event count was seen between both approaches (Figure 5.8 (A and B)).

Next, we wished to determine if these events were in fact interfering with CTC attachment to the glass bottom plate. Again, since we assume the cancer cells to be heavier, they should plate down first, meaning the "anucleated" cells may not be a source of experimental error. For this purpose, parallel CD36-kit spiked CTC isolates were either distributed into 3 wells or into 1 well of a 24-well glass bottom plate. Then Hoechst positive cells (accounting for all nucleated

cells i.e., PBMCs and CTCs) were counted and we found 18387 cells and 34910 cells when distributed in to 1 well or 3 wells of a 24-well glass bottom plate respectively (Table 5.5). We found 15 cytokeratin positive cells when the cells were placed in one well whereas we found an average of 8 cytokeratin positive cells per well when the cells were distributed in three wells of the glass bottom plate (Table 5.5). Thus, these results show that CTC attachment may be affected to some degree by residual lymphocytes and anucleated cells, but the loss of CTCs is not as dramatic as we had expected. If indeed the presence of high numbers of PBMCs and anucleated cells would prevent cancer cells from adhesion, then one would expect fewer cancer cells attaching due to competition in the one well. However, we found more cancer cells adhering in the one well than the average for each of the three wells. This might be due to the reason that CTCs are big cells as compared to other cells, and so might fall to the bottom of the plate faster. Nevertheless, the one well yielded fewer cancer cells overall than the three wells combined. Given the potential antibody costs if using three wells for every staining cycle, we decided that a compromise may be the best way forward. Adding the CTCs recovered using the CD36-kit into one well instead of three wells may be associated with some (37%) loss of CTCs to analyse, but that loss may be necessary as the strategy is far more compatible with our research budget.



(A)



(B)

Figure 5. 8 Anucleated cells vs. nucleated cells

9 mL healthy donor blood was processed to see whether by removing top plasma layer helps to get less numbers of anucleated cells which can interfere with the attachment of cancer cells to the surface. Cells were stained by using Hoechst and imaged by using fluorescent microscopy. Black dots showing nuclear stain were present while there were also anucleated cells (grey). There was no apparent difference in both conditions (Figure 5.8A and B).

Table 5. 5 Number of CTCs after immunostaining

Residual lymphocytes	Average cytokeratin positive cells
18387	8
34910	15

After isolation of CTCs, the immunostaining was done (n=2), and we found that CTC recovery would be not that much affected even if we put all the cells in one well.

5.3 CTC Immobilisation

Note: the data for this section were accumulated in parallel with the CTC kit comparisons and the concentration of adherent defined in this section were also used to coat the above used glass bottom plates to compare CTC capture by various methods.

Multiplex immunocytostaining involves multiple cycles of washing, staining, imaging, elution of antibodies and restaining. In this strategy it is crucial that cells remain in the exact location in the glass bottom plate during the serial staining and data acquisition cycles so we can overlay the accumulated data for each single cell. Thus, losing cells due to poor attachment especially for rare cells such as CTCs, has to be limited as far as possible. Preliminary experiments suggested using a cell adhesive may improve cell adhesion. We had preliminary data which showed Cell-Tak was a suited adhesive to improve cell attachment and is optically inert, so it does not interfere with microscopy. Cell-Tak is a cell and tissue adhesive derived from a marine mussel known as *Mytilus edulis*, which is used to attach cells or tissue sections to many types of surfaces, including plastic, glass, metal, FEP Polymer, and biological materials. Importantly, it is inert optically, and even in the process of fluorescence microscopy, it produces limited background [283]. The most commonly used concentration of Cell-Tak is 3.5 $\mu\text{g}/\text{cm}^2$ of surface area. pH (6.5-8.0) is an important factor in the regulation of adsorption, so any buffers can be used to neutralise Cell-Tak; 0.1 M sodium bicarbonate (NaHCO_3 (pH 8.0)) works best. 1 N sodium hydroxide (NaOH), equal to half the volume of Cell-Tak, used can be added in combination to a neutral buffer to neutralise the pH. To test which Cell-Tak dilution works best, the following experiment was designed:

Wells of a 24-well glass bottom plate were coated by using three different dilutions of Cell-Tak: 1:5, 1:7 and 1:10 and the plate left at room temperature on the work bench overnight. The next day, the plate was washed with sterile water and PBS. PC3 cells were harvested with

PBS/EDTA, and cells were counted using a haemocytometer; 1000 cells per well were added in a volume of 800 μ L PBS.

The plate was spun at 200 x g for 5 minutes using a special swinging adapter for spinning 24-well glass bottomed plates. The cells were then fixed with 4% PFA containing Hoechst (nuclear stain diluted to 1x solution) for 10 minutes. My co-supervisor, Dr Lock, who has developed multiplex single cell immunostaining techniques has previously developed a gentler protocol for rotating wash and other solutions in the various steps. The method is based on never removing the entire fluid volume in the wells on top of the cells in order to avoid losing cells during washing steps. This approach was adopted, and some volume of PBS was always left in the wells, in this case 400 μ L per well. For washing, PBS (200 μ L) was added to the volume 800 μ L of PBS already in the well and then 600 μ L of liquid was removed. Additional PBS (600 μ L) was added, and the same volume was removed several times until the PFA was diluted to negligible levels. Then the Hoechst positive cells were counted by using fluorescent microscopy.

5.3.1 Results and Discussion of CTC Adhesion Optimisation

To produce firm cell adherence to glass bottom plates, and to prevent cells from dislodging during the multiple wash and elution steps required to perform multiplex immunostaining experiments in future, we tested a series of Cell-Tak dilutions (in NaOH and NaHCO₃): 1:5, 1:7 and 1:10 compared to no Cell-Tak as a control. Duplicate wells per condition were included, and the experiments were repeated three times. The results show that the cells generally adhere better in the presence of Cell-Tak than without Cell-Tak; the latter Cell-Tak-free experiment only retaining 43% of cells on the glass bottom plate. While any Cell-Tak seemed advantageous, the best dilution was 1:5 (78%) closely followed by 1:7 and 1:10 (both

showed 68% cell retention) (Figure 5.9). Without Cell-Tak, an unacceptably high number of cells may be washed away during washing steps.

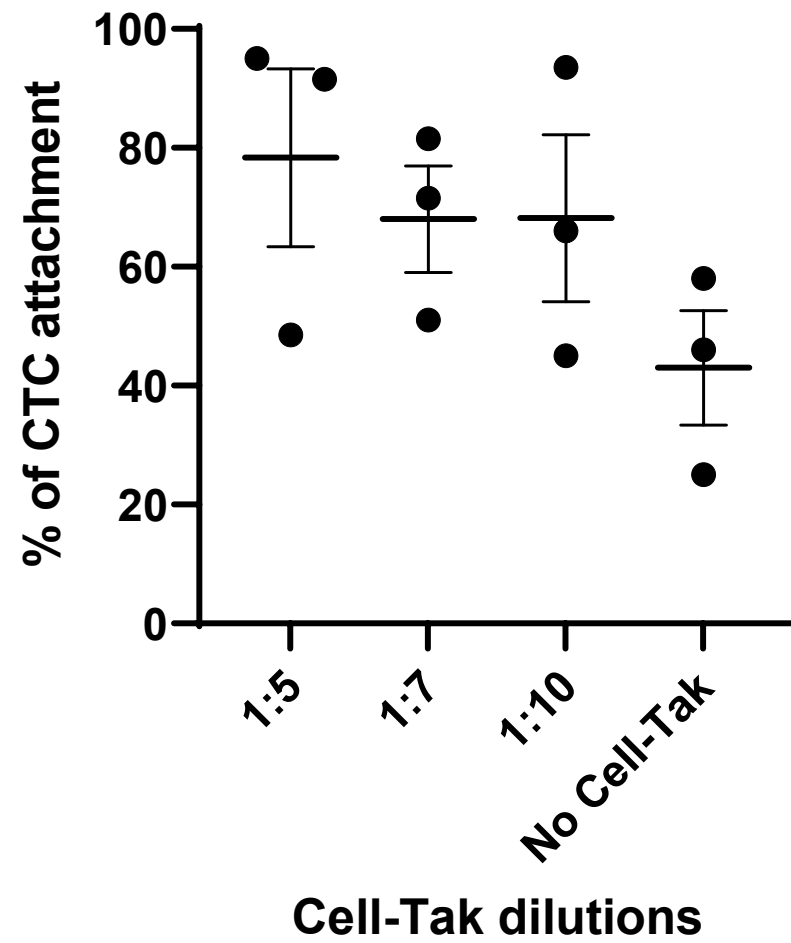


Figure 5. 9 Cell immobilisation by using Cell-Tak

The comparison of different dilutions of Cell-Tak to check the attachment of cancer cells (n=3). 1:5 dilution of Cell-Tak gives better attachment of the cells (78%) as compared to 1:7, 1:10 (68%) or no Cell-Tak (43%). P value for % CTC attachment is 0.01 for no Cell-Tak vs 1:5, 0.05 for no Cell-Tak vs 1:7 and 1:10 (One-way Anova multiple comparisons was performed using prism).

5.4 Antigen and Antibody Selection and Optimisation

To be able to move closer towards the overarching aim of this project, namely, to analyse the correlation of AR/AR-V7-AKT-Hippo pathways and EMT in PCa cells and CTCs, a decision needed to be made which antigens/antibodies would be most informative to use for future multiplex staining (Figure 5.10). Consequently, an extensive literature search was conducted to define the most useful antigens and relevant antibodies.

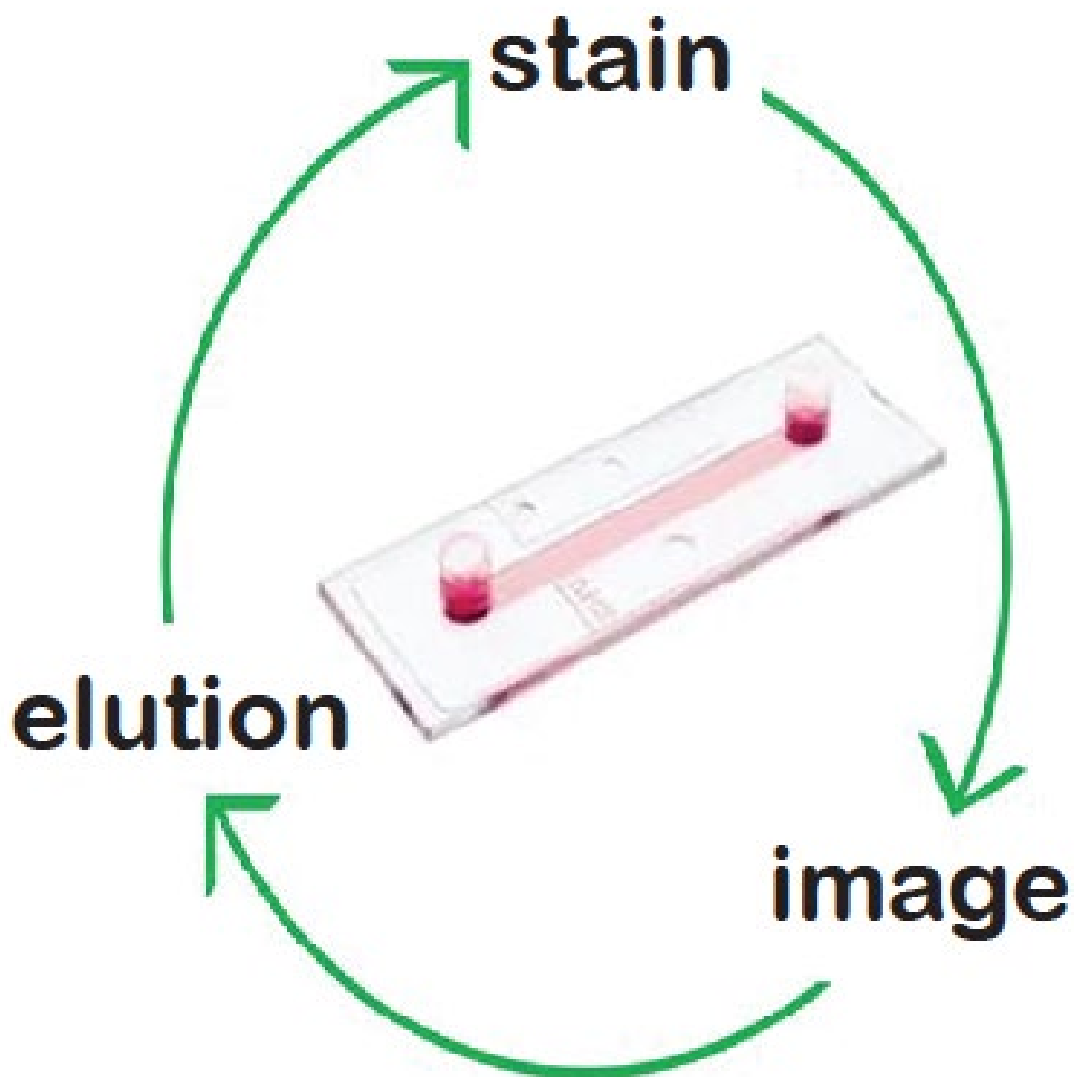


Figure 5. 10 Steps in multiplex proteomics

This figure presents the three steps are involved in each cycle of multiplex staining: immunocytostaining (stain), imaging (image), elution (bleaching) and then the cycle is repeated multiple times to cover all markers to be screened. The slide shown is a specialized Ibidi slide that can be used for these experiments and allows all processes to be performed on the microscope stage (with small tubes attached to inlet and outlet tubes to pump through washing and staining solutions).

The selected markers are listed in Table 5.6. These markers include EMT-MET markers, namely EpCAM, E-Cadherin and cytokeratin as epithelial markers and vimentin, NCAM, N-Cadherin as mesenchymal markers. As CTCs are rare cells, and the protocol developed involves isolating CTCs using the unbiased CD36-kit, we expect to detect epithelial as well as mesenchymal CTCs representing various EMT stages. In order to differentiate normal blood cells from CTCs, we will include CD45 as a blood cell marker and also stain for MCAM, which is an endothelial marker and able to differentiate CTCs from circulating endothelial cells that are present at various numbers in blood samples from healthy and cancer individuals [198]. As the aim is to study the complex interaction among AR, AKT and Hippo signalling pathways in PCa cells and ultimately in CTCs by performing multiplexing, the following markers were also chosen AR-FL, AR-V7, PSMA, pAKT, PTEN, YAP and BIRC5 (see Table 5.6). We selected these markers due to our literature review (Chapter 1). Analysing their expression and cellular localisation will help us to define the activity of the AR and related pathways.

Table 5. 6 List of shortlisted antigens for the AR/AR-V7–AKT–Hippo pathway study including cell line status for antibody optimisation

Antigen	Relevance[ref]	Positive cell lines	Negative cell lines
<i>CYTOKERATIN</i>	Epithelial & cytoskeletal protein, cytoplasm, CTC identification [284-286]	LNCaP, 22RV1, PC3	PBMCs
<i>EpCAM</i>	Epithelial protein CTC isolation / identification [287]	PC3, DU145, LNCaP	HN-3 (HNSCC), PBMCs
<i>E-CADHERIN</i>	Epithelial protein <u>EMT</u> marker [288-292]	DU145, LNCaP, PC3, 22RV1	MDA-MB231, U251, U2OS,
<i>N-CADHERIN</i>	Mesenchymal protein; <u>EMT</u> marker [288]	PC3	DU145, LNCaP
<i>VIMENTIN</i>	Mesenchymal protein <u>EMT</u> marker [293, 294]	PC3, LNCaP, DU145 (LOW)	MCF-7
<i>MCAM</i>	Endothelial marker distinguishes, endothelial cells from CTCs [198, 295, 296]	DU145, PC3, U251-HUMAN ATLAS WEBSITE	LNCaP, MCF7

<i>CD45</i>	CTC identification, distinguishes lymphocytic cells from CTCs [142]	PBMCs	CTCs
<i>Actin (detected by phalloidin)</i>	Cytoplasmic marker, cytoskeletal, cell shape and plasticity [297-301]	PC3, LNCaP, VCaP, 22RV1, DU145	NA
<i>ARFL</i>	Hormone driven transcription factor, driver of PCa [284, 296]	22RV1, LNCaP, VCaP	PC3
<i>AR-V7</i>	AR variant, driver of CRPC [284]	22RV1, VCaP	LNCaP, PC3
<i>PSMA</i>	AR target expressed on most PCa cells, target for isotope therapy & imaging [285]	LNCaP, 22RV1(Low)	PC3, DU145
<i>PD-L1</i>	Checkpoint protein (target of checkpoint inhibitors to enhance anti-cancer immunity) [296, 302]	22RV1, LNCaP, DU145	MCF-7

<i>pAKT (Ser473)</i>	Activation associated with CRPC [303]	LNCaP, PC3	22RV1, DU145
<i>PTEN</i>	Phosphatase/tumour suppressor, AKT inhibitor [304]	DU145, 22RV1	PC3
<i>YAP1</i>	Transcriptional co-activator downstream Hippo pathway [296]	U2OS	Cell signaling antibodies comparison, Normal B cells
<i>BIRC5</i>	Active YAP induces higher BIRC5 expression, Oncogene “surviving” [296]	U2-OS	PBMCs (not tested due to COVID)

In PCa cells and particularly CRPC cells, AR may be overactivated due to mutagenesis, amplification or expression of variants [26]. Often that renders the AR pathway active even in the absence of ligand and results in resistance to ADT, increased survival and proliferation [26]. The AR pathway markers we wish to evaluate are AR-FL, AR-V7, and PSMA, which is a cell surface protein commonly expressed in advanced PCa [305] and its expression is directly regulated by AR [306]. For AKT pathway evaluation, the important markers selected in this study are AKT and PTEN. PTEN is a tumour suppressor gene whose function is lost in 50% of advanced PCa and is associated with EMT [157, 307]. PTEN loss results in the activation of the AKT pathway and downstream components such as mTOR, resulting in apoptosis, autophagy and metastasis [307]. We hypothesise that there will be a positive correlation between AR-V7 and AKT activation as measured by PTEN loss and AKT phosphorylation in CTCs from ADT resistant patients [214]. The Hippo pathway is an important pathway in the development of PCa [159], and the markers selected for this pathway are YAP1 and BIRC5. As outlined in Chapter 1, Section 1.6, YAP activity is determined by its cellular localisation (active when in the nucleus) and active YAP induces high expression of BIRC5 which would result in increased tumour development [157]. From the literature, we found that YAP and AR interact with each in the nucleus. AR target genes can be suppressed by downregulating YAP [96], and hence can conclude that there is a positive relationship between YAP and AR-FL [96] and might result in poor prognosis and increased growth, while YAP activation results in loss of PTEN and then tumour formation [157]. PD-L1 was selected as an immune checkpoint marker, while Hoechst is a nuclear marker and actin (detected by phalloidin which directly binds to organised actin structures) is a cytoplasmic marker.

Table 5. 7 List of antibodies with company details, species and results

Antibodies, conjugate anti-	Clone	Catalogue #	Supplier	Host species		Optimised in this project
PE Cytokeratin	C11	5075S	Cell Signaling	M	1:100	Y
PE EpCAM	VU1D9	8995S	Cell Signaling	M	1:100	Y
FITC E- Cadherin	67A4	MA1-10194	Thermofisher	M	1:100	Y
PE N-Cadherin	8C11	12-3259-42	Thermofisher	M	1:50	Y
FITC Vimentin	V9	NBP1- 97670F	Invitro	M	1:50	Y

FITC MCAM	P1H12	11-1469-42	Thermofisher	M	1:50	Poor staining
PE CD45	HI-30	30400	BioLegend	M	1:100	Y
Actin (detected by phalloidin)	ab235137	ab235137	abcam	NA	1:4000	Y
PE AR-FL	D6F11	8428S	Cell Signaling	R	1:100	Y
APC AR-V7	E308L	36154BC	Cell Signaling	R	1:100	Y
APC PSMA	LNI-17	12702S	Cell Signaling	M	1:100	Y
PE PD-L1	E1L3N	14123S	Cell Signaling	R	1:100	Poor staining
APC p-AKT	D9E	11962S	Cell Signaling	R	1:50	Y

APC PTEN	1C3	250626-APC	Assay Matrix	M	1:100	N (stains PTEN negative cells)
FITC YAP	2F12	135472-APC	Assay Matrix	M	1:100	Y
FITC Survivin	5B10	134109- FITC	Assay Matrix	M	1:100	Y

Y: yes, N: no, M: mouse, R: rabbit

Once the markers to probe for, and the correlating antibodies were decided on and purchased, protocols had to be optimised to work in our hands for immunocytostaining with methods that will allow future incorporation into multiplex staining protocols.

I also did a literature search to identify cell lines that are either negative or positive for the markers of interest so that they could be used as negative and positive controls for antibody optimisation (see Table 5.6).

For antibody optimisation, defined numbers of relevant cells (positive and negative control cells) were seeded on sterile coverslips (see Chapter 2, Section 2.3.2 for cell culture conditions). Cells were fixed after 72 hours with 4% PFA. The fixed cells were permeabilized by using 0.2% Triton X-100 for 10 minutes followed by one PBS wash. The cells were then blocked by using 10% BSA for 30 minutes followed by another PBS wash. The cells were incubated with the relevant conjugated antibodies (see Table 5.7 for dilutions) for one hour at room temperature followed by Hoechst staining (nuclear staining) for 10 minutes, two PBS-T washes, one PBS wash and one mili-Q water wash. The coverslips were transferred to slides with mounting media and sealed by using nail polish. Imaging was done using an Olympus microscope.

5.4.1 Results

To study the complex interaction between different pathways, we selected proteins that, if detected by immunocytostaining, allow us to make conclusions about their activity. For example, YAP a co-transcription factor, kept in its inactive form by Hippo-signalling in the cytoplasm and is potentially involved in regulation of EMT and CRPC as detailed in Chapter 1, Section 1.6. YAP may be located in the nucleus as its active form, while the cytoplasmic form is prone to degradation and not functionally active [95, 163]. The proteins/antigens we selected are listed in Table 5.6.

All antibody optimisation included staining of positive (cell line expressing the antigen) and negative (cell lines not expressing the antigens) controls. A literature search was done to find the relative cell lines. PBMCs were selected as negative controls for some markers if sufficient evidence was found that they do not express these markers. Generally, adhered cell lines were used if applicable due to the ease of performing staining on adhered cells. Images of a representative staining experiment are shown for the anti- PE AR-FL antibody (Figure 5.11). Clear, predominantly nuclear staining is observed in AR-FL positive 22RV1 cells, while AR-FL negative PC3 cells stain negative in the same experiment. Similarly, both no-antibody controls show no background fluorescence in both cell lines. All antibody optimisation used the same strategy and information regarding optimisation in this project is included in Table 5.7, with most antibodies successfully optimized. Two antibodies, anti-PD-L1 and anti-MCAM, showed poor staining and one antibody, anti-PTEN, evidently bound non-specifically to cells, with apparent staining in the negative control cells regardless of concentration trialled.

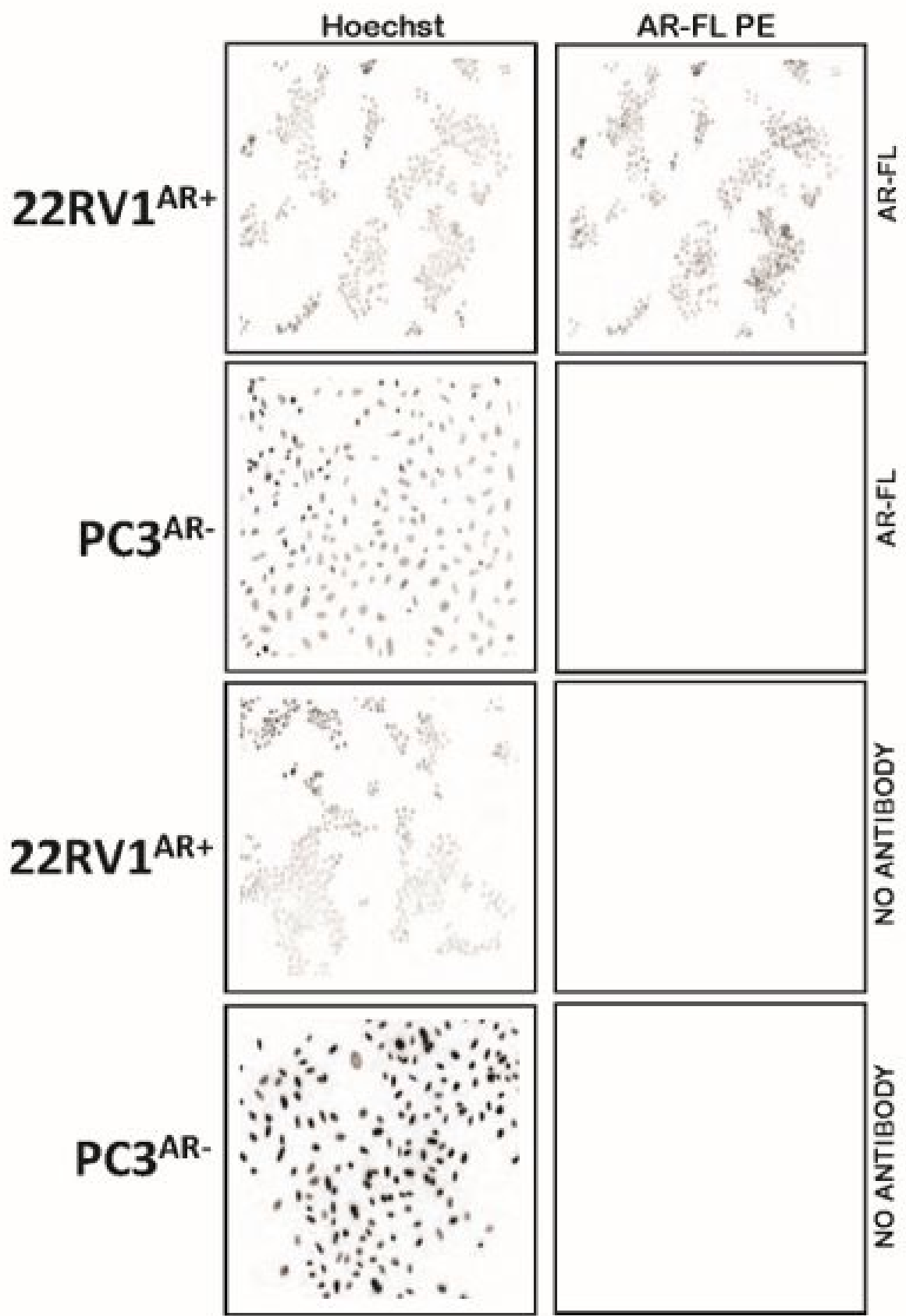


Figure 5. 11 AR-FL antibody staining

AR-FL staining in AR⁺ (22RV1) and AR⁻ (PC3). PCa cells were stained with AR-FL PE conjugated antibody. The images were generated at 20x objective by using Olympus microscope. Hoechst staining shows nuclear staining. No antibody experimental procedures were included to check for background fluorescence.

5.5 Mass spectrometry

When optimising AR-V7 antibodies (Chapter 4), Western analysis produced bands with a different, generally smaller, size than AR-V7. We thought it of interest to determine whether such bands were of proteins that may have some relation (homology) to AR-V7 to explain cross-reactivities detected. Some antibodies produced strong reaction to proteins of other size than that of AR-V7 (~80 kDa) in all cell lines, including those that are AR-V7 negative, with one band appearing relatively dominant just below the 28 kDa range (Fig 4.1C). There was also one protein band detected by two antibodies, including EPR15656, in AR-V7 negative PC3 cells that appeared just below the size of AR-V7. Despite the fact that we deemed it unlikely that PC3 expresses a protein homologue to AR-V7 this band and the other ones different from AR-V7 size prompted us to consider what proteins do cross-react with an assumed specific anti-AR-V7 antibody. To determine whether sequences homologous to AR-V7 were dominantly present in these bands, detected by antibody EPR15656, mass spectrometry was performed on bands of interest excised and eluted following polyacrylamide gel electrophoresis (PAGE).

First, total protein lysate from 22RV1 and PC3 prostate cancer cells was separated on 4-12% SDS PAGE gels and five bands corresponding to major cross-reactive bands were excised. The size of those bands (1, 2 and 3) was approximately 75 kDa, 62 kDa, 20 kDa from 22RV1 proteins and bands (4 and 5) from PC3 proteins were approximately 62 kDa and 20 kDa. After excision, the gel with the cut bands was transferred to PVDF membrane (Figure 5.12) and probed with AR-V7 antibody (EPR15656) to see whether the bands were fully excised. As shown in Figure 5.12, reactivity to these bands was lost after excision in the blot of the gel from which the bands had removed, confirming that the bands had been appropriately isolated. Two independent gels were run to isolate and analyse protein bands of interest in duplicate.

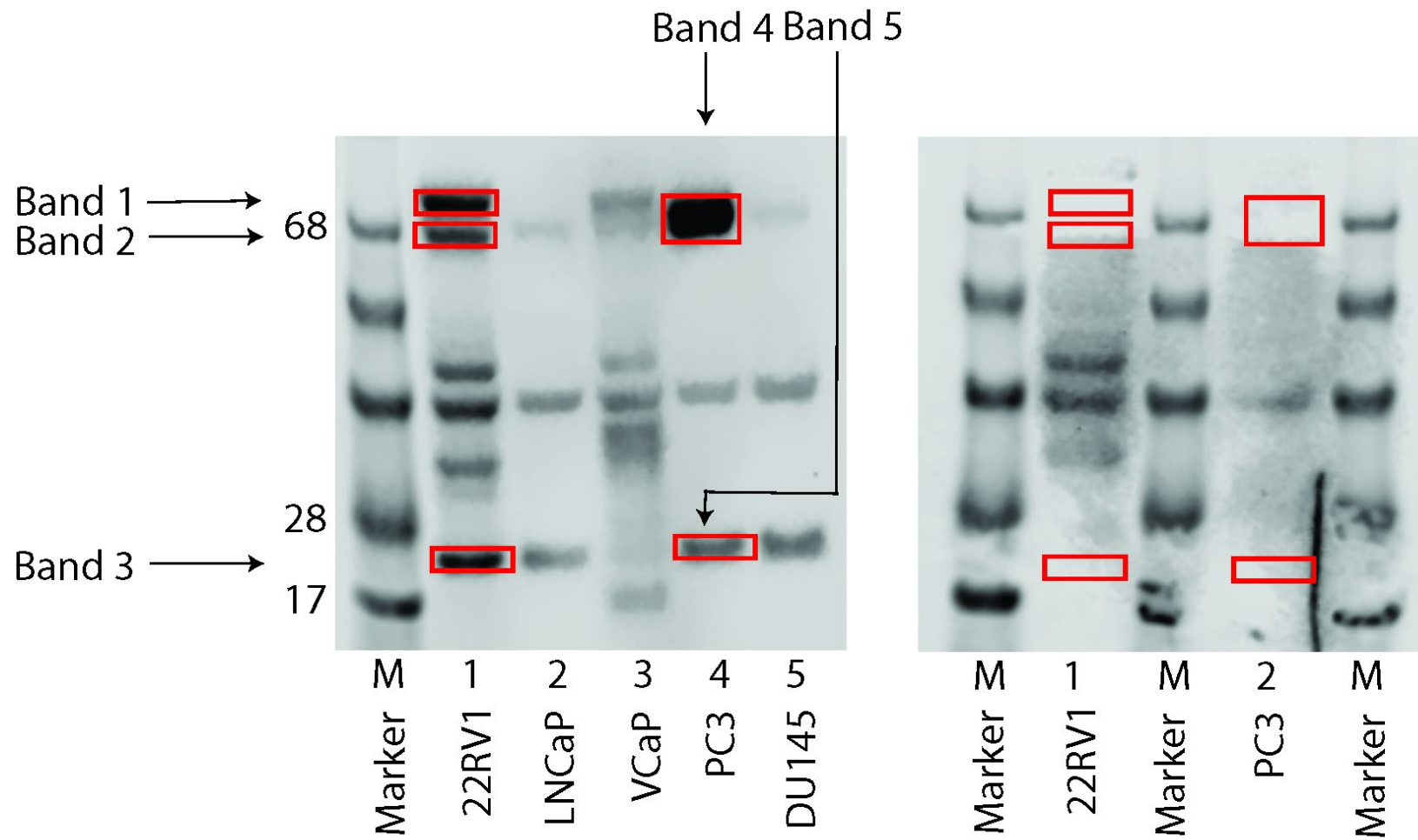


Figure 5. 12 Isolation of cross-reacting bands identified on SDS PAGE gel electrophoresis and western blot with antibody EPR15656

The immunoblot on the left shows proteins separated by SDS PAGE from the indicated cell lines probed with EPR15656 as described (Chapter 4, Section 4.5) and highlights the bands of interest (red framed) we wished to isolate from the 22RV1 and PC3 cell lines. To do so 22RV1 and PC3 protein lysates were run on another SDS gel with the same, coloured protein marker on each side of each lane. Coloured markers guided excision of the relevant bands relative to the R_f values of the markers prior to transfer. Probing the membrane with EPR15656 confirmed the relevant cross-reacting bands were successfully excised (right immunoblot, marked in red boxes). Bands were eluted and eluates analysed by mass spectrometry to identify major proteins in each band. Sample elution, preparation and mass spectrometry was performed in collaboration with Dr David Harman in the Western Sydney University Mass Spectrometry Facility).

The bands were eluted, samples prepared, and mass spectrometry performed in order to determine whether peptide homology to the AR or its variant 7 (AR-V7) could be detected.

Sample preparation was performed as follows. Gel slices were placed in protein Low-Bind tubes (500 μ L, Eppendorf). Proteins were fixed by treatment with 10% MeOH, 7% acetic acid (200 μ L) for 20 minutes. Slices were washed twice with ultrapure water (200 μ L per wash). Dehydration was performed by Speedivac and the shrunken slices were treated with 10 mM DTT in 100 mM aqueous ammonium bicarbonate (200 μ L). After heating at 60°C for 45 minutes, supernatants were aspirated and discarded. Alkylation was accomplished by the addition of 50 mM iodoacetamide in 100 mM ammonium bicarbonate (100 μ L), for 30 minutes at room temperature. Gel pieces were then washed with 100 mM ammonium bicarbonate (100 μ L) and dehydrated once more *via* Speedivac. Dried spots were treated with trypsin (20 μ L, 10 ng/ μ L) in 100 mM ammonium bicarbonate and placed on ice for 45 minutes while rehydrating. Digestion was continued at 22°C for 17 hours.

Supernatants were aspirated and placed in fresh 500 μ L tubes. Remaining peptides were extracted twice with 50% aqueous acetonitrile, 2% formic acid (50 μ L), with bath sonication for 10 minutes. Combined extracts were evaporated by Speedivac and peptides were reconstituted with 0.1% aqueous formic acid (15 μ L), using sonication for 10 minutes. Tubes were centrifuged for 10 minutes at 20,913 x g and the supernatants placed in Total Recovery chromatography vials (Thermo).

The digested peptides were separated by UPLC-MS using a Waters nanoAcquity UPLC sample manager fitted with a binary solvent manager. Separation consisted of two mobile phases. Mobile Phase A (0.1% formic acid in Milli-Q water) and Mobile Phase B (0.1% formic acid in ACN). The trapping column was a Waters nanoEase M/Z Symmetry C18 trap column (180 μ m x 20 mm) and the analytical column was a Waters nanoAcquity UPLC 1.7 μ m BEH130 C18 column (75 μ m x 100 mm) thermostated to 35°C. Elution was achieved at a flow rate of 300

nL/minute with each sample run for 50 minutes. The gradient was 0-minute 1% B; 2 minutes 10% B; 40 minutes 40% B; 42 minutes 85% B and 50 minutes 85% B. Samples were suspended in 0.1% formic acid and 1 μ L injected for each run.

Mass spectrometric detection was conducted using a Waters Synapt G2-Si, fitted with a nanoESI source, run in positive ion mode with a capillary voltage of 3 kV and a sampling cone voltage of 30 V as well as a source offset of 30 V for electrospray ionizations. The source temperature was set at 80°C. A desolvation flow of nitrogen gas at 600 L/hour and a desolvation temperature of 350°C was used. Lock spray configuration was conducted every 60 seconds with [Glu1]-fibrinopeptide B as the reference compound. Data acquisition was conducted over the mass to charge range of 50–2000. The data independent acquisition used an MSE experiment employing both low and high energy collision-induced dissociation of parent ions. Low energy collision was done at 6 V in the trap collision cell and at 4 V in the transfer collision cell. High energy collision used a collision energy ramp from 17 V to 60 V in the transfer collision cell. Scan time was 0.5 seconds and after each scan the system would switch from high to low energy collision.

Analysis of raw data was conducted using ProteinLynx Global Server (Waters), searching against the UniProt database using a Human taxonomic restriction. Variable modifications of carbamidomethyl (C), deamidated (NQ), oxidation (M) and propionamide (C) were used.

Identities of top five proteins in the gel slices is provided in Table 5.8–5.17. Those proteins detected in each of the duplicate bands are highlighted in grey. The molecular weight is given in kDa, The PLGS score is like a confidence score, the higher the better. The peptides identified is the number of peptides identified and % coverage is the proportion of all peptides in the protein identified.

Table 5. 8 22RV1 Band 1 (1)

Protein	Molecular weight (kDa)	PLGS score	Peptides identified	% Coverage
PRDX1_HUMAN	22.3	13258	18	67
SAR1A_HUMAN	22.5	4278	7	49
RL11_HUMAN	20.5	4194	7	28
Q5VVC8_HUMAN	20.2	3020	6	23
G3V1A4_HUMAN	17.0	3496	3	24

Table 5. 9 22RV1 Band 1 (duplicate)

Protein	Molecular weight (kDa)	PLGS score	Peptides identified	% Coverage
HSP7C_HUMAN	71.1	31335	34	54
Q53FA3_HUMAN	70.8	7755	8	20
F8W026_HUMAN	5.5	2673	3	40
HNRPM_HUMAN	77.8	22028	32	47
EZRI_HUMAN	69.5	20871	42	63

Table 5. 10 22RV1 Band 2 (1)

Protein	Molecular weight (kDa)	PLGS score	Peptides identified	% Coverage
DDX17_HUMAN	80.9	1099	4	11
ACADV_HUMAN	70.7	559	11	31
PUR9_HUMAN	65.1	211	13	33
DPYL2_HUMAN	62.7	186	9	32
MARCS_HUMAN	31.7	154	3	18

Table 5. 11 22RV1 Band 2 (duplicate)

Protein	Molecular weight (kDa)	PLGS score	Peptides identified	% Coverage
TKT_HUMAN	68.5	2597	20	33
ACADV_HUMAN	70.8	2251	15	36
DDX5_HUMAN	69.7	2031	14	31
HS71A_HUMAN	70.3	1343	22	53
PUR9_HUMAN	65.1	1319	19	44

Table 5. 12 22RV1 Band 3 (1)

Protein	Molecular weight (kDa)	PLGS score	Peptides identified	% Coverage
PRDX1_HUMAN	22.3	1988	9	53
MOR0P7_HUMAN	16.3	1614	4	28
PPIB_HUMAN	23.8	834	8	53
TAGL2_HUMAN	22.6	637	6	37
PEBP1_HUMAN	21.1	293	8	62

Table 5. 13 22RV1 Band 3 (duplicate)

Protein	Molecular weight (kDa)	PLGS score	Peptides identified	% Coverage
PRDX1_HUMAN	22.3	62689	23	79
RAB1B_HUMAN	22.3	25360	14	70
K7EMA7_HUMAN	7.9	23416	7	70
PPIB_HUMAN	23.8	22719	21	63
PEBP1_HUMAN	21.1	24712	16	88

Table 5. 14 PC3 Band 4 (1)

Protein	Molecular weight (kDa)	PLGS score	Peptides identified	% Coverage
HSP7C_HUMAN	71.1	71145	53	68
GRP75_HUMAN	73.9	28103	36	60
DDX5_HUMAN	69.7	25438	27	39
PABP1_HUMAN	70.9	19804	26	45
PUR9_HUMAN	65.1	19797	28	63

Table 5. 15 PC3 Band 4 (duplicate)

Protein	Molecular weight (kDa)	PLGS score	Peptides identified	% Coverage
HSP7C_HUMAN	71.1	70027	51	67
TKT_HUMAN	68.6	25098	42	68
PUR9_HUMAN	65.1	24792	24	70
DDX5_HUMAN	69.7	23432	29	46
GRP75_HUMAN	80.0	22735	36	56

Table 5. 16 PC3 Band 5 (1)

Protein	Molecular weight (kDa)	PLGS score	Peptides identified	% Coverage
PRDX1_HUMAN	22.3	54832	25	80
RAB1B_HUMAN	23.3	42642	11	59
COF1_HUMAN	18.7	20956	6	58
GSTP1_HUMAN	23.6	16653	5	30
PEBP1_HUMAN	21.2	15745	7	40

Table 5. 17 PC3 Band 5 (duplicate)

Protein	Molecular weight (kDa)	PLGS score	Peptides identified	% Coverage
PRDX1_HUMAN	22.3	13258	18	67
SAR1A_HUMAN	22.5	4278	7	49
RL11_HUMAN	20.5	4194	7	28
COF1_HUMAN	18.7	3496	3	22
SAR1B_HUMAN	22.5	3488	3	22

No homology to AR-V7 (or AR) was detected by mass spectroscopy for any of the bands (the top ones listed in the above tables or any others (data not shown)). Interestingly, in duplicate bands the top 5 detected proteins were not always identical (any identical ones found in both duplicate bands highlighted in grey) with the best match of 4 of the 5 top proteins detected for the PC3 band 4 that runs close to the molecular weight of AR-V7. To confirm this result, as a next step to test if there are indeed any proteins with homology to AR-V7 specific peptide sequences used as antigens to generate the anti-AR-V7 antibodies, a BLAST homology search of human proteins in the UniProt database with the unique peptide present in the AR-V7 sequence (See Chapter 4, Fig 4.1A) was performed using default parameters. The only sequence identified was AR-V7 itself.

5.6 Discussion

Studying the complex signalling pathway interactions in PCa has some challenges. For example, a current tumour biopsy is often not available, or multiple, sequential biopsies cannot be done. Therefore, liquid biopsies are a better option in this scenario, because this approach is less invasive and multiple liquid biopsies can be taken sequentially to track disease progress. CTCs are being studied in different types of cancer [308], but current approaches have limitations. For example, the most common method of CTC isolation is EpCAM-based isolation, in which CTCs that do not express this marker may be missed [282]. In the past, our team used the IsoFlux method in which CTCs were enriched by immunomagnetically targeting the cell surface molecule EpCAM [210]. It is also of note, there is already a commercial test offered for AR-V7 in CTCs by Epic sciences (<https://www.epicsciences.com/ar-v7-test/>). They process blood samples by first lysing red blood cells and then collecting nucleated cells on glass slides to probe for AR-V7 by immunostaining. In this study, we compared different CTC isolation methods with a focus on relatively fast, unbiased methods to retain the cellular protein landscape. We found that the CD36-kit performed better than the other tested CTC enrichment methods. However, the isolation efficiency was lower than that indicated by manufacturer which is over 80%. Our data of about 40-60% is consistently found in our lab by different operators. Other methods enrich CTCs based on cell surface markers such as EpCAM. For multiplex staining, we opted for unbiased depletion of lymphocytes to enrich as many CTCs as possible. In our hands, RosetteSep™ CTC enrichment cocktail containing anti-CD36 (Stemcell Technologies) performs well for enrichment of viable CTCs that can be cultured [277]. While testing another novel method, (OncoQuick vs. CD36-kit), we found a lot of aggregates with the OncoQuick CTC isolation method. Although there was no obvious reason for this consistent result, we excluded this method as CTC enrichment method going forward.

Secondly, we wanted to attach CTCs firmly to the glass surface for imaging. Maintaining the number of CTCs bound to each slide or glass bottom well is important for repeated manipulations during multiplex staining procedures. We found that cell adhesive called Cell-Tak improves the attachment of cells.

The work for this chapter also identified a set of 17 markers that, if immunocytostained for, are likely to have potential to inform not only about a cell's EMT status but also about the activity and possible interaction of AR/AR-V7 with the AKT and Hippo pathways in single cells. Antibodies detecting these markers were purchased and immunocytostaining procedures for these markers were optimised. The next step is combining these antibodies in multiplex staining of cultured PCa cells and PCa patient CTCs.

This chapter further describes some experiments and analysis to examine the anti-AR-V7 antibodies compared in Chapter 4. We were intrigued by some of the cross-reactive bands and were able to test their identity by mass spectrometry. However, the data from mass spectrometry and the BLAST search analysis showed no homology with the AR-V7 sequence that would explain why the antibodies interacted with them. While not as informative as we hoped, it is interesting that analysis of the PC3 (AR-V7 negative) band that runs close to AR-V7 in size, showed the most consistent data with 4 out of 5 top proteins detected in both duplicate bands. Whether one of these proteins indeed is the protein that cross reacts with the EPR15656 would however remain speculative, but if so, that may explain the band being very strong as the proteins appear abundant. Alternatively, the affinity of the antibody for the cross-reacting bands is likely to be very high if the cross-reacting protein is a minor component of the proteins eluted for the band. Overall, the mass spectrometry results indicate that the cross-reacting sequences present in the western blot are not a major component of the proteins in the samples obtained from these 1-dimensional gels. Further work in this area was not pursued but

could involve running these samples on 2D gels followed by western blot identification of specific protein spots prior to mass spectrometry. Despite not identifying the source of the cross-reactivity, the detection of cross-reacting bands in SDS PAGE is a concern, especially if immunocytochemistry as described in Chapter 4 produces background by antibodies that clearly also interact with unrelated proteins in Western analysis. It is important to highlight that our favoured anti-AR-V7 E308L antibody showed the “cleanest” immunoblot suggesting it will mainly detect AR-V7 in immunocytostaining compared to the EPR15656 clone.

5.7 Limitations

Despite identifying the best CTC isolation method of the ones tested, still only just over 50% of CTCs are captured. Nevertheless, this efficiency of CTC detection is well in line with the literature. CTC isolation efficiencies between 30->90% have been reported in recent comprehensive reviews of the literature [282, 309] for various methods, and these reviews also highlight that unbiased CTC isolation (depletion of lymphocytes) performs similarly. Thus, although it is desirable to improve CTC detection, the CTC enrichment efficiency data presented here are within an expected range. Given we are aiming ultimately to perform multiplex immunocytostaining which involves various cycles of staining and elution and washing, our methods need to retain enough CTCs immobilised to glass surfaces to allow multiple analysis steps. With some cell losses unavoidable and compromises to our methods proposed (to reduce the volume of antibodies needed), only testing *via* actual multiplex staining will confirm feasibility, and that was beyond the scope of this project. It needs also to be highlighted that actual loss of CTCs in numbers is relatively low. For example, if we counted 10 CTCs in a patient’s 10 mL blood sample, and were to recover over 50%, we would maximally lose 5 CTCs. If placing the sample into one well and other processing were to cause as much as another 20% loss that would lose another 2 CTCs. Thus, we still would expect to

analyse 3 CTCs in depth for >17 biomarkers. This may sound as if there are too few cells for analysis, but it is possible to improve CTC enrichment and immobilisation by increasing patient sample blood volume. If we start with 30 or 50 CTCs in a given sample, that will allow analysis of >17 markers in 9-15 CTCs, which is enough to allow us to detect heterogeneity to some extent.

5.8 Future directions

The next step is to progress towards multiplex staining in PCa CTCs which would not only pave the way for such a proof of concept, but it would also help to understand the complex biology of PCa. Ultimately, a robust method to detect true CTCs, in all EMT phenotypes, and with an almost real-time analysis of biological response to various therapies through multiplex immunocytostaining, could result in better methods for personalised treatment.

Chapter 6: General Discussion

Summary of the project This PhD project aimed to study the relationship between the signalling pathways that are responsible for the transition from hormone sensitive PCa to CRPC. In particular, this project was planned to develop strategies that ultimately will allow future analysis of multiple pathways in CTCs at the single cell level. The overarching aim for this project was set to study the complex relationship between AR/AR-V7, pTEN/AKT and Hippo/YAP signalling which can, as reviewed in Chapter 1, contribute to the oncogenic driver role that confers ADT resistance. Project specific, the feasible aims were to make first steps towards this goal, with a major focus on AR-V7, one of the most promising prognostic CRPC biomarkers.

For that purpose, the set aims were:

Aim 1: To systematically review and perform meta-analysis on the clinical relevance of liquid biopsy detection of the known CRPC biomarker AR-V7.

Aim 2: To determine the best anti-AR-V7 antibody to reliably detect AR-V7 in CTCs.

Aim 3: To optimise a range of methods as prerequisite for the use of multiplex immunofluorescence to analyse AR, AR-V7, AKT and Hippo pathway components, as well as markers for EMT using both cultured cells and CTCs.

Aim 1 was addressed in Chapter 3. The systematic review and meta-analysis were performed to study prognostic and predictive value of liquid biopsy-based AR-V7 detection. Our data show that AR-V7 detection in liquid biopsy was significantly associated with poor outcomes to AR signalling inhibitor treatment as shown for OS, PFS, PSA-PFS ($P < 0.001$). So, AR-V7 expression in CRPC patients can be used as a prognostic and predictive biomarker. In the taxane treated sub-group, AR-V7

expression was also significantly associated with poor OS ($P = 0.04$) while PFS ($P = 0.21$) or PSA-PFS ($P = 0.93$) was insignificant.

The reliability of systematic reviews is dependent on the quality of published literature. In the case of this study, of the 1180 papers identified, 37 (3%) papers were included in the final analysis. This number of analysed publications is greater than what is generally accepted in the field [310]. To include as much data as possible, if HR was not given, we calculated this by using the available method. Therefore, coupled with robust analysis procedures followed, we have confidence in the associations that systematic review has identified. A potential limitation of the study is that, at the time of writing, there were no randomised clinical trials looking at AR-V7 as measured by liquid biopsy. Consequently, there may be selection biased in the analysis.

Aim 2 was addressed in Chapter 4 which thoroughly compared all commercially available anti-AR-V7 antibodies. Our laboratory had the advantage of having available well characterised PCa cell lines with known AR-V7 status [51]. After confirming the AR-V7 status using our well established ddPCR AR-V7 test, Western analysis and immunocytostaining experiments were performed which ultimately resulted in finding that the anti-AR-V7 antibody clone E308L is best suited for AR-V7 immunocytostaining. Importantly, when I compared the E308L clone with the anti-AR-V7 clone EPR15656 previously used to detect AR-V7 in patient CTCs [42] E308L clearly outperformed EPR15656 as I consistently detected more PCa CTCs using E308L in all patient samples tested.

With the best anti-AR-V7 antibody at hand and optimised, **Aim 3** addressed in Chapter 5, embarked on optimisation of a range of methods which are a prerequisite for multiplex immunofluorescence to ultimately analyse pathway relations between AR,

AR-V7, AKT, Hippo pathway components and EMT using both cultured cells and patient CTCs. Firstly, I succeeded in defining the best unbiased method to enrich CTCs from blood samples (CD36-kit). I also identified and worked out the best concentration of a cell adhesive that assists in immobilisation of CTCs, which is critically important to progress to multiplex staining of these cells. Moreover, after extensive literature research and discussion with my supervisory team 17 critical markers for AR, AKT, Hippo signalling as well as EMT pathways were selected and antibodies recognizing these markers were optimised for future multiplex staining in CTCs. Although time did not allow me to utilise these technologies in multiplexed immunocytostaining, this work has laid the necessary foundations as the basis for multiplex immunocytostaining of patient CTCs.

6.1 Implications and Considerations for Clinical Translation

In Australia, PCa is the most commonly diagnosed cancer in men and second most lethal cancer [4]. AR signalling is important in normal prostate cells but often aberrantly regulated in malignant PCa cells [311]. Consequently, inhibition of the AR pathway by ADT is a critical way to treat PCa [312]. The expression of AR splice variants has been implicated as a mechanism for the resistance to ADT, ultimately resulting in progression to CRPC where enzalutamide and abiraterone have been proposed as a second line of treatment. Although these drugs are effective in the treatment of CRPC patients, some patients do not respond to this therapy, or alternatively, some patients develop resistance after some time. In PCa, tissue biopsy is not always acceptable to the patient, or possible, and multiple, sequential biopsies to follow changes of the cancer during progression are almost impossible. In CRPC, liquid biopsies can be used to monitor tumour progression [2] and multiple sequential timepoints can be studied.

The AR variant, AR-V7, has been studied in both normal and transformed prostate tissue [313]. AR-V7 remains constitutively active even in the absence of ligand binding and has been proposed as a means of resistance to different treatments.

The systematic review and meta-analysis presented here showed clear association of liquid biopsy-based AR-V7 with survival in patients treated with early or new generation AR pathway inhibitors suggesting AR-V7 testing may guide treatment decisions and as such may be an important marker to implement for clinical trials. Interestingly, AR-V7 was even a marker of poorer outcome for taxane-based chemotherapy in our study. While more data are needed to confirm this finding, straight forward liquid biopsy-based AR-V7 may prove to be clinically useful in many clinical scenarios, including being tested as an eligibility criterion for future clinical trials in CRPC patients.

Although liquid biopsy-based biomarkers testing has been promoted for a long time, clinical uptake of such tests remains limited, especially in Australia. Here, ctDNA testing for EGFR activating or first-line inhibitor resistance mutations has made some clinical headway for patients with non-small cell lung cancer [314], but apart from this liquid biopsy diagnostics is still in its infancy. Internationally, however, liquid biopsy testing is becoming more mainstream patient management, reimbursed by the relevant medicare equivalent, or paid for by the patients. One provider of commercial liquid biopsy testing is Epic Sciences in the USA, who conduct reimbursed tests for AR-V7 using CTCs from CRPC patients. Interestingly, our personal communication with Prof Howard Sher, a pioneer in immunocytostaining detection of AR-V7 in CTCs and collaborator of the Epic team, suggests that the EPR15656 anti-AR-V7 clone is used for the Epic assay. My results demonstrated that EPR15656 produced unspecific background in AR/AR-V7 negative cells and detected fewer CTCs than the E308L antibody

clone in our hands. Thus, development of a better diagnostic AR-V7 test than provided by Epics Sciences is possible.

In addition to the clinical benefits of AR-V7 testing by liquid biopsy described above, AR-V7 biology investigation through immunocytostaining has advantages that can be further developed for the future. For example, this approach allows the detection, quantitation and definition of cellular localisation of target proteins at a single cell level. This capability opens the potential to study the impact of cellular heterogeneity on disease outcome which may lead to a highly specific assay to stratify patients according to their single cell target protein status. The capability to examine cellular localisation of multiple proteins also opens the potential to examine the spatial location of several proteins in the same cell, thus providing a method for identifying protein-protein interactions of clinically relevant markers in clinically relevant cells. Based on the extensive literature analysis of relevant signalling pathways in PCa presented here, the molecular complexity and interactions of the AR/AKT/Hippo pathways are important interactions to study. The new capabilities developed in this thesis will add significantly to the scope with which this complex biology underlying CRPC development and progression are explored in the future by our team and others.

This project also defined the best CTC isolation method for down-stream multiplex staining of CTCs. We reasoned that an unbiased method, not preselecting CTCs by expression of cell surface markers such as EpCAM, that would also be relatively fast and gentle on the cells so as to avoid disturbing their proteomic landscape, was preferred. Since we already knew that the CD36-kit was able to isolate viable CTCs that may be cultured [277], it was satisfying to find it and the most effective CTC enrichment method of the ones tested. While still not ideal (efficiency around 50%), this optimized method is likely to be scaleable to a clinical setting, although further work will be necessary to evaluate this necessary goal.

This project also defined a method to immobilize CTCs on glass surfaces, which is critically important for future multiplex analysis that relies on imaging the same cells in different staining cycles and to overlay images. This is only possible if the cells are found at the same position in every staining cycle. Overall, this project made critical steps for future CTC analysis by multiplex immunocytostaining (proteomic microscopy).

6.2 Limitations of This Project

Chapter 3: The limitations for the systematic review and meta-analysis presented here were the heterogeneous methods of AR-V7 detection in multiple types of liquid biopsies from patients with a range of treatment regimens, in the various studies. With AR-V7 still being a relatively novel biomarker, the liquid biopsy research field still developing and clinicians making therapy decisions based on multiple parameters, this was not surprising. Given this variability, reports using different methods and liquid biopsy types were combined to increase the depth of the study and ultimately, the patient number included. Where possible, and the number of studies and patient numbers allowed it, sub-analyses were performed for the detection of AR-V7 in liquid biopsies based on different methods or patient treatments. Our data suggest predictive value of AR-V7 and found association of AR-V7 with response to the various treatments. The unexpected findings were that for AR-V7 positive patients it appeared that taxanes therapy was associated with better outcome. However, we realise that the limitation because most studies were not proper randomised trials. Despite the limitations, overall correlation with disease outcomes was evident in the analysis. Nevertheless, this study made it clear that development of one highly sensitive and specific method to detect AR-V7 would be desirable to progress to routine diagnostic settings.

Chapter 4: Although the use of well-characterised PCa cell models with respect to AR-V7 expression allowed us to convincingly identify the best anti-AR-V7 antibody for

immunocytostaining, the potential to validate this antibody in PCa patients was limited to testing AR-V7 immunodetection in CTCs of only six patients (patient recruitment was beyond our control, see COVID impact statement). Nevertheless, I detected consistently more CTCs with the best E308L antibody in this small patient cohort, providing strong evidence, albeit from few patients, that E308L is the best anti-AR-V7 antibody to detect AR-V7 in patient CTCs. Larger patient cohorts are certainly needed to compare AR-V7 detection by immunocytochemistry with AR-V7 detection at the mRNA level by ddPCR. These studies should include correlation with disease outcomes to fully understand if combining both methods versus using one over the other is the best approach for development of practical assays for diagnostic settings. Cost, time, equipment and expertise needed to do the assays should also be considered. Even if these studies may not show added value of immunocytostaining for simple evaluation if a patient's AR-V7 status is positive vs. negative, it is expected that AR-V7 immunocytochemistry detection in CTCs will reveal heterogeneity, and heterogeneity may be a powerful predictor if mono- or combination therapy is the better clinical approach for patient management or provide guidance to clinicians for next line therapy choices.

Chapter 5: The most disappointing limitation of this project was that it did not reach the end point of performing multiplex staining of either cultured cells or patient CTCs. Nevertheless, important steps towards this goal were made. The best of the tested methods for unbiased CTC enrichment was defined in this study. For multiplex immunostaining, we want to isolate as many CTCs as possible in order to do multiple rounds of staining to probe for various markers, washing and then re-staining. We wanted to isolate CTCs independent of any cell surface markers in order to study the selected markers and in our comparison the CD36-kit (Stemcell Technologies) proved the best method. Regardless, this method has an efficiency of only capturing about 50%, which means only about half of a patient's CTCs are expected to be

captured, which is suboptimal. CTC enrichment is a critical step if we want to perform multiplex CTC immunocytostaining in the future. Not enriching CTCs and instead analysing simply all the cells in a blood sample to avoid losing CTCs due to technical issues may appear an option. However, the number of blood cells in the sample make this a non-viable solution for multiplex staining. For instance, there are methods such as CTC detection using the Rarecyte CTC platform (Rarecyte Precision Biology for Life Sciences) [315] that essentially use a density gradient as only CTC enrichment, followed by spreading the entire PBMC/CTC fraction from 7.5 mL blood over 8 complete glass slides for immunostaining. 8 complete slides are necessary to achieve single cell layers for microscopy due to the large PBMC numbers. Given the rarity of CTCs, to analyse most CTCs, most slides will need to be immunostained. For multiplex staining that would lead to unaffordable costs of antibodies. As an example, my supervisors' current NHMRC grant to develop CTC multiplex staining budgets ~\$50,000 for antibodies (assuming staining on much smaller specialised ibidi slides (Fig 5.10)), however, if staining would need to be done on 8 complete slides for each patient and each biomarker to be tested, costs would increase to >\$1,000,000 for antibodies alone.

As indicated, the COVID-19 pandemic (see COVID impact statement) prevented further work on multiplex staining of CTCs or even PCa cell lines. This was due to limited access to the UNSW laboratories central to multiplex staining procedures. These events were mitigated by changes to the project plan and timeline which included i) addition of the initially unplanned systematic review, ii) detailed analysis based on the identified need to find the best anti-AR-V7 antibody and iii) adding mass spectrometry analysis to interrogate certain anti-AR-V7 antibody cross-reactions.

6.3 Future Directions

While our laboratory has established an extremely sensitive ddPCR-based method of AR-V7 (transcript) detection from as low as a single CTC [51], and also previously confirmed that CTCs are the best liquid biopsy source to detect AR-V7 [210], it is tempting to speculate that our method may be the basis of a standardised liquid biopsy testing for AR-V7 that could become a globally used diagnostic test. Further, I would propose that the ddPCR based detection of AR-V7 (transcript) would be complemented by also detecting AR-V7 protein by immunocytostaining of CTCs. My project has provided a basis for this as I identified the best suitable anti-AR-V7 antibody for AR-V7 detection in CTCs.

A possible limitation of this study is that CTCs identified by antibody E308L may be false positives. The specificity and sensitivity of E308L was clearly shown to be superior to other antibodies by performing western blotting and immunocytostaining of AR-V7 positive and negative cell lines. To further confirm the specificity, future studies could include spiking defined numbers of cultured cells into blood to model CTCs and identify them by using these antibodies. AR-V7 protein detection would allow to observe heterogeneity and analyse cellular localisation as well as co-localisation with other proteins that may improve our understanding of AR-V7 biology.

Clearly, future studies on larger patient cohorts are needed to work out how to best test for AR-V7 and compare utility of combined transcript (ddPCR) and protein (immunocytostaining) detection from liquid biopsy. This could become a future PhD project together with taking the final steps to progress my work of CTC isolation, immobilisation and optimisation of antibodies for probing CTCs to finally perform full CTC multiplex immunocytostaining combined with sophisticated analysis.

6.4 Conclusion

This project was designed to study AR-V7 in liquid biopsies at the single cell level and the interaction with AKT and Hippo pathway in PCa. The important results of this project are:

1. A thorough review of the AR/AR-V7 pathway and its interaction with other cancer associated signalling pathways has been performed.
2. Liquid biopsy detection of AR-V7 has been confirmed as an important biomarker and its detection is associated with poor disease outcomes.
3. Sensitivity and specificity of commercially available anti-AR-V7 antibodies varies widely and data presented here point towards the clone E308L being the best anti-AR-V7 antibody for immunocytostaining, including in the detection of CTCs.
4. RosetteSep CD36-kit is the best CTC isolation method of the ones tested.
5. Cell-Tak is a suitable component to help attaching CTCs to glass bottom plates for immunocytostaining and imaging.
6. 17 antigens/antibodies were identified in a literature review and are proposed to allow analysis of the AR/AR-V7 pathway, as well as interaction with the AKT and Hippo pathways and EMT status in CTCs. The relevant antibodies were purchased and optimised for immunocytostaining, and the developed optimisation can be transferred to multiplex CTC staining in the future.

The translational goals of this project remain critically important, and the data from this project have added to the body of work that indicate these goals are achievable and necessary. The next step is to perform proteomic microscopy at the single CTC level in order to study the complex interactions of signalling pathways. Ultimately, these analyses may reveal key components of these pathways that could be screened for as novel biomarkers in down-scaled multiplex approaches that would be feasible for

automated staining platforms already available in many diagnostic labs. If this goal is achieved in the future, my project has provided the initial steps to aid better diagnostics followed by personalised treatment decisions in the clinic for men with currently incurable disease. Furthermore, it would have helped to revolutionise the utility of CTCs and liquid biopsies by assessing multiple relevant biomarkers at once. The latter is likely applicable to other biomarkers in other cancers.

While the project had some limitations, these were either overcome, or analysis of data was valid despite those limitations, or the direction of the PhD project was meaningfully changed to pursue achievable goals in the circumstances posed by the pandemic. The project resulted in the delivery of novel outcomes that pave the way for future projects including multiplex immunocytostaining of CTCs.

Chapter 7: References

7.1 References Uncategorized References

1. Khan, T., et al., *The Prospect of Identifying Resistance Mechanisms for Castrate-Resistant Prostate Cancer Using Circulating Tumor Cells: Is Epithelial-to-Mesenchymal Transition a Key Player?* 2020. **2020**.
2. Khan, T., et al., *Prognostic and Predictive Value of Liquid Biopsy-Derived Androgen Receptor Variant 7 (AR-V7) in Prostate Cancer: A Systematic Review and Meta-Analysis*. 2022. **12**.
3. Jemal, A., et al., *Global cancer statistics*. CA: a cancer journal for clinicians, 2011. **61**(2): p. 69-90.
4. *Prostate cancer in Australia statistics*. 2022 11-03-2022 [cited 2022 04-05-2022]; Available from: <https://www.canceraustralia.gov.au/cancer-types/prostate-cancer/statistics>.
5. Huggins, C. and C.V.J.C.r. Hodges, *Studies on prostatic cancer. I. The effect of castration, of estrogen and of androgen injection on serum phosphatases in metastatic carcinoma of the prostate*. 1941. **1**(4): p. 293-297.
6. Anderson, K. and S.J.N. Liao, *Selective retention of dihydrotestosterone by prostatic nuclei*. 1968. **219**(5151): p. 277-279.
7. Bruchovsky, N. and J.D.J.J.o.B.C. Wilson, *The intranuclear binding of testosterone and 5 α -androstano-17 β -ol-3-one by rat prostate*. 1968. **243**(22): p. 5953-5960.
8. Mainwaring, W.J.J.o.E., *A soluble androgen receptor in the cytoplasm of rat prostate*. 1969. **45**(4): p. 531-541.
9. Agoulnik, I.U., et al., *Androgens modulate expression of transcription intermediary factor 2, an androgen receptor coactivator whose expression level correlates with early biochemical recurrence in prostate cancer*. Cancer research, 2006. **66**(21): p. 10594-10602.
10. Kim, Y., et al., *Update on Hsp90 inhibitors in clinical trial*. Current topics in medicinal chemistry, 2009. **9**(15): p. 1479-1492.
11. Shafi, A.A., A.E. Yen, and N.L. Weigel, *Androgen receptors in hormone-dependent and castration-resistant prostate cancer*. Pharmacology & therapeutics, 2013. **140**(3): p. 223-238.
12. Koochekpour, S., *Androgen receptor signaling and mutations in prostate cancer*. Asian journal of andrology, 2010. **12**(5): p. 639.
13. Dehm, S.M. and D.J. Tindall, *Molecular regulation of androgen action in prostate cancer*. Journal of cellular biochemistry, 2006. **99**(2): p. 333-344.
14. Jernberg, E., A. Bergh, and P. Wikström, *Clinical relevance of androgen receptor alterations in prostate cancer*. Endocrine connections, 2017. **6**(8): p. R146-R161.
15. Nadiminty, N., et al., *NF- κ B2/p52 induces resistance to enzalutamide in prostate cancer: role of androgen receptor and its variants*. Molecular cancer therapeutics, 2013. **12**(8): p. 1629-1637.
16. Mostaghel, E.A., et al., *Resistance to CYP17A1 inhibition with abiraterone in castration-resistant prostate cancer: induction of steroidogenesis and androgen receptor splice variants*. Clinical cancer research, 2011. **17**(18): p. 5913-5925.
17. Hu, R., et al., *Ligand-independent androgen receptor variants derived from splicing of cryptic exons signify hormone-refractory prostate cancer*. Cancer research, 2009. **69**(1): p. 16-22.
18. Guo, Z., et al., *A novel androgen receptor splice variant is up-regulated during prostate cancer progression and promotes androgen depletion-resistant growth*. Cancer research, 2009. **69**(6): p. 2305-2313.
19. Abeshouse, A., et al., *The molecular taxonomy of primary prostate cancer*. Cell, 2015. **163**(4): p. 1011-1025.
20. Lu, C. and J. Luo, *Decoding the androgen receptor splice variants*. Translational andrology and urology, 2013. **2**(3): p. 178.

21. Li, Y., et al., *Androgen receptor splice variants mediate enzalutamide resistance in castration-resistant prostate cancer cell lines*. *Cancer research*, 2013. **73**(2): p. 483-489.
22. Cao, B., et al., *Androgen receptor splice variants activating the full-length receptor in mediating resistance to androgen-directed therapy*. *Oncotarget*, 2014. **5**(6): p. 1646.
23. Xu, D., et al., *Androgen receptor splice variants dimerize to transactivate target genes*. *Cancer research*, 2015. **75**(17): p. 3663-3671.
24. Qu, Y., et al., *Constitutively active AR-V7 plays an essential role in the development and progression of castration-resistant prostate cancer*. *Scientific reports*, 2015. **5**: p. 7654.
25. Haffner, M.C., et al., *Genomic and phenotypic heterogeneity in prostate cancer*. 2021. **18**(2): p. 79-92.
26. Ehsani, M., F.O. David, and A.J.C. Baniahmad, *Androgen receptor-dependent mechanisms mediating drug resistance in prostate cancer*. 2021. **13**(7): p. 1534.
27. Formaggio, N., M.A. Rubin, and J.-P.J.O. Theurillat, *Loss and revival of androgen receptor signaling in advanced prostate cancer*. 2021. **40**(7): p. 1205-1216.
28. Hoang, D.T., et al., *Androgen receptor-dependent and-independent mechanisms driving prostate cancer progression: Opportunities for therapeutic targeting from multiple angles*. *Oncotarget*, 2017. **8**(2): p. 3724.
29. Shapiro, D. and B. Tareen, *Current and emerging treatments in the management of castration-resistant prostate cancer*. *Expert review of anticancer therapy*, 2012. **12**(7): p. 951-964.
30. Chen, C.D., et al., *Molecular determinants of resistance to antiandrogen therapy*. *Nature medicine*, 2004. **10**(1): p. 33.
31. Knudsen, K.E. and H.I. Scher, *Starving the addiction: new opportunities for durable suppression of AR signaling in prostate cancer*. *Clinical Cancer Research*, 2009. **15**(15): p. 4792-4798.
32. Longo, D.L., *New therapies for castration-resistant prostate cancer*. 2010, Mass Medical Soc.
33. De Bono, J.S., et al., *Abiraterone and increased survival in metastatic prostate cancer*. *New England Journal of Medicine*, 2011. **364**(21): p. 1995-2005.
34. Ryan, C.J., et al., *Abiraterone in metastatic prostate cancer without previous chemotherapy*. *New England Journal of Medicine*, 2013. **368**(2): p. 138-148.
35. Beer, T.M., et al., *Enzalutamide in metastatic prostate cancer before chemotherapy*. *New England Journal of Medicine*, 2014. **371**(5): p. 424-433.
36. Scher, H.I., et al., *Increased survival with enzalutamide in prostate cancer after chemotherapy*. *New England Journal of Medicine*, 2012. **367**(13): p. 1187-1197.
37. Fizazi, K., et al., *Abiraterone acetate for treatment of metastatic castration-resistant prostate cancer: final overall survival analysis of the COU-AA-301 randomised, double-blind, placebo-controlled phase 3 study*. *The lancet oncology*, 2012. **13**(10): p. 983-992.
38. Fang, M., et al., *Efficacy of abiraterone and enzalutamide in pre-and postdocetaxel castration-resistant prostate cancer: a trial-level meta-analysis*. *Prostate cancer*, 2017. **2017**.
39. Linder, S., et al., *Enzalutamide therapy for advanced prostate cancer: efficacy, resistance and beyond*. *Endocrine-related cancer*, 2018. **1**(aop).
40. Mittal, V., *Epithelial mesenchymal transition in tumor metastasis*. *Annual Review of Pathology: Mechanisms of Disease*, 2018. **13**: p. 395-412.
41. Nieto, M.A., et al., *EMT: 2016*. *Cell*, 2016. **166**(1): p. 21-45.
42. Scher, H.I., et al., *Association of AR-V7 on circulating tumor cells as a treatment-specific biomarker with outcomes and survival in castration-resistant prostate cancer*. *JAMA oncology*, 2016. **2**(11): p. 1441-1449.
43. Scher, H.I., et al., *Nuclear-specific AR-V7 Protein Localization is Necessary to Guide Treatment Selection in Metastatic Castration-resistant Prostate Cancer*. *Eur Urol*, 2017. **71**(6): p. 874-882.
44. Scher, H.I., et al., *Assessment of the validity of nuclear-localized androgen receptor splice variant 7 in circulating tumor cells as a predictive biomarker for castration-resistant prostate cancer*. *JAMA oncology*, 2018. **4**(9): p. 1179-1186.

45. Antonarakis, E.S., et al., *AR-V7 and resistance to enzalutamide and abiraterone in prostate cancer*. New England Journal of Medicine, 2014. **371**(11): p. 1028-1038.
46. Cristofanilli, M., et al., *Circulating tumor cells, disease progression, and survival in metastatic breast cancer*. New England Journal of Medicine, 2004. **351**(8): p. 781-791.
47. Mateo, J., et al., *Accelerating precision medicine in metastatic prostate cancer*. 2020. **1**(11): p. 1041-1053.
48. Ignatiadis, M., G.W. Sledge, and S.S.J.N.r.C.o. Jeffrey, *Liquid biopsy enters the clinic—Implementation issues and future challenges*. 2021. **18**(5): p. 297-312.
49. Yu, M., et al., *Circulating tumor cells: approaches to isolation and characterization*. 2011. **192**(3): p. 373-382.
50. Ferreira, M.M., V.C. Ramani, and S.S.J.M.o. Jeffrey, *Circulating tumor cell technologies*. 2016. **10**(3): p. 374-394.
51. Ma, Y., et al., *Droplet digital PCR based androgen receptor variant 7 (AR-V7) detection from prostate cancer patient blood biopsies*. International journal of molecular sciences, 2016. **17**(8): p. 1264.
52. Young, F.P., et al., *Biomarkers of Castrate Resistance in Prostate Cancer: Androgen Receptor Amplification and T877A Mutation Detection by Multiplex Droplet Digital PCR*. Journal of Clinical Medicine, 2022. **11**(1): p. 257.
53. Ding, P.N., et al., *Plasma next generation sequencing and droplet digital PCR-based detection of epidermal growth factor receptor (EGFR) mutations in patients with advanced lung cancer treated with subsequent-line osimertinib*. 2019. **10**(10): p. 1879-1884.
54. Caixeiro, N.J., et al., *Circulating tumour cells—a bona fide cause of metastatic cancer*. Cancer and Metastasis Reviews, 2014. **33**(2-3): p. 747-756.
55. Wang, Y., et al., *Liquid biopsy in prostate cancer: current status and future challenges of clinical application*. 2021. **24**(1): p. 58-71.
56. Yao, D., C. Dai, and S. Peng, *Mechanism of the mesenchymal–epithelial transition and its relationship with metastatic tumor formation*. Molecular cancer research, 2011. **9**(12): p. 1608-1620.
57. Stylianou, N., et al., *A molecular portrait of epithelial–mesenchymal plasticity in prostate cancer associated with clinical outcome*. Oncogene, 2018: p. 1.
58. Cheng, M., et al., *Circulating tumor cells are associated with bone metastasis of lung cancer*. Asian Pacific Journal of Cancer Prevention, 2014. **15**(15): p. 6369-6374.
59. Yang, Y.J., et al., *Phenotypes of circulating tumour cells predict time to castration resistance in metastatic castration-sensitive prostate cancer*. BJU international, 2019. **124**(2): p. 258-267.
60. Chen, J., et al., *Metabolic reprogramming-based characterization of circulating tumor cells in prostate cancer*. Journal of Experimental & Clinical Cancer Research, 2018. **37**(1): p. 127.
61. Steeg, P.S., *Tumor metastasis: mechanistic insights and clinical challenges*. Nature medicine, 2006. **12**(8): p. 895.
62. Montanari, M., et al., *Epithelial-mesenchymal transition in prostate cancer: an overview*. Oncotarget, 2017. **8**(21): p. 35376.
63. Lo, U., et al., *The role and mechanism of epithelial-to-mesenchymal transition in prostate cancer progression*. International journal of molecular sciences, 2017. **18**(10): p. 2079.
64. Stemmler, M.P., et al., *Non-redundant functions of EMT transcription factors*. Nat Cell Biol, 2019. **21**(1): p. 102-112.
65. Santamaria, P.G., G. Moreno-Bueno, and A. Cano, *Contribution of Epithelial Plasticity to Therapy Resistance*. J Clin Med, 2019. **8**(5).
66. Yang, M.-H., et al., *Direct regulation of TWIST by HIF-1 α promotes metastasis*. Nature cell biology, 2008. **10**(3): p. 295.
67. Imai, T., et al., *Hypoxia attenuates the expression of E-cadherin via up-regulation of SNAIL in ovarian carcinoma cells*. The American journal of pathology, 2003. **163**(4): p. 1437-1447.

68. Yang, J. and R.A. Weinberg, *Epithelial-mesenchymal transition: at the crossroads of development and tumor metastasis*. *Developmental cell*, 2008. **14**(6): p. 818-829.
69. Katoh, Y. and M. Katoh, *Hedgehog signaling, epithelial-to-mesenchymal transition and miRNA*. *International journal of molecular medicine*, 2008. **22**(3): p. 271-275.
70. De Craene, B. and G. Berx, *Regulatory networks defining EMT during cancer initiation and progression*. *Nature Reviews Cancer*, 2013. **13**(2): p. 97.
71. Huber, M.A., H. Beug, and T. Wirth, *Epithelial-mesenchymal transition: NF- κ B takes center stage*. *Cell cycle*, 2004. **3**(12): p. 1477-1480.
72. Moustakas, A. and C.H. Heldin, *Signaling networks guiding epithelial-mesenchymal transitions during embryogenesis and cancer progression*. *Cancer science*, 2007. **98**(10): p. 1512-1520.
73. Christofori, G., *New signals from the invasive front*. *Nature*, 2006. **441**(7092): p. 444.
74. Thiery, J.P., *Epithelial-mesenchymal transitions in tumour progression*. *Nature Reviews Cancer*, 2002. **2**(6): p. 442.
75. Thiery, J.P., et al., *Epithelial-mesenchymal transitions in development and disease*. *cell*, 2009. **139**(5): p. 871-890.
76. Kalluri, R. and R.A. Weinberg, *The basics of epithelial-mesenchymal transition*. *The Journal of clinical investigation*, 2009. **119**(6): p. 1420-1428.
77. Lin, C.Y., et al., *Elevation of androgen receptor promotes prostate cancer metastasis by induction of epithelial-mesenchymal transition and reduction of KAT5*. *Cancer science*, 2018. **109**(11): p. 3564.
78. Miao, L., et al., *Disrupting androgen receptor signaling induces Snail-mediated epithelial-mesenchymal plasticity in prostate cancer*. *Cancer research*, 2017. **77**(11): p. 3101-3112.
79. Kong, D., et al., *Androgen receptor splice variants contribute to prostate cancer aggressiveness through induction of EMT and expression of stem cell marker genes*. *The Prostate*, 2015. **75**(2): p. 161-174.
80. Lavery, D.N. and C.L. Bevan, *Androgen receptor signalling in prostate cancer: the functional consequences of acetylation*. *BioMed Research International*, 2010. **2011**.
81. Tan, M.E., et al., *Androgen receptor: structure, role in prostate cancer and drug discovery*. *Acta Pharmacologica Sinica*, 2015. **36**(1): p. 3.
82. Puche-Sanz, I., et al., *A comprehensive study of circulating tumour cells at the moment of prostate cancer diagnosis: biological and clinical implications of EGFR, AR and SNPs*. *Oncotarget*, 2017. **8**(41): p. 70472-70480.
83. Podolak, J., et al., *Androgen receptor amplification is concordant between circulating tumor cells and biopsies from men undergoing treatment for metastatic castration resistant prostate cancer*. *Oncotarget*, 2017. **8**(42): p. 71447.
84. Jiang, Y., et al., *Detection of androgen receptor mutations in circulating tumor cells in castration-resistant prostate cancer*. *Clinical chemistry*, 2010. **56**(9): p. 1492-1495.
85. Xu, W., Z. Yang, and N. Lu, *A new role for the PI3K/Akt signaling pathway in the epithelial-mesenchymal transition*. *Cell adhesion & migration*, 2015. **9**(4): p. 317-324.
86. Dong, J., et al., *Activation of phosphatidylinositol 3-kinase/AKT/snail signaling pathway contributes to epithelial-mesenchymal transition-induced multi-drug resistance to sorafenib in hepatocellular carcinoma cells*. *PLoS One*, 2017. **12**(9): p. e0185088.
87. Fang, F., et al., *Juglone suppresses epithelial-mesenchymal transition in prostate cancer cells via the protein kinase B/glycogen synthase kinase-3 β /Snail signaling pathway*. *Oncology letters*, 2018. **16**(2): p. 2579-2584.
88. Sittadjody, S., et al., *Non-androgen signaling pathways in castration-resistant prostate cancer*, in *Managing metastatic prostate cancer in your urological oncology practice*. 2016, Springer. p. 35-63.
89. da Silva, H.B., et al., *Dissecting major signaling pathways throughout the development of prostate cancer*. *Prostate cancer*, 2013. **2013**.

90. Kallergi, G., et al., *Phosphorylated EGFR and PI3K/Akt signaling kinases are expressed in circulating tumor cells of breast cancer patients*. Breast cancer research, 2008. **10**(5): p. R80.
91. Li, J., et al., *pERK/pAkt phenotyping in circulating tumor cells as a biomarker for sorafenib efficacy in patients with advanced hepatocellular carcinoma*. Oncotarget, 2016. **7**(3): p. 2646.
92. Punnoose, E.A., et al., *PTEN loss in circulating tumour cells correlates with PTEN loss in fresh tumour tissue from castration-resistant prostate cancer patients*. British Journal Of Cancer, 2015. **113**: p. 1225.
93. Shao, D.D., et al., *KRAS and YAP1 converge to regulate EMT and tumor survival*. Cell, 2014. **158**(1): p. 171-184.
94. Ou, H., et al., *Frizzled 2-induced epithelial-mesenchymal transition correlates with vasculogenic mimicry, stemness, and Hippo signaling in hepatocellular carcinoma*. Cancer Science, 2019. **110**(4): p. 1169.
95. Zhang L, et al., *The hippo pathway effector YAP regulates motility, invasion, and castration-resistant growth of prostate cancer cells*. Molecular and cellular biology, 2015. **35**(8): p. 1350-62.
96. Salem, O. and C.G. Hansen, *The Hippo Pathway in Prostate Cancer*. Cells, 2019. **8**(4): p. 370.
97. Wu, M., et al., *TAZ expression in three distinct circulating tumor cells of NSCLC patients*. INTERNATIONAL JOURNAL OF CLINICAL AND EXPERIMENTAL PATHOLOGY, 2017. **10**(5): p. 5721-5729.
98. Qiao, Y., et al., *YAP regulates actin dynamics through ARHGAP29 and promotes metastasis*. Cell reports, 2017. **19**(8): p. 1495-1502.
99. Huang, M., et al., *MAPK pathway mediates epithelial-mesenchymal transition induced by paraquat in alveolar epithelial cells*. Environmental toxicology, 2016. **31**(11): p. 1407-1414.
100. Hawsawi, O., et al., *High mobility group A2 (HMGA2) promotes EMT via MAPK pathway in prostate cancer*. Biochemical and biophysical research communications, 2018. **504**(1): p. 196-202.
101. Gui, T., et al., *The Roles of Mitogen-Activated Protein Kinase Pathways in TGF-beta-Induced Epithelial-Mesenchymal Transition*. J Signal Transduct, 2012. **2012**: p. 289243.
102. Mukherjee, R., et al., *Upregulation of MAPK pathway is associated with survival in castrate-resistant prostate cancer*. British journal of cancer, 2011. **104**(12): p. 1920.
103. Rodríguez-Berriguete, G., et al., *MAP kinases and prostate cancer*. Journal of signal transduction, 2012. **2012**.
104. Sergeant, G., et al., *Pancreatic cancer circulating tumour cells express a cell motility gene signature that predicts survival after surgery*. BMC cancer, 2012. **12**(1): p. 527.
105. Loree, J.M., S. Kopetz, and K.P. Raghav, *Current companion diagnostics in advanced colorectal cancer; getting a bigger and better piece of the pie*. Journal of gastrointestinal oncology, 2017. **8**(1): p. 199.
106. Reid, A.L., et al., *Detection of BRAF-V600E and V600K in melanoma circulating tumour cells by droplet digital PCR*. Clinical biochemistry, 2015. **48**(15): p. 999-1002.
107. Cheng, Z.-X., et al., *Nuclear Factor- κ B-Dependent Epithelial to Mesenchymal Transition Induced by HIF-1 α Activation in Pancreatic Cancer Cells under Hypoxic Conditions*. PLoS One, 2011. **6**(8): p. e23752.
108. Nomura, A., et al., *Inhibition of NF-kappa B pathway leads to deregulation of epithelial-mesenchymal transition and neural invasion in pancreatic cancer*. Laboratory Investigation, 2016. **96**(12): p. 1268.
109. Verzella, D., et al., *Targeting the NF- κ B pathway in prostate cancer: a promising therapeutic approach?* Current Drug Targets, 2016. **17**(3): p. 311-320.
110. Staal, J. and R. Beyaert, *Inflammation and NF- κ B signaling in prostate cancer: Mechanisms and clinical implications*. Cells, 2018. **7**(9): p. 122.

111. Mariscal, J., et al., *Molecular Profiling of Circulating Tumour Cells Identifies Notch1 as a Principal Regulator in Advanced Non-Small Cell Lung Cancer*. Scientific Reports, 2016. **6**: p. 37820.
112. Lo, U.-G., et al., *IFN γ -Induced IFIT5 Promotes Epithelial-to-Mesenchymal Transition in Prostate Cancer via miRNA Processing*. Cancer research, 2019. **79**(6): p. 1098-1112.
113. Xiong, H., et al., *Roles of STAT3 and ZEB1 proteins in E-cadherin down-regulation and human colorectal cancer epithelial-mesenchymal transition*. Journal of Biological Chemistry, 2012. **287**(8): p. 5819-5832.
114. Zhang, M., et al., *RHBDD1 promotes colorectal cancer metastasis through the Wnt signaling pathway and its downstream target ZEB1*. Journal of Experimental & Clinical Cancer Research, 2018. **37**(1): p. 22.
115. Lee, M.S., et al., *The metastasis suppressor CD82/KAI1 represses the TGF- β 1 and Wnt signalings inducing epithelial-to-mesenchymal transition linked to invasiveness of prostate cancer cells*. The Prostate, 2019.
116. Chen, C.-J., et al., *Epithelial-type CD133+ stem-like lung cancer cells emerge higher drug resistance through MDFIC-mediated Wnt/ β -catenin signaling pathway*. 2017, AACR.
117. Yang, J., et al., *Role of Jagged1/STAT 3 signalling in platinum-resistant ovarian cancer*. Journal of cellular and molecular medicine, 2019. **23**(6): p. 4005-4018.
118. Orzechowska, M., et al., *PO-151 Notch signalling differentiates disease-free survival in prostate cancer patients by affecting the epithelial-to-mesenchymal transition-associated processes*. 2018, BMJ Publishing Group Limited.
119. Sprouse, M.L., et al., *PMN-MDSCs Enhance CTC Metastatic Properties through Reciprocal Interactions via ROS/Notch/Nodal Signaling*. International journal of molecular sciences, 2019. **20**(8): p. 1916.
120. Figiel, S., et al., *Clinical significance of epithelial-mesenchymal transition markers in prostate cancer*. Human pathology, 2017. **61**: p. 26-32.
121. Behnsawy, H.M., et al., *Expression patterns of epithelial–mesenchymal transition markers in localized prostate cancer: significance in clinicopathological outcomes following radical prostatectomy*. BJU international, 2013. **111**(1): p. 30-37.
122. Burton, L.J., et al., *Association of Epithelial Mesenchymal Transition with prostate and breast health disparities*. PloS one, 2018. **13**(9): p. e0203855.
123. Whiteland, H., et al., *Putative prognostic epithelial-to-mesenchymal transition biomarkers for aggressive prostate cancer*. Experimental and molecular pathology, 2013. **95**(2): p. 220-226.
124. Padmanaban, V., et al., *E-cadherin is required for metastasis in multiple models of breast cancer*. Nature, 2019. **573**(7774): p. 439-444.
125. Cheaito, K.A., et al., *EMT Markers in Locally-Advanced Prostate Cancer: Predicting Recurrence?* Frontiers in Oncology, 2019. **9**: p. 131.
126. Lyu, P., et al., *Identification of TWIST-interacting genes in prostate cancer*. Science China Life Sciences, 2017. **60**(4): p. 386-396.
127. Abdelrahman, A.E., S.A. Arafa, and R.A. Ahmed, *Prognostic value of twist-1, E-cadherin and EZH2 in prostate cancer: An immunohistochemical study*. Turk Patoloji Derg, 2017. **1**(1): p. 198-210.
128. Gravdal, K., et al., *A switch from E-cadherin to N-cadherin expression indicates epithelial to mesenchymal transition and is of strong and independent importance for the progress of prostate cancer*. Clinical Cancer Research, 2007. **13**(23): p. 7003-7011.
129. Alonso-Magdalena, P., et al., *A role for epithelial-mesenchymal transition in the etiology of benign prostatic hyperplasia*. Proceedings of the National Academy of Sciences, 2009. **106**(8): p. 2859-2863.
130. Zhu, M.-L. and N. Kyprianou, *Role of androgens and the androgen receptor in epithelial-mesenchymal transition and invasion of prostate cancer cells*. The FASEB Journal, 2010. **24**(3): p. 769-777.

131. Sun, Y., et al., *Androgen deprivation causes epithelial–mesenchymal transition in the prostate: implications for androgen-deprivation therapy*. *Cancer research*, 2012. **72**(2): p. 527-536.
132. Klarman, G.J., et al., *Invasive prostate cancer cells are tumor initiating cells that have a stem cell-like genomic signature*. *Clinical & experimental metastasis*, 2009. **26**(5): p. 433-446.
133. Kong, D., et al., *Epithelial to mesenchymal transition is mechanistically linked with stem cell signatures in prostate cancer cells*. *PloS one*, 2010. **5**(8): p. e12445.
134. Mani, S.A., et al., *The epithelial-mesenchymal transition generates cells with properties of stem cells*. *Cell*, 2008. **133**(4): p. 704-715.
135. Santisteban, M., et al., *Immune-induced epithelial to mesenchymal transition in vivo generates breast cancer stem cells*. *Cancer research*, 2009. **69**(7): p. 2887-2895.
136. Zhang, X., et al., *Androgen receptor variants occur frequently in castration resistant prostate cancer metastases*. *PloS one*, 2011. **6**(11): p. e27970.
137. Watson, P.A., et al., *Constitutively active androgen receptor splice variants expressed in castration-resistant prostate cancer require full-length androgen receptor*. *Proceedings of the national academy of sciences*, 2010. **107**(39): p. 16759-16765.
138. Sun, S., et al., *Castration resistance in human prostate cancer is conferred by a frequently occurring androgen receptor splice variant*. *The Journal of clinical investigation*, 2010. **120**(8): p. 2715-2730.
139. Marín-Aguilera, M., et al., *Epithelial-to-mesenchymal transition mediates docetaxel resistance and high risk of relapse in prostate cancer*. *Molecular cancer therapeutics*, 2014. **13**(5): p. 1270-1284.
140. Wang, X., et al., *A luminal epithelial stem cell that is a cell of origin for prostate cancer*. *Nature*, 2009. **461**(7263): p. 495.
141. Chen, C.L., et al., *Single-cell analysis of circulating tumor cells identifies cumulative expression patterns of EMT-related genes in metastatic prostate cancer*. *The Prostate*, 2013. **73**(8): p. 813-826.
142. Armstrong, A.J., et al., *Circulating tumor cells from patients with advanced prostate and breast cancer display both epithelial and mesenchymal markers*. *Molecular cancer research*, 2011. **9**(8): p. 997-1007.
143. Miyamoto, D.T., et al., *Androgen receptor signaling in circulating tumor cells as a marker of hormonally responsive prostate cancer*. *Cancer discovery*, 2012. **2**(11): p. 995-1003.
144. Bluemn, E.G., et al., *Androgen receptor pathway-independent prostate cancer is sustained through FGF signaling*. *Cancer cell*, 2017. **32**(4): p. 474-489. e6.
145. Komiya, A., et al., *The prognostic significance of loss of the androgen receptor and neuroendocrine differentiation in prostate biopsy specimens among castration-resistant prostate cancer patients*. *Mol Clin Oncol*, 2013. **1**(2): p. 257-262.
146. Crumbaker, M., L. Khoja, and A. Joshua, *AR signaling and the PI3K pathway in prostate cancer*. *Cancers*, 2017. **9**(4): p. 34.
147. Jamaspishvili, T., et al., *Clinical implications of PTEN loss in prostate cancer*. *Nature Reviews Urology*, 2018. **15**(4): p. 222.
148. Carver, B.S., et al., *Reciprocal feedback regulation of PI3K and androgen receptor signaling in PTEN-deficient prostate cancer*. *Cancer cell*, 2011. **19**(5): p. 575-586.
149. Mulholland, D.J., et al., *Cell autonomous role of PTEN in regulating castration-resistant prostate cancer growth*. *Cancer cell*, 2011. **19**(6): p. 792-804.
150. Murillo, H., et al., *Role of PI3K signaling in survival and progression of LNCaP prostate cancer cells to the androgen refractory state*. *Endocrinology*, 2001. **142**(11): p. 4795-4805.
151. Lee, S.H., et al., *Crosstalking between androgen and PI3K/AKT signaling pathways in prostate cancer cells*. *Journal of Biological Chemistry*, 2015. **290**(5): p. 2759-2768.
152. Choucair, K., et al., *PTEN genomic deletion predicts prostate cancer recurrence and is associated with low AR expression and transcriptional activity*. *BMC cancer*, 2012. **12**(1): p. 543.

153. Ha, S., et al., *Androgen receptor levels are upregulated by Akt in prostate cancer*. *Endocrine-related cancer*, 2011. **18**(2): p. 245-255.
154. Sircar, K., et al., *PTEN genomic deletion is associated with p-Akt and AR signalling in poorer outcome, hormone refractory prostate cancer*. *The Journal of Pathology: A Journal of the Pathological Society of Great Britain and Ireland*, 2009. **218**(4): p. 505-513.
155. Kaarbø, M., et al., *PI3K-AKT-mTOR pathway is dominant over androgen receptor signaling in prostate cancer cells*. *Analytical Cellular Pathology*, 2010. **32**(1-2): p. 11-27.
156. Wang, Y., et al., *Differential regulation of PTEN expression by androgen receptor in prostate and breast cancers*. *Oncogene*, 2011. **30**(42): p. 4327.
157. Mulholland, D.J., et al., *Pten loss and RAS/MAPK activation cooperate to promote EMT and metastasis initiated from prostate cancer stem/progenitor cells*. *Cancer research*, 2012. **72**(7): p. 1878-1889.
158. Song, L.-B., et al., *The polycomb group protein Bmi-1 represses the tumor suppressor PTEN and induces epithelial-mesenchymal transition in human nasopharyngeal epithelial cells*. *The Journal of clinical investigation*, 2009. **119**(12): p. 3626-3636.
159. Collak, F.K., U. Demir, and F. Sagir, *YAP1 Is Involved in Tumorigenic Properties of Prostate Cancer Cells*. *Pathology & Oncology Research*, 2019.
160. Xu, W., et al., *PTEN lipid phosphatase inactivation links the hippo and PI3K/Akt pathways to induce gastric tumorigenesis*. *Journal of Experimental & Clinical Cancer Research*, 2018. **37**(1): p. 198.
161. Edgar, B.A., *From cell structure to transcription: Hippo forges a new path*. *Cell*, 2006. **124**(2): p. 267-273.
162. Yu, F.-X., B. Zhao, and K.-L. Guan, *Hippo pathway in organ size control, tissue homeostasis, and cancer*. *Cell*, 2015. **163**(4): p. 811-828.
163. Zhao, B., et al., *Inactivation of YAP oncoprotein by the Hippo pathway is involved in cell contact inhibition and tissue growth control*. *Genes & development*, 2007. **21**(21): p. 2747-2761.
164. Lei, Q.-Y., et al., *TAZ promotes cell proliferation and epithelial-mesenchymal transition and is inhibited by the hippo pathway*. *Molecular and cellular biology*, 2008. **28**(7): p. 2426-2436.
165. Zhou, D., et al., *Mst1 and Mst2 maintain hepatocyte quiescence and suppress hepatocellular carcinoma development through inactivation of the Yap1 oncogene*. *Cancer cell*, 2009. **16**(5): p. 425-438.
166. Zhao, B., et al., *TEAD mediates YAP-dependent gene induction and growth control*. *Genes & development*, 2008. **22**(14): p. 000-000.
167. Wu, S., et al., *The TEAD/TEF family protein Scalloped mediates transcriptional output of the Hippo growth-regulatory pathway*. *Developmental cell*, 2008. **14**(3): p. 388-398.
168. Lee, H.-C., et al., *YAP1 overexpression contributes to the development of enzalutamide resistance by induction of cancer stemness and lipid metabolism in prostate cancer*. 2021. **40**(13): p. 2407-2421.
169. Kang, W., et al., *Yes-associated protein 1 exhibits oncogenic property in gastric cancer and its nuclear accumulation associates with poor prognosis*. *Clinical Cancer Research*, 2011: p. clincanres. 2467.2010.
170. Lee, S., et al., *RAF kinase inhibitor-independent constitutive activation of Yes-associated protein 1 promotes tumor progression in thyroid cancer*. *Oncogenesis*, 2013. **2**(7): p. e55.
171. Xu, C., et al., *Mst1 overexpression inhibited the growth of human non-small cell lung cancer in vitro and in vivo*. *Cancer gene therapy*, 2013. **20**(8): p. 453.
172. Konsavage, W.M., et al., *Wnt/ β -catenin signaling regulates Yes-associated protein (YAP) gene expression in colorectal carcinoma cells*. *Journal of Biological Chemistry*, 2012: p. jbc. M111. 327767.
173. Ge, L., et al., *Yes-associated protein expression in head and neck squamous cell carcinoma nodal metastasis*. *PLoS one*, 2011. **6**(11): p. e27529.

174. Steinhardt, A.A., et al., *Expression of Yes-associated protein in common solid tumors*. Human pathology, 2008. **39**(11): p. 1582-1589.
175. Wang, C., et al., *Differences in Yes-associated protein and mRNA levels in regenerating liver and hepatocellular carcinoma*. Molecular medicine reports, 2012. **5**(2): p. 410-414.
176. Jiang, N., et al., *In vivo quantitative phosphoproteomic profiling identifies novel regulators of castration-resistant prostate cancer growth*. Oncogene, 2015. **34**(21): p. 2764.
177. Kuser-Abali, G., et al., *YAP1 and AR interactions contribute to the switch from androgen-dependent to castration-resistant growth in prostate cancer*. Nature communications, 2015. **6**: p. 8126.
178. Overholtzer, M., et al., *Transforming properties of YAP, a candidate oncogene on the chromosome 11q22 amplicon*. Proceedings of the National Academy of Sciences, 2006. **103**(33): p. 12405-12410.
179. Liu, R., et al., *FGF8 promotes colorectal cancer growth and metastasis by activating YAP1*. Oncotarget, 2015. **6**(2): p. 935.
180. Hu, Q., et al., *LncRNAs-directed PTEN enzymatic switch governs epithelial–mesenchymal transition*. Cell research, 2019. **29**(4): p. 286.
181. Yu, M., et al., *YAP1 contributes to NSCLC invasion and migration by promoting Slug transcription via the transcription co-factor TEAD*. Cell death & disease, 2018. **9**(5): p. 464.
182. Tang, Y., et al., *Snail/Slug binding interactions with YAP/TAZ control skeletal stem cell self-renewal and differentiation*. Nat Cell Biol, 2016. **18**(9): p. 917-29.
183. Wang, Y., et al., *Twist-mediated Epithelial-mesenchymal Transition Promotes Breast Tumor Cell Invasion via Inhibition of Hippo Pathway*. Sci Rep, 2016. **6**: p. 24606.
184. Wei, S.C., et al., *Matrix stiffness drives epithelial-mesenchymal transition and tumour metastasis through a TWIST1-G3BP2 mechanotransduction pathway*. Nat Cell Biol, 2015. **17**(5): p. 678-88.
185. Morgan, C., et al., *The role of adhesion molecules as biomarkers for the aggressive prostate cancer phenotype*. PloS one, 2013. **8**(12): p. e81666.
186. Knights, A.J., et al., *Holding tight: cell junctions and cancer spread*. Trends in cancer research, 2012. **8**: p. 61.
187. Tuomi, S., et al., *PKCε Regulation of an α5 Integrin–ZO-1 Complex Controls Lamellae Formation in Migrating Cancer Cells*. Sci. Signal., 2009. **2**(77): p. ra32-ra32.
188. Smalley, K.S., et al., *Up-regulated expression of zonula occludens protein-1 in human melanoma associates with N-cadherin and contributes to invasion and adhesion*. The American journal of pathology, 2005. **166**(5): p. 1541-1554.
189. Dekky, B., et al., *Correction: Proteomic screening identifies the zonula occludens protein ZO-1 as a new partner for ADAM12 in invadopodia-like structures*. Oncotarget, 2018. **9**(87): p. 35795.
190. Lehmann, W., et al., *ZEB1 turns into a transcriptional activator by interacting with YAP1 in aggressive cancer types*. Nat Commun, 2016. **7**: p. 10498.
191. Selth, L.A., et al., *A ZEB1-miR-375-YAP1 pathway regulates epithelial plasticity in prostate cancer*. Oncogene, 2017. **36**(1): p. 24.
192. Chen, H., Q. Chen, and Q. Luo, *Expression of netrin-1 by hypoxia contributes to the invasion and migration of prostate carcinoma cells by regulating YAP activity*. Experimental cell research, 2016. **349**(2): p. 302-309.
193. Park, J., et al., *Switch-like enhancement of epithelial-mesenchymal transition by YAP through feedback regulation of WT1 and Rho-family GTPases*. Nat Commun, 2019. **10**(1): p. 2797.
194. Tumaneng, K., et al., *YAP mediates crosstalk between the Hippo and PI (3) K–TOR pathways by suppressing PTEN via miR-29*. Nature cell biology, 2012. **14**(12): p. 1322.
195. Lin, H.-K., et al., *Regulation of androgen receptor signaling by PTEN (phosphatase and tensin homolog deleted on chromosome 10) tumor suppressor through distinct mechanisms in prostate cancer cells*. Molecular endocrinology, 2004. **18**(10): p. 2409-2423.

196. Becker, T.M., et al., *New frontiers in circulating tumor cell analysis: A reference guide for biomolecular profiling toward translational clinical use*. International journal of cancer, 2014. **134**(11): p. 2523-2533.
197. Thalgott, M., et al., *Detection of circulating tumor cells in different stages of prostate cancer*. Journal of cancer research and clinical oncology, 2013. **139**(5): p. 755-763.
198. Po, J.W., et al., *Improved ovarian cancer EMT-CTC isolation by immunomagnetic targeting of epithelial EpCAM and mesenchymal N-cadherin*. Journal of circulating biomarkers, 2018. **7**: p. 1849454418782617.
199. Polioudaki, H., et al., *Variable expression levels of keratin and vimentin reveal differential EMT status of circulating tumor cells and correlation with clinical characteristics and outcome of patients with metastatic breast cancer*. BMC Cancer, 2015. **15**: p. 399.
200. Horimoto, Y., et al., *Analysis of circulating tumour cell and the epithelial mesenchymal transition (EMT) status during eribulin-based treatment in 22 patients with metastatic breast cancer: a pilot study*. J Transl Med, 2018. **16**(1): p. 287.
201. Zhao, X.H., et al., *Molecular detection of epithelial-mesenchymal transition markers in circulating tumor cells from pancreatic cancer patients: Potential role in clinical practice*. World J Gastroenterol, 2019. **25**(1): p. 138-150.
202. Po, J.W., et al., *Importance and Detection of Epithelial-to-Mesenchymal Transition (EMT) Phenotype in CTCs, in Tumor Metastasis*. 2016.
203. Qi, L.N., et al., *Circulating Tumor Cells Undergoing EMT Provide a Metric for Diagnosis and Prognosis of Patients with Hepatocellular Carcinoma*. Cancer Res, 2018. **78**(16): p. 4731-4744.
204. Armstrong, A.J., et al., *Prospective multicenter validation of androgen receptor splice variant 7 and hormone therapy resistance in high-risk castration-resistant prostate cancer: The PROPHECY study*. Journal of Clinical Oncology, 2019. **37**(13): p. 1120-1129.
205. Leversha, M.A., et al., *Fluorescence in situ hybridization analysis of circulating tumor cells in metastatic prostate cancer*. Clin Cancer Res, 2009. **15**(6): p. 2091-7.
206. Steinestel, J., et al., *Detecting predictive androgen receptor modifications in circulating prostate cancer cells*. Oncotarget, 2019. **10**(41): p. 4213-4223.
207. Reyes, E.E., et al., *Quantitative characterization of androgen receptor protein expression and cellular localization in circulating tumor cells from patients with metastatic castration-resistant prostate cancer*. J Transl Med, 2014. **12**: p. 313.
208. Darshan, M.S., et al., *Taxane-induced blockade to nuclear accumulation of the androgen receptor predicts clinical responses in metastatic prostate cancer*. Cancer Res, 2011. **71**(18): p. 6019-29.
209. Sharp, A., et al., *Androgen receptor splice variant-7 expression emerges with castration resistance in prostate cancer*. J Clin Invest, 2019. **129**(1): p. 192-208.
210. Nimir, M., et al., *Detection of AR-V7 in liquid biopsies of castrate resistant prostate cancer patients: a comparison of AR-V7 analysis in circulating tumor cells, circulating tumor RNA and exosomes*. 2019. **8**(7): p. 688.
211. Luk, A., et al., *CTC-mRNA (AR-V7) Analysis from blood samples—impact of blood collection tube and storage time*. International journal of molecular sciences, 2017. **18**(5): p. 1047.
212. Wang, Z., et al., *The Prognostic Value of Androgen Receptor Splice Variant 7 in Castration-Resistant Prostate Cancer Treated With Novel Hormonal Therapy or Chemotherapy: A Systematic Review and Meta-analysis*. Front Oncol, 2020. **10**: p. 572590.
213. Worroll, D., et al., *Androgen receptor nuclear localization correlates with AR-V7 mRNA expression in circulating tumor cells (CTCs) from metastatic castration resistance prostate cancer patients*. Phys Biol, 2019. **16**(3): p. 036003.
214. Attard, G., et al., *Characterization of ERG, AR and PTEN gene status in circulating tumor cells from patients with castration-resistant prostate cancer*. Cancer research, 2009. **69**(7): p. 2912-2918.

215. Maas, M., et al., *Circulating tumor cells and their role in prostate cancer*. Asian journal of andrology, 2019. **21**(1): p. 24.
216. Gao, Y., et al., *Single-cell sequencing deciphers a convergent evolution of copy number alterations from primary to circulating tumor cells*. Genome Res, 2017. **27**(8): p. 1312-1322.
217. Bredemeier, M., et al., *Comparison of the PI3KCA pathway in circulating tumor cells and corresponding tumor tissue of patients with metastatic breast cancer*. Mol Med Rep, 2017. **15**(5): p. 2957-2968.
218. Ting, D.T., et al., *Single-cell RNA sequencing identifies extracellular matrix gene expression by pancreatic circulating tumor cells*. Cell Rep, 2014. **8**(6): p. 1905-1918.
219. Sharma, S., et al., *Circulating tumor cell isolation, culture, and downstream molecular analysis*. Biotechnology advances, 2018. **36**(4): p. 1063-1078.
220. Li, X., et al., *Strategies for enrichment of circulating tumor cells*. Translational Cancer Research, 2020. **9**(3): p. 2012.
221. Diamond, E.S., et al., *Isolation and characterization of circulating tumor cells in prostate cancer*. 2012. **2**: p. 131.
222. Kallergi, G., et al., *Phosphorylation of FAK, PI-3K, and impaired actin organization in CK-positive micrometastatic breast cancer cells*. Molecular Medicine, 2007. **13**(1-2): p. 79-88.
223. Tinhofer, I., et al., *Monitoring of circulating tumor cells and their expression of EGFR/phospho-EGFR during combined radiotherapy regimens in locally advanced squamous cell carcinoma of the head and neck*. International Journal of Radiation Oncology* Biology* Physics, 2012. **83**(5): p. e685-e690.
224. Yokoi, K., et al., *Identification and validation of SRC and phospho-SRC family proteins in circulating mononuclear cells as novel biomarkers for pancreatic cancer*. Translational oncology, 2011. **4**(2): p. 83-91.
225. Shin, S.J., et al., *Circulating vascular endothelial growth factor receptor 2/pAkt-positive cells as a functional pharmacodynamic marker in metastatic colorectal cancers treated with antiangiogenic agent*. Investigational new drugs, 2013. **31**(1): p. 1-13.
226. Lonergan, P.E. and D.J. Tindall, *Androgen receptor signaling in prostate cancer development and progression*. Journal of carcinogenesis, 2011. **10**: p. 20-20.
227. Cattrini, C.A.-O., et al., *Optimal Sequencing and Predictive Biomarkers in Patients with Advanced Prostate Cancer*. LID - 10.3390/cancers13184522 [doi] LID - 4522. (2072-6694 (Print)).
228. Wyatt, A.W., et al., *Concordance of Circulating Tumor DNA and Matched Metastatic Tissue Biopsy in Prostate Cancer*. LID - 10.1093/jnci/djx118 [doi] LID - djx118. (1460-2105 (Electronic)).
229. Shafi, A.A., et al., *Differential regulation of metabolic pathways by androgen receptor (AR) and its constitutively active splice variant, AR-V7, in prostate cancer cells*. (1949-2553 (Electronic)).
230. Stuoopelyte, K., et al., *Analysis of AR-FL and AR-V1 in Whole Blood of Patients with Castration Resistant Prostate Cancer as a Tool for Predicting Response to Abiraterone Acetate*. J Urol. **204**(1): p. 71-78.
231. Todenhöfer, T., et al., *AR-V7 Transcripts in Whole Blood RNA of Patients with Metastatic Castration Resistant Prostate Cancer Correlate with Response to Abiraterone Acetate*. J Urol. **197**(1): p. 135-142.
232. Sharp, A., et al., *Clinical Utility of Circulating Tumour Cell Androgen Receptor Splice Variant-7 Status in Metastatic Castration-resistant Prostate Cancer*. Eur Urol. **76**(5): p. 676-685.
233. Del Re, M., et al., *Androgen receptor gain in circulating free DNA and splicing variant 7 in exosomes predict clinical outcome in CRPC patients treated with abiraterone and enzalutamide*. Prostate Cancer Prostatic Dis.
234. Del Re, M., et al., *AR-V7 and AR-FL expression is associated with clinical outcome: a translational study in patients with castrate resistant prostate cancer*. BJU Int.

235. Liberati, A., et al., *The PRISMA Statement for Reporting Systematic Reviews and Meta-Analyses of Studies That Evaluate Health Care Interventions: Explanation and Elaboration*. PLOS Medicine, 2009. **6**(7): p. e1000100.
236. Tierney, J.F., et al., *Practical methods for incorporating summary time-to-event data into meta-analysis*. Trials, 2007. **8**: p. 16-16.
237. Wang, J., et al., *Prognostic Value of Androgen Receptor Splice Variant 7 in the Treatment of Metastatic Castration-Resistant Prostate Cancer: A Systematic Review and Meta-Analysis*. Front Oncol, 2020. **10**: p. 562504.
238. Antonarakis, E.S., et al., *Androgen Receptor Splice Variant 7 and Efficacy of Taxane Chemotherapy in Patients With Metastatic Castration-Resistant Prostate Cancer*. JAMA Oncol. **1**(5): p. 582-91.
239. Antonarakis, E.S., et al., *Clinical Significance of Androgen Receptor Splice Variant-7 mRNA Detection in Circulating Tumor Cells of Men With Metastatic Castration-Resistant Prostate Cancer Treated With First- and Second-Line Abiraterone and Enzalutamide*. J Clin Oncol. **35**(19): p. 2149-2156.
240. Armstrong, A.J., et al., *Prospective multicenter study of circulating tumor cell AR-V7 and taxane versus hormonal treatment outcomes in metastatic castration-resistant prostate cancer*. JCO Precision Oncology, 2020. **4**: p. 1285-1301.
241. Belderbos, B.P.S., et al., *Associations between AR-V7 status in circulating tumour cells, circulating tumour cell count and survival in men with metastatic castration-resistant prostate cancer*. Eur J Cancer. **121**: p. 48-54.
242. Cattrini, C., et al., *Role of circulating tumor cells (CTC), androgen receptor full length (AR-FL) and androgen receptor splice variant 7 (AR-V7) in a prospective cohort of castration-resistant metastatic prostate cancer patients*. Cancers, 2019. **11**(9).
243. Chung, J.S., et al., *Circulating Tumor Cell-Based Molecular Classifier for Predicting Resistance to Abiraterone and Enzalutamide in Metastatic Castration-Resistant Prostate Cancer*. Neoplasia (United States), 2019. **21**(8): p. 802-809.
244. De Laere, B., et al., *TP53 Outperforms Other Androgen Receptor Biomarkers to Predict Abiraterone or Enzalutamide Outcome in Metastatic Castration-Resistant Prostate Cancer*. Clin Cancer Res. **25**(6): p. 1766-1773.
245. Del Re, M., et al., *The Detection of Androgen Receptor Splice Variant 7 in Plasma-derived Exosomal RNA Strongly Predicts Resistance to Hormonal Therapy in Metastatic Prostate Cancer Patients*. European Urology, 2017. **71**(4): p. 680-687.
246. Erb, H.H.H., et al., *AR-V7 Protein Expression in Circulating Tumour Cells Is Not Predictive of Treatment Response in mCRPC*. Urologia Internationalis, 2020. **104**(3): p. 253-262.
247. Graf, R.P., et al., *Clinical Utility of the Nuclear-localized AR-V7 Biomarker in Circulating Tumor Cells in Improving Physician Treatment Choice in Castration-resistant Prostate Cancer*. European Urology, 2020. **77**(2): p. 170-177.
248. Gupta, S., et al., *Discordant and heterogeneous clinically relevant genomic alterations in circulating tumor cells vs plasma DNA from men with metastatic castration resistant prostate cancer*. Genes Chromosomes Cancer. **59**(4): p. 225-239.
249. Joncas, F.H., et al., *Plasma extracellular vesicles as phenotypic biomarkers in prostate cancer patients*. Prostate, 2019. **79**(15): p. 1767-1776.
250. Kwan, E.M., et al., *Prognostic Utility of a Whole-blood Androgen Receptor-based Gene Signature in Metastatic Castration-resistant Prostate Cancer*. Eur Urol Focus.
251. Di Lorenzo, G., et al., *Assessment of Total, PTEN(-), and AR-V7(+) Circulating Tumor Cell Count by Flow Cytometry in Patients with Metastatic Castration-Resistant Prostate Cancer Receiving Enzalutamide*. (1938-0682 (Electronic)).
252. Maillet, D., et al., *Improved Androgen Receptor Splice Variant 7 Detection Using a Highly Sensitive Assay to Predict Resistance to Abiraterone or Enzalutamide in Metastatic Prostate Cancer Patients*. Eur Urol Oncol.

253. Marín-Aguilera, M., et al., *Androgen Receptor and Its Splicing Variant 7 Expression in Peripheral Blood Mononuclear Cells and in Circulating Tumor Cells in Metastatic Castration-Resistant Prostate Cancer*. *Cells*. **9**(1).
254. Markowski, M.C., et al., *A Multicohort Open-label Phase II Trial of Bipolar Androgen Therapy in Men with Metastatic Castration-resistant Prostate Cancer (RESTORE): A Comparison of Post-abiraterone Versus Post-enzalutamide Cohorts*. *Eur Urol*.
255. Miyamoto, D.T., et al., *An RNA-based digital circulating tumor cell signature is predictive of drug response and early dissemination in prostate cancer*. *Cancer Discovery*. **8**(3): p. 288-303.
256. Okegawa, T., et al., *AR-V7 in circulating tumor cells cluster as a predictive biomarker of abiraterone acetate and enzalutamide treatment in castration-resistant prostate cancer patients*. *Prostate*, 2018. **78**(8): p. 576-582.
257. Onstenk, W., et al., *Efficacy of Cabazitaxel in Castration-resistant Prostate Cancer Is Independent of the Presence of AR-V7 in Circulating Tumor Cells*. *European Urology*, 2015. **68**(6): p. 939-945.
258. Qu, F., et al., *Association of AR-V7 and prostate-specific antigen RNA levels in blood with efficacy of abiraterone acetate and enzalutamide treatment in men with prostate cancer*. *Clinical Cancer Research*, 2017. **23**(3): p. 726-734.
259. Scher, H.I., et al., *Assessment of the validity of nuclear-localized androgen receptor splice variant 7 in circulating tumor cells as a predictive biomarker for castration-resistant prostate cancer*. *JAMA Oncology*, 2018. **4**(9): p. 1179-1186.
260. Seitz, A.K., et al., *AR-V7 in Peripheral Whole Blood of Patients with Castration-resistant Prostate Cancer: Association with Treatment-specific Outcome Under Abiraterone and Enzalutamide*. *European Urology*, 2017. **72**(5): p. 828-834.
261. Sepe, P., et al., *Could circulating tumor cells and ARV7 detection improve clinical decisions in metastatic castration-resistant prostate cancer? The istituto nazionale dei tumori (INT) experience*. *Cancers*, 2019. **11**(7).
262. Škereňová, M., et al., *Gene Expression Analysis of Immunomagnetically Enriched Circulating Tumor Cell Fraction in Castration-Resistant Prostate Cancer*. *Molecular Diagnosis and Therapy*, 2018. **22**(3): p. 381-390.
263. Tagawa, S.T., et al., *Expression of AR-V7 and ARv(567es) in Circulating Tumor Cells Correlates with Outcomes to Taxane Therapy in Men with Metastatic Prostate Cancer Treated in TAXYNERGY*. *Clin Cancer Res*. **25**(6): p. 1880-1888.
264. Tommasi, S., et al., *Standardization of CTC AR-V7 PCR assay and evaluation of its role in castration resistant prostate cancer progression*. *Prostate*. **79**(1): p. 54-61.
265. Wang, S., et al., *Expression of androgen receptor variant 7 (AR-V7) in circulated tumor cells and correlation with drug resistance of prostate cancer cells*. *Medical Science Monitor*, 2018. **24**: p. 7051-7056.
266. Galletti, G., et al., *Mechanisms of resistance to systemic therapy in metastatic castration-resistant prostate cancer*. *Cancer Treatment Reviews*, 2017. **57**: p. 16-27.
267. Zhang, G., et al., *Androgen receptor splice variants circumvent AR blockade by microtubule-targeting agents*. *Oncotarget*; Vol 6, No 27, 2015.
268. Zhou, J. and R. Liu, *The association between androgen receptor splice variant 7 status and prognosis of metastatic castration-resistant prostate cancer: A systematic review and meta-analysis*. *Andrologia*, 2020. **52**(7): p. e13642.
269. Zhu, Y., et al., *Novel junction-specific and quantifiable in situ detection of AR-V7 and its clinical correlates in metastatic castration-resistant prostate cancer*. 2018. **73**(5): p. 727-735.
270. Carpenter, A.E., et al., *CellProfiler: image analysis software for identifying and quantifying cell phenotypes*. 2006. **7**(10): p. 1-11.
271. Berthold, M.R., et al., *KNIME-the Konstanz information miner: version 2.0 and beyond*. 2009. **11**(1): p. 26-31.

272. Kanayama, M., et al., *Ar splicing variants and resistance to ar targeting agents*. 2021. **13**(11): p. 2563.
273. Lock, J.G., et al. *Visual analytics of single cell microscopy data using a collaborative immersive environment*. in *Proceedings of the 16th ACM SIGGRAPH International Conference on Virtual-Reality Continuum and its Applications in Industry*. 2018.
274. Eslami-S, Z., L.E. Cortés-Hernández, and C. Alix-Panabières, *Epithelial cell adhesion molecule: an anchor to isolate clinically relevant circulating tumor cells*. *Cells*, 2020. **9**(8): p. 1836.
275. Huang, C., et al., *Distribution and Clinical Analysis of EpCAM+/Vimentin+ Circulating Tumor Cells in High-Risk Population and Cancer Patients*. *Frontiers in Oncology*, 2021. **11**: p. 1674.
276. De Wit, S., et al., *EpCAMhigh and EpCAMlow circulating tumor cells in metastatic prostate and breast cancer patients*. *Oncotarget*, 2018. **9**(86): p. 35705.
277. Brungs, D., et al., *Establishment of novel long-term cultures from EpCAM positive and negative circulating tumour cells from patients with metastatic gastroesophageal cancer*. *Scientific reports*, 2020. **10**(1): p. 1-13.
278. Po, J.W., et al., *Immunomagnetic isolation of circulating melanoma cells and detection of PD-L1 status*. *PLoS One*, 2019. **14**(2): p. e0211866.
279. Gertler, R., et al., *Detection of circulating tumor cells in blood using an optimized density gradient centrifugation*, in *Molecular Staging of Cancer*. 2003, Springer. p. 149-155.
280. Menyailo, M.E., M.S. Tretyakova, and E.V. Denisov, *Heterogeneity of circulating tumor cells in breast cancer: identifying metastatic seeds*. *International Journal of Molecular Sciences*, 2020. **21**(5): p. 1696.
281. Ghazani, A.A., et al., *Sensitive and direct detection of circulating tumor cells by multimarker μ -nuclear magnetic resonance*. *Neoplasia*, 2012. **14**(5): p. 388-IN2.
282. Bankó, P., et al., *Technologies for circulating tumor cell separation from whole blood*. *Journal of hematology & oncology*, 2019. **12**(1): p. 1-20.
283. Corning. *Corning® Cell-Tak™ Cell and Tissue Adhesive Frequently Asked Questions*.
284. Hille, C., et al., *Detection of Androgen Receptor Variant 7 (ARV7) mRNA Levels in EpCAM-Enriched CTC Fractions for Monitoring Response to Androgen Targeting Therapies in Prostate Cancer*. *Cells*, 2019. **8**(9): p. 1067.
285. Gorges, T.M., et al., *Heterogeneous PSMA expression on circulating tumor cells-a potential basis for stratification and monitoring of PSMA-directed therapies in prostate cancer*. *Oncotarget*, 2016. **7**(23): p. 34930.
286. Lazar, D.C., et al., *Cytometric comparisons between circulating tumor cells from prostate cancer patients and the prostate-tumor-derived LNCaP cell line*. *Physical biology*, 2012. **9**(1): p. 016002.
287. Ni, J., et al., *Epithelial cell adhesion molecule (EpCAM) is associated with prostate cancer metastasis and chemo/radioresistance via the PI3K/Akt/mTOR signaling pathway*. *The international journal of biochemistry & cell biology*, 2013. **45**(12): p. 2736-2748.
288. Tran, N.L., et al., *N-cadherin expression in human prostate carcinoma cell lines: an epithelial-mesenchymal transformation mediating adhesion with stromal cells*. *The American journal of pathology*, 1999. **155**(3): p. 787-798.
289. Liu, C.-Y., et al., *Vimentin contributes to epithelial-mesenchymal transition cancer cell mechanics by mediating cytoskeletal organization and focal adhesion maturation*. *Oncotarget*, 2015. **6**(18): p. 15966.
290. Jones, J., et al., *Nuclear Kaiso indicates aggressive prostate cancers and promotes migration and invasiveness of prostate cancer cells*. *The American journal of pathology*, 2012. **181**(5): p. 1836-1846.
291. Lewis-Tuffin, L.J., et al., *Misregulated E-cadherin expression associated with an aggressive brain tumor phenotype*. *PLoS one*, 2010. **5**(10): p. e13665.




292. Shiota, M., et al., *Crosstalk between epithelial-mesenchymal transition and castration resistance mediated by Twist1/AR signaling in prostate cancer*. *Endocrine-related cancer*, 2015. **22**(6): p. 889-900.
293. Steinmetz, N.F., et al., *Two domains of vimentin are expressed on the surface of lymph node, bone and brain metastatic prostate cancer lines along with the putative stem cell marker proteins CD44 and CD133*. *Cancers*, 2011. **3**(3): p. 2870-2885.
294. D'Anselmi, F., et al., *Microenvironment promotes tumor cell reprogramming in human breast cancer cell lines*. *PloS one*, 2013. **8**(12): p. e83770.
295. Wu, G.J., et al., *Expression of a human cell adhesion molecule, MUC18, in prostate cancer cell lines and tissues*. *The Prostate*, 2001. **48**(4): p. 305-315.
296. *The Human Protein Atlas Available from: <https://www.proteinatlas.org/>*.
297. Cui, Y. and S. Yamada, *N-cadherin dependent collective cell invasion of prostate cancer cells is regulated by the N-terminus of α -catenin*. *PloS one*, 2013. **8**(1): p. e55069.
298. Kregel, S., et al., *Acquired resistance to the second-generation androgen receptor antagonist enzalutamide in castration-resistant prostate cancer*. *Oncotarget*, 2016. **7**(18): p. 26259.
299. Tiwari, R., et al., *Androgen deprivation upregulates SPINK1 expression and potentiates cellular plasticity in prostate cancer*. *Nature communications*, 2020. **11**(1): p. 1-19.
300. Subbarayan, V., et al., *Differential expression of cyclooxygenase-2 and its regulation by tumor necrosis factor- α in normal and malignant prostate cells*. *Cancer research*, 2001. **61**(6): p. 2720-2726.
301. Pogoda, K., et al., *In search of the correlation between nanomechanical and biomolecular properties of prostate cancer cells with different metastatic potential*. *Archives of Biochemistry and Biophysics*, 2021. **697**: p. 108718.
302. Gevensleben, H., et al., *The immune checkpoint regulator PD-L1 is highly expressed in aggressive primary prostate cancer*. *Clinical Cancer Research*, 2016. **22**(8): p. 1969-1977.
303. Shukla, S., et al., *Activation of PI3K-Akt signaling pathway promotes prostate cancer cell invasion*. *International journal of cancer*, 2007. **121**(7): p. 1424-1432.
304. Fraser, M., et al., *PTEN Deletion in Prostate Cancer Cells Does Not Associate with Loss of RAD51 Function: Implications for Radiotherapy and Chemotherapy* *PTEN and RAD51 in Prostate Cancer*. *Clinical Cancer Research*, 2012. **18**(4): p. 1015-1027.
305. O'Keefe, D.S., et al., *A perspective on the evolving story of PSMA biology, PSMA-based imaging, and endoradiotherapeutic strategies*. *Journal of Nuclear Medicine*, 2018. **59**(7): p. 1007-1013.
306. Cimadamore, A., et al., *New prostate cancer targets for diagnosis, imaging, and therapy: focus on prostate-specific membrane antigen*. *Frontiers in oncology*, 2018. **8**: p. 653.
307. Jamaspishvili, T., et al., *Clinical implications of PTEN loss in prostate cancer*. *Nature Reviews Urology*, 2018. **15**(4): p. 222-234.
308. Lin, D., et al., *Circulating tumor cells: Biology and clinical significance*. *Signal transduction and targeted therapy*, 2021. **6**(1): p. 1-24.
309. Lampignano, R., et al., *Enrichment, isolation and molecular characterization of EpCAM-negative circulating tumor cells*. *Isolation and Molecular Characterization of Circulating Tumor Cells*, 2017: p. 181-203.
310. Ahn, E. and H. Kang, *Introduction to systematic review and meta-analysis*. *Korean journal of anesthesiology*, 2018. **71**(2): p. 103-112.
311. Uo, T., C.C. Sprenger, and S.R. Plymate, *Androgen receptor signaling and metabolic and cellular plasticity during progression to castration resistant prostate cancer*. *Frontiers in Oncology*, 2020. **10**: p. 2275.
312. Tang, Q., et al., *The Role of Androgen Receptor in Cross Talk Between Stromal Cells and Prostate Cancer Epithelial Cells*. *Frontiers in cell and developmental biology*, 2021: p. 2678.
313. Sobhani, N., et al., *AR-V7 in Metastatic Prostate Cancer: A Strategy beyond Redemption*. *International Journal of Molecular Sciences*, 2021. **22**(11): p. 5515.

314. Usui, K., et al., *Plasma ctDNA monitoring during epidermal growth factor receptor (EGFR)-tyrosine kinase inhibitor treatment in patients with EGFR-mutant non-small cell lung cancer (JP-CLEAR trial)*. Japanese Journal of Clinical Oncology, 2019. **49**(6): p. 554-558.
315. Kaldjian, E.P., et al., *The RareCyte® platform for next-generation analysis of circulating tumor cells*. Cytometry Part A, 2018. **93**(12): p. 1220-1225.

Appendices

Review Article

The Prospect of Identifying Resistance Mechanisms for Castrate-Resistant Prostate Cancer Using Circulating Tumor Cells: Is Epithelial-to-Mesenchymal Transition a Key Player?

Tanzila Khan ^{1,2,3}, Kieran F. Scott ^{1,2}, Therese M. Becker ^{1,2,3,4}, John Lock,⁵
Mohammed Nimir,^{2,3,4,6} Yafeng Ma,^{2,3,4} and Paul de Souza^{1,2,3,6,7}

¹School of Medicine, Western Sydney University, Campbelltown, NSW 2560, Australia

²Medical Oncology, Ingham Institute of Applied Medical Research, Liverpool, NSW 2170, Australia

³Centre of Circulating Tumour Cells Diagnostics & Research, Ingham Institute of Applied Medical Research, Liverpool, NSW 2170, Australia

⁴South West Sydney Clinical School, University of New South Wales, Liverpool Hospital, Liverpool, NSW 2170, Australia

⁵School of Medical Sciences, University of New South Wales, Kensington, Australia

⁶Medical Oncology, Liverpool Hospital, Liverpool, NSW 2170, Australia

⁷School of Medicine, University of Wollongong, Wollongong, NSW 2522, Australia

Correspondence should be addressed to Tanzila Khan; 19153083@student.westernsydney.edu.au

Received 3 September 2019; Revised 19 November 2019; Accepted 14 February 2020; Published 30 March 2020

Academic Editor: Craig Robson

Copyright © 2020 Tanzila Khan et al. This is an open access article distributed under the Creative Commons Attribution License, which permits unrestricted use, distribution, and reproduction in any medium, provided the original work is properly cited.

Prostate cancer (PCa) is initially driven by excessive androgen receptor (AR) signaling with androgen deprivation therapy (ADT) being a major therapeutic approach to its treatment. However, the development of drug resistance is a significant limitation on the effectiveness of both first-line and more recently developed second-line ADTs. There is a need then to study AR signaling within the context of other oncogenic signaling pathways that likely mediate this resistance. This review focuses on interactions between AR signaling, the well-known phosphatidylinositol-3-kinase/AKT pathway, and an emerging mediator of these pathways, the Hippo/YAP1 axis in metastatic castrate-resistant PCa, and their involvement in the regulation of epithelial-mesenchymal transition (EMT), a feature of disease progression and ADT resistance. Analysis of these pathways in circulating tumor cells (CTCs) may provide an opportunity to evaluate their utility as biomarkers and address their importance in the development of resistance to current ADT with potential to guide future therapies.

1. Introduction

Prostate cancer (PCa) is highly prevalent in the Western world; it ranks sixth among cancers in regard to mortality among men [1]. There were 1,276,106 new cases of PCa and 358,989 deaths due to PCa worldwide in 2018 [2]. Despite dramatic improvements in five-year survival, mortality from PCa is poised to remain a major health problem due to increasing longevity, particularly in western countries. The most significant factors associated with morbidity and mortality are the development of metastatic spread to other organs, particularly bone, and emerging resistance to therapy.

On the molecular level, PCa is almost always initially driven by excessive signaling through the androgen receptor (AR) pathway (reviewed in [3]). Consequently, men with metastatic PCa will be offered androgen deprivation therapy (ADT) as the primary treatment. After a median of around 18–24 months, the disease tends to become resistant to hormonal manipulation and progresses towards so-called metastatic castration-resistant prostate cancer (mCRPC). In mCRPC, the concentration of the current blood-based clinical PCa biomarker, prostate-specific antigen (PSA), continues to increase over time. As PSA is regulated *via* AR signaling, this suggests, in general, the common ongoing

involvement of AR signaling in disease progression to mCRPC [4–7]. Abiraterone [8, 9] and enzalutamide [10, 11] have been developed to be used for mCRPC, as “second-generation” ADT treatments, and responses are generally good, but a median progression-free survival of 5.6 months [8] suggests resistance to treatment once again supervenes. Indeed, despite the difference in mechanisms of action, cross-resistance between enzalutamide and abiraterone is very common [8, 12–14], suggesting the development of true hormone resistance following second-line ADT therapy, as opposed to castrate resistance. Thus, androgen signaling through AR within the context of the oncogenic effect of other signaling pathways remains an important area of research as there are, yet, no effective treatments or markers for true hormone resistance. Here, we review the involvement of two critical signaling pathways, the phosphatidylinositol-3-kinase/AKT (PI3K/AKT) and Hippo/YAP pathway, which interact with the AR pathway in mCRPC and which have links to epithelial-to-mesenchymal transition (EMT). EMT is thought to play an important role in the development of both metastasis and therapy resistance [15, 16]. Our literature research indicates that the analysis of circulating tumor cells (CTCs) isolated from PCa patients may allow CTCs to be used as a tool to define how these signaling pathways interact with the AR pathway to cause ADT resistance and thereby investigate the mechanism by which these pathways may contribute to castrate resistance. In addition, CTCs may thus emerge as a useful PCa biomarker for personalized therapy.

2. Circulating Tumor Cells and EMT in Metastasis

Metastasis in PCa is integrally linked to mCRPC. At the cellular level, metastasis involves a sequence of steps, and current evidence suggests that EMT and the reverse process mesenchymal-to-epithelial transition (MET) (reviewed in [17]) are important mechanisms by which tumor cells migrate and reestablish themselves at distant sites. Cancer cells are believed to lose their tight adhesion to neighboring cells and become more mobile when undergoing EMT, which, in turn, favors their ability to shed from the tumor mass, intravasate into the bloodstream, and thus become CTCs. MET, on the other hand, is thought to aid CTCs after leaving the vascular system to be able to settle in other tissues and form new tumors [18, 19] (Figure 1). Thus, CTC numbers have been recognized as a marker of metastatic disease, and importantly, EMT markers have been screened for in patient CTCs including those of 54 patients with PCa, 53% of these patients had advanced metastatic disease and intermittent epithelial-to-mesenchymal phenotype of CTCs correlated with metastasis in these patients, while another study found that the mesenchymal CTC phenotype correlated with increased rates of progression to CRPC in a cohort of 108 PCa patients recruited with high volume metastatic disease at hormone-sensitive disease stage and longitudinally followed during the study [20–22].

Metastatic spread of cancer is thought to involve different stages (Figure 1(a)) in which cancer cells (i) lose cell-

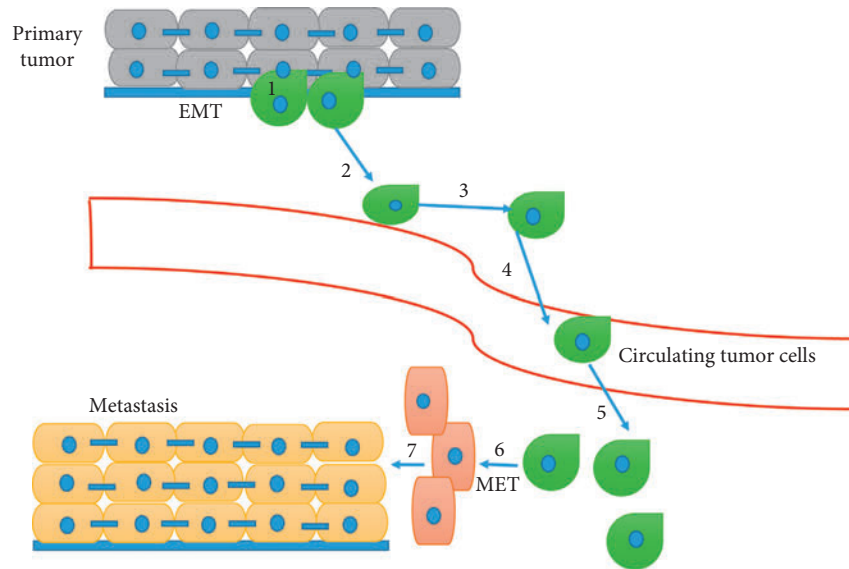
cell tight junctions and detach from the primary site/organ, (ii) penetrate the basal lamina and enter nearby tissue, (iii) evade programmed cell death normally induced by loss of substrate adhesion (anoikis), (iv) breach blood or lymphatic vessels and migrate to other sites *via* blood/lymphatic circulation, (v) leave the bloodstream or lymphatic vessels at distant organs, (vi) form a micrometastatic core, and finally (vii) adjust and reprogram the surrounding stroma to form detectable macrometastases [23]. At a molecular level, EMT has been implicated in various cancers, including PCa. In the development of mCRPC, it has been proposed that activation of transcription factors (TFs) results in the loss of epithelial properties and acquisition of mesenchymal characteristics as well as the change of cell shape, leading to enhanced invasion and increased mortality [24, 25].

EMT is inducible by environmental factors such as radiation or hypoxia (Figure 1(b)), and there is accumulating evidence that radiation or chemotherapy, used to treat earlier stage PCa, may induce EMT changes [26, 27]. Hypoxia induces the production of hypoxia-inducible factor (HIF), and HIF-1 α stimulates transcription factors (TFs), such as Snail and Twist, to trigger EMT [28, 29]. EMT then results from activation of a mesenchymal transcriptional program induced by specific transcription factors (EMT-TFs) [26]. Mechanistically, central EMT-TFs ZEB1, Snail, Slug, and Twist along with other TFs such as TCF4 and FOXC2 suppress the expression of key epithelial markers such as cytokeratin, E-cadherin, occludin, and claudin while causing upregulation of mesenchymal markers such as N-cadherin, fibronectin, and vimentin, which enable cancer cells to be more motile and consequently more aggressive (Figure 1(c)).

Regulation by signaling cascades and signaling molecules including EGF, Hedgehog, Wnt, FGF, Notch, TGF- β , and HGF in turn induces signaling *via* NF- κ B, MAPK, PI3K/AKT, or Wnt/ β -catenin pathways to regulate EMT-TFs and ultimately induce EMT phenotypic changes. More recently, the Hippo pathway has been implicated in regulating EMT *via* its downstream transcriptional modulator Yes-associated protein (YAP) and the transcriptional coactivator TAZ [28, 30–38]. Importantly, there is evidence in the literature that these pathways can be successfully analysed in CTCs even though in some cases these analyses may not have yet been reported for PCa CTCs. Table 1 summarises some of the evidence implicating signaling pathways in EMT of PCa as well as the analysis of these pathways in CTCs mainly from other cancers. CTC studies from other cancers are included because they indicate the feasibility of investigating these pathways in PCa CTC.

3. Clinical Relevance of EMT Markers in PCa

Several studies have assessed EMT markers for their clinical importance at various stages of human PCa. Table 2 shows typical EMT markers detected in PCa tissue. A possible clinical utility of these EMT markers at different phases of the disease is suggested by their prognostic correlation with both recurrence-free and overall survival. For example, EMT markers Twist and vimentin as measured by

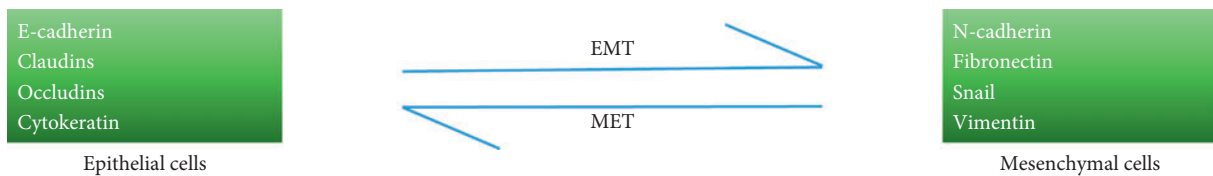


- (1) Detachment and movement from the primary site/organ
- (2) Invasion into nearby organ
- (3) Evade programmed cell death after detachment from the primary site
- (4) Invasion in the blood or lymphatic vessel
- (5) Extravasation of the blood stream/lymphatic vessel at a distant organ
- (6) Form a micrometastatic nodule
- (7) Form macrometastasis

(a)

Environmental factors Hypoxia Radiation	Signaling molecules EGF, Hedgehog, Wnt, FGF, Notch, TGF- β , HGF, FGF,	Signaling cascades Notch, NF-KB, Hippo, MAPK, AKT, Wnt/ β - catenin, AR	Transcription regulators/coactivators ZEB1, TCF4, YAP1, Snail 1, Twist, FOXC2, and Snail 2
---	---	--	--

(b)



(c)

FIGURE 1: EMT in cancer metastasis. (a) Schematic representation of the role of EMT in cancer metastasis. (b) A cascade of transcriptional regulation underlies the transition from an epithelial to a mesenchymal phenotype, and (c) during EMT, epithelial markers are down-regulated while mesenchymal markers are upregulated.

immunohistochemistry in radical prostatectomy samples are independent markers for biochemical recurrence as defined by a resurgence in serum prostate-specific antigen (PSA) levels postsurgery [84, 90]. A recent study found that Cathepsin L (Cat L), which is an EMT-associated target of the EMT-TF Snail, may be a biomarker of PCa progression [83]. In addition, loss of membrane-bound E-cadherin staining appears to be linked with higher Gleason score, advanced clinical stage, and poor prognosis in PCa [91]. EMT markers such as Zeb1, E-cadherin, and vimentin play important roles at different stages of disease progression from primary tumor stage 2 to CRPC. In CRPC, increased expression of Zeb1 correlated with decreased survival [84]. Further, in a study of

108 patients with newly diagnosed castrate-sensitive PCa, expression of mesenchymal markers in CTCs at baseline was found to be an independent prognostic factor that was predictive of time to progression to CRPC following standard ADT. Patients who had mesenchymal CTCs at baseline showed a significantly shorter time to progression to CRPC than patients without CTCs or patients whose CTCs were negative for mesenchymal markers [21]. Several studies show that E-cadherin suppresses invasion and metastasis *in vitro*, and consistent with these findings, E-cadherin staining in tumor tissue correlates with longer overall survival [84]. However, the relationship of E-cadherin to metastasis is not clear in all cases since, in a recent study, it has been shown that

TABLE 1: Signaling pathways implicated in EMT and relevance to PCa.

Pathway	Implication in cancer-related EMT	Roles in PCa	CTC analysis
AR	Opposing data: elevation of AR expression and AR signaling in prostate tumors promotes PCa metastasis by induction of EMT [39]; other data suggest AR reverses EMT and ADT can induce EMT [40, 41]	Cell proliferation and tumor progression [42, 43]	Different AR expression patterns, amplification, mutation, and variant expression in PCa CTC [44–47]
AKT	PI3K-AKT directly or in crosstalk with other signaling pathways can induce EMT [48, 49]. Drugs inhibiting EMT <i>via</i> the Akt/GSK-3 β /Snail pathway decrease the invasiveness of PCa cells [50]	Implicated in PCa cell proliferation and resistance to apoptosis [51, 52]	Phosphorylated EGFR and PI3K/Akt signaling kinases detected in breast cancer patient CTCs [53], pERK/Akt pathway in CTCs in hepatocellular carcinoma patients [54], PTEN loss in circulating tumor cells in CRPC patients [55]. No report in PCa CTCs
Hippo	Deregulation of the Hippo pathway contributes to EMT in colorectal cancer [56], and FZD2 could promote clinically relevant EMT in hepatocellular carcinoma involving Hippo pathway [57]	Emerging roles in PCa development, progression, EMT, and mCRPC [58, 59]	TAZ expression detected in NSCLC CTCs [60], YAP association with metastasis in human gastric cancer [61]. No report in PCa CTCs
MAPK	MAPK mediates epithelial-mesenchymal transition in cooperation with TGF- β /Smad2 signaling and increased Snail and Twist expression [62–64]	Linked to proliferation, early relapse, and development of mCRPC [65, 66]	MAPK gene expression signature shown in pancreatic CTCs [67], detection of mutant RAS and RAF in CRC and in melanoma CTCs [68, 69]. No report in PCa CTCs
NF- κ B	Hypoxia or overexpression of HIF-1 α induces the EMT <i>via</i> NF- κ B in pancreatic cancer cells [70] and inhibition of NF- κ B deregulates EMT [71]	Promotes PCa cell survival, tumor invasion, metastasis, and chemoresistance [72, 73]	NSCLC-CTC gene expression profile was associated with cellular movement, cell adhesion and differentiation, and cell-to-cell signaling linked to PI3K/AKT, ERK1/2, and NF- κ B pathways [74]. No report in PCa CTCs
JAK/STAT	IFN- γ can induce epithelial-to-mesenchymal transition (EMT) in PCa cells <i>via</i> the JAK-STAT signaling pathway [75], and STAT3 may directly mediate EMT progression and regulate ZEB1 expression in CRC [76]	PCa progression, cell proliferation, and inhibition of apoptosis [51, 52]	No direct analysis of these pathways in CTCs
Wnt/ β -catenin	Dysregulation of Wnt/ β -catenin signaling has been implicated in the development of cancer in different tissues such as lung, skin, liver, and prostate [52], <i>via</i> regulating Zeb1 in CRC [77]	Wnt/ β -catenin pathway promotes the metastatic spread of prostate cancer cells by inducing EMT [78]	Epithelial type CTCs and activation of Wnt/ β -catenin signaling in lung cancer cells [79]. No report in PCa CTCs
Notch	Crosstalk between the Jagged1/Notch and JAK/STAT3 signaling pathways by promoting EMT through Jagged-1 in ovarian cancer [80]	Notch signaling results in prostate tumor recurrence <i>via</i> EMT [81]	Increased production of ROS results in the upregulation of Notch1 in CTCs in metastatic breast and melanoma cancer [82]. No report in PCa CTCs

TABLE 2: EMT markers detected in PCa tissue.

Epithelial markers	Mesenchymal markers
E-cadherin [84]	Snail, Cat L [83]
Cytokeratin [85]	Vimentin, N-cadherin [84]
E-cadherin [88]	Vimentin [85]
E-cadherin, cytochrome [89]	Twist [86, 87]
	N-cadherin [88]

loss of E-cadherin reduced metastatic potential in invasive ductal carcinomas [92], suggesting that E-cadherin plays opposing roles in tumor progression by suppressing cancer cell invasion while promoting metastasis. Nonetheless, on balance, the data suggest that EMT markers may have predictive value with respect to recurrence and overall survival both in tissues and in CTCs [84]. Different studies

show that E-cadherin suppresses invasion and metastasis. However, in a recent study, it has been shown that loss of E-cadherin reduced metastatic potential in invasive ductal carcinomas [92].

4. AR, ADT, EMT, and Drug Resistance

The AR, located on the X chromosome (Figure 2(a)), is a hormone-dependent transcription factor [93]. In the unstimulated state, the receptor is cytoplasmic and bound by heat-shock proteins [94]. When its ligand, dihydrotestosterone (DHT) or testosterone, binds *via* the AR ligand-binding domain (LBD) (Figure 2(a)), a structural change results in the detachment of AR from the heat-shock protein 90 (HSP90) complex, homodimerization of the receptor, and nuclear translocation.

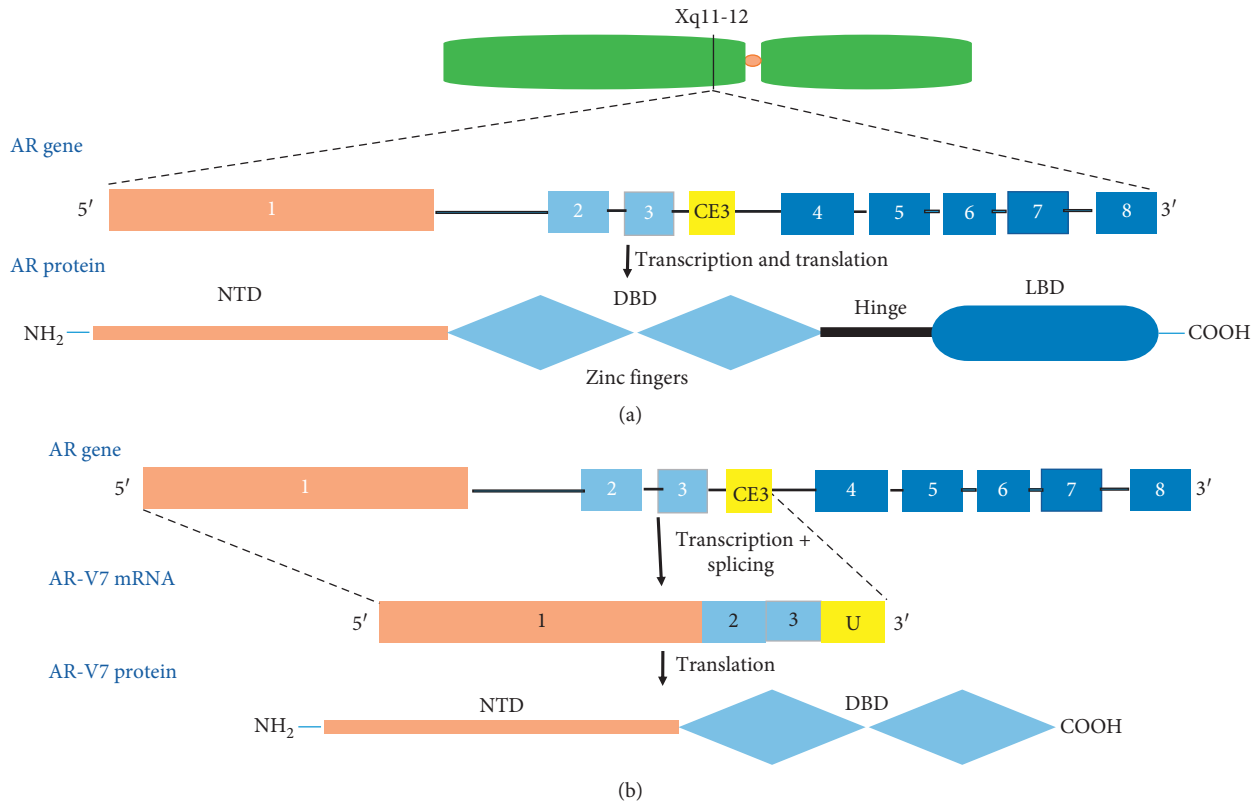


FIGURE 2: AR and AR-V7 gene and protein. The schematic indicates (a) the structural organisation of the AR gene and protein (NTD: amino terminal domain; DBD: DNA-binding domain; LBD: ligand-binding domain). (b) The transcription and translation of the AR-V7 protein including the exon/intron DNA composition of the AR, highlighting the cryptic exon CE3 (middle) and domains of the AR retained in the AR-V7 protein (bottom).

In the nucleus, AR acts as a transcription factor by binding to androgen-response elements (AREs) in the promoter region of androgen-regulated genes [95, 96]. AR transactivates genes which are responsible for cell growth, differentiation, and cell survival [97]. Consequently, increased AR signaling can potentially transform normal prostate cells into malignant PCa cells. Moreover, it has been shown that ADT therapy can select for cancer cells with further increased AR activity, for example, due to AR gene amplification [98].

The expression of alternative AR splice variants has been proposed as a mechanism underlying resistance to ADT [99, 100]. Most splice variants result in the translation of a truncated AR protein lacking a functional C-terminal LBD but containing a functional transactivating N-terminal domain. Without being capable of binding ligand, the resulting proteins are constitutively active as transcription factors and able to promote expression of certain target genes [97, 101]. At least 20 splice variants of AR have been identified in human prostate tissue and have been implicated in the development of mCRPC [101–104]. Amongst AR variants, AR-V7 is highly expressed in mCRPC and is the most frequently disease-associated variant identified in the clinic [105, 106]. The AR-V7 transcript results from alternative splicing of the AR gene such that the transcript contains exons 1, 2, and 3 together with a cryptic exon 3E (CE3) resulting in a truncated transcript (U), resulting in premature transcriptional termination (Figure 2(b)). AR-V7 is constitutively active

irrespective of androgen binding, which is a proposed mechanism of escape from ADT [107, 108].

There is no clear consensus with respect to the role of androgen signaling in the regulation of EMT. An early study using cell lines showed that androgen stimulation promoted EMT in both LNCaP and PC-3 cells but that there was an inverse relationship between AR receptor levels and androgen-mediated EMT marker expression and EMT-associated cytoskeletal changes. Low levels of AR induced by shRNA promoted PCa cell metastatic ability by inducing EMT while high levels did not [109]. In contrast, a recent study has shown that AR mRNA and protein expression is higher in metastatic tumor tissues than in primary tumors and increases with tumor stage and Gleason score. Patients with higher AR expression showed shorter recurrence-free survival, indicating a positive association between AR expression and tumor progression. Further, knockdown of AR using siRNA in C4-2B cells suppressed functional markers of EMT, *viz* cell migration and invasion, and mesenchymal marker proteins associated with EMT, while increasing the epithelial marker E-cadherin. These effects were recapitulated by treatment with the antiandrogen bicalutamide [39]. Thus, it appears that AR stimulation induces or suppresses EMT in cell culture in a cell-type-dependent fashion.

Studies with both normal mouse prostate and human prostate tumor models in mice have shown that androgen

deprivation through surgical castration, while suppressing tumor growth, induces mesenchymal markers of EMT and markers of a stem cell phenotype, while suppressing epithelial markers. These changes were also seen in tissues of patients treated with ADT [110], supporting the view that AR signaling suppresses EMT, while ADT promotes it.

In further support of this view, ADT with enzalutamide in C4-2 cells, but not in PC-3 cells, induced EMT markers in a Snail-dependent fashion. Induction of EMT required both suppression of AR signaling and activation of Snail. Interestingly, Snail was downregulated by androgen in AR-expressing C4-2 and VCaP cells but again, not in PC-3 cells. Importantly, the inverse correlation between AR signaling and Snail expression observed in C4-2 xenografts and castration-resistant patient-derived metastases in mice and in clinical samples supports the view that the induction of EMT is an adaptive response to ADT with enzalutamide [40]. ADT may favor acquisition of stem cell and EMT characteristics, expression of oncogenes, or suppression of tumor suppressor genes in AR-positive PCa cells, implying that mCRPC at least in part is achieved through EMT [41, 110–114].

Other data suggest that AR splice variants are involved in the development of drug resistance in PCa [105, 115–117]. One corollary of this hypothesis is that inhibition of the AR variants or their specific function might lead to reversal of EMT phenotype and that might in turn inhibit tumor spread [41, 118]. Overall, however, this area remains understudied, and more data are needed to fully understand how the AR pathway and its manipulation during therapy may regulate EMT and thus potentially metastasis. Since mCRPC is ultimately the principal cause of death in many patients, the fundamental biological processes for the development and establishment of mCRPC need to be understood [119]. It is noteworthy that there is now mounting evidence in CTCs that the expression of EMT markers is associated with mCRPC [120, 121], highlighting the potential benefit in the analysis of CTCs to address the role of AR in metastasis and drug resistance.

5. Akt Pathway in mCRPC

As indicated above, due to the hormone-independent nature of mCRPC, it is unresponsive to all current forms of ADT. At this stage, AR expression may even be completely lost [122–124], raising the question as to how survival and proliferation of PCa cells occur at this stage. The main oncogenic signaling pathway implicated at this juncture is the PI3K/AKT-pathway, predominantly activated through frequent functional loss of the inhibitory tumor suppressor phosphatase and tensin homolog (PTEN), which is less common in localized PCa (20–30%) but becomes more dominant and is found in up to 50–60% of mCRPCs. The result is uncontrolled, oncogenic Akt signaling (reviewed in [125, 126]). The PI3K/AKT and AR pathways are highly networked with both positive and negative feedback loops [125], and in mCRPC, current literature indicates that negative feedback dominates. That is, inhibition of one pathway leads to reciprocal activation of the other [127–130].

Carver and colleagues have elucidated part of this interaction, demonstrating that the AR reduces AKT activation through the intermediary PHLPP, while AKT can transcriptionally downregulate AR output via HER kinase activity [127]. The exact role of PTEN in mediating this interaction is controversial. On the one hand, PTEN deletion has been associated with AKT activation and reduced AR levels [128, 131], and on the other hand, it may independently increase AR gene expression by removing transcriptional repression [130, 132–134]. Given the interconnected signaling network, outcomes of AR and AKT signaling or silencing may affect overall outcomes in a context-specific fashion, which is likely dependent on the presence and activity of other proteins that can affect the balance of feedback loops. For example, it has been shown that AR can transcriptionally repress PTEN expression in PCa cells while it increases PTEN expression in breast cancer cells and the report suggested this may be due to tissue-dependent availability of transcriptional cofactors [135]. Moreover, ADT may also affect the balance in these interconnected signaling pathways. Importantly, loss of *PTEN* has been associated with EMT driven through the AKT pathway or in cooperation with RAS signaling; thereby, lack of PTEN function could promote metastasis [136, 137].

6. Hippo Signaling Pathway and Its Role in CRPC and EMT

As indicated above, several signaling pathways may contribute to the induction of EMT and ultimately metastasis, with the AKT pathway of importance in the context of PCa. More recently, the YAP1 transcriptional coactivator regulated by the Hippo pathway has emerged as an important player in this scenario and in regulating PCa cell motility [138]. In the context of gastric cancer, PTEN inactivation has been proposed to link the Hippo and PI3K/Akt pathways to promote cancer development and tumorigenesis [139]. In normal tissue, the Hippo signaling pathway appears central to cell growth control and limits organ size by coordinating cell proliferation, growth, and death [140]. Different signals like cell polarity, cell-cell contact, extracellular matrix characteristics, and stress can result in the activation of the Hippo pathway (reviewed in [141]). Hippo signaling through a kinase cascade results in phosphorylation of oncogenic cotranscription factors known as YAP and TAZ, promoting their cytoplasmic retention and proteasomal degradation [142–144] (Figure 3).

Inactivation of the Hippo pathway allows for YAP and TAZ activation *via* dephosphorylation, which is required for translocation into the nucleus. Although TAZ and YAP lack intrinsic DNA-binding domains, they are recruited by and enhance the activity of other transcription factors at their target promoters [145, 146].

Hippo signaling can act as a tumor suppressor. Functional impairment of Hippo signaling is often due to the loss of MST1/2 or LATS1/2 function or due to *YAP1* gene amplification. YAP1 is the most studied YAP isoform, and aberrant YAP1 activation is associated with the etiology of various malignancies including stomach [147], thyroid

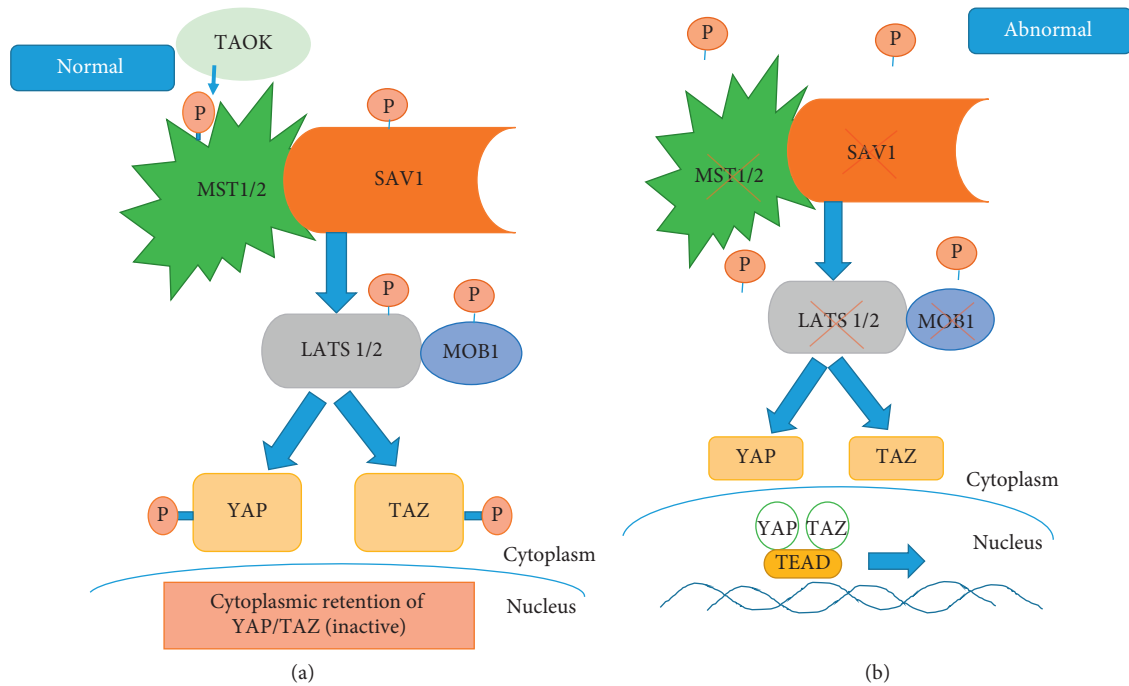


FIGURE 3: Hippo signaling pathway. Active Hippo signaling represses YAP and TAZ *via* phosphorylation (a), while inactive Hippo leads to dephosphorylation, nuclear translocation, and thus activation of TFs (b). The crossed out symbol indicates pathway members frequently lost in cancer.

[148], lung [149], colon [150], head and neck [151] ovarian [152], liver [153], and prostate cancer [154].

Most interestingly, YAP1 and AR directly interact in PCa cells. One study demonstrates that unlike in hormone-sensitive prostate cancer cells, YAP1-AR interactions are androgen-insensitive and may cause resistance to enzalutamide in mCRPC cells. The WW/SH3 domain of YAP1 most likely facilitates the interaction with the AR amino terminal domain (NTD) [155].

One study proposes that increased nuclear YAP1, possibly due to the loss of Hippo signaling, may lead to increased complex formation between AR and YAP1 leading to androgen-independent binding of the complex to AREs in AR-driven promoters resulting in aberrant AR target gene expression possibly promoting mCRPC [58].

Importantly, YAP has been shown to promote metastasis through several mechanisms including EMT, and there is some evidence that the PTEN-AKT axis is involved in YAP1-induced EMT [145, 156, 157]. The underlying mechanisms of EMT regulation by YAP are still emerging, but given the role of YAP as a transcriptional coregulator, it is not surprising that the pathways centrally involve EMT-TFs. Critically, YAP1 has been shown to network with the main EMT-TFs. For instance, high glucose-induced poly-ubiquitination of PTEN results in alteration of its phosphatase targets, including an increased focus on dephosphorylation and activation of EMT regulators such as Twist, Snail, and YAP1 [158]. YAP1 was also reported to drive EMT and likely NSCLC metastasis by TEAD-dependent transcriptional induction of *SLUG* [159]. Focusing on YAP's role in osteoblast differentiation, one study identified

two links between YAP and Snail/Slug. In Snail/Slug-null skeletal stem/stromal cells, the levels of both YAP and TAZ were reduced *via* protein degradation due to activation of the Hippo pathway, while direct interaction of YAP with Snail and with Slug was shown to alter YAP/TEAD transcriptional activity [160]. Another study found that Twist-induced EMT in breast cancer cells is dependent on TAZ activity. The mechanism involved increased expression of the Hippo pathway inhibitors PAR-1 and PAR-3, which drive TAZ nuclear localisation. One would expect that YAP nuclear localisation may also be induced *via* PAR-1/-3 in this context, although this was not examined [161]. Another study revealed that increased extracellular matrix stiffness can induce EMT in breast cancer cells and that blocking β 1-integrin-mediated matrix stiffness prevented both Twist and YAP nuclear translocation albeit, interestingly, by different mechanisms [162].

In epithelial cells, cells are connected to each other by membrane structures called tight junctions, adherens junctions, and desmosomes. Any dysregulation in these junctions is implicated in metastasis and EMT [163, 164]. Zona occludens-1 (ZO-1) is a tight junction protein that is present in normal epithelial cells. Though not yet studied in PCa, in melanoma, lung cancer cells, and breast cancer, ZO-1 expression correlates with invasion properties of cancer cells [165–167]. One study found that YAP overexpression resulted in downregulation of ZO-1 and induced metastasis through EMT in NSCLC [159].

YAP (but not TAZ) has been shown to interact directly with ZEB1 and, remarkably, this interaction turns this transcriptional repressor into an activator. This is

highlighted by the fact that ZEB1-mediated CDH1 (E-cadherin) repression is independent of YAP binding. Critically, gene upregulation by the ZEB1-YAP complex correlated with gene expression signatures of claudin-low breast cancer, a breast cancer subtype overall exhibiting an EMT phenotype. More importantly, ZEB1-YAP complex-mediated gene expression was related to poor patient survival in hormone-independent breast cancers and linked to drug resistance and metastasis [168]. ZEB1 is known to repress several EMT-related miRNAs including miR375, which is associated with an epithelial phenotype. Nevertheless, miR375, a known YAP target, is commonly overexpressed in PCa and in fact has been indicated as a plasma marker of PCa. The suggested mechanism by which miR375 supports an epithelial phenotype is via feedback regulation, such that it targets and suppresses YAP transcript and thus YAP protein levels and thereby reversing EMT in PCa cells. Surprisingly however, high plasma miR375 level was associated with CTC positivity [169], suggesting that further investigations are needed to understand the complex network between YAP, ZEB1, miR375, EMT, and CTC formation. Additionally, hypoxia may, at least in part, induce EMT by stabilizing YAP and its nuclear translocation in PCa cell lines [170].

Not surprisingly, another study showed that inhibiting a key characteristic of epithelial tissue, namely, E-cadherin-mediated cell-cell interaction, resulted in EMT and increased dissemination of Madin–Darby canine kidney cells. Interestingly, dissemination could be partially prevented by YAP knockdown. The same study found that not only is YAP required to allow nuclear entry of the MET initiating Wilms tumor protein 1 (WT1), but both WT1 and YAP form a complex at the *CDH1* (E-cadherin) promoter and repress its transcription. These data, together with confirmation that E-cadherin inhibition upregulates YAP levels, indicate a double-negative feedback where E-cadherin and YAP mutually inhibit each other. This may be part of a switch between EMT and MET, thus potentially explaining the plasticity of the EMT process [171].

7. YAP Crosstalk with AR, AKT and AR Pathways

Interestingly, one possible mechanism for PTEN loss of function is mediated by YAP. The pathway involves nuclear YAP-mediated activation of the TEAD family of transcription factors, leading to synthesis of the PTEN transcriptional repressor miRNA29c. Conversely, when YAP is inactivated via phosphorylation, PTEN levels are restored and the oncogenic function of YAP is inhibited [172]. Moreover, as mentioned above, PTEN ubiquitination can dephosphorylate and thus activate YAP causing its nuclear accumulation indicating a possible positive feedback regulation [158].

On the other hand, PTEN was identified as a negative regulator of AR activity such that the AR/PTEN interaction may mediate a tumor suppressor role for PTEN via suppression of AR and apoptosis induction in PCa cells [173]. However, as outlined above, the PTEN and AR network is

still poorly understood, and data are conflicting. This is exemplified by another study with opposing findings, wherein PTEN deletion reduces both AR expression and AR transcriptional activity in PCa [131].

Taken together, emerging evidence indicates that YAP is part of the complex functional network that connects the AR and AKT pathways and thereby modulates PCa and mCRPC—at least in part—*via* EMT (Figure 4). However, more work is needed to better understand this interplay and its implications for the development of strategies to treat advanced PCa.

8. Analysis of PCa CTCs to Explore the AR-AKT-YAP Connection and EMT

The evaluation of molecular pathways underlying mCRPC is challenging because tissue biopsies are generally not available from late disease stages and animal models; further, although examination of tissue can provide some signaling pathway information, this mode of studying PCa has limitations. Liquid biopsies, and analysis of mCRPC CTCs, may be an alternative. While diagnostic CTC analysis in PCa is still in its infancy, there is ample evidence of its utility in this disease. Certainly, CTCs have been investigated by imaging and molecular technologies for expression of proteins, gene amplifications, mutations, and transcript expression on both targeted and comprehensive levels [174]. For PCa, increased CTC counts are associated with earlier disease progression and shorter OS, with enumeration of PCa CTCs using the CellSearch CTC platform gaining FDA approval as a prognostic indicator [175]. While common CTC isolation and analysis techniques favour epithelial CTCs, there have been numerous advances in improving capture, detection, and analysis of EMT-CTCs by screening for epithelial and mesenchymal marker expression [176–181]. Equally, as Table 1 shows, several major signaling pathways implicated in EMT have, to some extent, been analysed in CTC samples. In this review, we focussed on the AR, AKT, and Hippo pathways as being central to mCRPC, at least in part *via* EMT regulation. It is now important to consider how these pathways have been explored in CTCs, in order to gauge the potential for CTC analysis to advance our understanding of these pathways in mCRPC. Accordingly, we note that DNA-, RNA-, and protein-centric analyses for AR and AR-V7 levels in isolated CTCs have become a busy field of PCa research. Moreover, efforts are being made to translate CTC-based AR and AR-V7 detection into clinical settings aimed initially at stratifying patients to define either eligibility criteria or outcome markers for clinical trials (<https://clinicaltrials.gov>) [182].

mCRPC-associated AR amplification and mutation analysis have been performed in CTCs using hybridization techniques such as fluorescent *in situ* hybridization (FISH) and other molecular approaches. In general, these studies were able to validate the association of CTC-based AR amplification or mutation with mCRPC, while the relevance of AR cellular localisation in CTCs was shown in mCRPC and in response to taxanes [46, 47, 183–186]. The presence of full-length AR and AR-V7 in CTCs has been studied

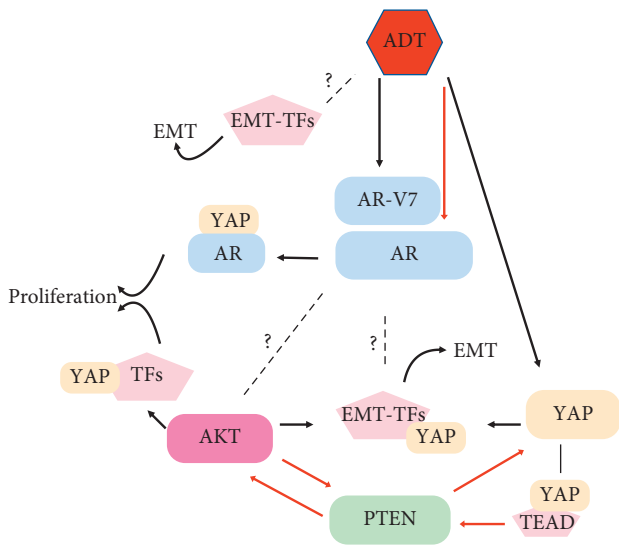


FIGURE 4: AR AKT and YAP interaction. Schematic presentation of reported and likely (dotted lines) network connections between ADT, AR, AKT, and YAP.

extensively at the RNA level and CTC-based AR-V7 in particular was found to correlate with mCRPC and primary resistance to abiraterone and enzalutamide [45, 182, 184, 187, 188]. Interestingly, there have also been efforts at detecting both AR and AR-V7 as biomarkers in other liquid biopsy entities, including plasma-derived circulating tumor RNA (ctRNA), exosomes, or even in urine. We recently compared some of these strategies and found both full-length AR and V7 RNA detection is more sensitive and specific if performed on CTC samples, as compared to ctRNA or exosomes. We also demonstrated that AR-V7 is detectable from CTC-RNA up to 48 h post blood draw into common EDTA vacutubes [189, 190]. With improved AR-V7-specific antibody availability, CTC immunocytostaining more recently revealed that specific detection of AR-V7 in CTC nuclei is an even better predictor of OS and PFS in CRPC patients [191, 192]. In general, it appears nuclear AR is found in most CTCs positive for AR-V7 RNA, reflecting the predominant tendency for AR-V7 to be nuclear localized in mCRPC tissue [188, 193]. In CRPC patients, AR-V7-positive CTCs have been shown to correlate with enzalutamide and abiraterone resistance [187]. In any case, when investigating the interplay of AR/AR-V7 with other pathways, especially transcriptional coactivators, immunocytodetection in CTCs appears to be the most logical strategy.

Several studies have also analysed PTEN loss in CTCs, which, as outlined above, may allow oncogenic activation of the AKT pathway and is an important PCa biomarker. Loss of *PTEN* and gain of AR copy numbers were reported in PCa CTCs [194–197], while testing for activation of the AKT pathway has been performed for example by phospho-Akt or phospho-S6 kinase immunostaining in breast cancer and multiple myeloma CTCs [198].

Reports on hippo signaling and YAP1 analysis in CTCs, by contrast, are still scarce. One study assessed expression of TAZ using RNA in situ hybridization (RNAish) probing of

NSCLC CTCs. TAZ expression was detected more frequently in EGFR wild-type cancers while its expression in CTCs was associated with lymph node status of the disease [60]. It is likely that YAP1 could be analysed in a similar fashion in CTCs or preferentially using immunocytostaining, as the latter would also reveal cellular localisation and thus activity as well as colocalisation with other proteins. However, to our knowledge, direct detection of YAP1 in CTCs has not yet been reported, although the relationship of YAP1 to EMT suggests that activated YAP1 should correlate with increased formation of CTCs. Some indirect evidence lends further strength to this idea, as a recent report showed that the Rho GTPase activating protein 29 (ARHGAP29) is a transcriptional target of YAP1 in gastric cancer. High ARHGAP29 levels were shown to regulate cytoskeletal actin and cell migration. Importantly, the authors also demonstrated using a mouse model that CTCs exhibited increased ARHGAP29 RNA levels compared with primary tumor site cells [61, 199]. Final proof of a YAP1-ARHGAP29 connection in CTCs remains pending, however. Another transcriptional target of YAP is miR375 which was associated with CTC positivity, yet a direct connection was again not shown in CTCs [169].

Taken together, the reviewed data suggest that AR-AKT-YAP1 network can be analysed in CTCs. Since tumor tissue is rarely available in the mCRPC setting, and blood samples can be easily taken, future endeavours in CTC analysis could open the way to better understand ADT resistance and thereby inform the development of improved diagnostic, prognostic, and therapeutic capabilities.

Analysis of CTCs has provided a foundation for liquid biopsy, especially in the absence of biopsy tissue. However, there are serious challenges with CTC isolation, detection, and downstream analysis. One is that CTC numbers are relatively small within large populations of blood cells and the volume of blood that can be taken depends on the patient's general condition. CTCs are quite heterogeneous in terms of physical properties (size, elasticity, and surface charge), biological characteristics, and expression of different tumor markers making enrichment or isolation of all CTCs difficult (reviewed in [200]). In general, the low CTC numbers make downstream analysis of CTCs another challenge. Protein detection is usually limited to immunocytostaining which relies on antibody-based detection and the number of microscope channels available with 3 usually dedicated to detection of a CTC marker (often cytokeratin), a nuclear marker such as DAPI, and exclusion of a blood cell marker usually CD45. Nevertheless, some studies have detected additional proteins such as EMT markers [21, 22, 176] or posttranslational modifications such as phosphorylation of pFAK, pPI3K, pSRC, pEGFR, and pAkt [53, 201–204].

9. Conclusion

Here, we reviewed connections between the AR pathway and the AKT and Hippo pathways, exploring a potential role for this signaling nexus in EMT and mCRPC. Though current literature supports the importance of this tripartite relationship, further study is now needed to better evaluate its

importance in PCa, as well as its clinical potential in defining biomarkers or drug targets. Analysis of PCa CTCs may facilitate deeper investigations into AR/AKT/Hippo pathway interactions, and how these drive EMT as well as ADT resistance. Such analyses may ultimately mediate the emergence of new diagnostic/prognostic assays directed towards PCa, though at this time insufficient data are available to establish feasibility of this concept. Indeed, while some aspects of these pathways have already been investigated in CTCs, optimisation of more comprehensive CTC analysis methods is now needed to permit the dissection of these pathway interactions, as a precursor to this significant goal.

Conflicts of Interest

The authors declare that there are no conflicts of interest regarding the publication of this paper.

Acknowledgments

This work was funded by the Centre for Oncology Education & Research Translation (CONCERT) through Cancer Institute NSW under grant number 13/TRC/1-01. TK is recipient of a Western Sydney University Androgen Receptor Research Scholarship.

References

- [1] A. Jemal, F. Bray, M. M. Center, J. Ferlay, E. Ward, and D. Forman, "Global cancer statistics," *CA: A Cancer Journal for Clinicians*, vol. 61, no. 2, pp. 69–90, 2011.
- [2] F. Bray, J. Ferlay, I. Soerjomataram, R. L. Siegel, L. A. Torre, and A. Jemal, "Global cancer statistics 2018: GLOBOCAN estimates of incidence and mortality worldwide for 36 cancers in 185 countries," *CA: A Cancer Journal for Clinicians*, vol. 68, no. 6, pp. 394–424, 2018.
- [3] D. T. Hoang, K. A. Iczkowski, D. Kilari, W. See, and M. T. Nevalainen, "Androgen receptor-dependent and-independent mechanisms driving prostate cancer progression: opportunities for therapeutic targeting from multiple angles," *Oncotarget*, vol. 8, no. 2, p. 3724, 2017.
- [4] D. Shapiro and B. Tareen, "Current and emerging treatments in the management of castration-resistant prostate cancer," *Expert Review of Anticancer Therapy*, vol. 12, no. 7, pp. 951–964, 2012.
- [5] C. D. Chen, D. S. Welsbie, C. Tran et al., "Molecular determinants of resistance to antiandrogen therapy," *Nature Medicine*, vol. 10, no. 1, pp. 33–39, 2004.
- [6] K. E. Knudsen and H. I. Scher, "Starving the addiction: new opportunities for durable suppression of AR signaling in prostate cancer," *Clinical Cancer Research*, vol. 15, no. 15, pp. 4792–4798, 2009.
- [7] D. L. Longo, "New therapies for castration-resistant prostate cancer," *New England Journal of Medicine*, vol. 363, no. 5, pp. 479–481, 2010.
- [8] J. S. De Bono, C. J. Logothetis, A. Molina et al., "Abiraterone and increased survival in metastatic prostate cancer," *The New England Journal of Medicine*, vol. 364, no. 364, pp. 1995–2005, 2011.
- [9] C. J. Ryan, M. R. Smith, J. S. de Bono et al., "Abiraterone in metastatic prostate cancer without previous chemotherapy," *The New England Journal of Medicine*, vol. 368, no. 368, pp. 138–148, 2013.
- [10] T. M. Beer, A. J. Armstrong, D. E. Rathkopf et al., "Enzalutamide in metastatic prostate cancer before chemotherapy," *New England Journal of Medicine*, vol. 371, no. 5, pp. 424–433, 2014.
- [11] H. I. Scher, K. Fizazi, F. Saad et al., "Increased survival with enzalutamide in prostate cancer after chemotherapy," *New England Journal of Medicine*, vol. 367, no. 13, pp. 1187–1197, 2012.
- [12] K. Fizazi, H. I. Scher, A. Molina et al., "Abiraterone acetate for treatment of metastatic castration-resistant prostate cancer: final overall survival analysis of the COU-AA-301 randomised, double-blind, placebo-controlled phase 3 study," *The Lancet Oncology*, vol. 13, no. 10, pp. 983–992, 2012.
- [13] M. Fang, M. Nakazawa, E. S. Antonarakis, and C. Li, "Efficacy of abiraterone and enzalutamide in pre-and post-docetaxel castration-resistant prostate cancer: a trial-level meta-analysis," *Prostate Cancer*, vol. 2017, Article ID 8560827, 8 pages, 2017.
- [14] S. Linder, H. G. van der Poel, A. M. Bergman, W. Zwart, and S. Prekovic, "Enzalutamide therapy for advanced prostate cancer: efficacy, resistance and beyond," *Endocrine-Related Cancer*, vol. 26, no. 1, pp. R31–R52, 2018.
- [15] V. Mittal, "Epithelial mesenchymal transition in tumor metastasis," *Annual Review of Pathology: Mechanisms of Disease*, vol. 13, no. 1, pp. 395–412, 2018.
- [16] M. A. Nieto, R. Y.-J. Huang, R. A. Jackson, and J. P. Thiery, "EMT: 2016," *Cell*, vol. 166, no. 1, pp. 21–45, 2016.
- [17] D. Yao, C. Dai, and S. Peng, "Mechanism of the mesenchymal-epithelial transition and its relationship with metastatic tumor formation," *Molecular Cancer Research*, vol. 9, no. 12, pp. 1608–1620, 2011.
- [18] N. J. Caixeiro, N. Kienzle, S. H. Lim et al., "Circulating tumour cells—a bona fide cause of metastatic cancer," *Cancer and Metastasis Reviews*, vol. 33, no. 2-3, pp. 747–756, 2014.
- [19] N. Stylianou, M. L. Lehman, C. Wang et al., "A molecular portrait of epithelial-mesenchymal plasticity in prostate cancer associated with clinical outcome," *Oncogene*, vol. 38, no. 7, pp. 913–934, 2019.
- [20] M. Cheng, L. Liu, H.-S. Yang, and G.-F. Liu, "Circulating tumor cells are associated with bone metastasis of lung cancer," *Asian Pacific Journal of Cancer Prevention*, vol. 15, no. 15, pp. 6369–6374, 2014.
- [21] Y.-J. Yang, Y.-Y. Kong, G.-X. Li, Y. Wang, D.-W. Ye, and B. Dai, "Phenotypes of circulating tumour cells predict time to castration resistance in metastatic castration-sensitive prostate cancer," *BJU International*, vol. 124, no. 2, pp. 258–267, 2019.
- [22] J. Chen, S. Cao, B. Situ et al., "Metabolic reprogramming-based characterization of circulating tumor cells in prostate cancer," *Journal of Experimental & Clinical Cancer Research*, vol. 37, no. 1, p. 127, 2018.
- [23] P. S. Steeg, "Tumor metastasis: mechanistic insights and clinical challenges," *Nature Medicine*, vol. 12, no. 8, pp. 895–904, 2006.
- [24] M. Montanari, S. Rossetti, C. Cavaliere et al., "Epithelial-mesenchymal transition in prostate cancer: an overview," *Oncotarget*, vol. 8, no. 21, p. 35376, 2017.
- [25] U.-G. Lo, C.-F. Lee, M.-S. Lee, and J.-T. Hsieh, "The role and mechanism of epithelial-to-mesenchymal transition in

- prostate cancer progression,” *International Journal of Molecular Sciences*, vol. 18, no. 10, p. 2079, 2017.
- [26] M. P. Stemmler, R. L. Eccles, S. Brabletz, and T. Brabletz, “Non-redundant functions of EMT transcription factors,” *Nature Cell Biology*, vol. 21, no. 1, pp. 102–112, 2019.
- [27] P. G. Santamaria, G. Moreno-Bueno, and A. Cano, “Contribution of epithelial plasticity to therapy resistance,” *Journal of Clinical Medicine*, vol. 8, no. 5, p. 676, 2019.
- [28] M.-H. Yang, M.-Z. Wu, S.-H. Chiou et al., “Direct regulation of TWIST by HIF-1 α promotes metastasis,” *Nature Cell Biology*, vol. 10, no. 3, pp. 295–305, 2008.
- [29] T. Imai, A. Horiuchi, C. Wang et al., “Hypoxia attenuates the expression of E-cadherin via up-regulation of SNAIL in ovarian carcinoma cells,” *The American Journal of Pathology*, vol. 163, no. 4, pp. 1437–1447, 2003.
- [30] J. Yang and R. A. Weinberg, “Epithelial-mesenchymal transition: at the crossroads of development and tumor metastasis,” *Developmental Cell*, vol. 14, no. 6, pp. 818–829, 2008.
- [31] Y. Katoh and M. Katoh, “Hedgehog signaling, epithelial-to-mesenchymal transition and miRNA,” *International Journal of Molecular Medicine*, vol. 22, no. 3, pp. 271–275, 2008.
- [32] B. D. Craene and G. Bercx, “Regulatory networks defining EMT during cancer initiation and progression,” *Nature Reviews Cancer*, vol. 13, no. 2, pp. 97–110, 2013.
- [33] M. A. Huber, H. Beug, and T. Wirth, “Epithelial-mesenchymal transition: NF- κ B takes center stage,” *Cell Cycle*, vol. 3, no. 12, pp. 1477–1480, 2004.
- [34] A. Moustakas and C.-H. Heldin, “Signaling networks guiding epithelial-mesenchymal transitions during embryogenesis and cancer progression,” *Cancer Science*, vol. 98, no. 10, pp. 1512–1520, 2007.
- [35] G. Christofori, “New signals from the invasive front,” *Nature*, vol. 441, no. 7092, pp. 444–450, 2006.
- [36] J. P. Thiery, “Epithelial-mesenchymal transitions in tumour progression,” *Nature Reviews Cancer*, vol. 2, no. 6, pp. 442–454, 2002.
- [37] J. P. Thiery, H. Acloque, R. Y. J. Huang, and M. A. Nieto, “Epithelial-mesenchymal transitions in development and disease,” *Cell*, vol. 139, no. 5, pp. 871–890, 2009.
- [38] R. Kalluri and R. A. Weinberg, “The basics of epithelial-mesenchymal transition,” *Journal of Clinical Investigation*, vol. 119, no. 6, pp. 1420–1428, 2009.
- [39] C.-Y. Lin, Y.-J. Jan, L.-K. Kuo et al., “Elevation of androgen receptor promotes prostate cancer metastasis by induction of epithelial-mesenchymal transition and reduction of KAT5,” *Cancer Science*, vol. 109, no. 11, pp. 3564–3574, 2018.
- [40] L. Miao, L. Yang, R. Li et al., “Disrupting androgen receptor signaling induces snail-mediated epithelial-mesenchymal plasticity in prostate cancer,” *Cancer Research*, vol. 77, no. 11, pp. 3101–3112, 2017.
- [41] D. Kong, S. Sethi, Y. Li et al., “Androgen receptor splice variants contribute to prostate cancer aggressiveness through induction of EMT and expression of stem cell marker genes,” *The Prostate*, vol. 75, no. 2, pp. 161–174, 2015.
- [42] D. N. Lavery and C. L. Bevan, “Androgen receptor signalling in prostate cancer: the functional consequences of acetylation,” *BioMed Research International*, vol. 2011, Article ID 862125, 7 pages, 2010.
- [43] M. E. Tan, J. Li, H. E. Xu, K. Melcher, and E.-I. Yong, “Androgen receptor: structure, role in prostate cancer and drug discovery,” *Acta Pharmacologica Sinica*, vol. 36, no. 1, pp. 3–23, 2015.
- [44] I. Puche-Sanz, M. J. Alvarez-Cubero, M. Pascual-Geler et al., “A comprehensive study of circulating tumour cells at the moment of prostate cancer diagnosis: biological and clinical implications of EGFR, AR and SNPs,” *Oncotarget*, vol. 8, no. 41, pp. 70472–70480, 2017.
- [45] Y. Ma, A. Luk, F. Young et al., “Droplet digital PCR based androgen receptor variant 7 (AR-V7) detection from prostate cancer patient blood biopsies,” *International Journal of Molecular Sciences*, vol. 17, no. 8, p. 1264, 2016.
- [46] J. Podolak, K. Eilers, T. Newby et al., “Androgen receptor amplification is concordant between circulating tumor cells and biopsies from men undergoing treatment for metastatic castration resistant prostate cancer,” *Oncotarget*, vol. 8, no. 42, p. 71447, 2017.
- [47] Y. Jiang, J. F. Palma, D. B. Agus, Y. Wang, and M. E. Gross, “Detection of androgen receptor mutations in circulating tumor cells in castration-resistant prostate cancer,” *Clinical Chemistry*, vol. 56, no. 9, pp. 1492–1495, 2010.
- [48] W. Xu, Z. Yang, and N. Lu, “A new role for the PI3K/Akt signaling pathway in the epithelial-mesenchymal transition,” *Cell Adhesion & Migration*, vol. 9, no. 4, pp. 317–324, 2015.
- [49] J. Dong, B. Zhai, W. Sun, F. Hu, H. Cheng, and J. Xu, “Activation of phosphatidylinositol 3-kinase/AKT/snail signaling pathway contributes to epithelial-mesenchymal transition-induced multi-drug resistance to sorafenib in hepatocellular carcinoma cells,” *PLoS One*, vol. 12, no. 9, Article ID e0185088, 2017.
- [50] F. Fang, S. Chen, J. Ma et al., “Juglone suppresses epithelial-mesenchymal transition in prostate cancer cells via the protein kinase B/glycogen synthase kinase-3 β /Snail signaling pathway,” *Oncology Letters*, vol. 16, no. 2, pp. 2579–2584, 2018.
- [51] S. Sittadjody, T. Thangasamy, B. NickKolgh, and K. C. Balaji, “Non-androgen signaling pathways in castration-resistant prostate cancer,” in *Managing Metastatic Prostate Cancer in Your Urological Oncology Practice*, pp. 35–63, Springer, Berlin, Germany, 2016.
- [52] H. B. da Silva, E. P. Amaral, E. L. Nolasco et al., “Dissecting major signaling pathways throughout the development of prostate cancer,” *Prostate Cancer*, vol. 2013, Article ID 920612, 23 pages, 2013.
- [53] G. Kallergi, S. Agelaki, A. Kalykaki, C. Stournaras, D. Mavroudis, and V. Georgoulis, “Phosphorylated EGFR and PI3K/Akt signaling kinases are expressed in circulating tumor cells of breast cancer patients,” *Breast Cancer Research*, vol. 10, no. 5, p. R80, 2008.
- [54] J. Li, L. Shi, X. Zhang et al., “pERK/pAkt phenotyping in circulating tumor cells as a biomarker for sorafenib efficacy in patients with advanced hepatocellular carcinoma,” *Oncotarget*, vol. 7, no. 3, p. 2646, 2016.
- [55] E. A. Punnoose, R. Ferraldeschi, E. Szafer-Glusman et al., “PTEN loss in circulating tumour cells correlates with PTEN loss in fresh tumour tissue from castration-resistant prostate cancer patients,” *British Journal Of Cancer*, vol. 113, no. 8, pp. 1225–1233, 2015.
- [56] D. D. Shao, W. Xue, E. B. Krall et al., “KRAS and YAP1 converge to regulate EMT and tumor survival,” *Cell*, vol. 158, no. 1, pp. 171–184, 2014.
- [57] H. Ou, Z. Chen, L. Xiang et al., “Frizzled 2-induced epithelial-mesenchymal transition correlates with vasculogenic mimicry, stemness, and Hippo signaling in hepatocellular carcinoma,” *Cancer Science*, vol. 110, no. 4, pp. 1169–1182, 2019.

- [58] L. Zhang, S. Yang, X. Chen et al., "The hippo pathway effector YAP regulates motility, invasion, and castration-resistant growth of prostate cancer cells," *Molecular and Cellular Biology*, vol. 35, no. 8, pp. 1350–1362, 2015.
- [59] O. Salem and C. G. Hansen, "The hippo pathway in prostate cancer," *Cells*, vol. 8, no. 4, p. 370, 2019.
- [60] M. Wu, Y. Wang, H. Wu, and K. Cai, "TAZ expression in three distinct circulating tumor cells of NSCLC patients," *International Journal of Clinical and Experimental Pathology*, vol. 10, no. 5, pp. 5721–5729, 2017.
- [61] Y. Qiao, J. Chen, Y. B. Lim et al., "YAP regulates actin dynamics through ARHGAP29 and promotes metastasis," *Cell Reports*, vol. 19, no. 8, pp. 1495–1502, 2017.
- [62] M. Huang, Y.-P. Wang, L.-Q. Zhu, Q. Cai, H.-H. Li, and H.-F. Yang, "MAPK pathway mediates epithelial-mesenchymal transition induced by paraquat in alveolar epithelial cells," *Environmental Toxicology*, vol. 31, no. 11, pp. 1407–1414, 2016.
- [63] O. Hawsawi, V. Henderson, L. J. Burton, J. Dougan, P. Nagappan, and V. Odero-Marah, "High mobility group A2 (HMGA2) promotes EMT via MAPK pathway in prostate cancer," *Biochemical and Biophysical Research Communications*, vol. 504, no. 1, pp. 196–202, 2018.
- [64] T. Gui, Y. Sun, A. Shimokado, and Y. Muragaki, "The roles of mitogen-activated protein kinase pathways in TGF- β -induced epithelial-mesenchymal transition," *Journal of Signal Transduction*, vol. 2012, Article ID 289243, 10 pages, 2012.
- [65] R. Mukherjee, D. H. McGuinness, P. McCall et al., "Upregulation of MAPK pathway is associated with survival in castrate-resistant prostate cancer," *British Journal of Cancer*, vol. 104, no. 12, pp. 1920–1928, 2011.
- [66] G. Rodríguez-Berriguete, B. Fraile, P. Martínez-Onsurbe, G. Olmedilla, R. Paniagua, and M. Royuel, "MAP kinases and prostate cancer," *Journal of Signal Transduction*, vol. 2012, Article ID 169170, 9 pages, 2012.
- [67] G. Sergeant, R. V. Eijdsen, T. Roskams, V. Van Duppen, and B. Topal, "Pancreatic cancer circulating tumour cells express a cell motility gene signature that predicts survival after surgery," *BMC Cancer*, vol. 12, no. 1, p. 527, 2012.
- [68] J. M. Loree, S. Kopetz, and K. P. S. Raghav, "Current companion diagnostics in advanced colorectal cancer; getting a bigger and better piece of the pie," *Journal of Gastrointestinal Oncology*, vol. 8, no. 1, pp. 199–212, 2017.
- [69] A. L. Reid, J. B. Freeman, M. Millward, M. Ziman, and E. S. Gray, "Detection of BRAF-V600E and V600K in melanoma circulating tumour cells by droplet digital PCR," *Clinical Biochemistry*, vol. 48, no. 15, pp. 999–1002, 2015.
- [70] Z.-X. Cheng, B. Sun, S. Wang et al., "Nuclear factor- κ B-dependent epithelial to mesenchymal transition induced by HIF-1 α activation in pancreatic cancer cells under hypoxic conditions," *PLoS One*, vol. 6, no. 8, Article ID e23752, 2011.
- [71] A. Nomura, K. Majumder, B. Giri et al., "Inhibition of NF- κ B pathway leads to deregulation of epithelial-mesenchymal transition and neural invasion in pancreatic cancer," *Laboratory Investigation*, vol. 96, no. 12, pp. 1268–1278, 2016.
- [72] D. Verzella, M. Fischietti, D. Capece et al., "Targeting the NF- κ B pathway in prostate cancer: a promising therapeutic approach?," *Current Drug Targets*, vol. 17, no. 3, pp. 311–320, 2016.
- [73] J. Staal and R. Beyaert, "Inflammation and NF- κ B signaling in prostate cancer: mechanisms and clinical implications," *Cells*, vol. 7, no. 9, p. 122, 2018.
- [74] J. Mariscal, M. Alonso-Nocelo, L. Muinelo-Romay et al., "Molecular profiling of circulating tumour cells identifies Notch1 as a principal regulator in advanced non-small cell lung cancer," *Scientific Reports*, vol. 6, p. 37820, 2016.
- [75] U.-G. Lo, R. Pong, D. Yang et al., "Ifny-induced IFIT5 promotes epithelial-to-mesenchymal transition in prostate cancer via miRNA processing," *Cancer Research*, vol. 79, no. 6, pp. 1098–1112, 2018.
- [76] H. Xiong, J. Hong, W. Du et al., "Roles of STAT3 and ZEB1 proteins in E-cadherin down-regulation and human colorectal cancer epithelial-mesenchymal transition," *Journal of Biological Chemistry*, vol. 287, no. 8, pp. 5819–5832, 2012.
- [77] M. Zhang, F. Miao, R. Huang et al., "RHBDD1 promotes colorectal cancer metastasis through the Wnt signaling pathway and its downstream target ZEB1," *Journal of Experimental & Clinical Cancer Research*, vol. 37, no. 1, p. 22, 2018.
- [78] M.-S. Lee, J. Lee, Y. M. Kim, and H. Lee, "The metastasis suppressor CD82/KAI1 represses the TGF- β 1 and Wnt signalings inducing epithelial-to-mesenchymal transition linked to invasiveness of prostate cancer cells," *The Prostate*, vol. 79, no. 12, pp. 1394–1405, 2019.
- [79] C.-J. Chen, C.-J. Yang, M.-S. Huang, and Y.-P. Liu, "Epithelial-type CD133+ stem-like lung cancer cells emerge higher drug resistance through MDFIC-mediated Wnt/ β -catenin signaling pathway," in *Proceedings of the AACR Annual Meeting 2017*, Washington, DC, USA, April 2017.
- [80] J. Yang, H. Xing, D. Lu et al., "Role of Jagged1/STAT 3 signalling in platinum-resistant ovarian cancer," *Journal of Cellular and Molecular Medicine*, vol. 23, no. 6, pp. 4005–4018, 2019.
- [81] M. Orzechowska, D. Jedroszka, R. Hamouz, and A. K. Bednarek, *PO-151 Notch Signalling Differentiates Disease-free Survival in Prostate Cancer Patients by Affecting the Epithelial-To-Mesenchymal Transition-Associated Processes*, BMJ Publishing Group Limited, London, UK, 2018.
- [82] M. L. Sprouse, T. Welte, D. Boral et al., "PMN-MDSCs enhance CTC metastatic properties through reciprocal interactions via ROS/Notch/Nodal signaling," *International Journal of Molecular Sciences*, vol. 20, no. 8, p. 1916, 2019.
- [83] L. J. Burton, O. Hawsawi, Q. Loyd et al., "Association of Epithelial Mesenchymal Transition with prostate and breast health disparities," *PLoS One*, vol. 13, no. 9, Article ID e0203855, 2018.
- [84] S. Figiel, C. Vasseur, F. Bruyere, F. Rozet, K. Maheo, and G. Fromont, "Clinical significance of epithelial-mesenchymal transition markers in prostate cancer," *Human Pathology*, vol. 61, pp. 26–32, 2017.
- [85] K. A. Cheaito, H. F. Bahmad, O. Hadadeh et al., "EMT markers in locally-advanced prostate cancer: predicting recurrence?," *Frontiers in Oncology*, vol. 9, p. 131, 2019.
- [86] P. Lyu, S.-D. Zhang, H.-F. Yuen et al., "Identification of TWIST-interacting genes in prostate cancer," *Science China Life Sciences*, vol. 60, no. 4, pp. 386–396, 2017.
- [87] A. E. Abdelrahman, S. A. Arafa, and R. A. Ahmed, "Prognostic value of twist-1, E-cadherin and EZH2 in prostate cancer: an immunohistochemical study," *Turkish Journal of Pathology*, vol. 1, no. 1, pp. 198–210, 2017.
- [88] K. Gravdal, O. J. Halvorsen, S. A. Haukaas, and L. A. Akslen, "A switch from E-cadherin to N-cadherin expression indicates epithelial to mesenchymal transition and is of strong and independent importance for the progress of prostate cancer," *Clinical Cancer Research*, vol. 13, no. 23, pp. 7003–7011, 2007.

- [89] P. Alonso-Magdalena, C. Brössner, A. Reiner et al., "A role for epithelial-mesenchymal transition in the etiology of benign prostatic hyperplasia," *Proceedings of the National Academy of Sciences*, vol. 106, no. 8, pp. 2859–2863, 2009.
- [90] H. M. Behnsawy, H. Miyake, K.-I. Harada, and M. Fujisawa, "Expression patterns of epithelial-mesenchymal transition markers in localized prostate cancer: significance in clinicopathological outcomes following radical prostatectomy," *BJU International*, vol. 111, no. 1, pp. 30–37, 2013.
- [91] H. Whiteland, S. Spencer-Harty, D. H. Thomas et al., "Putative prognostic epithelial-to-mesenchymal transition biomarkers for aggressive prostate cancer," *Experimental and Molecular Pathology*, vol. 95, no. 2, pp. 220–226, 2013.
- [92] V. Padmanaban, I. Krol, Y. Suhail et al., "E-cadherin is required for metastasis in multiple models of breast cancer," *Nature*, vol. 573, no. 7774, pp. 439–444, 2019.
- [93] I. U. Agoulnik, A. Vaid, M. Nakka et al., "Androgens modulate expression of transcription intermediary factor 2, an androgen receptor coactivator whose expression level correlates with early biochemical recurrence in prostate cancer," *Cancer Research*, vol. 66, no. 21, pp. 10594–10602, 2006.
- [94] Y. Kim, S. Alarcon, S. Lee et al., "Update on Hsp90 inhibitors in clinical trial," *Current Topics in Medicinal Chemistry*, vol. 9, no. 15, pp. 1479–1492, 2009.
- [95] A. A. Shafi, A. E. Yen, and N. L. Weigel, "Androgen receptors in hormone-dependent and castration-resistant prostate cancer," *Pharmacology & Therapeutics*, vol. 140, no. 3, pp. 223–238, 2013.
- [96] S. Koochekpour, "Androgen receptor signaling and mutations in prostate cancer," *Asian Journal of Andrology*, vol. 12, no. 5, pp. 639–657, 2010.
- [97] S. M. Dehm and D. J. Tindall, "Molecular regulation of androgen action in prostate cancer," *Journal of Cellular Biochemistry*, vol. 99, no. 2, pp. 333–344, 2006.
- [98] E. Jernberg, A. Bergh, and P. Wikström, "Clinical relevance of androgen receptor alterations in prostate cancer," *Endocrine Connections*, vol. 6, no. 8, pp. R146–R161, 2017.
- [99] N. Nadiminty, R. Tummala, C. Liu et al., "NF-B2/p52 induces resistance to enzalutamide in prostate cancer: role of androgen receptor and its variants," *Molecular Cancer Therapeutics*, vol. 12, no. 8, pp. 1629–1637, 2013.
- [100] E. A. Mostaghel, B. T. Marck, S. R. Plymate et al., "Resistance to CYP17A1 inhibition with abiraterone in castration-resistant prostate cancer: induction of steroidogenesis and androgen receptor splice variants," *Clinical Cancer Research*, vol. 17, no. 18, pp. 5913–5925, 2011.
- [101] R. Hu, T. A. Dunn, S. Wei et al., "Ligand-independent androgen receptor variants derived from splicing of cryptic exons signify hormone-refractory prostate cancer," *Cancer Research*, vol. 69, no. 1, pp. 16–22, 2009.
- [102] Z. Guo, X. Yang, F. Sun et al., "A novel androgen receptor splice variant is up-regulated during prostate cancer progression and promotes androgen depletion-resistant growth," *Cancer Research*, vol. 69, no. 6, pp. 2305–2313, 2009.
- [103] A. Abeshouse, J. Ahn, R. Akbani et al., "The molecular taxonomy of primary prostate cancer," *Cell*, vol. 163, no. 163, pp. 1011–1025, 2015.
- [104] C. Lu and J. Luo, "Decoding the androgen receptor splice variants," *Translational Andrology and Urology*, vol. 2, no. 3, p. 178, 2013.
- [105] Y. Li, S. C. Chan, L. J. Brand, T. H. Hwang, K. A. T. Silverstein, and S. M. Dehm, "Androgen receptor splice variants mediate enzalutamide resistance in castration-resistant prostate cancer cell lines," *Cancer Research*, vol. 73, no. 2, pp. 483–489, 2013.
- [106] B. Cao, G. Zhang, D. Xu et al., "Androgen receptor splice variants activating the full-length receptor in mediating resistance to androgen-directed therapy," *Oncotarget*, vol. 5, no. 6, p. 1646, 2014.
- [107] D. Xu, Y. Zhan, Y. Qi et al., "Androgen receptor splice variants dimerize to transactivate target genes," *Cancer Research*, vol. 75, no. 17, pp. 3663–3671, 2015.
- [108] Y. Qu, B. Dai, D. Ye et al., "Constitutively active AR-V7 plays an essential role in the development and progression of castration-resistant prostate cancer," *Scientific Reports*, vol. 5, p. 7654, 2015.
- [109] M.-L. Zhu and N. Kyprianou, "Role of androgens and the androgen receptor in epithelial-mesenchymal transition and invasion of prostate cancer cells," *The FASEB Journal*, vol. 24, no. 3, pp. 769–777, 2010.
- [110] Y. Sun, B.-E. Wang, K. G. Leong et al., "Androgen deprivation causes epithelial-mesenchymal transition in the prostate: implications for androgen-deprivation therapy," *Cancer Research*, vol. 72, no. 2, pp. 527–536, 2012.
- [111] G. J. Klarmann, E. M. Hurt, L. A. Mathews et al., "Invasive prostate cancer cells are tumor initiating cells that have a stem cell-like genomic signature," *Clinical & Experimental Metastasis*, vol. 26, no. 5, pp. 433–446, 2009.
- [112] D. Kong, S. Banerjee, A. Ahmad et al., "Epithelial to mesenchymal transition is mechanistically linked with stem cell signatures in prostate cancer cells," *PLoS One*, vol. 5, no. 8, Article ID e12445, 2010.
- [113] S. A. Mani, W. Guo, M.-J. Liao et al., "The epithelial-mesenchymal transition generates cells with properties of stem cells," *Cell*, vol. 133, no. 4, pp. 704–715, 2008.
- [114] M. Santisteban, J. M. Reiman, M. K. Asiedu et al., "Immune-induced epithelial to mesenchymal transition in vivo generates breast cancer stem cells," *Cancer Research*, vol. 69, no. 7, pp. 2887–2895, 2009.
- [115] X. Zhang, C. Morrissey, S. Sun et al., "Androgen receptor variants occur frequently in castration resistant prostate cancer metastases," *PLoS One*, vol. 6, no. 11, Article ID e27970, 2011.
- [116] P. A. Watson, Y. F. Chen, M. D. Balbas et al., "Constitutively active androgen receptor splice variants expressed in castration-resistant prostate cancer require full-length androgen receptor," *Proceedings of the National Academy of Sciences*, vol. 107, no. 39, pp. 16759–16765, 2010.
- [117] S. Sun, C. C. T. Sprenger, R. L. Vessella et al., "Castration resistance in human prostate cancer is conferred by a frequently occurring androgen receptor splice variant," *Journal of Clinical Investigation*, vol. 120, no. 8, pp. 2715–2730, 2010.
- [118] M. Marín-Aguilera, J. Codony-Servat, Ö. Reig et al., "Epithelial-to-mesenchymal transition mediates docetaxel resistance and high risk of relapse in prostate cancer," *Molecular Cancer Therapeutics*, vol. 13, no. 5, pp. 1270–1284, 2014.
- [119] X. Wang, M. K.-d. Julio, K. D. Economides et al., "A luminal epithelial stem cell that is a cell of origin for prostate cancer," *Nature*, vol. 461, no. 7263, pp. 495–500, 2009.
- [120] C.-L. Chen, D. Mahalingam, P. Osmulski et al., "Single-cell analysis of circulating tumor cells identifies cumulative expression patterns of EMT-related genes in metastatic prostate cancer," *The Prostate*, vol. 73, no. 8, pp. 813–826, 2013.

- [121] A. J. Armstrong, M. S. Marengo, S. Oltean et al., "Circulating tumor cells from patients with advanced prostate and breast cancer display both epithelial and mesenchymal markers," *Molecular Cancer Research*, vol. 9, no. 8, pp. 997–1007, 2011.
- [122] D. T. Miyamoto, R. J. Lee, S. L. Stott et al., "Androgen receptor signaling in circulating tumor cells as a marker of hormonally responsive prostate cancer," *Cancer Discovery*, vol. 2, no. 11, pp. 995–1003, 2012.
- [123] E. G. Bluemn, I. M. Coleman, J. M. Lucas et al., "Androgen receptor pathway-independent prostate cancer is sustained through FGF signaling," *Cancer Cell*, vol. 32, no. 4, pp. 474–489, 2017.
- [124] A. Komiya, K. Yasuda, A. Watanabe, Y. Fujiuchi, T. Tsuzuki, and H. Fuse, "The prognostic significance of loss of the androgen receptor and neuroendocrine differentiation in prostate biopsy specimens among castration-resistant prostate cancer patients," *Molecular and Clinical Oncology*, vol. 1, no. 2, pp. 257–262, 2013.
- [125] M. Crumbaker, L. Khoja, and A. Joshua, "AR signaling and the PI3K pathway in prostate cancer," *Cancers*, vol. 9, no. 12, p. 34, 2017.
- [126] T. Jamskishvili, D. M. Berman, A. E. Ross et al., "Clinical implications of PTEN loss in prostate cancer," *Nature Reviews Urology*, vol. 15, no. 4, pp. 222–234, 2018.
- [127] B. S. Carver, C. Chapinski, J. Wongvipat et al., "Reciprocal feedback regulation of PI3K and androgen receptor signaling in PTEN-deficient prostate cancer," *Cancer Cell*, vol. 19, no. 5, pp. 575–586, 2011.
- [128] D. J. Mulholland, L. M. Tran, Y. Li et al., "Cell autonomous role of PTEN in regulating castration-resistant prostate cancer growth," *Cancer Cell*, vol. 19, no. 6, pp. 792–804, 2011.
- [129] H. Murillo, H. Huang, L. J. Schmidt, D. I. Smith, and D. J. Tindall, "Role of PI3K signaling in survival and progression of LNCaP prostate cancer cells to the androgen refractory state," *Endocrinology*, vol. 142, no. 11, pp. 4795–4805, 2001.
- [130] S. H. Lee, D. Johnson, R. Luong, and Z. Sun, "Crosstalk between androgen and PI3K/AKT signaling pathways in prostate cancer cells," *Journal of Biological Chemistry*, vol. 290, no. 5, pp. 2759–2768, 2015.
- [131] K. Choucair, J. Ejdelman, F. Brimo, A. Aprikian, S. Chevalier, and J. Lapointe, "PTEN genomic deletion predicts prostate cancer recurrence and is associated with low AR expression and transcriptional activity," *BMC Cancer*, vol. 12, no. 1, p. 543, 2012.
- [132] S. Ha, R. Ruoff, N. Kahoud, T. F. Franke, and S. K. Logan, "Androgen receptor levels are upregulated by Akt in prostate cancer," *Endocrine Related Cancer*, vol. 18, no. 2, pp. 245–255, 2011.
- [133] K. Sircar, M. Yoshimoto, F. A. Monzon et al., "PTEN genomic deletion is associated with p-Akt and AR signalling in poorer outcome, hormone refractory prostate cancer," *The Journal of Pathology*, vol. 218, no. 4, pp. 505–513, 2009.
- [134] M. Kaarbø, Ø. L. Mikkelsen, L. Malerød et al., "PI3K-AKT-mTOR pathway is dominant over androgen receptor signaling in prostate cancer cells," *Analytical Cellular Pathology*, vol. 32, Article ID 290643, 17 pages, 2010.
- [135] Y. Wang, T. Romigh, X. He et al., "Differential regulation of PTEN expression by androgen receptor in prostate and breast cancers," *Oncogene*, vol. 30, no. 42, pp. 4327–4338, 2011.
- [136] D. J. Mulholland, N. Kobayashi, M. Ruscetti et al., "Pten loss and RAS/MAPK activation cooperate to promote EMT and metastasis initiated from prostate cancer stem/progenitor cells," *Cancer Research*, vol. 72, no. 7, pp. 1878–1889, 2012.
- [137] L.-B. Song, J. Li, W.-T. Liao et al., "The polycomb group protein Bmi-1 represses the tumor suppressor PTEN and induces epithelial-mesenchymal transition in human nasopharyngeal epithelial cells," *Journal of Clinical Investigation*, vol. 119, no. 12, pp. 3626–3636, 2009.
- [138] F. K. Collak, U. Demir, and F. Sagir, "YAP1 is involved in tumorigenic properties of prostate cancer cells," *Pathology & Oncology Research*, 2019.
- [139] W. Xu, Z. Yang, C. Xie et al., "PTEN lipid phosphatase inactivation links the hippo and PI3K/Akt pathways to induce gastric tumorigenesis," *Journal of Experimental & Clinical Cancer Research*, vol. 37, no. 1, p. 198, 2018.
- [140] B. A. Edgar, "From cell structure to transcription: hippo forges a new path," *Cell*, vol. 124, no. 2, pp. 267–273, 2006.
- [141] F.-X. Yu, B. Zhao, and K.-L. Guan, "Hippo pathway in organ size control, tissue homeostasis, and cancer," *Cell*, vol. 163, no. 4, pp. 811–828, 2015.
- [142] B. Zhao, X. Wei, W. Li et al., "Inactivation of YAP oncoprotein by the Hippo pathway is involved in cell contact inhibition and tissue growth control," *Genes & Development*, vol. 21, no. 21, pp. 2747–2761, 2007.
- [143] Q.-Y. Lei, H. Zhang, B. Zhao et al., "TAZ promotes cell proliferation and epithelial-mesenchymal transition and is inhibited by the hippo pathway," *Molecular and Cellular Biology*, vol. 28, no. 7, pp. 2426–2436, 2008.
- [144] D. Zhou, C. Conrad, F. Xia et al., "Mst1 and Mst2 maintain hepatocyte quiescence and suppress hepatocellular carcinoma development through inactivation of the Yap1 oncogene," *Cancer Cell*, vol. 16, no. 5, pp. 425–438, 2009.
- [145] B. Zhao, X. Ye, J. Yu et al., "TEAD mediates YAP-dependent gene induction and growth control," *Genes & Development*, vol. 22, no. 14, p. 000, 2008.
- [146] S. Wu, Y. Liu, Y. Zheng, J. Dong, and D. Pan, "The TEAD/TEF family protein Scalloped mediates transcriptional output of the Hippo growth-regulatory pathway," *Developmental Cell*, vol. 14, no. 3, pp. 388–398, 2008.
- [147] W. Kang, J. H. M. Tong, A. W. H. Chan et al., "Yes-associated protein 1 exhibits oncogenic property in gastric cancer and its nuclear accumulation associates with poor prognosis," *Clinical Cancer Research*, vol. 17, no. 8, pp. 2130–2139, 2011.
- [148] S. E. Lee, J. U. Lee, M. H. Lee et al., "RAF kinase inhibitor-independent constitutive activation of Yes-associated protein 1 promotes tumor progression in thyroid cancer," *Oncogenesis*, vol. 2, no. 7, p. e55, 2013.
- [149] C. M. Xu, W. W. Liu, C. J. Liu, C. Wen, H. F. Lu, and F. S. Wan, "Mst1 overexpression inhibited the growth of human non-small cell lung cancer in vitro and in vivo," *Cancer Gene Therapy*, vol. 20, no. 8, pp. 453–460, 2013.
- [150] W. M. Konsavage, S. L. Kyler, S. A. Rennoll, G. Jin, and G. S. Yochum, "Wnt/ β -catenin signaling regulates Yes-associated protein (YAP) gene expression in colorectal carcinoma cells," *Journal of Biological Chemistry*, vol. 287, no. 15, pp. 11730–11739, 2012.
- [151] L. Ge, M. Smal, W. Meng et al., "Yes-associated protein expression in head and neck squamous cell carcinoma nodal metastasis," *PLoS One*, vol. 6, no. 11, Article ID e27529, 2011.
- [152] A. A. Steinhardt, M. F. Gayyed, A. P. Klein et al., "Expression of Yes-associated protein in common solid tumors," *Human Pathology*, vol. 39, no. 11, pp. 1582–1589, 2008.
- [153] C. Wang, L. Zhang, Q. He et al., "Differences in Yes-associated protein and mRNA levels in regenerating liver and

- hepatocellular carcinoma,” *Molecular Medicine Reports*, vol. 5, no. 5, pp. 410–414, 2012.
- [154] N. Jiang, K. Hjorth-Jensen, O. Hekmat et al., “In vivo quantitative phosphoproteomic profiling identifies novel regulators of castration-resistant prostate cancer growth,” *Oncogene*, vol. 34, no. 21, pp. 2764–2776, 2015.
- [155] G. Kuser-Abali, A. Alptekin, M. Lewis, I. P. Garraway, and B. Cinar, “YAP1 and AR interactions contribute to the switch from androgen-dependent to castration-resistant growth in prostate cancer,” *Nature Communications*, vol. 6, p. 8126, 2015.
- [156] M. Overholtzer, J. Zhang, G. A. Smolen et al., “Transforming properties of YAP, a candidate oncogene on the chromosome 11q22 amplicon,” *Proceedings of the National Academy of Sciences*, vol. 103, no. 33, pp. 12405–12410, 2006.
- [157] R. Liu, S. Huang, Y. Lei et al., “FGF8 promotes colorectal cancer growth and metastasis by activating YAP1,” *Oncotarget*, vol. 6, no. 2, p. 935, 2015.
- [158] Q. Hu, C. Li, S. Wang et al., “LncRNAs-directed PTEN enzymatic switch governs epithelial-mesenchymal transition,” *Cell Research*, vol. 29, no. 4, pp. 286–304, 2019.
- [159] M. Yu, Y. Chen, X. Li et al., “YAP1 contributes to NSCLC invasion and migration by promoting Slug transcription via the transcription co-factor TEAD,” *Cell Death & Disease*, vol. 9, no. 5, p. 464, 2018.
- [160] Y. Tang, T. Feinberg, E. T. Keller, X.-Y. Li, and S. J. Weiss, “Snail/slugg binding interactions with YAP/TAZ control skeletal stem cell self-renewal and differentiation,” *Nature Cell Biology*, vol. 18, no. 9, pp. 917–929, 2016.
- [161] Y. Wang, J. Liu, X. Ying, P. C. Lin, and B. P. Zhou, “Twist-mediated epithelial-mesenchymal transition promotes breast tumor cell invasion via inhibition of hippo pathway,” *Scientific Reports*, vol. 6, p. 24606, 2016.
- [162] S. C. Wei, L. Fattet, J. H. Tsai et al., “Matrix stiffness drives epithelial-mesenchymal transition and tumour metastasis through a TWIST1-G3BP2 mechanotransduction pathway,” *Nature Cell Biology*, vol. 17, no. 5, pp. 678–688, 2015.
- [163] C. Morgan, S. A. Jenkins, H. G. Kynaston, and S. H. Doak, “The role of adhesion molecules as biomarkers for the aggressive prostate cancer phenotype,” *PLoS One*, vol. 8, no. 12, Article ID e81666, 2013.
- [164] A. J. Knights, A. P. Funnell, M. Crossley, and R. C. Pearson, “Holding tight: cell junctions and cancer spread,” *Trends in Cancer Research*, vol. 8, no. 8, pp. 61–69, 2012.
- [165] S. Tuomi, A. Mai, J. Nevo et al., “PKC regulation of an 5 integrin-ZO-1 complex controls lamellae formation in migrating cancer cells,” *Science Signaling*, vol. 2, no. 77, p. ra32, 2009.
- [166] K. S. M. Smalley, P. Brafford, N. K. Haass, J. M. Brandner, E. Brown, and M. Herlyn, “Up-regulated expression of zonula occludens protein-1 in human melanoma associates with N-cadherin and contributes to invasion and adhesion,” *The American Journal of Pathology*, vol. 166, no. 5, pp. 1541–1554, 2005.
- [167] B. Dekky, M. Ruff, D. Bonnier, V. Legagneux, and N. Th  ret, “Correction: proteomic screening identifies the zonula occludens protein ZO-1 as a new partner for ADAM12 in invadopodia-like structures,” *Oncotarget*, vol. 9, no. 87, p. 35795, 2018.
- [168] W. Lehmann, D. Mossmann, J. Kleemann et al., “ZEB1 turns into a transcriptional activator by interacting with YAP1 in aggressive cancer types,” *Nature Communications*, vol. 7, no. 1, p. 10498, 2016.
- [169] L. A. Selth, R. Das, S. L. Townley et al., “A ZEB1-miR-375-YAP1 pathway regulates epithelial plasticity in prostate cancer,” *Oncogene*, vol. 36, no. 1, pp. 24–34, 2017.
- [170] H. Chen, Q. Chen, and Q. Luo, “Expression of netrin-1 by hypoxia contributes to the invasion and migration of prostate carcinoma cells by regulating YAP activity,” *Experimental Cell Research*, vol. 349, no. 2, pp. 302–309, 2016.
- [171] J. Park, D.-H. Kim, S. R. Shah et al., “Switch-like enhancement of epithelial-mesenchymal transition by YAP through feedback regulation of WTI and Rho-family GTPases,” *Nature Communications*, vol. 10, no. 1, p. 2797, 2019.
- [172] K. Tumaneng, K. Schlegelmilch, R. C. Russell et al., “YAP mediates crosstalk between the Hippo and PI(3)K-TOR pathways by suppressing PTEN via miR-29,” *Nature Cell Biology*, vol. 14, no. 12, pp. 1322–1329, 2012.
- [173] H.-K. Lin, Y.-C. Hu, D. K. Lee, and C. Chang, “Regulation of androgen receptor signaling by PTEN (phosphatase and tensin homolog deleted on chromosome 10) tumor suppressor through distinct mechanisms in prostate cancer cells,” *Molecular Endocrinology*, vol. 18, no. 10, pp. 2409–2423, 2004.
- [174] T. M. Becker, N. J. Caixeiro, S. H. Lim et al., “New frontiers in circulating tumor cell analysis: a reference guide for biomolecular profiling toward translational clinical use,” *International Journal of Cancer*, vol. 134, no. 11, pp. 2523–2533, 2014.
- [175] M. Thalgott, B. Rack, T. Maurer et al., “Detection of circulating tumor cells in different stages of prostate cancer,” *Journal of Cancer Research and Clinical Oncology*, vol. 139, no. 5, pp. 755–763, 2013.
- [176] J. W. Po, A. Roohullah, D. Lynch et al., “Improved ovarian cancer EMT-CTC isolation by immunomagnetic targeting of epithelial EpCAM and mesenchymal N-cadherin,” *Journal of Circulating Biomarkers*, vol. 7, 2018.
- [177] H. Polioudaki, S. Agelaki, R. Chiotak et al., “Variable expression levels of keratin and vimentin reveal differential EMT status of circulating tumor cells and correlation with clinical characteristics and outcome of patients with metastatic breast cancer,” *BMC Cancer*, vol. 15, p. 399, 2015.
- [178] Y. Horimoto, E. Tokuda, F. Murakami et al., “Analysis of circulating tumour cell and the epithelial mesenchymal transition (EMT) status during eribulin-based treatment in 22 patients with metastatic breast cancer: a pilot study,” *Journal of Translational Medicine*, vol. 16, no. 1, p. 287, 2018.
- [179] X.-H. Zhao, Z.-R. Wang, C.-L. Chen et al., “Molecular detection of epithelial-mesenchymal transition markers in circulating tumor cells from pancreatic cancer patients: potential role in clinical practice,” *World Journal of Gastroenterology*, vol. 25, no. 1, pp. 138–150, 2019.
- [180] J. W. Po, D. Lynch, P. de Souza, and T. M. Becker, “Importance and detection of epithelial-to-mesenchymal transition (EMT) phenotype in CTCs,” in *Tumor Metastasis*, pp. 241–256, InTechOpen, London, UK, 2016.
- [181] L.-N. Qi, B.-D. Xiang, F.-X. Wu et al., “Circulating tumor cells undergoing EMT provide a metric for diagnosis and prognosis of patients with hepatocellular carcinoma,” *Cancer Research*, vol. 78, no. 16, pp. 4731–4744, 2018.
- [182] A. J. Armstrong, S. Halabi, J. Luo et al., “Prospective multicenter validation of androgen receptor splice variant 7 and hormone therapy resistance in high-risk castration-resistant prostate cancer: the PROPHECY study,” *Journal of Clinical Oncology*, vol. 37, no. 13, pp. 1120–1129, 2019.

- [183] M. A. Leversha, J. Han, Z. Asgari et al., "Fluorescence in situ hybridization analysis of circulating tumor cells in metastatic prostate cancer," *Clinical Cancer Research*, vol. 15, no. 6, pp. 2091–2097, 2009.
- [184] J. Steinestel, M. Luedeke, A. Arndt et al., "Detecting predictive androgen receptor modifications in circulating prostate cancer cells," *Oncotarget*, vol. 10, no. 41, pp. 4213–4223, 2019.
- [185] E. E. Reyes, D. J. VanderWeele, M. Isikbay et al., "Quantitative characterization of androgen receptor protein expression and cellular localization in circulating tumor cells from patients with metastatic castration-resistant prostate cancer," *Journal of Translational Medicine*, vol. 12, no. 1, p. 313, 2014.
- [186] M. S. Darshan, M. S. Loftus, M. Thadani-Mulero et al., "Taxane-induced blockade to nuclear accumulation of the androgen receptor predicts clinical responses in metastatic prostate cancer," *Cancer Research*, vol. 71, no. 18, pp. 6019–6029, 2011.
- [187] E. S. Antonarakis, C. Lu, H. Wang et al., "AR-V7 and resistance to enzalutamide and abiraterone in prostate cancer," *New England Journal of Medicine*, vol. 371, no. 11, pp. 1028–1038, 2014.
- [188] A. Sharp, I. Coleman, W. Yuan et al., "Androgen receptor splice variant-7 expression emerges with castration resistance in prostate cancer," *The Journal of Clinical Investigation*, vol. 129, no. 129, pp. 192–208, 2019.
- [189] M. Nimir, Y. Ma, S. A. Jeffreys et al., "Detection of AR-V7 in liquid biopsies of castrate resistant prostate cancer patients: a comparison of AR-V7 analysis in circulating tumor cells, circulating tumor RNA and exosomes," *Cells*, vol. 8, no. 7, p. 688, 2019.
- [190] A. Luk, Y. Ma, P. Ding et al., "CTC-mRNA (AR-V7) analysis from blood samples-impact of blood collection tube and storage time," *International Journal of Molecular Sciences*, vol. 18, no. 5, p. 1047, 2017.
- [191] H. I. Scher, R. P. Graf, N. A. Schreiber et al., "Nuclear-specific AR-V7 protein localization is necessary to guide treatment selection in metastatic castration-resistant prostate cancer," *European Urology*, vol. 71, no. 6, pp. 874–882, 2017.
- [192] H. I. Scher, D. Lu, N. A. Schreiber et al., "Association of AR-V7 on circulating tumor cells as a treatment-specific biomarker with outcomes and survival in castration-resistant prostate cancer," *JAMA Oncology*, vol. 2, no. 11, pp. 1441–1449, 2016.
- [193] D. Worroll, G. Galletti, A. Gjyrezi et al., "Androgen receptor nuclear localization correlates with AR-V7 mRNA expression in circulating tumor cells (CTCs) from metastatic castration resistance prostate cancer patients," *Physical Biology*, vol. 16, no. 3, Article ID 036003, 2019.
- [194] G. Attard, J. F. Swennenhuis, D. Olmos et al., "Characterization of ERG, AR and PTEN gene status in circulating tumor cells from patients with castration-resistant prostate cancer," *Cancer Research*, vol. 69, no. 7, pp. 2912–2918, 2009.
- [195] M. Maas, M. Hegemann, S. Rausch, J. Bedke, A. Stenzl, and T. Todenhöfer, "Circulating tumor cells and their role in prostate cancer," *Asian Journal of Andrology*, vol. 21, no. 1, p. 24, 2019.
- [196] M. Bredemeier, S. Kasimir-Bauer, H.-C. Kolberg et al., "Comparison of the PI3KCA pathway in circulating tumor cells and corresponding tumor tissue of patients with metastatic breast cancer," *Molecular Medicine Reports*, vol. 15, no. 5, pp. 2957–2968, 2017.
- [197] Y. Gao, X. Ni, H. Guo et al., "Single-cell sequencing deciphers a convergent evolution of copy number alterations from primary to circulating tumor cells," *Genome Research*, vol. 27, no. 8, pp. 1312–1322, 2017.
- [198] J. Zhang, K. Chen, and Z. Fan, "Circulating tumor cell isolation and analysis," in *Advances in Clinical Chemistry*, pp. 1–31, Elsevier, Amsterdam, The Netherlands, 2016.
- [199] D. T. Ting, B. S. Wittner, M. Ligorio et al., "Single-cell RNA sequencing identifies extracellular matrix gene expression by pancreatic circulating tumor cells," *Cell Reports*, vol. 8, no. 6, pp. 1905–1918, 2014.
- [200] S. Sharma, R. Zhuang, M. Long et al., "Circulating tumor cell isolation, culture, and downstream molecular analysis," *Biotechnology Advances*, vol. 36, no. 4, pp. 1063–1078, 2018.
- [201] G. Kallergi, D. Mavroudis, V. Georgoulas, and C. Stourmaras, "Phosphorylation of FAK, PI-3K, and impaired actin organization in CK-positive micrometastatic breast cancer cells," *Molecular Medicine*, vol. 13, no. 1–2, pp. 79–88, 2007.
- [202] I. Tinhofer, T. Hristozova, C. Stromberger, U. KeilhoIz, and V. Budach, "Monitoring of circulating tumor cells and their expression of EGFR/phospho-EGFR during combined radiotherapy regimens in locally advanced squamous cell carcinoma of the head and neck," *International Journal of Radiation Oncology*Biophysics*, vol. 83, no. 5, pp. e685–e690, 2012.
- [203] K. Yokoi, D. Hawke, C. J. Oborn et al., "Identification and validation of SRC and phospho-SRC family proteins in circulating mononuclear cells as novel biomarkers for pancreatic cancer," *Translational Oncology*, vol. 4, no. 2, pp. 83–91, 2011.
- [204] S. J. Shin, J. W. Hwang, J. B. Ahn, S. Y. Rha, J. K. Roh, and H. C. Chung, "Circulating vascular endothelial growth factor receptor 2/pAkt-positive cells as a functional pharmacodynamic marker in metastatic colorectal cancers treated with antiangiogenic agent," *Investigational New Drugs*, vol. 31, no. 1, pp. 1–13, 2013.



Prognostic and Predictive Value of Liquid Biopsy-Derived Androgen Receptor Variant 7 (AR-V7) in Prostate Cancer: A Systematic Review and Meta-Analysis

Tanzila Khan^{1,2,3}, Therese M. Becker^{2,3,4}, Kieran F. Scott^{1,2}, Joseph Descallar^{4,5}, Paul de Souza^{1,2,6}, Wei Chua^{1,2,4,7} and Yafeng Ma^{2,3,4*}

¹ School of Medicine, Western Sydney University, Campbelltown, NSW, Australia, ² Medical Oncology, Ingham Institute of Applied Medical Research, Liverpool, NSW, Australia, ³ Centre of Circulating Tumour Cell Diagnostics & Research, Ingham Institute of Applied Medical Research, Liverpool, NSW, Australia, ⁴ South West Sydney Clinical School, University of New South Wales, Liverpool Hospital, Liverpool, NSW, Australia, ⁵ Ingham Institute of Applied Medical Research, Liverpool, NSW, Australia, ⁶ School of Medicine, University of New South Wales, Kensington, NSW, Australia, ⁷ Medical Oncology, Liverpool Hospital, Liverpool, NSW, Australia

OPEN ACCESS

Edited by:

Riccardo Tellini,
Careggi University Hospital, Italy

Reviewed by:

Hideki Maeda,
Meiji Pharmaceutical University, Japan
Aasems Jacob,
Pikeville Medical Center, United States
Haoran Liu,
Stanford University, United States
Carlo Cattrini,
Azienda Ospedaliero Universitaria
Maggiore della Carità, Italy

*Correspondence:

Yafeng Ma
yafeng.ma@unsw.edu.au

Specialty section:

This article was submitted to
Genitourinary Oncology,
a section of the journal
Frontiers in Oncology

Received: 02 February 2022

Accepted: 21 February 2022

Published: 18 March 2022

Citation:

Khan T, Becker TM, Scott KF, Descallar J, de Souza P, Chua W and Ma Y (2022) Prognostic and Predictive Value of Liquid Biopsy-Derived Androgen Receptor Variant 7 (AR-V7) in Prostate Cancer: A Systematic Review and Meta-Analysis. *Front. Oncol.* 12:868031. doi: 10.3389/fonc.2022.868031

In advanced prostate cancer, access to recent diagnostic tissue samples is restricted and this affects the analysis of the association of evolving biomarkers such as AR-V7 with metastatic castrate resistance. Liquid biopsies are emerging as alternative analytes. To clarify clinical value of AR-V7 detection from liquid biopsies, here we performed a meta-analysis on the prognostic and predictive value of androgen receptor variant 7 (AR-V7) detected from liquid biopsy for patients with prostate cancer (PC), three databases, the Embase, Medline, and Scopus were searched up to September 2021. A total of 37 studies were included. The effects of liquid biopsy AR-V7 status on overall survival (OS), radiographic progression-free survival (PFS), and prostate-specific antigen (PSA)-PFS were calculated with RevMan 5.3 software. AR-V7 positivity detected in liquid biopsy significantly associates with worse OS, PFS, and PSA-PFS ($P < 0.00001$). A subgroup analysis of patients treated with androgen receptor signaling inhibitors (ARSi such as abiraterone and enzalutamide) showed a significant association of AR-V7 positivity with poorer OS, PFS, and PSA-PFS. A statistically significant association with OS was also found in taxane-treated patients ($P = 0.04$), but not for PFS ($P = 0.21$) or PSA-PFS ($P = 0.93$). For AR-V7 positive patients, taxane treatment has better OS outcomes than ARSi ($P = 0.01$). Study quality, publication bias and sensitivity analysis were integrated in the assessment. Our data show that liquid biopsy AR-V7 is a clinically useful biomarker that is associated with poor outcomes of ARSi-treated castrate resistant PC (CRPC) patients and thus has the potential to guide patient management and also to stratify patients for clinical trials. More studies on chemotherapy-treated patients are warranted.

Systematic Review Registration: PROSPERO, CRD42021239353.

Keywords: prostate cancer, AR-V7, liquid biopsy, prognosis, meta-analysis

INTRODUCTION

Prostate cancer (PC) is one of the most common male cancers. The androgen receptor (AR) pathway is critical in maintaining normal prostate tissue homeostasis, cancer development and progression (1). Therapies for PC include surgery and radiation for localized or early-stage cancer, while for advanced or metastatic PC, androgen deprivation therapy (ADT), with or without chemotherapy is the standard of care. However, patients eventually develop castration resistant PC (CRPC). Recent incorporation of novel androgen receptor signaling inhibitors (ARSi, e.g., enzalutamide (Enz), abiraterone (Abi)) and taxane-based chemotherapy have improved outcomes of CRPC patients over the past two decades (2).

Biomarkers detected in liquid biopsy (such as circulating tumor cells and cell-free tumor DNA) demonstrate good concordance with biomarkers detected in conventional tissue biopsy, especially for metastatic CRPC (3). Liquid biopsy is emerging as a reliable source of biological data for biomarker discovery, especially in advanced PC when tissue biopsy is often not obtainable or can be used longitudinally to monitor tumor evolution and changes in biomarker characteristics. In CRPC, one of most promising prognostic markers is the constitutively active AR splice variant 7 (AR-V7). AR-V7 lacks the ligand binding domain and substitutes for functional AR even in the absence of the ligand testosterone, and differentially regulates AR-dependent gene expression (4). Thus far, current literature suggests that expression or nuclear subcellular location of AR-V7 is associated with overall survival (OS) and progression free survival (PFS) when found in tissue biopsy (5) or liquid biopsy [whole blood (6, 7), circulating tumor cells (8), and exosomes (9, 10)]. However, the study cohorts are variable in patient numbers and stages and also treatment options; the clinical relevance of AR-V7, especially liquid biopsy detectable AR-V7, is still not clear or widely accepted and need further investigation.

To clarify the clinical utility of AR-V7 detection from liquid biopsies, we undertook a comprehensive systematic review and meta-analysis to evaluate the available data from the clinical studies published up to September 2021. Prognostic and predictive value of liquid biopsy derived AR-V7 data in PC patients were evaluated from 37 studies that met the inclusion criteria.

METHODS

Study Design and Literature Searches

This study was conducted according to preferred reporting items for systematic reviews and meta-analysis (PRISMA) (11). The protocol has been registered on PROSPERO (CRD42021239353). Detailed literature searches up to September 10, 2021 in the Embase, PubMed, and Scopus databases were conducted thoroughly to check the prognostic role of AR-V7 in PC. The used search terms were (~Androgen Receptor Variant 7) OR (~ARV7) OR (~AR3) AND (~"prostate cancer"). The searched study citations were imported to EndNote (version X9) for duplicate checking and title and/or abstract screening and then

uploaded to the online systematic review research tool Rayyan (<https://www.rayyan.ai/>) for independent systematic review according to selection criteria. Two independent, blinded observers (TK and YM) reviewed all candidate articles. Any discrepancies in the article selections were resolved by discussion.

Selection Criteria

Pre-set exclusion criteria of this study were: (1) publication type: review articles, letters, comments, questionnaires, conference papers, corrections, reply to editor, case reports, book chapters, abstracts only, research highlights, summaries; (2) non-human studies (animal or cell line study); (3) non-prostate cancer; (4) AR-V7 data are not derived from human; (5) survival data not related to AR-V7 or with insufficient data to calculate the hazard ratios (HRs) and their 95% CIs, or the Kaplan–Meier (K–M) curve unable to calculate HRs and 95% CI parameters. Finally, studies were only included when they met the following criteria: (1) AR-V7 assayed in liquid biopsies (whole blood, circulating tumor cells, PBMC, plasma, exosome); (2) A reported relationship between AR-V7 and prognostic/predictive indicators, namely, OS, PFS, and PSA-PFS; (3) patient cohorts with $n > 25$, and (4) English language only.

Data Extraction and Quality Assessment

This study focuses on the prognostic value of AR-V7 detected from liquid biopsy and its predictive value for ARSi and chemotherapy. According to a pre-designed table, the items of data extraction included the last name of the first author, publication year, study country, number of patients included, age of patient, sample resource (processing method) and AR-V7 detection method, type of therapies, endpoints of oncological outcomes, HRs and 95% CIs (from univariate or multivariate Cox analysis), follow-up durations and definitions of OS, PFS, and PSA-PFS (**Supplementary Table 1**). When HRs and 95% CIs were not presented in the study, an Engauge Digitizer (version 12.1) was used to digitalize the K–M survival curve to re-calculate HRs and 95% CI as described previously (12). Data was extracted by two authors (TK and YM) independently and any inconsistencies were resolved by discussion. Notably, when several publications were retrieved reporting the same trial or patient cohort or from same author(s), study question and data from this publication were discussed by two authors (TK and YM) and uniqueness of the included data was ensured.

The adapted Newcastle–Ottawa Scale (NOS) scales for cohort study (13) were used to evaluate the quality of enrolled studies, which embraced three aspects, namely, patient selection, comparability, and assessment of outcome with a total score of 9. In addition, the quality of statistical evaluation was assessed to give a maximal score of 1 as described in **Supplementary Table 2**; a score of 7 or more is considered as high-quality and a score of 6 or less is considered as low quality.

Statistical Analysis

Pooled HR and 95% CI were used to evaluate the prognostic and predictive value of AR-V7 presence or high expression (in some studies, authors set a threshold to discriminate high or low expression level) on the patient survival parameters (OS, PFS,

PFA-PFS) in Review Manager 5.3 software (RevMan v.5.3, Denmark). The Cochran Q and I^2 statistical methods were applied to evaluate the heterogeneity among included studies and a random effects model was used for data consolidation. If the heterogeneity was very high, only a descriptive score was given. Further subgroup analysis based on patient treatment was also conducted. The inverted funnel plots with Egger's test were used to analyze potential publication bias with R software. A sensitivity analysis was carried out to assess the influence of each individual study on the pooled results by sequentially excluding each study. A two-tailed p-value <0.05 was regarded as statistically significant.

RESULTS

Search Results, Study and Patient Characteristics

The flowchart outlining the results of the literature search and application of the strategic inclusion and exclusion criteria is presented in **Figure 1**. A total of 1,180 relevant articles were identified in initial database searches (Embase: 321, Medline: 537, Scopus: 322). After screening research title and abstract to remove duplicates (n = 410) and excluding the non-relevant studies based on publication type (n = 353), non-human studies (n = 193), non-prostate cancer (n = 5) and foreign language (n = 3) followed by a review of full text for eligibility, 37 articles were identified based on inclusion criteria 'human data', 'AR-V7', 'liquid biopsy', and 'survival'. Although we initially only searched quite a broad terminology 'prostate cancer', all 37 studies investigated CRPC (n = 4) or metastatic CRPC (mCRPC) (n = 33) as defined in the reports (**Supplementary Table 1**). Baseline characteristics of all eligible articles are listed in **Table 1**. All articles were published from 2014 to 2021 and included studies from Europe (46%), America and Canada (46%), and Asia-Pacific (8%). Liquid biopsy AR-V7 was detected from CTC (n = 28), PBMC (n = 2), whole blood (n = 4) or exosomes (n = 3). The patient cohort size ranged from 26 to 202 and the median or mean patient age ranged from 56 to 78. CTC enrichment methods included (modified) AdnaTest[®] (Qiagen) (n = 13), Oncoquick[®] (Greiner Bio-One GmbH) (n = 1), red blood cell (RBC) lysis (n = 3), and immunomagnetic beads-based methods (such as CellSearch[®] or IsoFlux[®], dynabeads) (n = 9). The method of AR-V7 detection was primarily by PCR (quantitative PCR and droplet digital PCR, 92%). Endpoint of patient outcomes include OS (n = 30), PFS (n = 28) and PSA-PFS (n = 10) (**Table 1**).

Thirty studies including 976 AR-V7 positive (or high level, as defined by authors) and 2,056 AR-V7 negative (or low level) patients were used for OS comparison, while 28 studies including 697 AR-V7 positive and 1,553 AR-V7 negative patients were used for PFS analysis and 10 studies including 216 AR-V7 positive and 425 AR-V7 negative patients for PSA-PFS analysis. Most patients in the cohort of studies were treated with ARSi (either enzalutamide, abiraterone, or not specified) or taxane-based chemotherapy. Some reports included miscellaneous treatments [such as Bipolar Androgen-based therapy (32)]. Overall AR-V7 positive patients had significantly worse OS (HR 3.36, 95% CI 2.56–4.41,

P <0.00001), PFS (HR 2.96, 95% CI 2.20–3.98, P <0.00001) and PSA-PFS (HR 4.34, 95% CI 2.15–8.76, P <0.00001) than AR-V7 negative patients. Due to significant study heterogeneity ($I^2 \geq 80\%$), random effects model was applied to calculate HR value and 95% CI for all survival parameters.

Predictive Value of AR-V7 for ARSi-Treatment

AR-V7 positive patients treated with ARSi (enzalutamide or abiraterone) had significant poorer OS (HR 4.34, 95% CI 3.00–6.28, P <0.00001), PFS (HR 2.89, 95% CI 2.15–3.87, P <0.00001) and PSA-PFS (HR 4.69, 95% CI 2.50–8.82, P <0.0001) compared with AR-V7 negative patients (**Figures 2–4**). When analyzed based on specific treatment, compared to negative patients, AR-V7 positive patients also had significant worse OS (Enz: HR 2.93, 95% CI 1.71–5.01, P <0.0001; Abi: HR 6.59, 95% CI 2.18–19.94, P = 0.0008, respectively) (**Figure 2**), PFS (Enz: HR 4.38, 95% CI 2.44–7.84, P <0.0001; Abi: HR 6.88, 95% CI 1.99–23.73, P = 0.002, respectively) (**Figure 3**) and PSA-PFS (Enz: HR 7.40, 95% CI 2.66–20.60, one study, P = 0.0008; Abi: HR 11.39, 95% CI 4.53–28.67, two studies, P <0.00001, respectively) (**Figure 4**).

Chemotherapy-Treated Patients and Outcome Association With AR-V7

In the subgroup analysis of the patients treated with taxane-based chemotherapy, the association of AR-V7 positivity with worse OS was observed (HR 1.70, 95% CI 1.03–2.81, P = 0.04) (**Figure 2**), but no conclusive association between AR-V7 positive status and worse PFS and PSA-PFS were apparent, likely due to inadequate power (PFS: HR 1.81, 95% CI 0.71–4.61, P = 0.21, **Figure 3**; PSA-PFS: HR 0.93, 95% CI 0.21–4.22, P = 0.93, **Figure 4**). It is to be emphasised that data is only derived from two studies and a total of 129 patients (**Figure 4**).

AR-V7 Effect on Non-Defined (Miscellaneous) Treatments

For the studies in which the authors did not clarify treatments and were unable to be classified as either ARSi or taxane chemotherapy, AR-V7 presence is associated with worse OS (HR 3.47, 95% CI 1.85–6.49, P = 0.0001, 5 studies) and PFS (3 studies, HR 1.68, 95% CI 1.03–2.76, P = 0.04) (**Figures 2, 3**).

ARSi vs. Chemotherapy in AR-V7 Positive or Negative Patients

Four studies compared treatment response in AR-V7 positive or negative patients. Taxane treatment is linked to superior OS (HR 0.54, 95% CI 0.34–0.87, P = 0.01) in patients positive for AR-V7, compared to ARSi (**Figure 5A**). In contrast, for AR-V7 negative patients, OS in taxane or ARSi treated patients is not significantly different (HR 1.17, 95% CI 0.71–1.92, P = 0.54) (**Figure 5B**).

Quality Assessment, Publication Bias and Sensitivity Analysis

Thirty five articles were assessed as high-quality studies while 2 were deemed low quality studies (**Table 1** and **Supplementary Table 2**). Overall, the average quality of studies is 8.5. Publication

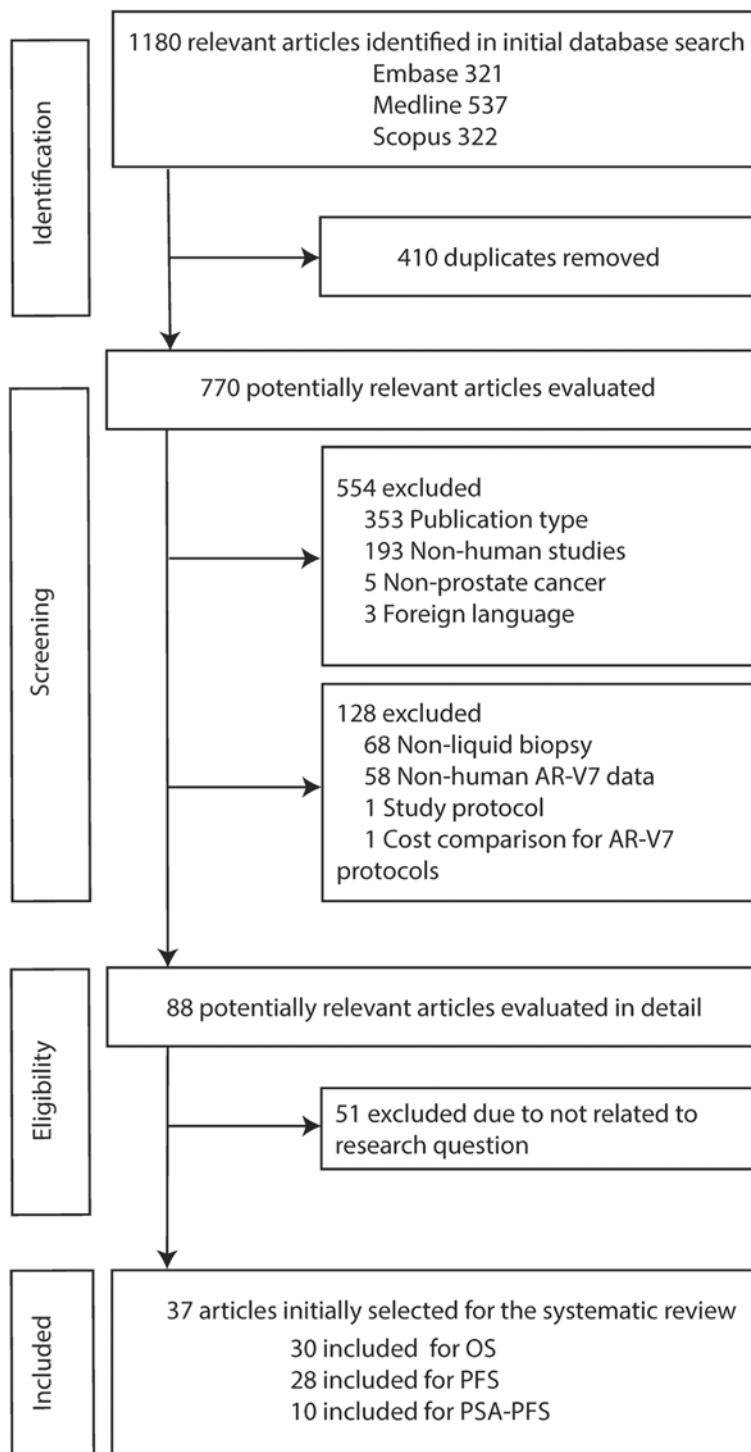


FIGURE 1 | Flow chart of literature search and study selection.

biases were evaluated for subgroups with more than 10 publications; no publication bias was observed for OS (Egger's test $P = 0.9925$, 15 publications, **Supplementary Figure 1A**) whereas publication bias was observed for PFS (Egger's test $P =$

0.0411 , 17 publications, **Supplementary Figure 1B**) in ARSi-treated subgroups. Sensitivity analyses were performed on the subgroups of more than 6 studies and the results were relatively stable except for overall survival in chemotherapy-treated group,

TABLE 1 | The basic characteristics of eligible studies.

Study	Year, country	Study type	Patients	Age	Resource, method	Treatment	Endpoint outcome	Follow up (month)	NOS score
Antonarakis et al. (14)	2015 US	Pros	37 CTC+	67 (46–82) ^b	CTCs (mAdna), qRT-PCR	Taxane	OS, PFS, PSA-PFS	7.7 (0.7– 19.0) ^b	10
Antonarakis et al. (15)	2017 US	Pros	53 CTC–, 113 CTC+/AR-V7–, 36 CTC+/AR-V7+	70 71 70 ^a	CTCs (mAdna), qRT-PCR	Abi/Enz	OS, PFS, PSA-PFS	CTC–:15.0 CTC+/ ARV7–: 21.7 CTC+/ ARV7+: 14.6 ^a	9
Antonarakis et al. (16)	2014 US	Pros	Enz:31, Abi: 31	Enz:70 (56–84), Abi:69 (48–79) ^b	CTCs (mAdna), qRT-PCR	Abi/Enz	OS, r PFS, PSA-PFS	Enz: 5.4 (1.4–9.9) Abi: 4.6 (0.9–8.2) ^b	9
Armstrong et al. (17)	2019 US	Pros, blinded, multi- center	118	73 (45–92) ^b	CTCs (Adna, CellSearch), qRT-PCR	Abi/Enz	OS, PFS	19.6 ^a	10
Armstrong et al. (18)	2020 US	Pros, blinded	ARSi:118 Taxane: 51	72 (48–82) 72 (45–87) ^b	CTCs (Adna, CellSearch), qRT- PCR	ARSi, Taxane	OS, PFS	ARSi:35 Tax:23 ^a	9
Belderbos et al. (19)	2019 Netherlands	Pros	94	69 (65–75) ^c	CTCs (CellSearch), qRT-PCR	Cabazitaxel ARSi	OS	NA	9
Catrinini et al. (20)	2019 Italy	Pros	39	72 (56–84) ^b	CTCs (Adna), qRT- PCR	ARSi, Taxane	OS	NA	8
Chung et al. (21)	2019 US	Pros	37	72 (67–79) ^c	CTCs (Dynabeads), qRT- PCR	Abi/Enz	OS, rPFS, PSA-PFS	11.4 (4.7– 21.3) ^c	7
De Laere et al. (22)	2019 Belgium	Pros multi- center	168	76 ± 7.7 ^e	CTCs (CellSearch), RNA-seq	Abi/Enz	OS, PFS	12.4 (7– 17.3) ^c	10
Del Re et al. (23)	2017 Italy	Pros	36	66 (51–81) ^b	Plasma exosomes (exoRNeasy), ddPCR	ARSi	OS, PFS	9 (2.0– 31.0) ^b	8
Del Re et al. (9)	2021 Italy	Retros	84	78 (47–91) ^b	Plasma exosomes (exoRNeasy), ddPCR	ARSi	OS, PFS	NA	9
Del Re et al. (10)	2019 Italy	Retros	73	NA	Plasma exosomes (exoRNeasy), ddPCR	Abi/Enz	OS, PFS	NA	7
Erb et al. (24)	2020 Germany	Pros	26	74.3 ± 9 ^a	CTCs (OncoQuick), IHC	ARSi, Taxane	PFS	NA	6
Graf et al. (25)	2020 US	Pros, cross- sectional	193	69 (62.5–75) ^c	CTCs (RBC lysis), IF	ARSi, Taxane	OS	28.4 (24.4– 33.0) ^c	9
Gupta et al. (26)	2019 US	Pros	ARSi:120 Radium:20	ARSi:73 (45–92) Radium:72 (54–86) ^b	CTCs (Adna, CellSearch), qRT- PCR and Epic assay	Abi/Enz, Radium	PFS	NA	9
Joncas et al. (27)	2019 Canada	Pros	35	75 (67,79) ^c	EVs (UC, miRNeasy), ddPCR	ARSi, Taxane	OS, PFS	27 (16,33) ^c	8
Kwan et al. (28)	2019 Australia	Pros	115	72 (46–91) ^b	WB, qRT-PCR	ARSi, Taxane	OS	15.5 (1.4– 29) ^b	10
Lorenzo et al. (29)	2021 Italy	Pros, multi- center	53 (45 data only)	72.1 (54–86) ^b	CTCs, (Flow cytometry)	Enz	OS, rPFS	27 ^a	10
Maillet et al. (30)	2019 France	Pros	41	73 ^a	CTCs (AdnaTest), qRT-PCR	ARSi	OS, rPFS, PSA-PFS	31 ARSi treated patients: 10.5 ^a	8
Marin et al. (31)	2020 Spain	Pros	136	ARSi:70.2 (53.3–93.3)	PBMC and CTCs (IsoFlux) qRT-PCR	Abi/Enz, Taxane	OS, rPFS, PSA-PFS	ARSi:14.9 (1.5–57.9) Tax:13.8	10

(Continued)

TABLE 1 | Continued

Study	Year, country	Study type	Patients	Age	Resource, method	Treatment	Endpoint outcome	Follow up (month)	NOS score
Markowski et al. (32)	2021 US	Multicohort phase II	Post-Abi: 29, Post-Enz: 30	Tax: 62.8 (32.8–79.4) ^b Post-Abi: 71 (49–85) Post-Enz: 74 (50–89) ^b	CTCs (Adna), qRT-PCR	BAT, ARSi	rPFS	(1.37– 82.27) ^a NA	7
Miyamoto et al. (33)	2018 US	Pros	27	67 ^d	CTCs (CTC-iChip), ddPCR	Abi	OS, rPFS	13.0 ^a	8
Okegawa et al. (34)	2018 Japan	Retros	49 CTC–, 23 CTC+/AR-V7–, 26 CTC+/AR-V7+	69 71 72 ^d	CTCs (on-chip FC), PCR	Abi/Enz	OS, rPFS, PSA-PFS	20.7 (3.0– 37.0) ^b	9
Onstenk et al. (35)	2015 Netherlands	Pros, multi- center, phase II	29	70 ± 7 ^e	CTCs (CellSearch), qRT-PCR	Cabazitaxel	OS, PFS	7 (2–27) ^b	7
Qu et al. (36)	2017 US	Retros	Abi: 81, Enz: 51	Abi: 68.3 (62–74) Enz: 69.0 (63–74) ^c	PBMC(Ficol), ddPCR	Abi/Enz	OS, PFS (TTF)	29.7 (3.6– 47.5) 23.9 (0.9– 48.3) ^b	10
Scher et al. (37)	2018 US	Pros, cross- sectional	142	69.5 ± 9.6 ^e	CTCs (RBC lysis), IF	ARSi, Taxane	OS	4.3 years	8
Scher et al. (38)	2017 US	Pros, cross- sectional	161	68 (45–91) ^b	CTCs (RBC lysis), IF	ARSi, Taxane	OS	11 (1–30) ^a	9
Scher et al. (39)	2016 US	Pros, cross- sectional	161	68 (45–91) ^b	CTCs, IF	ARSi, Taxane	OS, PFS	36	10
Seitz et al. (40)	2017 Germany	Pros	85	71 (66–74) ^c	WB, ddPCR	Abi/Enz	OS, rPFS, PSA-PFS	7.6 (4.7– 12.7) ^c	8
Sepe et al. (41)	2019 Italy	Pros	Abi:26, Enz: 11	75 (68–80) ^b	CTCs (Adna), qRT-PCR	Abi/Enz	OS, rPFS, PSA-PFS	25 ^a	9
Sharp et al. (8)	2019 UK	Pros	181	CTC–:71.0 (66.8–75.6), CTC +/AR-V7–: 69.6 (64.9–72.3), CTC +/AR-V7+: 70.4 (65.3–74.6) ^c	CTCs (Adna, CellSearch), qRT-PCR	ARSi, Taxane	OS	19 (11–31) ^c	10
Škereňová et al. (42)	2018 Czech Republic	Retros	41	71 (54–82) ^b	CTCs (Adna), qRT-PCR	Docetaxel	OS	23.5 ^a	7
Stuopelyte et al. (6)	2020 Lithuania	Pros	102	75.4 (11.4) ^c	WB, qRT-PCR	Abi	PFS, OS	30.5 ^a	9
Tagawa et al. (43)	2019 US	Pros	54	71 (53–84) ^b	CTCs, ddPCR	Taxane	PFS	NA	7
Todenhöfer et al. (7)	2016, Canada	Pros	37	70 (53–87) ^b	WB, qRT-PCR	Abi	OS PSA-PFS	NA	8
Tommasi et al. (44)	2018 Italy	Pros	44	71.5 (55–87) ^b	CTCs (Adna), qRT-PCR	ARSi, Taxane	PFS	20.5 ^a	7
Wang et al. (45)	2018 China	Pros	36	56.2 ± 8.6 ^e	CTCs (immuno- beads), qRT-PCR	Abi/Enz	PFS	NA	6

Studies are labeled as last name of first author, et al. and presented in alphabetical order; Patient number and age are all patients included in study; Pros, prospective; Retros, retrospective. ^amedian, ^bmedian (range), ^cmedian IQR, ^dmean, ^emean ± STD. WB, whole blood; CTC, circulating tumor cells; RBC, red blood cell lysis; PBMC, peripheral blood mononuclear cell; Ficoll, density gradient medium; Adna, AdnaTest ProstateCancerPanel AR-V7; mAdna, modified Adna; IF, immunofluorescent staining; qRT-PCR, quantitative real time-polymerase chain reaction; ddPCR, droplet digital PCR; UC, ultracentrifuge; FC, flow cytometry; ARSi, androgen receptor signaling inhibitor; Abi, abiraterone; Enz, Enzalutamide; BAT, bipolar androgen therapy; NA, not available; some studies include healthy control for threshold setting or discovery cohort (the data is lack and not included in table).

where missing data in one study (31) had a significant effect on data outcome (**Supplementary Table 3**).

DISCUSSION

AR splice variants have been proposed as a cause of resistance to ARSi and taxane-based chemotherapy (46). AR-V7, the most-

studied AR splice variant, is emerging as a clinically relevant biomarker in CRPC, with a detection incidence ranging between 20 and 60%, depending on biopsy source, detection methods, and disease stage. Given that tumor tissue of advanced PC is rarely available and archival tissue may not reflect the biology of the current tumor stage, liquid biopsies, mainly blood, are becoming attractive resources for AR-V7 and other biomarker evaluation. Technical advances, different detection methods for

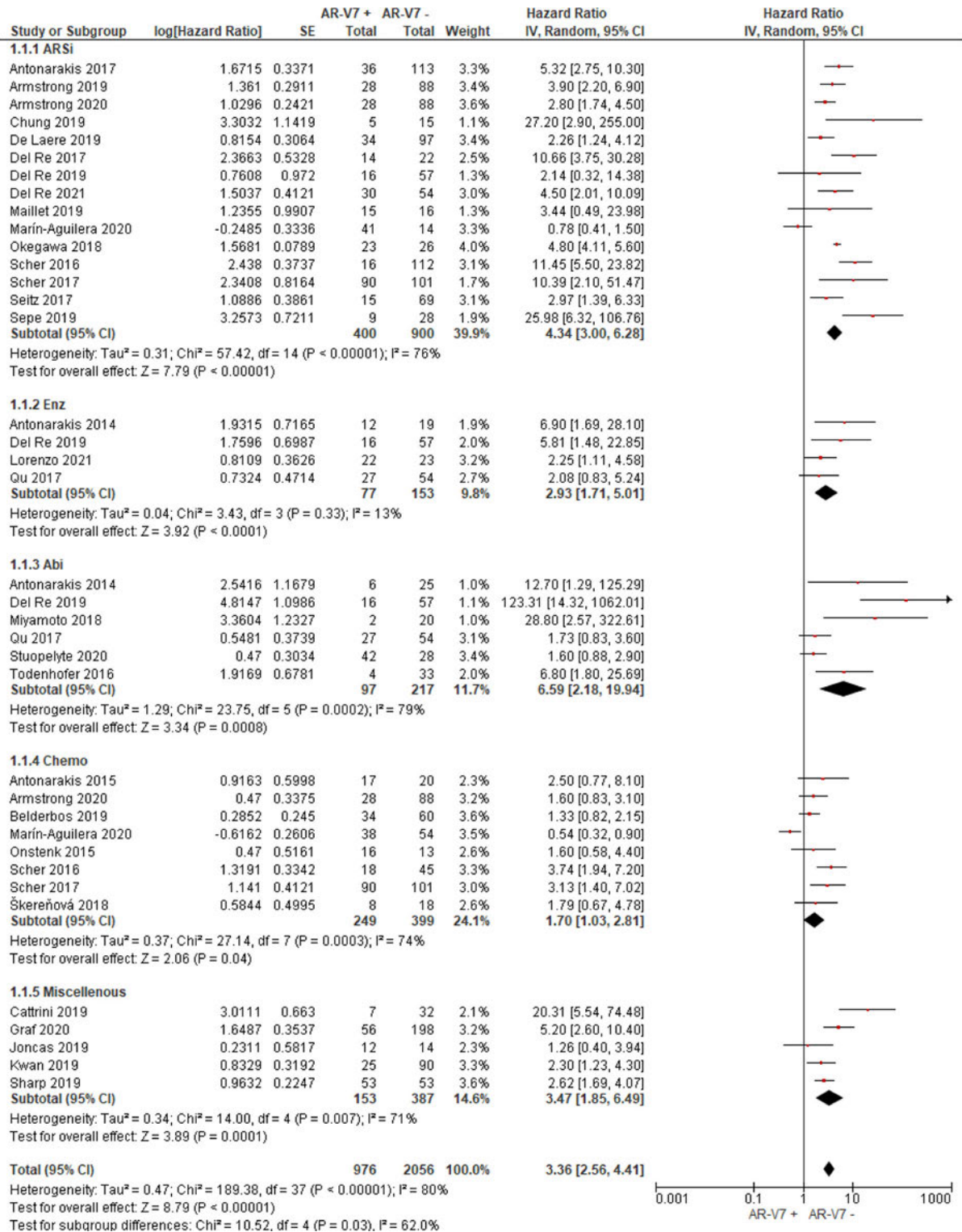


FIGURE 2 | Forest plot of hazard ratios (HRs) for association of liquid biopsy AR-V7 status with overall survival (OS) in all included studies. Pooled HRs were calculated using random effect model. AR-V7, androgen receptor splice variant 7; CI, confidence interval and bars indicate 95% CIs. Subgroup analysis (ARSi, enzalutamide or abiraterone; Enz, enzalutamide; Abi, abiraterone; Chemo, taxane based chemotherapy; Miscellaneous, treatments that do not belong to above treatments or not clearly defined) were assessed.

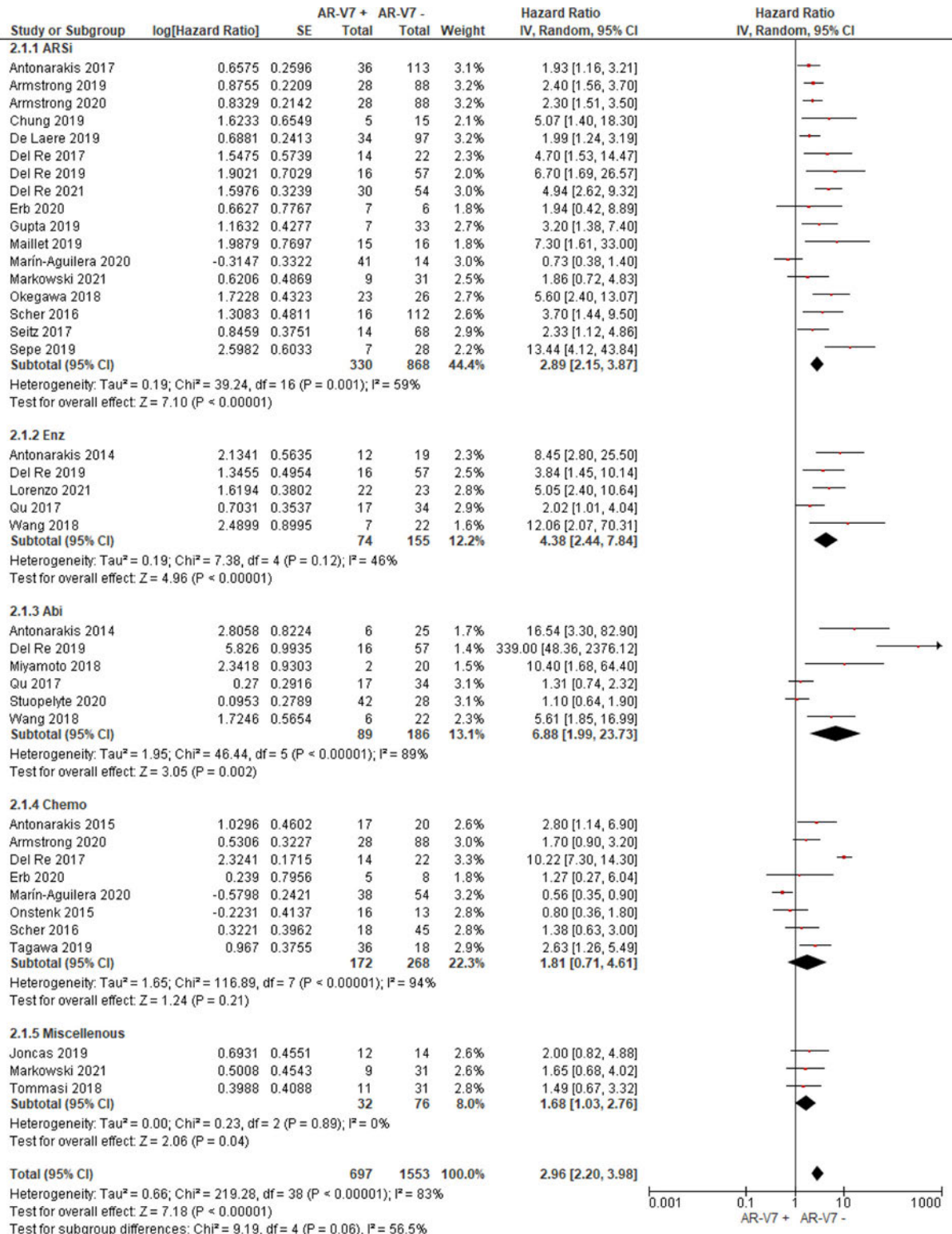


FIGURE 3 | Forest plot of hazard ratios (HRs) for association of liquid biopsy AR-V7 status with PFS in all studies. Pooled HRs were calculated using random effect model. AR-V7: androgen receptor splice variant 7. CI, confidence interval and bars indicate 95% CIs. Subgroup analysis (ARSi, enzalutamide or abiraterone; Enz, enzalutamide; Abi, abiraterone; Chemo, taxane based chemotherapy; Miscellaneous, treatments that do not belong to above treatments or not clearly defined) were assessed.

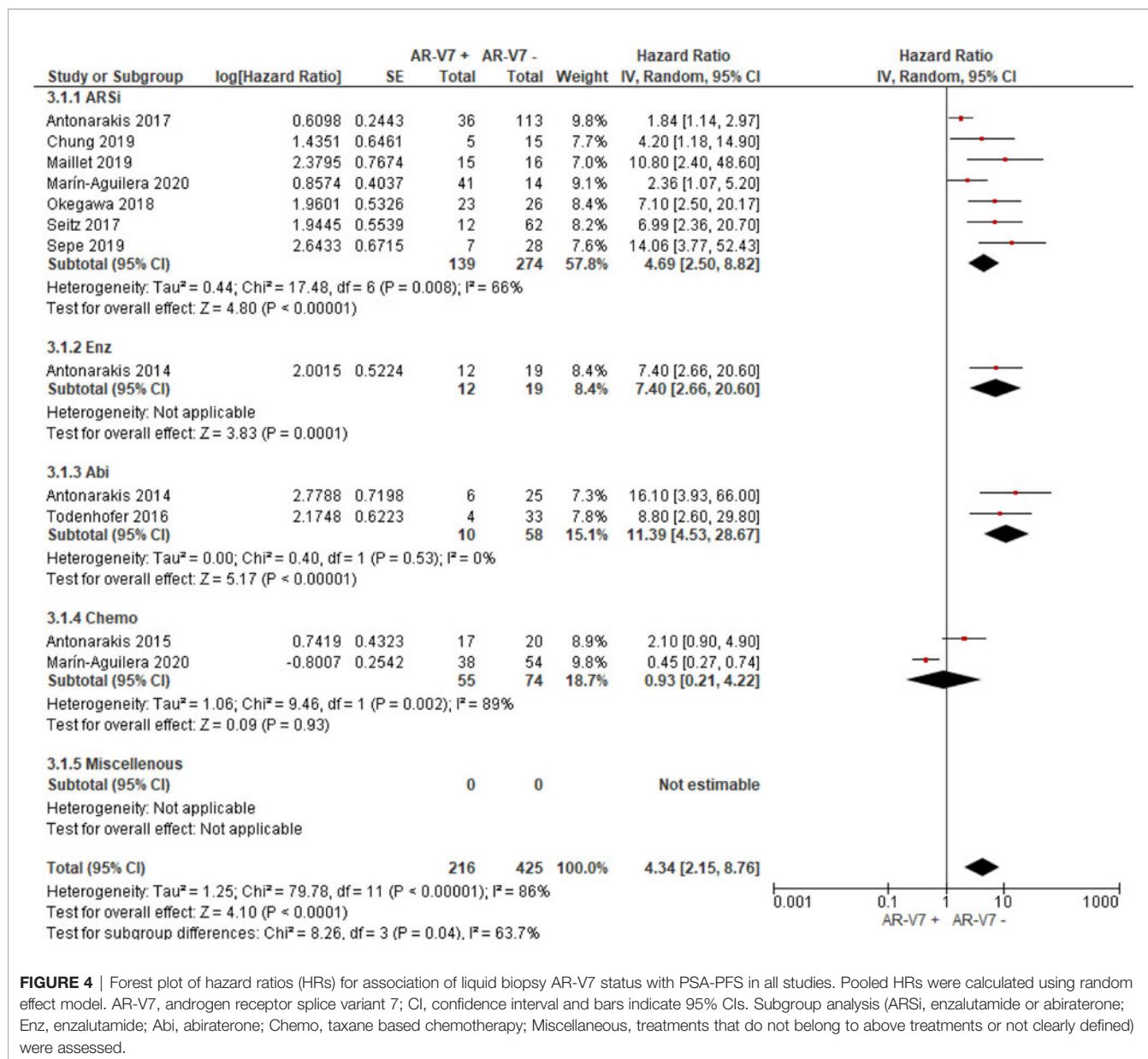


FIGURE 4 | Forest plot of hazard ratios (HRs) for association of liquid biopsy AR-V7 status with PSA-PFS in all studies. Pooled HRs were calculated using random effect model. AR-V7, androgen receptor splice variant 7; CI, confidence interval and bars indicate 95% CIs. Subgroup analysis (ARSi, enzalutamide or abiraterone; Enz, enzalutamide; Abi, abiraterone; Chemo, taxane based chemotherapy; Miscellaneous, treatments that do not belong to above treatments or not clearly defined) were assessed.

AR-V7 from liquid biopsies are now available, including modified AdnaTest ProstateCancer, and droplet digital PCR of CTCs enriched by various CTC isolation platforms (see **Table 1**). We recently confirmed CTC-based AR-V7 testing is more reliable than exosomal RNA and cell free tumor RNA in plasma (47). Accumulating reports on the association of AR-V7 detectability in liquid biopsy with therapy response and patient survival have prompted us to perform this systematic review and meta-analysis on the prognostic and predictive utility of liquid biopsy-based AR-V7 identification. Our data show that liquid biopsy detectable AR-V7 significantly associates with poor outcomes to ARSi treatment as shown for OS, PFS, PSA-PFS (P < 0.001). This strongly supports the notion that AR-V7 detection from CRPC patient liquid biopsies has prognostic and predictive power. This observation is highly clinically relevant and could

affect how clinicians make treatment decisions for patients with (metastatic) CRPC and when to transition patients to taxane-based chemotherapy.

While on taxane-based treatment, the association of AR-V7 presence with poorer outcome is still significant (P = 0.04) for OS data and lack adequate power for PFS (P = 0.21) or PSA-PFS (P = 0.93). However, there are relatively fewer publications in this subgroup, so these conclusions are based on weaker datasets compared to the ARSi treated subgroup; for instance, the omitting one publication changes the P-value and AR-V7 impact on OS would no longer be significant (**Supplementary Table 3**). Our data agree with a recent report that AR-V7 may contribute to taxane resistance by circumventing taxane-induced inhibitory effects both *in vitro* (cell lines) and *in vivo* (PC tissue) (43, 48). On the other hand, we cannot exclude the possibility

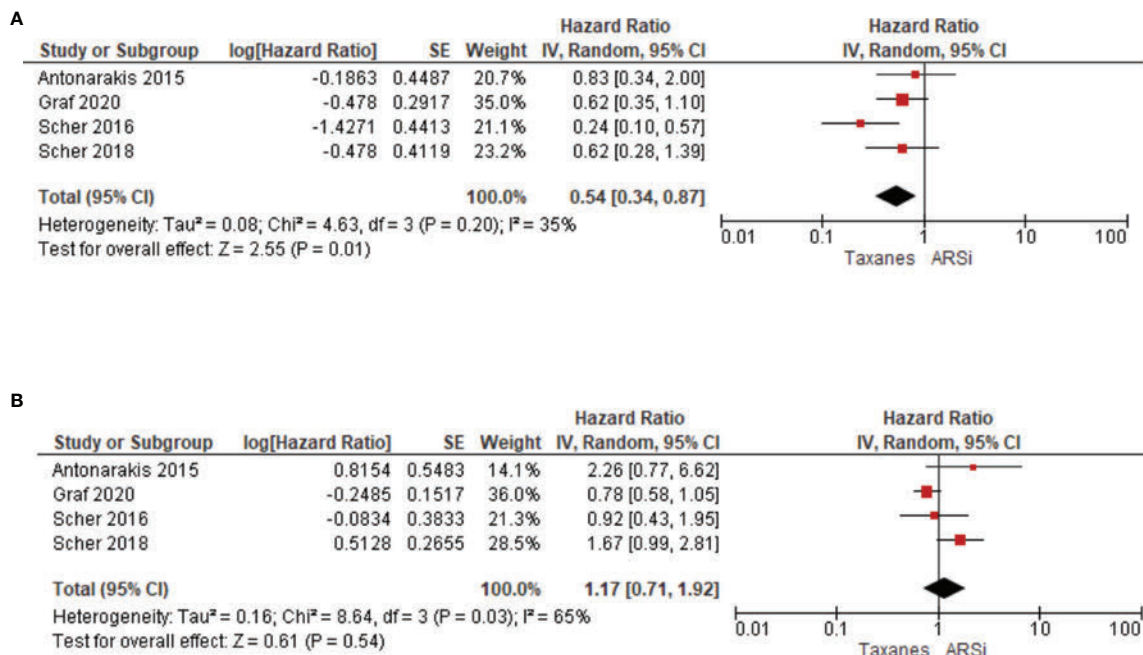


FIGURE 5 | Forest plots for association of liquid biopsy AR-V7 status with OS in **(A)** AR-V7 positive (ARSi vs. Chemotherapy) and **(B)** AR-V7 negative patients (ARSi vs. Chemotherapy). Pooled HRs were calculated using random effect model. AR-V7, androgen receptor splice variant 7; CI, confidence interval and bars indicate 95% CIs.

that AR-V7 expression was induced in CRPC patients who had received ARSi prior to chemotherapy, and that its effect on OS has not been completely washed out by taxanes. We note that four studies suggest that chemotherapy would be a better option compared to ARSi (HR 0.54, $P = 0.01$) in AR-V7 positive CRPC, suggesting that AR-V7 determination is important in chemotherapy-treated patients. More studies in this subgroup are warranted.

Three other meta-analyses on AR-V7 prognostication (13, 49, 50) have been published recently, but given the common inaccessibility of current tissue biopsies, our meta-analysis exclusively focuses on liquid biopsies and includes the most up-to-date studies. Further, we not only include all studies with author self-reported HR and 95% CI, but also calculate HR and 95% CI with established methods (12) for some papers with insufficient and incomplete statistical reporting. Nevertheless, our systematic review has limitations. We only examined OS, PFS, and PSA-PFS, and did not assess other treatment outcomes such as PSA response. Discrepancies in the definition of PSA response (e.g., extent of PSA fall in a specific timeframe) exist across studies and given our selection criteria, papers were excluded if they only reported PSA response without survival data. Secondly, statistical power was limited by the numbers of studies available and small sample sizes in some of the subgroups analysed. Thirdly, included study designs differed greatly in biological material investigated (type of liquid biopsy and content such as CTCs or exosomes). For some studies, patients were enrolled from a single centre, potentially leading to

publication bias and selection bias. Also, no randomized study has ever directly compared the predictive value of AR-V7 in patients treated with chemotherapy vs. ARSi. Therefore, the results are indirect with potential bias. Lastly, the variability of techniques used to determine AR-V7 positivity, namely, qRT-PCR and ddPCR of mRNA derived from CTC, whole blood, exosome, could result in differing conclusions. The cut-off value is essential in defining and interpretation of AR-V7 positivity, due to the continuous nature of this variable; more work is required to answer the question of whether the degree of AR-V7 presence is important. Last but not least, other CTC AR detection methods have been adopted such as RNA-seq and immunostaining. Despite the variety of methodologies, we found that liquid biopsy detectable AR-V7 correlates with disease outcomes (**Supplementary Figure 2**).

In conclusion, ARSi and taxane-based chemotherapy are approved treatment options for CRPC patients and are used globally. Use of emerging methodologies, such as liquid biopsy-determined AR-V7, to optimize utility of a known predictive biomarker could help to guide the optimal treatment sequencing pathway for each patient in a personalised manner and is therefore of clinical importance. Standardization of liquid biopsy AR-V7 detection would underpin utility in clinical practice. Avoiding ineffective therapies or early switching to more effective approaches should ensure better outcomes for patients. However, further studies on chemotherapy-treated patient cohort and direct comparison of chemotherapy vs. ARSi are warranted.

DATA AVAILABILITY STATEMENT

The original contributions presented in the study are included in the article/**Supplementary Material**. Further inquiries can be directed to the corresponding author.

AUTHOR CONTRIBUTIONS

Project development, methodology, data collection and analysis: TK and YM. Conceptualization: YM and TK. Project development: TB, KS, PDS and WC. Statistics: JD, TK and YM. Manuscript writing, editing, and reviewing: all authors. All authors listed have made a substantial, direct, and intellectual contribution to the work and approved it for publication.

FUNDING

TK received an Ingham Institute/Narellan Rotary Club Men's health grant 2018 and a WSU School of Medicine Androgen Receptor Research scholarship.

REFERENCES

- Lonergan PE, Tindall DJ. Androgen Receptor Signaling in Prostate Cancer Development and Progression. *J Carcinog* (2011) 10:20–. doi: 10.4103/1477-3163.83937
- Cattrini CA-O, España R, Mennitto A, Bersanelli MA-O, Castro EA-O, Olmos D, et al. Optimal Sequencing and Predictive Biomarkers in Patients With Advanced Prostate Cancer. *Cancers* (2021) 13:4522. doi: 10.3390/cancers13184522
- Wyatt AW, Annala M, Aggarwal R, Beja K, Feng F, Youngren J, et al. Concordance of Circulating Tumor DNA and Matched Metastatic Tissue Biopsy in Prostate Cancer. *J Natl Cancer Inst* (2017) 109:djx118. doi: 10.1093/jnci/djx118
- Shafi AA, Putluri V, Arnold JM, Tsouko E, Maity S, Roberts JM, et al. Differential Regulation of Metabolic Pathways by Androgen Receptor (AR) and its Constitutively Active Splice Variant, AR-V7, in Prostate Cancer Cells. *Oncotarget* (2015) 6:31997–2012. doi: 10.18632/oncotarget.5585
- Sharp A, Coleman I, Yuan W, Sprenger C, Dolling D, Rodrigues DN, et al. Androgen Receptor Splice Variant-7 Expression Emerges With Castration Resistance in Prostate Cancer. *J Clin Invest* (2019) 129:192–208. doi: 10.1172/JCI122819
- Stuopelyte K, Sabaliauskaitė R, Bakavicius A, Hafliadótir BS, Visakorpi T, Väänänen RM, et al. Analysis of AR-FL and AR-V1 in Whole Blood of Patients With Castration Resistant Prostate Cancer as a Tool for Predicting Response to Abiraterone Acetate. *J Urol* (2020) 204(1):71–8. doi: 10.1097/JU.0000000000000803
- Todenhöfer T, Azad A, Stewart C, Gao J, Eigl BJ, Gleave ME, et al. AR-V7 Transcripts in Whole Blood RNA of Patients With Metastatic Castration Resistant Prostate Cancer Correlate With Response to Abiraterone Acetate. *J Urol* (2016) 197(1):135–42. doi: 10.1016/j.juro.2016.06.094
- Sharp A, Welti JC, Lambros MBK, Dolling D, Rodrigues DN, Pope L, et al. Clinical Utility of Circulating Tumour Cell Androgen Receptor Splice Variant-7 Status in Metastatic Castration-Resistant Prostate Cancer. *Eur Urol* (2019) 76(5):676–85. doi: 10.1016/j.eururo.2019.04.006
- Del Re M, Conteduca V, Crucitta S, Gurioli G, Casadei C, Restante G, et al. Androgen Receptor Gain in Circulating Free DNA and Splicing Variant 7 in Exosomes Predict Clinical Outcome in CRPC Patients Treated With Abiraterone and Enzalutamide. *Prostate Cancer Prostatic Dis* (2021) 24(2):524–31. doi: 10.1038/s41391-020-00309-w
- Del Re M, Crucitta S, Sbrana A, Rofi E, Paolieri F, Gianfilippo G, et al. AR-V7 and AR-FL Expression Is Associated With Clinical Outcome: A Translational

SUPPLEMENTARY MATERIAL

The Supplementary Material for this article can be found online at: <https://www.frontiersin.org/articles/10.3389/fonc.2022.868031/full#supplementary-material>

Supplementary Table 2 | Quality assessment of included studies based on adapted NOS scales.

Supplementary Table 3 | Sensitivity analysis of subgroups with more than 6 studies.

Supplementary Figure 1 | Inverted funnel plot to evaluate potential publication bias in OS **(A)** and PFS **(B)** of ARSI treated patients.

Supplementary Figure 2 | Forest plot of hazard ratios (HRs) for association of liquid biopsy AR-V7 status with OS **(A)**, PFS **(B)**, PSA-PFS **(C)** in all studies. Subgroup analysis were performed based on AR-V7 detection technique type. Pooled HRs were calculated using random effect model. AR-V7: androgen receptor splice variant 7. CI: confidence interval and bars indicate 95% CIs. PCR, polymerase chain reaction; qRT-PCR, quantitative real time PCR; ddPCR, droplet digital PCR; IF, immunofluorescence; IHC, immunohistochemistry; FC, flow cytometry; RNA-seq, RNA-sequencing.

- Study in Patients With Castrate Resistant Prostate Cancer. *BJU Int* (2019) 124:693–700. doi: 10.1111/bju.14792
- Liberati A, Altman DG, Tetzlaff J, Mulrow C, Gøtzsche PC, Ioannidis JPA, et al. The PRISMA Statement for Reporting Systematic Reviews and Meta-Analyses of Studies That Evaluate Health Care Interventions: Explanation and Elaboration. *PLoS Med* (2009) 6(7):e1000100. doi: 10.1136/bmj.b2700
 - Tierney JF, Stewart LA, Ghersi D, Burdett S, Sydes MR. Practical Methods for Incorporating Summary Time-to-Event Data Into Meta-Analysis. *Trials* (2007) 8:16–. doi: 10.1186/1745-6215-8-16
 - Wang J, Zhang Y, Wei C, Gao X, Yuan P, Gan J, et al. Prognostic Value of Androgen Receptor Splice Variant 7 in the Treatment of Metastatic Castration-Resistant Prostate Cancer: A Systematic Review and Meta-Analysis. *Front Oncol* (2020) 10:562504. doi: 10.3389/fonc.2020.562504
 - Antonarakis ES, Lu C, Luber B, Wang H, Chen Y, Nakazawa M, et al. Androgen Receptor Splice Variant 7 and Efficacy of Taxane Chemotherapy in Patients With Metastatic Castration-Resistant Prostate Cancer. *JAMA Oncol* (2015) 1(5):582–91. doi: 10.1001/jamaoncol.2015.1341
 - Antonarakis ES, Lu C, Luber B, Wang H, Chen Y, Zhu Y, et al. Clinical Significance of Androgen Receptor Splice Variant-7 Mrna Detection in Circulating Tumor Cells of Men With Metastatic Castration-Resistant Prostate Cancer Treated With First- and Second-Line Abiraterone and Enzalutamide. *J Clin Oncol* (2017) 35(19):2149–56. doi: 10.1200/JCO.2016.70.1961
 - Antonarakis ES, Lu C, Wang H, Luber B, Nakazawa M, Roeser JC, et al. AR-V7 and Resistance to Enzalutamide and Abiraterone in Prostate Cancer. *New Engl J Med* (2014) 371(11):1028–38. doi: 10.1056/NEJMoa1315815
 - Armstrong AJ, Halabi S, Luo J, Nanus DM, Giannakakou P, Szmulewitz RZ, et al. Prospective Multicenter Validation of Androgen Receptor Splice Variant 7 and Hormone Therapy Resistance in High-Risk Castration-Resistant Prostate Cancer: The PROPHECY Study. *J Clin Oncol* (2019) 37(13):1120–9. doi: 10.1200/JCO.18.01731
 - Armstrong AJ, Luo J, Nanus DM, Giannakakou P, Szmulewitz RZ, Danila DC, et al. Prospective Multicenter Study of Circulating Tumor Cell AR-V7 and Taxane Versus Hormonal Treatment Outcomes in Metastatic Castration-Resistant Prostate Cancer. *JCO Precis Oncol* (2020) 4:1285–301. doi: 10.1200/PO.20.00200
 - Belderbos BPS, Sieuwerts AM, Hoop EO, Mostert B, Kraan J, Hamberg P, et al. Associations Between AR-V7 Status in Circulating Tumour Cells, Circulating Tumour Cell Count and Survival in Men With Metastatic Castration-Resistant Prostate Cancer. *Eur J Cancer* (2019) 121:48–54. doi: 10.1016/j.ejca.2019.08.005

20. Cattrini C, Rubagotti A, Zinoli L, Cerbone L, Zanardi E, Capaia M, et al. Role of Circulating Tumor Cells (CTC), Androgen Receptor Full Length (AR-FL) and Androgen Receptor Splice Variant 7 (AR-V7) in a Prospective Cohort of Castration-Resistant Metastatic Prostate Cancer Patients. *Cancers* (2019) 11(9):1365. doi: 10.3390/cancers11091365
21. Chung JS, Wang Y, Henderson J, Singhal U, Qiao Y, Zaslavsky AB, et al. Circulating Tumor Cell-Based Molecular Classifier for Predicting Resistance to Abiraterone and Enzalutamide in Metastatic Castration-Resistant Prostate Cancer. *Neoplasia (United States)* (2019) 21(8):802–9. doi: 10.1016/j.neo.2019.06.002
22. De Laere B, Oeyen S, Mayrhofer M, Whittington T, van Dam PJ, Van Oyen P, et al. TP53 Outperforms Other Androgen Receptor Biomarkers to Predict Abiraterone or Enzalutamide Outcome in Metastatic Castration-Resistant Prostate Cancer. *Clin Cancer Res* (2019) 25(6):1766–73. doi: 10.1158/1078-0432.CCR-18-1943
23. Del Re M, Biasco E, Crucitta S, Derosa L, Rofi E, Orlandini C, et al. The Detection of Androgen Receptor Splice Variant 7 in Plasma-Derived Exosomal RNA Strongly Predicts Resistance to Hormonal Therapy in Metastatic Prostate Cancer Patients. *Eur Urol* (2017) 71(4):680–7. doi: 10.1016/j.eururo.2016.08.012
24. Erb HHH, Sparwasser P, Diehl T, Hemmerlein-Thomas M, Tsaur I, Jünger E, et al. AR-V7 Protein Expression in Circulating Tumour Cells is Not Predictive of Treatment Response in MCRPC. *Urologia Internationalis* (2020) 104(3):253–62. doi: 10.1159/000504416
25. Graf RP, Hullings M, Barnett ES, Carbone E, Dittamore R, Scher HI. Clinical Utility of the Nuclear-Localized AR-V7 Biomarker in Circulating Tumor Cells in Improving Physician Treatment Choice in Castration-Resistant Prostate Cancer. *Eur Urol* (2020) 77(2):170–7. doi: 10.1016/j.eururo.2019.08.020
26. Gupta S, Hovelson DH, Kemeny G, Halabi S, Foo WC, Anand M, et al. Discordant and Heterogeneous Clinically Relevant Genomic Alterations in Circulating Tumor Cells vs Plasma DNA From Men With Metastatic Castration Resistant Prostate Cancer. *Genes Chromosomes Cancer* (2019) 59(4):225–39. doi: 10.1002/gcc.22824
27. Joncas FH, Lucien F, Rouleau M, Morin F, Leong HS, Pouliot F, et al. Plasma Extracellular Vesicles as Prognostic Biomarkers in Prostate Cancer Patients. *Prostate* (2019) 79(15):1767–76. doi: 10.1002/pros.23901
28. Kwan EM, Fettke H, Docanto MM, To SQ, Bukczynska P, Mant A, et al. Prognostic Utility of a Whole-Blood Androgen Receptor-Based Gene Signature in Metastatic Castration-Resistant Prostate Cancer. *Eur Urol Focus* (2021) 7:63–70. doi: 10.1016/j.euf.2019.04.020
29. Di Lorenzo G, Zappavigna S, Crocetto F, Giuliano M, Ribera D, Morra R, et al. Assessment of Total, PTEN(-), and AR-V7(+) Circulating Tumor Cell Count by Flow Cytometry in Patients With Metastatic Castration-Resistant Prostate Cancer Receiving Enzalutamide. *Clin Genitourin Cancer* (2021) 19:e286–98. doi: 10.1016/j.clgc.2021.03.021
30. Maillot D, Allioli N, Peron J, Plesa A, Decaussin-Petrucci M, Tartas S, et al. Improved Androgen Receptor Splice Variant 7 Detection Using a Highly Sensitive Assay to Predict Resistance to Abiraterone or Enzalutamide in Metastatic Prostate Cancer Patients. *Eur Urol Oncol* (2021) 4:609–17. doi: 10.1016/j.euo.2019.08.010
31. Marin-Aguilera M, Jiménez N, Reig Ò, Montalbo R, Verma AK, Castellano G, et al. Androgen Receptor and its Splicing Variant 7 Expression in Peripheral Blood Mononuclear Cells and in Circulating Tumor Cells in Metastatic Castration-Resistant Prostate Cancer. *Cells* (2020) 9(1):203. doi: 10.3390/cells9010203
32. Markowski MC, Wang H, Sullivan R, Rifkind I, Sinibaldi V, Schweizer MT, et al. A Multicohort Open-Label Phase II Trial of Bipolar Androgen Therapy in Men With Metastatic Castration-Resistant Prostate Cancer (RESTORE): A Comparison of Post-Abiraterone Versus Post-Enzalutamide Cohorts. *Eur Urol* (2021) 79:692–9. doi: 10.1016/j.eururo.2020.06.042
33. Miyamoto DT, Lee RJ, Kalinich M, LiCausi JA, Zheng Y, Chen T, et al. An RNA-Based Digital Circulating Tumor Cell Signature is Predictive of Drug Response and Early Dissemination in Prostate Cancer. *Cancer Discovery* (2018) 8(3):288–303. doi: 10.1158/2159-8290.CD-16-1406
34. Okegawa T, Ninomiya N, Masuda K, Nakamura Y, Tambo M, Nutahara K. AR-V7 in Circulating Tumor Cells Cluster as a Predictive Biomarker of Abiraterone Acetate and Enzalutamide Treatment in Castration-Resistant Prostate Cancer Patients. *Prostate* (2018) 78(8):576–82. doi: 10.1002/pros.23501
35. Onstenk W, Sieuwerts AM, Kraan J, Van M, Nieuweboer AJM, Mathijssen RHJ, et al. Efficacy of Cabazitaxel in Castration-Resistant Prostate Cancer is Independent of the Presence of AR-V7 in Circulating Tumor Cells. *Eur Urol* (2015) 68(6):939–45. doi: 10.1016/j.eururo.2015.07.007
36. Qu F, Xie W, Nakabayashi M, Zhang H, Jeong SH, Wang X, et al. Association of AR-V7 and Prostate-Specific Antigen RNA Levels in Blood With Efficacy of Abiraterone Acetate and Enzalutamide Treatment in Men With Prostate Cancer. *Clin Cancer Res* (2017) 23(3):726–34. doi: 10.1158/1078-0432.CCR-16-1070
37. Scher HI, Graf RP, Schreiber NA, Jayaram A, Winquist E, McLaughlin B, et al. Assessment of the Validity of Nuclear-Localized Androgen Receptor Splice Variant 7 in Circulating Tumor Cells as a Predictive Biomarker for Castration-Resistant Prostate Cancer. *JAMA Oncol* (2018) 4(9):1179–86. doi: 10.1001/jamaoncol.2018.1621
38. Scher HI, Graf RP, Schreiber NA, McLaughlin B, Lu D, Louw J, et al. Nuclear-Specific AR-V7 Protein Localization is Necessary to Guide Treatment Selection in Metastatic Castration-Resistant Prostate Cancer. *Eur Urol* (2017) 71(6):874–82. doi: 10.1016/j.eururo.2016.11.024
39. Scher HI, Lu D, Schreiber NA, Louw J, Graf RP, Vargas HA, et al. Association of AR-V7 on Circulating Tumor Cells as a Treatment-Specific Biomarker With Outcomes and Survival in Castration-Resistant Prostate Cancer. *JAMA Oncol* (2016) 2(11):1441–9. doi: 10.1001/jamaoncol.2016.1828
40. Seitz AK, Thoene S, Bietenbeck A, Nawroth R, Tauber R, Thalgot M, et al. AR-V7 in Peripheral Whole Blood of Patients With Castration-Resistant Prostate Cancer: Association With Treatment-Specific Outcome Under Abiraterone and Enzalutamide. *Eur Urol* (2017) 72(5):828–34. doi: 10.1016/j.eururo.2017.07.024
41. Sepe P, Verzoni E, Miodini P, Claps M, Ratta R, Martinetti A, et al. Could Circulating Tumor Cells and ARV7 Detection Improve Clinical Decisions in Metastatic Castration-Resistant Prostate Cancer? The Istituto Nazionale Dei Tumori (INT) Experience. *Cancers* (2019) 11(7):980. doi: 10.3390/cancers11070980
42. Škereňová M, Mikulová V, Čapoun O, Švec D, Kološťová K, Soukup V, et al. Gene Expression Analysis of Immunomagnetically Enriched Circulating Tumor Cell Fraction in Castration-Resistant Prostate Cancer. *Mol Diagnosis Ther* (2018) 22(3):381–90. doi: 10.1007/s40291-018-0333-0
43. Tagawa ST, Antonarakis ES, Gjyrezi A, Galletti G, Kim S, Worroll D, et al. Expression of AR-V7 and Arv(567es) in Circulating Tumor Cells Correlates With Outcomes to Taxane Therapy in Men With Metastatic Prostate Cancer Treated in TAXYNERGY. *Clin Cancer Res* (2019) 25(6):1880–8. doi: 10.1158/1078-0432.CCR-18-0320
44. Tommasi S, Pilato B, Carella C, Lasorella A, Danza K, Vallini I, et al. Standardization of CTC AR-V7 PCR Assay and Evaluation of its Role in Castration Resistant Prostate Cancer Progression. *Prostate* (2018) 79(1):54–61. doi: 10.1002/pros.23710
45. Wang S, Yang S, Nan C, Wang Y, He Y, Mu H. Expression of Androgen Receptor Variant 7 (AR-V7) in Circulated Tumor Cells and Correlation With Drug Resistance of Prostate Cancer Cells. *Med Sci Monitor* (2018) 24:7051–6. doi: 10.12659/MSM.909669
46. Galletti G, Leach BI, Lam L, Tagawa ST. Mechanisms of Resistance to Systemic Therapy in Metastatic Castration-Resistant Prostate Cancer. *Cancer Treat Rev* (2017) 57:16–27. doi: 10.1016/j.ctrv.2017.04.008
47. Nimir M, Ma Y, Jeffreys SA, Opperman T, Young F, Khan T, et al. Detection of AR-V7 in Liquid Biopsies of Castrate Resistant Prostate Cancer Patients: A Comparison of AR-V7 Analysis in Circulating Tumor Cells, Circulating Tumor RNA and Exosomes. *Cells* (2019) 8(7):688. doi: 10.3390/cells8070688
48. Zhang G, Liu X, Li J, Ledet E, Alvarez X, Qi Y, et al. Androgen Receptor Splice Variants Circumvent AR Blockade by Microtubule-Targeting Agents. *Oncotarget* (2015) 6(27):23358–71. doi: 10.18632/oncotarget.4396
49. Wang Z, Shen H, Ma N, Li Q, Mao Y, Wang C, et al. The Prognostic Value of Androgen Receptor Splice Variant 7 in Castration-Resistant Prostate Cancer Treated With Novel Hormonal Therapy or Chemotherapy: A Systematic Review and Meta-Analysis. *Front Oncol* (2020) 10:572590. doi: 10.3389/fonc.2020.572590
50. Zhou J, Liu R. The Association Between Androgen Receptor Splice Variant 7 Status and Prognosis of Metastatic Castration-Resistant Prostate Cancer: A

Systematic Review and Meta-Analysis. *Andrologia* (2020) 52(7):e13642. doi: 10.1111/and.13642

Conflict of Interest: The authors declare that the research was conducted in the absence of any commercial or financial relationships that could be construed as a potential conflict of interest.

Publisher's Note: All claims expressed in this article are solely those of the authors and do not necessarily represent those of their affiliated organizations, or those of the publisher, the editors and the reviewers. Any product that may be evaluated in

this article, or claim that may be made by its manufacturer, is not guaranteed or endorsed by the publisher.

Copyright © 2022 Khan, Becker, Scott, Descallar, de Souza, Chua and Ma. This is an open-access article distributed under the terms of the Creative Commons Attribution License (CC BY). The use, distribution or reproduction in other forums is permitted, provided the original author(s) and the copyright owner(s) are credited and that the original publication in this journal is cited, in accordance with accepted academic practice. No use, distribution or reproduction is permitted which does not comply with these terms.



OPEN

Choice of antibody is critical for specific and sensitive detection of androgen receptor splice variant-7 in circulating tumor cells

Tanzila Khan^{1,2,3,5}✉, John G. Lock^{3,4}, Yafeng Ma^{1,2,3,5}, David G. Harman⁶, Paul de Souza^{1,2,3}, Wei Chua^{1,2,5,7}, Bavanthi Balakrishnar⁷, Kieran F. Scott^{1,2} & Therese M. Becker^{1,2,3,5}✉

Androgen receptor variant 7 (AR-V7) is an important biomarker to guide treatment options for castration-resistant prostate cancer (CRPC) patients. Its detectability in circulating tumour cells (CTCs) opens non-invasive diagnostic avenues. While detectable at the transcript level, AR-V7 protein detection in CTCs may add additional information and clinical relevance. The aim of this study was to compare commercially available anti-AR-V7 antibodies and establish reliable AR-V7 immunocytochemical staining applicable to CTCs from prostate cancer (PCa) patients. We compared seven AR-V7 antibodies by western blotting and immunocytochemical staining using a set of PCa cell lines with known AR/AR-V7 status. The emerging best antibody was validated for detection of CRPC patient CTCs enriched by negative depletion of leucocytes. The anti-AR-V7 antibody, clone E308L emerged as the best antibody in regard to signal to noise ratio with a specific nuclear signal. Moreover, this antibody detects CRPC CTCs more efficiently compared to an antibody previously shown to detect AR-V7 CTCs. We have determined the best antibody for AR-V7 detection of CTCs, which will open future studies to correlate AR-V7 subcellular localization and potential co-localization with other proteins and cellular structures to patient outcomes.

Abbreviations

aa	Amino acid
ADT	Androgen deprivation therapy
AR	Androgen receptor
AR-V7	Androgen receptor variant 7
CRPC	Castration-resistant prostate cancer
CTCs	Circulating tumour cells
CE3	Cryptic exon E3
DBD	DNA binding domain
ddPCR	Droplet digital PCR
FBS	Fetal Bovine Serum
AR-FL	Full length AR
Knime	Konstanz Information Miner
LBD	Ligand binding domain
NTD	N-terminal domain
PVDF	Polyvinyl difluoride
PCa	Prostate cancer
TBS-T	Tris-buffered saline with 0.1% Tween 20 detergent

¹School of Medicine, Western Sydney University, Campbelltown, NSW 2560, Australia. ²Medical Oncology, Ingham Institute of Applied Medical Research, Liverpool, NSW 2170, Australia. ³Centre of Circulating Tumour Cells Diagnostics & Research, Ingham Institute for Applied Medical Research, Liverpool, NSW 2170, Australia. ⁴School of Medical Sciences, University of New South Wales, Sydney, Australia. ⁵South Western Sydney Clinical School, University of New South Wales, Liverpool Hospital, Liverpool, NSW 2170, Australia. ⁶School of Science, Western Sydney University, Campbelltown, NSW 2560, Australia. ⁷Department of Medical Oncology, Liverpool Hospital, Liverpool, NSW 2170, Australia. ✉email: 19153083@student.westernsydney.edu.au; therese.becker@inghaminstitute.org.au

Aberrant activity of the androgen receptor (AR) is central to prostate cancer development and first line therapy for metastatic prostate cancer is androgen deprivation therapy (ADT) which targets AR signalling^{1,2}. However, ADT resistance inevitably occurs, and disease is then referred to as castrate resistant prostate cancer (CRPC).

The expression of altered AR proteins translated from alternative AR splice variants has been proposed as a mechanism of ADT resistance^{3,4}. Expression of the AR splice variant 7 (AR-V7), is correlated with CRPC and is the most frequently identified disease associated variant. AR-V7 is proposed to be ligand independent and constitutively active as a nuclear transcription factor^{5,6}.

Splicing of the AR gene including exon 1, 2 and 3 together with a cryptic exon 3E (CE3) results in the AR-V7 transcript (Fig. 1A). The unique cryptic exon has allowed the generation of highly sensitive and specific assays to detect AR-V7 at the mRNA level^{7–10}. Importantly, given the general lack of matching tumor tissue for biomarker analysis at the CRPC stage these methods have been used to successfully detect AR-V7 transcripts from liquid biopsies, such as urine, plasma, exosomes and circulating tumor cells (CTCs) with the most reliable data originating from AR-V7 analysis in CTCs¹¹. Our recent metanalysis emphasises the potential of AR-V7 detection in liquid biopsies as clinical biomarker, as it demonstrates significant correlation with patient survival overall and in context of specific treatment¹. The presence of full-length AR (AR-FL) and AR-V7 in CTCs has been investigated at the RNA level in a number of studies and CTC-based AR-V7 was found to correlate with metastatic CRPC and primary resistance to abiraterone and enzalutamide^{8,12–15}.

The AR-V7 protein has 16 distinctive C-terminal amino acids, encoded by an alternate cryptic exon 3 producing a unique AR-V7 C-terminal protein domain, allowing for generation of specific antibodies. To our knowledge seven antibodies are now commercially available designated to specifically detect the AR-V7 protein and have been raised to C-terminal peptides (Fig. 1A). AR-V7 protein detection opens opportunities for immunohistological analysis, however as outlined above tissue is rarely available for advanced prostate cancer analysis. Again, liquid biopsy derived CTCs lend themselves for immunocytostaining of AR-V7 to add to mRNA information that is readily obtained from these samples. Indeed, Scher et al. reported that information regarding AR-V7 subcellular localization within CTCs may add important information correlating to disease progression and therapy response^{13,16,17}. This is an important finding as it potentially increases the value of AR-V7 screening as a biomarker in prostate cancer. Additionally, cellular AR-V7 protein analysis may enable future detailed investigations into interactions of AR-V7 with other proteins and nucleic acids to help understanding its CRPC related functions.

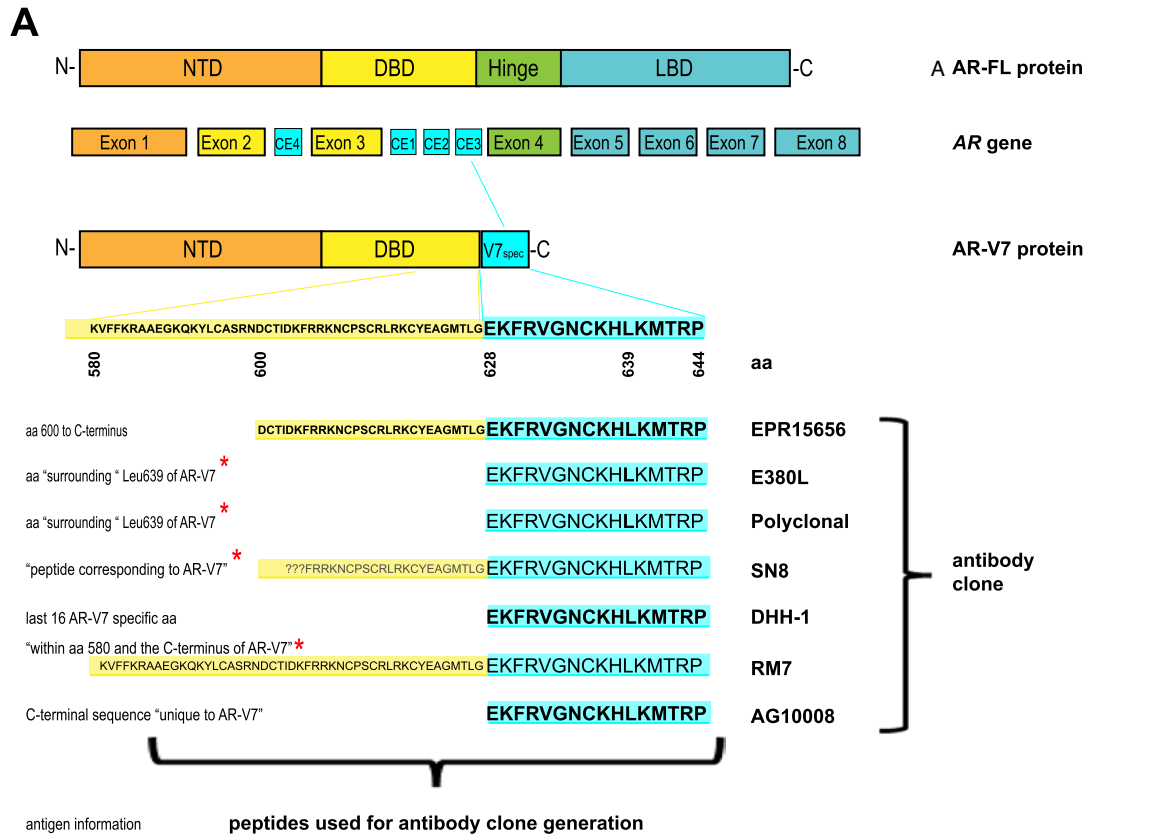
Here, using a cohort of well characterised prostate cancer cell lines with known and experimentally validated AR-V7 expression, we thoroughly tested the seven commercially available AR-V7 antibodies for their ability to truly detect AR-V7 by immunoblotting and immunocytostaining. Our findings highlight sensitivity, specificity and cross reactivities of antibodies and point towards an antibody of choice for AR-V7 immunocytostaining of CTCs. The antibody prioritised in this study performed well when employed for detection of CTCs from CRPC patients by immunocytostaining. Our finding is highly relevant to enhance AR-V7 utility to screen patients for therapy decisions or to stratify patients for relevant clinical trials.

Methods

Cell lines. 22RV1, LNCaP, VCaP, PC3 and DU145 prostate cancer cell lines are here referred to as 22RV1^{AR+/AR-V7+++}, LNCaP^{AR+/AR-V7-}, VCaP^{AR+++/AR-V7+}, PC3^{AR(+/-)/AR-V7-}, DU145^{AR-/AR-V7-} according to their published and in this study validated AR-FL and AR-V7 expression^{18–20} and cells were grown in DMEM supplemented with 10% Foetal Bovine Serum (FBS), 2 mM L-Glutamine, 4 nM HEPES or MEM supplemented with 10% FBS, 2 mM L-Glutamine, 4 nM HEPES at 37 °C in 5% CO₂. Cell lines were obtained directly or through Australian distributors (Merck/Sigma-Aldrich, Castle Hill; Invitro, Lane Cove, Australia) of the European Collection of Authenticated Cell Cultures (ECACC) or American Type Culture Collection (ATCC) and tested to be mycoplasma free (MycAlert Mycoplasma Detection Kit, Lonza, Rockland, USA) and STR authenticated (AGRF, Melbourne, Australia). Cells were seeded at approximately 30–40% confluency and harvested after 72-h culture for immunoblotting and gene expression analysis.

Antibodies. Six rabbit anti-human-AR-V7 antibodies were compared in this study: clone EPR15656 (Abcam, VIC, Australia), clone E308L and “polyclonal antibody” (Cell Signalling, Danvers, MA, USA), clone SN8 (Creative Diagnostic, Shirley, NY, USA), clone DHH-1 (RQ4683, Assay Matrix, VIC, Australia), and clone RM7 (RevMab Biosciences, San Francisco, CA, USA), as well as the mouse anti-human-AR-V7 clone AG10008 (Precision Antibody, Columbia, MD, USA). The available information of antigens used for the anti-AR-V7 antibody generation is shown in Fig. 1A. Additional antibodies used in this study are: mouse anti-human AR-FL, clone ER179 (Abcam, NSW, Australia), rabbit anti-GAPDH clone 14C10 (Cell Signaling, VIC, Australia), Alexa fluor 488 goat anti-rabbit IgG (H + L) (LOT 1423009) or Alexa fluor 488 goat anti-Mouse (H + L) (LOT 1252783) (Life technologies, Eugene, OR, USA), horseradish peroxidase-labelled donkey anti-Rabbit IgG (1:1000 dilution) (Lot 9526417, GE Healthcare, Buckinghamshire, UK) or sheep anti-mouse IgG, Horseradish Peroxidase linked F(ab)₂ fragment (1:1000 dilution) (Lot 312511, Amersham, GE Healthcare, Buckinghamshire, UK) and Alexa fluor 555 Phalloidin (Abcam, NSW, Australia).

Droplet digital PCR (ddPCR). In brief, total RNA was extracted with ISOLATE II RNA Mini Kit (Bioline, London, UK) from approximately 5 × 10⁶ cells. Quality and quantity of RNA was tested using a fragment analyser (5200 Fragment Analyzer System, CA, USA). cDNA was synthesised from 1 µg of total RNA per cell line using the SensiFAST cDNA Synthesis Kit (Bioline, London, UK). ddPCR to detect AR-V7 and full-length AR (AR-FL) was performed as described previously¹⁵. Quality of RNA was confirmed by conducting GAPDH ddPCR as described previously¹¹.



B

	22RV1 ^{AR+/AR-V7+++}	LNCaP ^{AR+/AR-V7-}	VCaP ^{AR+++/AR-V7+}	PC3 ^{AR(+)/AR-V7-}	DU145 ^{AR-/AR-V7-}
AR-FL	+	+	+++	(+/-)	-
AR-V7	+++	-	+	-	-

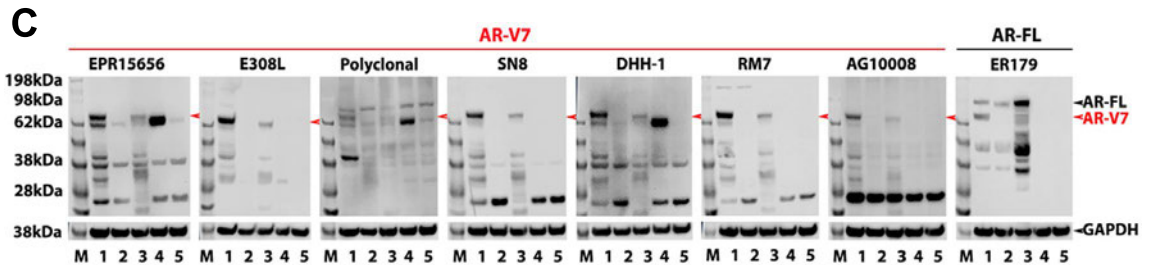


Figure 1. AR-V7 specific peptide and antigens for antibody generation. (A) Schematic presentation of the AR-gene encoding full length androgen receptor (AR-FL) and androgen receptor variant 7 (AR-V7) proteins. Amino acid (aa) sequences of cryptic exon (CE) 3 encoded AR-V7 specific domain (V7^{spec}) and a section of DNA binding domain (DBD) shared with AR-FL are displayed and aa sequences representing antigens for antibody generation is indicated for the clones. Antigen information: as published by supplier or provided on request (*: information is considered ambivalent for four peptides, consequently shown aa sequences may not reflect exact antigen peptides, but are based on "informed assumption" that the V7 specific unique 16 aa are part of all peptides and uncertain proportions of the DBD shared with AR-FL as indicated); ???: DBD aa sequences uncertain; NTD: N-terminal domain; LBD: ligand binding domain; N-: N-terminal; -C: C-terminal. (B) Validation of AR-FL and AR-V7 mRNA expression in the indicated cell lines by ddPCR. - no detection; (+/-) low, but detectable; + detection; +++ high levels of AR-V7 or AR-FL copies; (C) Immunoblotting of total protein lysates from the indicated cell lines for AR-V7 (separate gels for each antibody, left), or AR-FL (right) using the indicated antibodies in reference to GAPDH (cropped from probing of the same membrane shown below each plot). M: size marker; 1: 22RV1^{AR+/AR-V7+++}, 2: LNCaP^{AR+/AR-V7-}, 3: VCaP^{AR+++/AR-V7+}, 4: PC3^{AR(+)/AR-V7-}, 5: DU145^{AR-/AR-V7-}.

Western blotting. Approximately 1×10^6 cultured cells were harvested and lysed in RIPA lysis buffer (50 mM Tris–Cl pH7.5, 150 mM NaCl, 0.5% Triton X-100, 2 mM EDTA, 2 mM EGTA 25 mM NaF, 10% glycerol) containing 1 \times protease inhibitors (Roche, Basel, Switzerland) for 30 min placed on ice, followed by maximum microfuge centrifugation speed (11,700 \times g, 4 °C, 20 min) and recovery of supernatant. Protein concentrations were determined using the DC protein assay kit (Bio-Rad Laboratories, Hercules, CA). 30 μ g total protein per sample was separated on 4–12% Bis–Tris gels (Invitrogen, Life Technologies) and transferred to Polyvinylidene difluoride (PVDF) membrane (Amersham, GE Healthcare, Buckinghamshire, UK). Membranes were incubated with primary antibodies (dilutions see Supp. Table S1) overnight under gentle agitation at 4 °C. After three Tris-buffered saline with 0.1% Tween 20 detergent (TBS-T) washes, membranes were incubated with horseradish peroxidase-conjugated donkey anti-rabbit IgG (1:1000 dilution) or sheep anti-mouse IgG, horseradish peroxidase linked F(ab)₂ fragment (1:1000 dilution) for 1 h at room temperature and again washed three times. Membranes were developed using Western Lightning™ Plus-ECL Enhanced Luminol Reagent Plus (LOT 275–13,481) and Western Lightning™ Plus-ECL Oxidizing Reagent Plus (LOT 265-13481) (PerkinElmer, Waltham, MA, USA) and imaging was performed with an Odyssey imager (LI-Cor Biosciences, Lincoln, NE).

Immunocytostaining of cell lines and PBMC. For each cell line approximately 20,000 cells were seeded on sterile, round coverslips in 12-well plates and cultured for 72 h followed by fixation with 3.7% paraformaldehyde for 10 min. In case of PBMC probing cells were cytospun onto superfrost + slides. Cells were permeabilized with 0.2% Triton-X for 10 min and blocked using 10% goat serum in PBS for 30 min. Primary antibodies were diluted in 0.5% FBS in PBS (Supplementary Table S1) and incubated for 1 h. Secondary antibodies conjugated with Alexa fluor 488 goat anti-rabbit IgG (H + L) (1:5000) or Alexa fluor 488 goat anti-mouse (H + L) (1:5000) were diluted in PBS with 0.5% goat serum and incubated 30 min. Cells were stained with Alexa fluor 555 phalloidin for 0.5 h followed by nuclear staining by using 1 \times Hoechst (Fluorochrome, San Francisco, CA, USA) in PBS for 10 min. Coverslips were mounted with Pro Long™ Glass Antifade Mountant (Eugene, OR, USA). Monochrome images were taken with Olympus IX71 microscope (Olympus, Tokyo, Japan) at $\times 20$ magnification with identical acquisition settings, below any pixel intensity saturation in the brightest cell labelling conditions.

CTC enrichment and immunocytostaining. To validate AR-V7 CTC detection six prostate cancer patients with advanced CRPC, likely to yield high CTC counts, were recruited. For each patient, 2 \times 9 mL peripheral blood was collected into 2 EDTA vacutubes (Greiner Bio-One) and processed within 24 h. 2 \times 9 mL blood was used to isolate CTCs using RosetteSep™ CTC enrichment cocktail containing anti-CD36 (Stemcell Technologies, Victoria, Australia) according to supplier's instructions. In brief, blood was incubated with antibody cocktail for 10 min and then diluted with 2% FBS in PBS as recommended by manufacturer, transferred to a Sepmate tube containing lymphoprep density gradient medium (Stemcell technologies, VIC, Australia) and centrifuged at 1200 \times g for 10 min. The supernatant with cellular layer was recovered and topped up to 50 mL with 2% FBS in PBS and gently mixed. After a 10-min 300 \times g spin, the supernatant was discarded, and cells were suspended in residual fluid by gentle tapping. Cells were washed once with PBS and spun again (300 \times g, 10 min), resuspended in 1.5 mL PBS and transferred to a well of a 24-well glass bottom plate (Greiner Bio-One GmbH, Frickenhausen, Germany) coated with 3.5 μ g of CellTak (FAL354240, InVitro technologies, VIC, Australia) per cm². After spinning the cells onto the glass (200 \times g, 10 min) immunocytostaining was essentially performed as above including anti-AR-V7 (E308L or EPR15656) staining and probing for CD45 to exclude lymphocytes and Hoechst to secure nucleated cellular identity. All patient CTC samples were stained in parallel to a positive control 22RV1 sample. To identify CTCs the definition CD45-, AR-V7 + and Hoechst positive was used, where AR-V7 positivity was determined by the parallel 22RV1 probing. Typically, weak but clear AR-V7 staining in 22RV1 was around an intensity value of 2000 (AR488 channel, Olympus cellSens Dimension image analysis software). Consequently, events with intensities below 2000 were considered AR-V7 negative (not CTCs) for patient CTC samples. Images in Fig. 4 are displayed using pseudocolors to allow for merging of images from various channels.

Image analysis and statistics. Image J (1.53c, National Institute of Health, USA) was used for RGB stacking and merging of immunostaining images from cell lines before doing quantitative image analysis using CellProfiler (Broad Institute, MIT, Massachusetts, USA) an automated image analysis software to measure biological phenotypes in images²¹. CellProfiler segmented cell data for at least 150 cells per sample (nucleus and cytoplasm) based on staining and extracted data on nucleus, cell body and cytoplasm and AR-V7 intensity were saved in excel to transfer to Konstanz Information Miner (Knime)²². The quantitative data from CellProfiler was used in Knime to compare the intensity of AR-V7 detected by different antibodies as well as cellular localization of AR-V7.

Ethical approval and consent to participate. All methods were performed in accordance with the relevant guidelines and regulations and the study was approved by the South Western Sydney Local Health District Human Ethics Committee (HREC/13/LPOOL/158). Written informed consent was obtained from all patients participating in the study.

Consent for publication. All authors agree on the submitted version of the manuscript.

Results

For any antibody to be selective for AR-V7, it must recognise a C-terminal peptide epitope corresponding to the 16 amino acid peptide sequence (EKFRVGNCKHLKMTRP) unique to AR-V7, encoded by the cryptic exon 3. Supplier information regarding the exact antigens used for antibody generation is considered imprecise for five of the seven antibodies tested here. Nevertheless, one can deduce that the entire 16 amino acids or most are part of any antigenic peptide used for antibody generation. Three of the antibodies are known or implied to have antigen peptides additionally containing parts of at least the DNA binding domain (DBD) shared by AR-V7 and AR-FL (Fig. 1A).

To be able to thoroughly compare these antibodies, AR-V7 status of several prostate cancer cell lines was validated. ddPCR confirmed high and detectable AR-V7 in 22RV1^{AR+/AR-V7+++} and lower but readily detectable transcript AR-V7 expression in VCaP^{AR+++/AR-V7+}, while AR-V7 is negative for LNCap^{AR+/AR-V7-}, PC3^{AR(+/-)/AR-V7-}, DU145^{AR-/AR-V7-}, ddPCR also confirmed known AR-FL status for all lines (Fig. 1B)¹⁵.

To test whether all of the anti-AR-V7 antibodies interact with a protein of the expected AR-V7 size of ~80 kDa in our AR-V7 expressing cell lines, or whether the antibodies may cross react with other proteins we first tested the antibodies by immunoblotting of full protein lysates from all cell lines (Fig. 1C). We also included an anti-AR-FL antibody to clarify whether the AR-V7 antibodies identified protein bands of AR-FL size. None of the specific anti-AR-V7 antibodies produced a band considered AR-FL. Interestingly, only the anti-AR-V7 antibody clones E308L, SN8, RM7 and AG1008 produced a distinct band appearing around the expected AR-V7 size for AR-V7 positive 22RV1^{AR+/AR-V7+++} and VCaP^{AR+++/AR-V7+} cells, while not detecting anything above background in AR-V7 negative cell lines in that protein size range. However, there was clearly some cross-reactivity detected for proteins of smaller size. We considered E308L was the “cleanest” antibody with negligible cross-reactivity detected for AR-V7 negative cell lines. SN8, RM7 and especially AG1008 produced strong reaction to proteins of sizes other than 80 kDa in all, including AR-V7 negative cell lines with one band appearing relatively dominant just below the 28 kDa range.

Two anti-AR-V7 antibodies (EPR15656 and DHH-1), while detecting protein bands corresponding to AR-V7 size in 22RV1^{AR+/AR-V7+++} and VCaP^{AR+++/AR-V7+} cells, additionally detected a very strong band in AR-V7 negative PC3^{AR(+/-)/AR-V7-} cells, while additional bands across cell lines evidenced further cross-reactivity for these antibodies. The prominent PC3^{AR(+/-)/AR-V7-} protein band was just below the expected AR-V7 size. AR-V7 detection with the polyclonal antibody proved to be highly nonspecific. (Fig. 1C). Complete raw data (images of all immunoblots) are provided as Supplementary Fig. S1.

Although deemed very unlikely that PC3^{AR(+/-)/AR-V7-} with undetectable AR-V7 transcript express a slightly truncated form of AR-V7, we wished to rule out AR-V7 identity of this band detected close to 80 kDa. Firstly, we conducted protein Blast searches (blast.ncbi.nlm.nih.gov/Blast.cgi?PAGE=Proteins) of the full AR-V7 specific 16 amino acid sequence as well as the sequence from amino acid 580 and 600 (see Fig. 1A) to the C-terminus of AR-V7 against the human protein database (<https://www.uniprot.org>), which identified only the AR-V7 splice variant and for the 580/600 to C-terminus peptide additionally to AR-V7 the partially homologue AR variant 5 (see ref²³ for review of AR variants). Additionally, we were able to elute the ~62 kDa PC3^{AR(+/-)/AR-V7-} band of interest from a gel to perform mass spectroscopy and the retrieved data confirmed our Blast data with no proteins detected that share homology to AR-V7 or AR-FL in the excised protein band of interest from PC3^{AR(+/-)/AR-V7-} cells. Out of interest the same was done for the 28 kDa band as cross reactivities for that size were detected by several anti-AR-V7 antibodies, no AR(-V7) homology was found. The datasets generated for these analyses are available (<https://doi.org/10.26183/7d43-ze13>).

With Western analysis already pointing towards clear specificity differences between the tested antibodies we excluded two antibodies from further analysis, the polyclonal due to lack of specificity for AR-V7 detection sensitivity and specificity by Western analysis, and the mouse monoclonal AG10008. The latter was excluded due to very strong cross-reactivity in all cell lines with a protein band at ~28 kDa compared to specific AR-V7 band intensity and since ultimately, we aim to perform AR-V7 detection by immunocytostaining of CTCs. In our established CTC workflow antibodies of rabbit origin are more easily integrated for technical reasons. Initial immunocytostaining analysis of the five remaining antibodies was performed focusing on the AR-V7-positive cell line, 22RV1^{AR+/AR-V7+++} and the AR-V7-negative cell line LNCap^{AR+/AR-V7-}.

Representative immunocytostaining images of all remaining antibodies in the two cell lines used for monochromatic analysis of staining intensity and subcellular localization are shown in Fig. 2. In comparison to “no primary” control staining we analysed intensity of staining, and subcellular localization of staining as specific AR-V7 staining is expected to be predominantly nuclear²⁴. Initial subjective visual analysis clearly favours the E308L and SN8 antibodies that show distinct nuclear AR-V7 staining in 22RV1^{AR+/AR-V7+++}, however SN8 produces what appears to be cross-reactivity with nucleolar structures in the negative control LNCap^{AR+/AR-V7-} cells. EPR15656, DHH-1 and RM7 appear to produce less distinct staining in 22RV1^{AR+/AR-V7+++} vs LNCap^{AR+/AR-V7-} cells. Analysing images using unbiased digital image analysis essentially confirmed these observations, presented in Fig. 3 for nuclear intensity. E308L produced the second highest nuclear staining intensity after SN8 in 22RV1^{AR+/AR-V7+++} cells, and that corresponded to the second lowest nuclear staining intensity in AR-V7 negative LNCap^{AR+/AR-V7-}. Since the staining in LNCap^{AR+/AR-V7-} can be attributed to unspecific antibody binding, E308L is the antibody with the best signal detection to noise ratio for AR-V7 immunocytostaining.

The goal of the presented antibody comparison was to find the best suited anti-AR-V7 antibody to probe and analyse AR-V7 in CTCs. With E308L emerging as the favourite candidate anti-AR-V7 antibody while EPR15656 was previously published to be used for AR-V7 immunocytostaining in CTCs^{20,24}, a final validation of both antibodies, E308L and EPR15656, was by detection of CTCs isolated from a small number of CRPC patients (to validate antibody staining this pilot study focussed on patients with advanced CRPC only, see Table 1). It is evident that E308L detected prostate cancer patient CTC numbers are consistently higher, indicating higher sensitivity

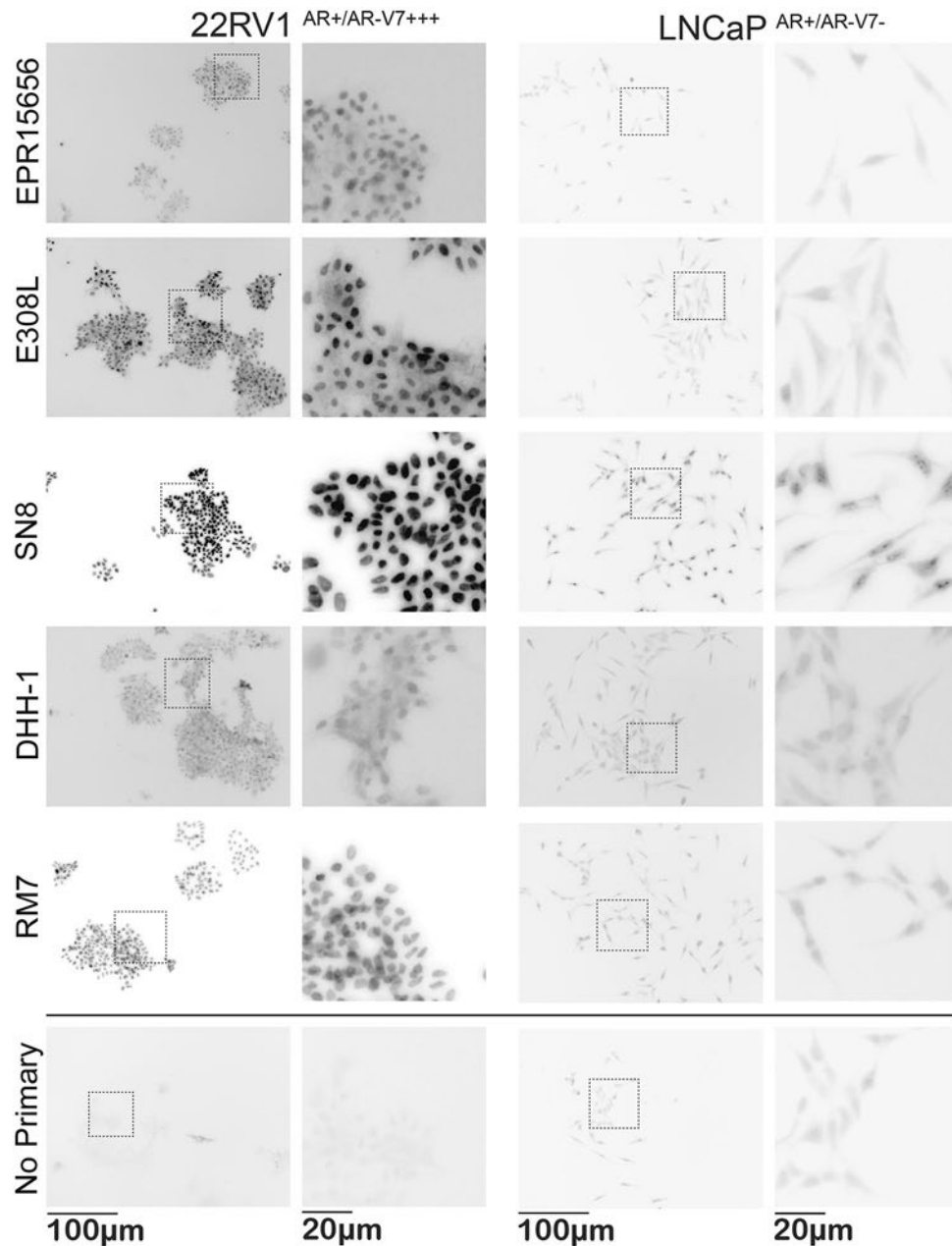


Figure 2. AR-V7 staining with different antibodies in AR-V7 positive and negative cells. Immunocytochemistry was performed with the indicated antibodies on 22RV1^{AR+/AR-V7+++} and LNCaP^{AR+/AR-V7-} cells in comparison to no-primary antibody controls. Images were acquired with identical acquisition settings, with no pixel intensity saturation in the brightest cell labelling conditions. This enables quantitative comparison of intensity values across all antibodies and cell lines. Here, monochrome images are presented inverted, allowing easier visual detection of low intensity labelling patterns. Overview visual fields of stained cells are shown to the left with higher magnification images for representative regions (dotted boxes) to the right.

of E308L CTC detection. Additionally, heterogeneity of AR-V7 expression is apparent as detection efficiencies are between 7–308% higher using E308L (Table 1). Representative CTC detection with both antibodies is shown in Fig. 4. Importantly, using both antibodies on three healthy donor PBMCs, confirmed negligible background staining for residual blood cells with the anti-AR-V7 antibodies in blood cells (Supplementary Fig. S2).

Discussion

Here we compared various antibodies to establish specific detection of AR-V7 by immunocytochemistry with ultimate focus to detect AR-V7 positive CTCs from prostate cancer patient bloods. Initially PCa cell lines with known and here confirmed status of AR-V7 expression (Fig. 1B) provided the tools to precisely judge cross-reactivity of antibodies in AR-V7 negative cells while specific staining and its subcellular localization could

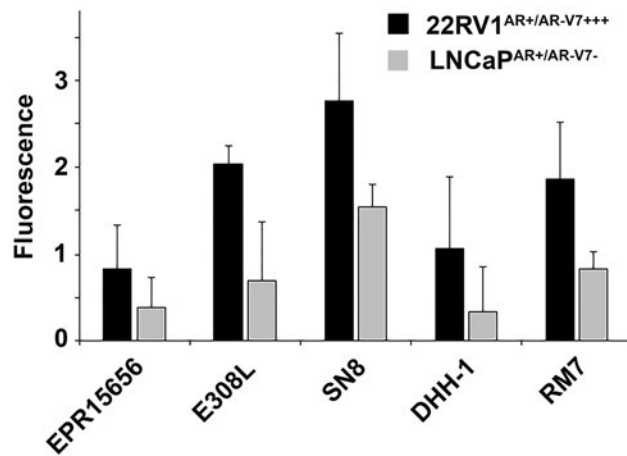


Figure 3. AR-V7 staining nuclear intensity. Cells (imaged as presented in Fig. 2) were segmented using CellProfiler based on identification of Hoechst as a nuclear marker and Alexa fluor 555 phalloidin as a cell body marker. This permitted selective measurement of AR-V7 labelling intensities in individual whole cells, as well as in nuclear and cytoplasmic compartments, per cell. Here, nuclear AR-V7 labelling intensity (average and standard deviation of at least 150 cells per condition) is depicted after normalisation to control values (no primary antibody labelling), allowing comparison of antibody signals in 22RV1^{AR+/AR-V7+++} and LNCaP^{AR+/AR-V7-} cells. Fluorescence (Y-axis): in arbitrary units.

Patient	Age	Clinical notes	CTC counts	
			E308L	EPR15656
1	75	High grade disease, lymph node involvement (PSMA PET)	38	23
2	78	Widespread pelvic disease with vesical and rectal fistula	29	20
3	77	Widespread bone metastases, on chemotherapy, anemia	69	64
4	85	Widespread bone metastases, starting clinical trial (failed standard therapies)	45	5
5	84	Aggressive soft tissue disease in neck lymph nodes and meningeal metastases despite chemotherapy	173	95
6	77	Metastatic bone disease, Gleason grade 4+5=9	184	45

Table 1. AR-V7 staining CTC detection by antibody in advanced CRPC patients. CTCs were enriched (RosetteSep) and immunocytostained for detection. Nucleated (Hoechst staining) events were included in CTC counts if negative for CD45 and positive for AR-V7 using the indicated anti-AR-V7 antibodies.

be determined in AR-V7 expressing cells. Western analysis helped to determine sensitivity and specificity of antibodies first, since higher cross-reactivity for immunocytostaining is likely mirrored by the appearance of cross-reactive bands in AR-V7 negative cells and for molecular weights other than the ~80 kDa of AR-V7 in positive cells. Indeed the “cleanest” antibody by Western analysis, E308L, in the end also emerged as our favoured antibody for immunocytostaining as well. The other antibody that performed highly for immunocytostaining in AR-V7 positive 22RV1^{AR+/AR-V7+++} cells, clone SN8, caused however clearly noticeable nuclear staining in AR-V7 negative LNCaP^{AR+/AR-V7-} cells, interestingly of nucleolar appearance. This means use of this antibody for CTC detection likely would cause false positive AR-V7 detection in the cellular compartment that has been linked to AR-V7 activity²⁴, affecting potential for “true” biomarker detection.

AR-V7 detection in CTCs by immunocytostaining has been reported previously using the ERP15656 antibody^{20,24}. This prompted us to do a direct comparison of CTC detection in parallel patient blood samples with our favourite E308L as well as the ERP15656 antibody. For proof-of-concept, we focused on a small highly advanced CRPC patient cohort (Table 1) to increase likelihood of high CTC numbers. We also used unbiased CTC enrichment using lymphocyte depletions as AR-V7 has been reported more common in EpCAM-negative CTCs²⁵. Interestingly the E308L did not only consistently detect more CTCs in the small cohort of 6 patients (Table 1), but did so marginally to dramatically, which likely reflects heterogeneous AR-V7 protein levels in patient CTCs. More work is needed to verify the extent and heterogeneity of AR-V7 levels in CTCs. So far EPR15656 staining has shown correlation of AR-V7 CTC staining with patient outcome²⁴. Nevertheless, evaluation in larger patient cohorts is needed to clarify if AR-V7 detection in CTCs by immunocytostaining is better suited to predict patient outcome than detection by mRNA, or if indeed a combination of both methods may have benefit. A clear benefit of detecting the AR-V7 protein rather than only mRNA in CTCs is that it opens opportunities to evaluate cell by cell heterogeneity and how AR-V7 expression and sub-cellular localization is related to that of other proteins, which may not only add to our understanding of AR-V7 function but reveal ways of therapeutically targeting it in the future.

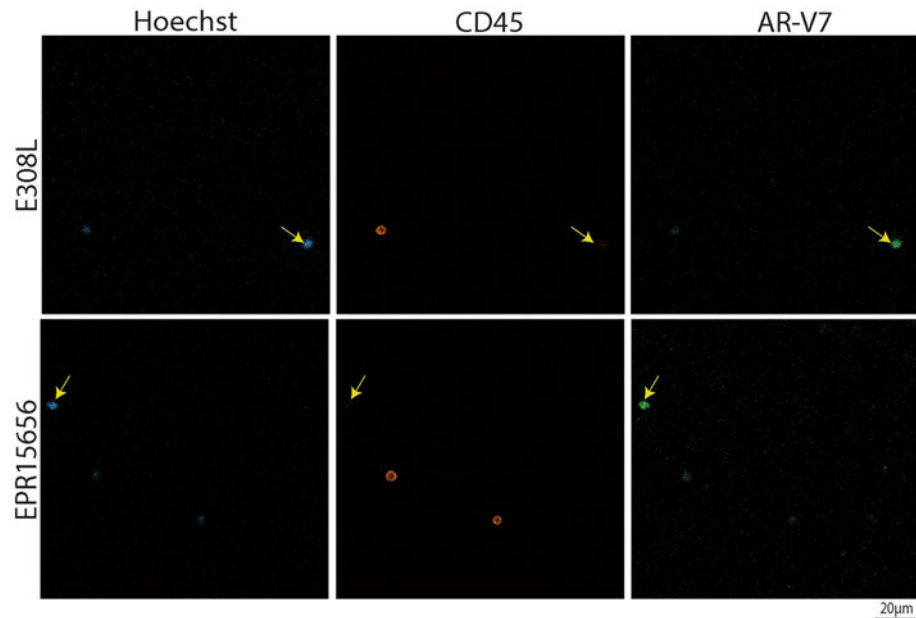


Figure 4. AR-V7 CTC detection. CTCs were identified based on AR-V7 staining. In brief, nucleated (blue, Hoechst) events were included in CTC counts if negative for CD45 (orange) and positive for AR-V7 (green) using the indicated anti-AR-V7 antibodies. AR-V7 was considered positive if intensities (Olympus cellSens Dimension image analysis software) were comparable or above intensities of cells weak but clearly identifiable (by operator) AR-V7 staining in 22RV1 (included as positive controls in each staining run).

Conclusion

Here we evaluated the commercially available antibodies against AR-V7 for utility in immunocytostaining of cell lines with known AR-V7 status and CRPC patient CTCs. The clone E308L emerged as the favoured antibody considering sensitivity and specificity as shown by immunoblotting and signal to noise ratio in immunocytostaining. With the growing attraction of liquid biopsies in diagnostic settings, identification of the best antibody to detect AR-V7 in CTCs may help to develop a standardised approach for AR-V7 screening in patient CTCs.

Data availability

All data generated in this study are included either in this article or in a supplementary table. Mass Spectroscopy datasets generated and/or analysed during the current study are available in the Western Sydney University ResearchDirect repository, <https://doi.org/10.26183/7d43-ze13>.

Received: 10 May 2022; Accepted: 8 September 2022

Published online: 28 September 2022

References

- Khan, T. *et al.* Prognostic and predictive value of liquid biopsy-derived androgen receptor variant 7 (AR-V7) in prostate cancer: A systematic review and meta-analysis. *Front. Oncol.* **12**, 963 (2022).
- Lonergan, P. E. & Tindall, D. J. Androgen receptor signaling in prostate cancer development and progression. *J. Carcinogen.* **10**, 20 (2011).
- Mostaghel, E. A. *et al.* Resistance to CYP17A1 inhibition with abiraterone in castration-resistant prostate cancer: Induction of steroidogenesis and androgen receptor splice variants. *Clin. Cancer Res.* **17**, 5913–5925 (2011).
- Nadiminty, N. *et al.* NF- κ B/p52 induces resistance to enzalutamide in prostate cancer: Role of androgen receptor and its variants. *Mol. Cancer Ther.* **12**, 1629–1637 (2013).
- Cao, B. *et al.* Androgen receptor splice variants activating the full-length receptor in mediating resistance to androgen-directed therapy. *Oncotarget* **5**, 1646 (2014).
- Li, Y. *et al.* Androgen receptor splice variants mediate enzalutamide resistance in castration-resistant prostate cancer cell lines. *Cancer Res.* **73**, 483–489 (2013).
- Antonarakis, E. S. *et al.* Clinical significance of androgen receptor splice variant-7 mRNA detection in circulating tumor cells of men with metastatic castration-resistant prostate cancer treated with first- and second-line abiraterone and enzalutamide. *J. Clin. Oncol.* **35**, 2149 (2017).
- Antonarakis, E. S. *et al.* AR-V7 and resistance to enzalutamide and abiraterone in prostate cancer. *Engl. J. Med.* **371**, 1028–1038 (2014).
- Onstenk, W. *et al.* Efficacy of cabazitaxel in castration-resistant prostate cancer is independent of the presence of AR-V7 in circulating tumor cells. *Eur. Urol.* **68**, 939–945 (2015).
- Qu, F. *et al.* Association of AR-V7 and prostate-specific antigen RNA levels in blood with efficacy of abiraterone acetate and enzalutamide treatment in men with prostate cancer. *Clin. Cancer Res.* **23**, 726–734 (2017).
- Nimir, M. *et al.* Detection of AR-V7 in liquid biopsies of castrate resistant prostate cancer patients: A comparison of AR-V7 analysis in circulating tumor cells, circulating tumor RNA and exosomes. *Cells* **8**, 688 (2019).

12. Steinestel, J. *et al.* Detecting predictive androgen receptor modifications in circulating prostate cancer cells. *Oncotarget* **10**, 4213–4223. <https://doi.org/10.18632/oncotarget.3925> (2019).
13. Armstrong, A. J. *et al.* Prospective multicenter validation of androgen receptor splice variant 7 and hormone therapy resistance in high-risk castration-resistant prostate cancer: The PROPHECY study. *J. Clin. Oncol.* **37**, 1120–1129. <https://doi.org/10.1200/JCO.18.01731> (2019).
14. Sharp, A. *et al.* Androgen receptor splice variant-7 expression emerges with castration resistance in prostate cancer. *J. Clin. Invest.* **129**, 192–208. <https://doi.org/10.1172/JCI122819> (2019).
15. Ma, Y. *et al.* Droplet digital PCR based androgen receptor variant 7 (AR-V7) detection from prostate cancer patient blood biopsies. *Int. J. Mol. Sci.* **17**, 1264 (2016).
16. Armstrong, A. J. *et al.* Prospective multicenter study of circulating tumor cell AR-V7 and taxane versus hormonal treatment outcomes in metastatic castration-resistant prostate cancer. *JCO Precis. Oncol.* **4**, 1285–1301 (2020).
17. Scher, H. I. *et al.* Assessment of the validity of nuclear-localized androgen receptor splice variant 7 in circulating tumor cells as a predictive biomarker for castration-resistant prostate cancer. *JAMA* **4**, 1179–1186 (2018).
18. Zhu, Y. *et al.* Novel junction-specific and quantifiable in situ detection of AR-V7 and its clinical correlates in metastatic castration-resistant prostate cancer. *Eur. Urol.* **73**, 727–735 (2018).
19. Hu, R. *et al.* Ligand-independent androgen receptor variants derived from splicing of cryptic exons signify hormone-refractory prostate cancer. *Cancer Res.* **69**, 16–22 (2009).
20. Scher, H. I. *et al.* Association of AR-V7 on circulating tumor cells as a treatment-specific biomarker with outcomes and survival in castration-resistant prostate cancer. *JAMA* **2**, 1441–1449 (2016).
21. Carpenter, A. E. *et al.* Cell profiler: Image analysis software for identifying and quantifying cell phenotypes. *Genome Biol.* **7**, 1–11 (2006).
22. Berthold, M. R. *et al.* KNIME-the Konstanz information miner: Version 2.0 and beyond. *ACM SIGKDD Explor. Newsl.* **11**, 26–31 (2009).
23. Kanayama, M., Lu, C., Luo, J. & Antonarakis, E. S. Ar splicing variants and resistance to ar targeting agents. *Cancers* **13**, 2563 (2021).
24. Scher, H. I. *et al.* Nuclear-specific AR-V7 protein localization is necessary to guide treatment selection in metastatic castration-resistant prostate cancer. *Eur. Urol.* **71**, 874–882 (2017).
25. Gjyrezi, A. *et al.* Androgen receptor variant shows heterogeneous expression in prostate cancer according to differentiation stage. *Commun. Biol.* **4**, 785. <https://doi.org/10.1038/s42003-021-02321-9> (2021).

Acknowledgements

We wish to thank the patients that consented to participate in the study.

Author contributions

Conceptualisation: T.K., J.L., K.S., T.B.; Experimental/Analysis: T.K., J.L., Y.M., D.H., K.S., T.B.; Patient recruitment: Pd.S., W.C., B.B.; Manuscript drafting: T.K., K.S., T.B.; Manuscript finalisation: all authors.

Funding

The study was funded by the NHMRC Ideas Grant APP1184009.

Competing interests

The authors declare no competing interests.

Additional information

Supplementary Information The online version contains supplementary material available at <https://doi.org/10.1038/s41598-022-20079-w>.

Correspondence and requests for materials should be addressed to T.K. or T.M.B.

Reprints and permissions information is available at www.nature.com/reprints.

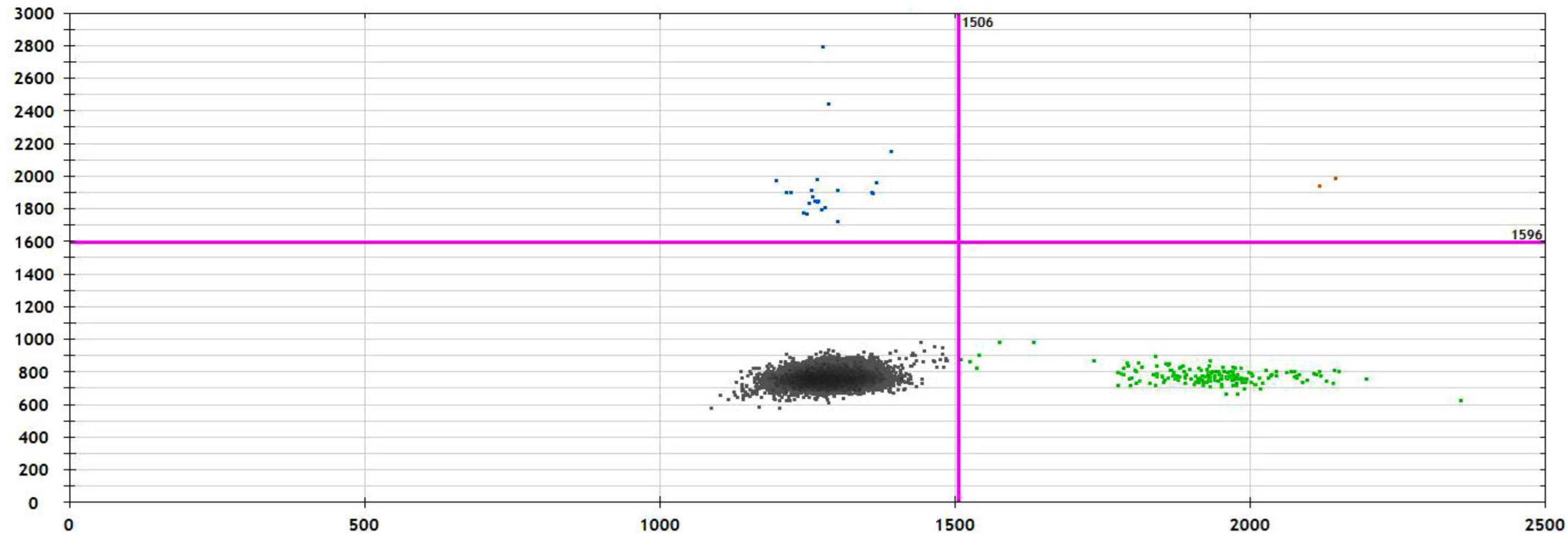
Publisher's note Springer Nature remains neutral with regard to jurisdictional claims in published maps and institutional affiliations.



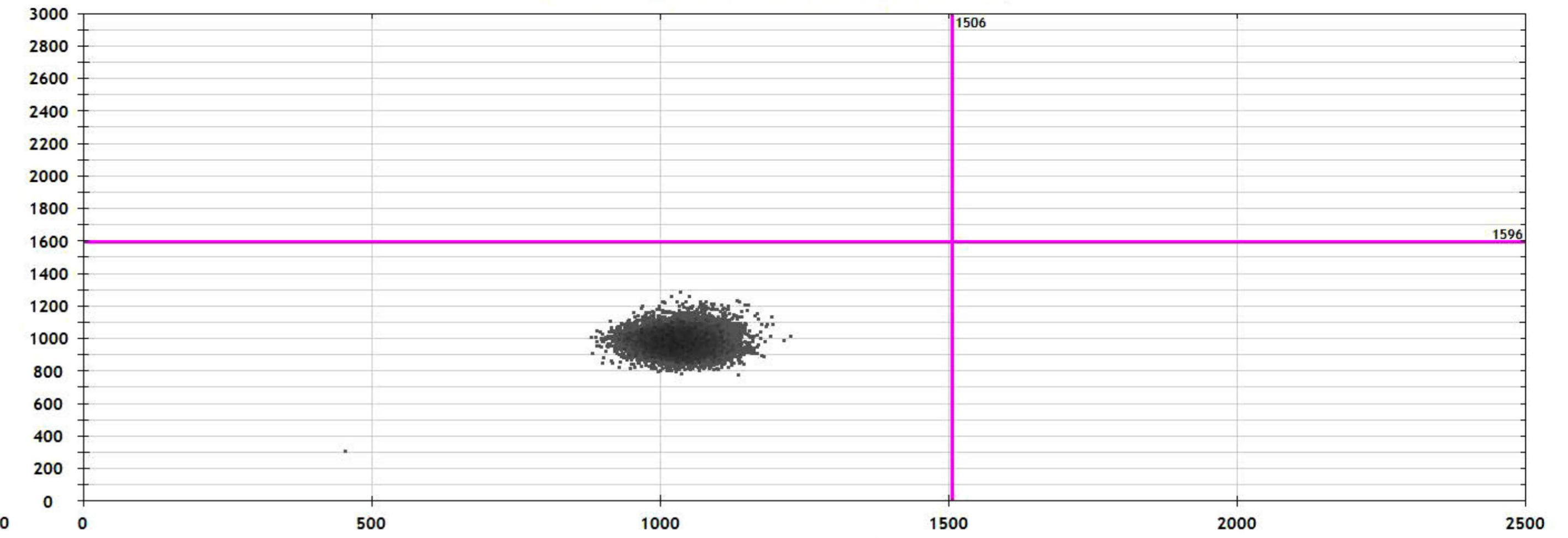
Open Access This article is licensed under a Creative Commons Attribution 4.0 International License, which permits use, sharing, adaptation, distribution and reproduction in any medium or format, as long as you give appropriate credit to the original author(s) and the source, provide a link to the Creative Commons licence, and indicate if changes were made. The images or other third party material in this article are included in the article's Creative Commons licence, unless indicated otherwise in a credit line to the material. If material is not included in the article's Creative Commons licence and your intended use is not permitted by statutory regulation or exceeds the permitted use, you will need to obtain permission directly from the copyright holder. To view a copy of this licence, visit <http://creativecommons.org/licenses/by/4.0/>.

© The Author(s) 2022

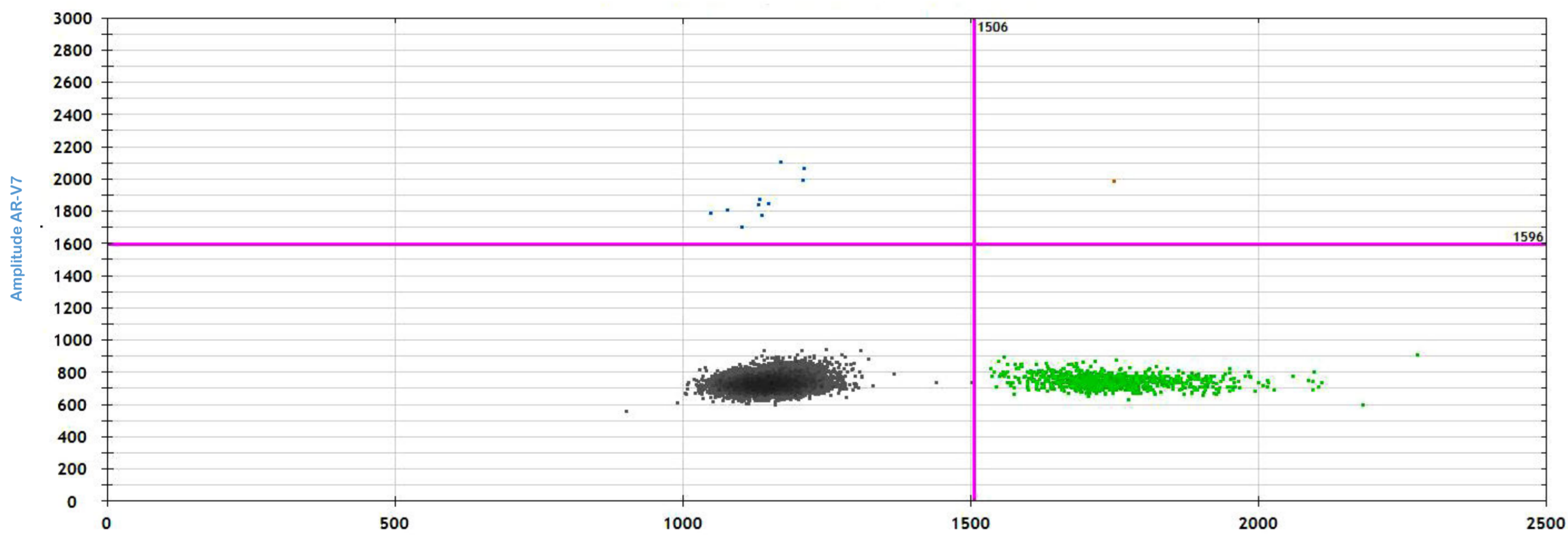
22RV1 AR+/AR-V7+++



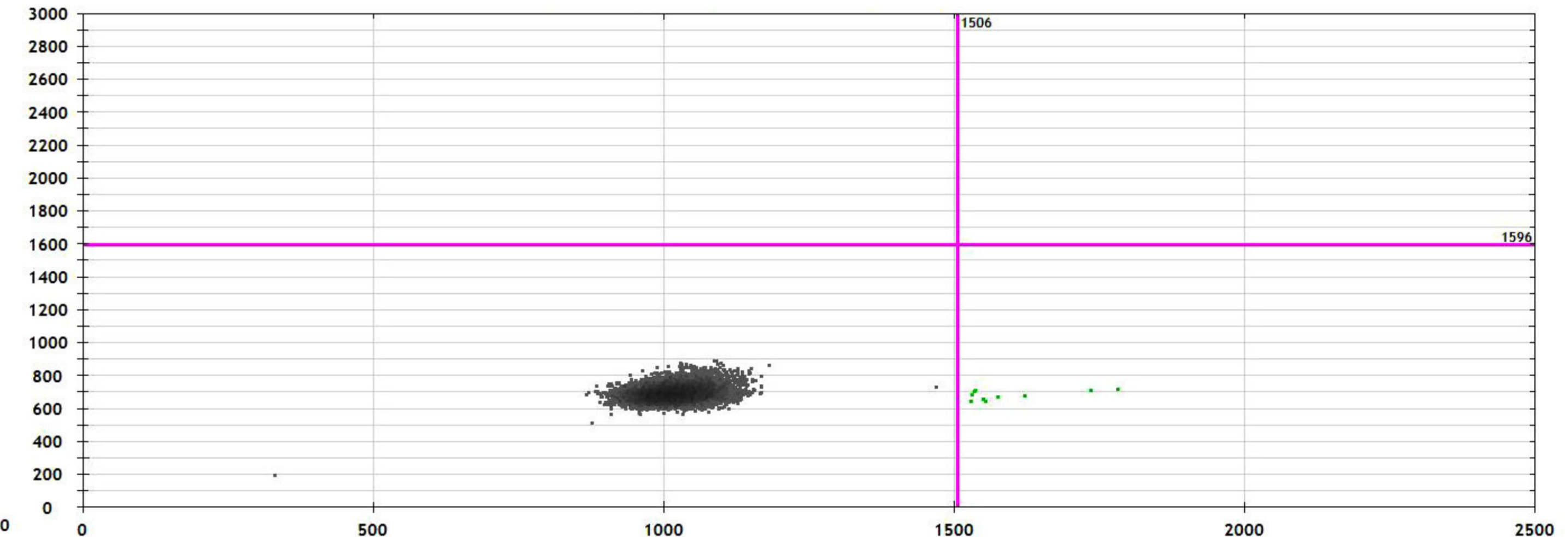
DU145 AR-/AR-V7-



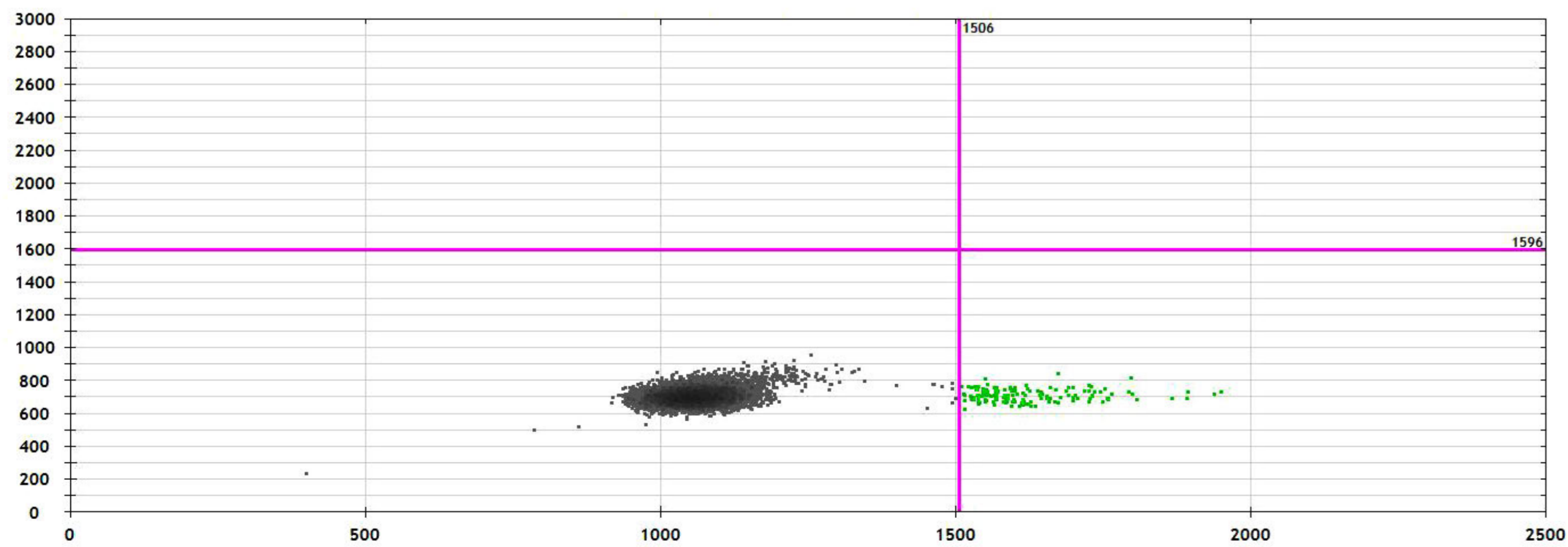
VCaP AR+++/AR-V7+



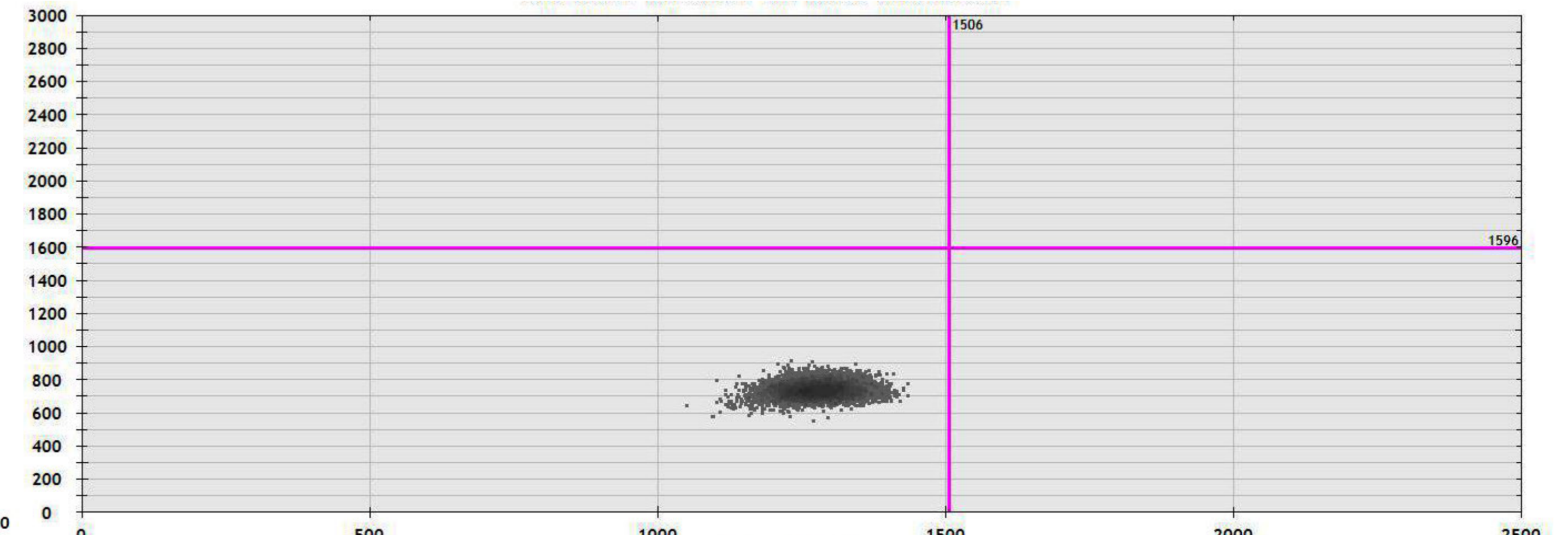
PC3 AR-/AR-V7-



LNCaP AR+++/AR-V7-



No template



Amplitude AR-FL